ISSN 1007-9327 (print)
ISSN 2219-2840 (online)

World Journal of *Gastroenterology*

World J Gastroenterol 2019 May 21; 25(19): 2271-2401

Published by Baishideng Publishing Group Inc

World Journal of Gastroenterology

Contents

Weekly Volume 25 Number 19 May 21, 2019

Contents

World Journal of Gastroenterology

Volume 25 Number 19 May 21, 2019

ABOUT COVER

Editorial board member of *World Journal of Gastroenterology*, C. Mel Wilcox, MD, Doctor, Professor, Division of Gastroenterology and Hepatology, Department of Medicine, University of Alabama at Birmingham, Birmingham, AL 35294, United States

AIMS AND SCOPE

World Journal of Gastroenterology (*World J Gastroenterol*, *WJG*, print ISSN 1007-9327, online ISSN 2219-2840, DOI: 10.3748) is a peer-reviewed open access journal. The *WJG* Editorial Board consists of 642 experts in gastroenterology and hepatology from 59 countries.

The primary task of *WJG* is to rapidly publish high-quality original articles, reviews, and commentaries in the fields of gastroenterology, hepatology, gastrointestinal endoscopy, gastrointestinal surgery, hepatobiliary surgery, gastrointestinal oncology, gastrointestinal radiation oncology, *etc*. The *WJG* is dedicated to become an influential and prestigious journal in gastroenterology and hepatology, to promote the development of above disciplines, and to improve the diagnostic and therapeutic skill and expertise of clinicians.

INDEXING/ABSTRACTING

The *WJG* is now indexed in Current Contents®/Clinical Medicine, Science Citation Index Expanded (also known as SciSearch®), Journal Citation Reports®, Index Medicus, MEDLINE, PubMed, PubMed Central, Scopus and Directory of Open Access Journals. The 2018 edition of Journal Citation Report® cites the 2017 impact factor for *WJG* as 3.300 (5-year impact factor: 3.387), ranking *WJG* as 35th among 80 journals in gastroenterology and hepatology (quartile in category Q2).

RESPONSIBLE EDITORS FOR THIS ISSUE

Responsible Electronic Editor: *Yu-Jie Ma* **Proofing Editorial Office Director:** *Ze-Mao Gong*

NAME OF JOURNAL
World Journal of Gastroenterology

ISSN
ISSN 1007-9327 (print) ISSN 2219-2840 (online)

LAUNCH DATE
October 1, 1995

FREQUENCY
Weekly

EDITORS-IN-CHIEF
Subrata Ghosh, Andrzej S Tarnawski

EDITORIAL BOARD MEMBERS
http://www.wjgnet.com/1007-9327/editorialboard.htm

EDITORIAL OFFICE
Ze-Mao Gong, Director

PUBLICATION DATE
May 21, 2019

INSTRUCTIONS TO AUTHORS
https://www.wjgnet.com/bpg/gerinfo/204

GUIDELINES FOR ETHICS DOCUMENTS
https://www.wjgnet.com/bpg/GerInfo/287

GUIDELINES FOR NON-NATIVE SPEAKERS OF ENGLISH
https://www.wjgnet.com/bpg/gerinfo/240

PUBLICATION MISCONDUCT
https://www.wjgnet.com/bpg/gerinfo/208

ARTICLE PROCESSING CHARGE
https://www.wjgnet.com/bpg/gerinfo/242

STEPS FOR SUBMITTING MANUSCRIPTS
https://www.wjgnet.com/bpg/GerInfo/239

ONLINE SUBMISSION
https://www.f6publishing.com

World Journal of Gastroenterology

Submit a Manuscript: https://www.f6publishing.com

World J Gastroenterol 2019 May 21; 25(19): 2271-2278

DOI: 10.3748/wjg.v25.i19.2271

ISSN 1007-9327 (print) ISSN 2219-2840 (online)

OPINION REVIEW

Cyst fluid glucose: An alternative to carcinoembryonic antigen for pancreatic mucinous cysts

César Vivian Lopes

ORCID number: César Vivian Lopes (0000-0003-1820-7192).

Author contributions: Lopes CV defined the concept of the study, evaluated the literature, wrote the manuscript, and provided the figures and tables.

Conflict-of-interest statement: Author does not have any conflicts of interest.

Manuscript source: Invited manuscript

Received: January 7, 2019
Peer-review started: January 7, 2019
First decision: March 14, 2019
Revised: March 30, 2019
Accepted: April 19, 2019
Article in press: April 19, 2019
Published online: May 21, 2019

P-Reviewer: Cianci P
S-Editor: Yan JP
L-Editor: A
E-Editor: Ma YJ

César Vivian Lopes, Department of Gastroenterology and Digestive Endoscopy, Santa Casa Hospital, Porto Alegre 91410-000, Brazil

Corresponding author: César Vivian Lopes, MD, PhD, Doctor, Department of Gastroenterology and Digestive Endoscopy, Santa Casa Hospital, Rua Prof. Cristiano Fischer 668/1001, Porto Alegre 91410-000, Brazil. drcvlopes@gmail.com
Telephone: +55-51-999628623
Fax: +55-51-999628623

Abstract

Pancreatic cystic lesions (PCLs) have been increasingly recognized in clinical practice. Although inflammatory cysts (pseudocysts) are the most common PCLs detected by cross-sectional imaging modalities in symptomatic patients in a setting of acute or chronic pancreatitis, incidental pancreatic cysts with no symptoms or history of pancreatitis are usually neoplastic cysts. For these lesions, it is imperative to identify mucinous cysts (intraductal papillary mucinous neoplasms and mucinous cystic neoplasms) due to the risk of their progression to malignancy. However, no single imaging modality alone is sufficient for a definitive diagnosis of all PCLs. The cyst fluid obtained by endoscopic ultrasound-guided fine needle aspiration provides additional information for the differential diagnosis of PCLs. Current recommendations suggest sending cyst fluid for cytology evaluation and measurement of carcinoembryonic antigen (CEA) levels. Unfortunately, the sensitivity of cytology is greatly limited, and cyst fluid CEA has demonstrated insufficient accuracy as a predictor of mucinous cysts. More recently, cyst fluid glucose has emerged as an alternative to CEA for distinguishing between mucinous and nonmucinous lesions. Herein, the clinical utility of cyst fluid glucose and CEA for the differential diagnosis of PCLs was evaluated.

Key words: Carcinoembryonic antigen; Differential diagnosis; Fine-needle biopsy; Glucose; Pancreatic cyst; Tumor marker

Core tip: Incidental pancreatic cysts have been found in far more patients with the improvement of cross-sectional imaging tests. Many of these lesions have malignant potential, especially the mucinous lesions, and imaging alone is not enough to guarantee definitive diagnosis. Cyst fluid carcinoembryonic antigen (CEA) has been used as the most important cyst fluid marker to distinguish mucinous from nonmucinous cysts. More

recently, glucose has emerged as a useful cyst fluid marker for the identification of pancreatic mucinous cysts with an accuracy similar to or even better than CEA.

Citation: Lopes CV. Cyst fluid glucose: An alternative to carcinoembryonic antigen for pancreatic mucinous cysts. *World J Gastroenterol* 2019; 25(19): 2271-2278
URL: https://www.wjgnet.com/1007-9327/full/v25/i19/2271.htm
DOI: https://dx.doi.org/10.3748/wjg.v25.i19.2271

INTRODUCTION

Pancreatic cystic lesions (PCLs) have been detected in between 2.4% and 19.6% of the general population during imaging tests [computed tomography (CT), magnetic resonance imaging (MRI)] for unrelated reasons[1,2]. In the absence of previous episodes of acute pancreatitis, which could increase the chance of pseudocysts, most of these lesions are neoplasms, and some of them have significant malignant potential, especially the intraductal papillary mucinous neoplasms (IPMNs) and mucinous cystic neoplasms (MCN)[3-5].

The accurate diagnosis of PCLs is critical to guarantee the best management for these patients, whether through surgical resection or periodic surveillance[6-8]. Unfortunately, there is no a single test accurate enough to assure a definitive diagnosis for all PCLs, particularly for those that are isolated unilocular cystic lesions, with neither perceptible communication with the main pancreatic duct (MPD) nor previous episodes of pancreatitis[9]. Therefore, a combination of information obtained from demographics, clinical history and imaging, as well as cytopathology and cyst fluid markers obtained by endoscopic ultrasound-guided fine needle aspiration (EUS-FNA), has been used for the differential diagnosis of PCLs (Table 1).

Recently, a few studies reported on the value of cyst fluid glucose as an addition to the differential diagnosis of pancreatic cysts[10-12]. However, carcinoembryonic antigen (CEA) has been the most used cyst fluid marker to date. This review aimed to compare the roles of cyst fluid glucose and CEA for the diagnosis of mucinous and nonmucinous PCLs.

IMAGING OF PANCREATIC CYSTIC LESIONS

Noninvasive cross-sectional imaging tests (CT and MRI) are usually responsible for detecting unsuspected PCLs and represent the first diagnostic approach for these lesions. EUS is a complementary tool when the diagnosis is undetermined by clinical and cross-sectional imaging data, when there are worrisome features present, or if surgery is believed to pose a high risk. Regarding the characteristics of mucinous lesions, IPMNs are radiographically classified according to the dilation of the ductal system as main duct-IPMN (MD-IPMN), branch duct-IPMN (BD-IPMN), or mixed type-IPMN. MD-IPMN is characterized by focal or diffuse dilation of the MPD to > 5 mm (Figure 1), and by the frequent presentation of a patulous aspect of the ampullary orifice with mucus secretion. Chronic pancreatitis and ductal adenocarcinoma are the most important differential diagnoses for this type of lesion. BD-IPMN is usually a multifocal disease with normal caliber MPD (Figure 2). Mixed type-IPMN shows a dilation of the MPD and the presence of dilated side branches (Figure 3). The MCN is classically a single macrocystic lesion in the body or tail of the pancreas (Figure 4). For nonmucinous cysts, the pseudocyst is usually a thin- or thick-walled unilocular lesion that almost always occurs in the setting of an episode of acute pancreatitis or pancreatic trauma, as well as in patients with chronic pancreatitis. For serous cystic lesions, numerous microcystic lesions with thin septa are the most common presentation. Central calcified fibrosis is a classic aspect of this type of lesion[13-15].

Nevertheless, there is not an ideal imaging modality to guarantee a correct diagnosis for all PCLs. There is a significant imaging overlap for different types of PCLs, and specific cystic lesions do not always disclose their most typical imaging features. The accuracy of CT and MRI/MR cholangiopancreatography in determining a definitive diagnosis is approximately 50%[16-18]. For EUS morphology alone, there is slightly more than chance interobserver agreement among experienced endosonographers for the diagnosis of the specific types of PCLs[19].

Since imaging alone is not sufficient for a definitive diagnosis of many PCLs, EUS-

Table 1 Differential diagnosis of pancreatic cystic lesions

	IPMN	MCN	PC	SCN	NET	SPN
Sex	M = F	F > M	M > F	F > M	M = F	F > M
Age (yr)	40-80	30-70	Variable	50-70	20-50	8-40
Clinical setting	Asymptomatic Pancreatitis	Asymptomatic Pain/mass	Pancreatitis	Asymptomatic Pain/mass	Asymptomatic Pain/mass	Asymptomatic Pain/mass
Appearance	Dilated MPD and/or branch-ducts. Fish- mouth papilla.	Well-circumscribed macrocystic lesion	Unilocular. Thin/thick- walled. Acute/chronic pancreatitis.	Microcystic with central fibrosis/ macrocystic and solid variants are possible	Associated mass	Mixed solid and cystic with well-defined borders.
Location	Head	Body/tail	Anywhere	Anywhere	Body/tail	Body/tail
Communication with MPD	Yes	Rare	Yes/no	No	No	No
Calcification	No	Peripheral	Related to chronic pancreatitis	Central	In necrotic lesions.	In necrotic lesions.
Fluid	Clear/viscous	Clear/viscous	Thin/dark	Clear/watery	Thin	Bloody
Epithelium	Columnar papillary mucinous.	Columnar/cuboidal mucinous.	No epithelium. Inflammatory cells.	Serous cuboidal. Stain for glycogen.	Endocrine. Stain for synaptophysin, chromogranin	Stain for vimentin, α_1-antitrypsin, β-catenin
Malignant potential	High	High	None	Rare	Low	Low
Cyst fluid CEA	Usually High	High	Low	Very low	Very low	Low
Cyst fluid amilase	High	Variable	High	Low	Low	Low

IPMN: Intraductal papillary mucinous neoplasm; MCN: Mucinous cystic neoplasm; PC: Pseudocyst; SCN: Serous cystic neoplasm; NET: Neuroendocrine tumor; SPN: Solid pseudopapillary neoplasm; MPD: Main pancreatic duct; CEA: Carcinoembryonic antigen.

FNA provides additional information that can be helpful in confirming the type of cyst. The aspirated cyst fluid allows cytological analysis, as well as assessment of biochemical and molecular factors and tumor markers.

PANCREATIC CYST FLUID ANALYSES

Cytology

Cytologic diagnosis using cystic fluid relies on the presence of confirmed malignant cells, mucin-containing cells, or glycogen-containing cells. The specificity of cytology in most studies is excellent and approaches 100%, but the sensitivity is usually unsatisfactory, especially due to the paucicellular nature of the samples and the presence of blood and benign epithelial cells from the gastric or duodenal mucosa. In a meta-analysis by Wang *et al*[20] of 16 studies and 1024 patients, the specificity of malignant cytology was 94%, but the sensitivity was only 51%. These data resemble those from another meta-analysis by Thornton *et al*[21].

Carcinoembryonic antigen

Given the unsatisfactory sensitivity of cytology for PCLs, the value of tumor markers in the aspirated cyst fluid has been examined. In the well-known multicenter prospective study by Brugge *et al*[22], a cut-off of 192 ng/mL for CEA demonstrated a sensitivity of 75%, specificity of 84%, and accuracy of 79% for the differential diagnosis between mucinous and nonmucinous cystic lesions. This performance was significantly better when compared to EUS morphology alone (51%) or cytology (59%) ($P < 0.05$). These results were corroborated in a meta-analysis by Thornton *et al*[21]. However, a multicenter study demonstrated a misdiagnosis of 40% for mucinous and 17% for nonmucinous lesions by using the same cut-off[23]. Given the risk of misclassification, other studies have used higher CEA thresholds in an attempt to improve the diagnostic accuracy for mucinous lesions, despite compromising the sensitivity of the marker[23-27]. A CEA level of > 800 ng/mL had a specificity ranging between 86% and 98% and a diagnostic accuracy between 58% and 79% for detecting mucinous lesions, but the sensitivity was too low, ranging from 33% to 48%[23,24,26]. On the other hand, similar results have been found with lower thresholds. Gaddam *et al*[23], using a cut-off value of 105 ng/mL, yielded a sensitivity of 70% and specificity of 63%, albeit 30% of mucinous lesions were misdiagnosed. With an even lower CEA

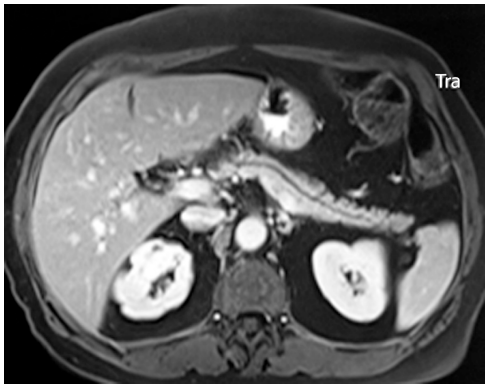

Figure 1 Main duct-intraductal papillary mucinous neoplasms. Magnetic resonance imaging of a uniform dilation of the main pancreatic duct.

cut-off of only 48.6 ng/mL, Oh *et al*[28] described a sensitivity, specificity, and accuracy for the diagnosis of mucinous cysts of 72.4%, 94.7%, and 81.3%, respectively.

Unlike the high CEA levels and the correlation with mucinous lesions, CEA levels of < 5 ng/mL are highly suggestive of nonmucinous lesions, with sensitivity ranging from 44% to 50%, specificity higher than 95%, and diagnostic accuracy ranging from 67% to 78%[24,26]. Most of these lesions were serous cystic neoplasms in the presence of low levels of amylase. However, in the experiment of Gaddam *et al*[23], despite median CEA levels for serous cysts having been found to be 1.7 ng/mL, 31% of serous cysts would have been misclassified when using a cut-off of 5 ng/mL.

Thus, cyst fluid CEA alone cannot be regarded as a perfect marker for the differential diagnosis of PCLs at this time. CEA levels have been demonstrated to be insufficiently accurate as a predictor of mucinous cysts, and the optimal cut-off is controversial. The ranges of cyst fluid CEA concentration from mucinous and nonmucinous cysts overlap considerably according to the CEA cut-off used[23,24]. Cysts with viscous fluid and CEA values between 10 ng/mL and 200 ng/mL represent the most important diagnostic challenge. Particularly for IPMNs, Yoon *et al*[29] demonstrated that cyst fluid CEA levels vary considerably by histologic type, with the gastric and pancreatobiliary types presenting the highest median CEA concentrations (619.8 and 270 ng/mL, respectively), and the intestinal and oncocytic types presenting the lowest median concentrations (83 and 5.1 ng/mL, respectively, P = 0.012). Furthermore, there has not been a significant correlation between the risk of malignancy and cyst fluid CEA levels[28,30,31]. CEA measurement is a laborious technique that requires specific laboratory capabilities that are costly and time-consuming. Commercially available methods for CEA measurement have been validated for the analysis of serum or plasma but not for pancreatic cyst fluid, and there could be significant variation in the results among different methods. Moreover, CEA thresholds are not necessarily transferable between different methods[32].

Molecular markers in pancreatic cyst fluid seem to be promising for the future, especially with the evaluation of GNAS and KRAS[33-35]. However, molecular markers are even more expensive than CEA, the analyses are performed using specialized technologies offered in few referral laboratories, and their results take a long time to be available. Additionally, molecular profiling remains under investigation and is not widely available. Currently, other cyst fluid markers are being sought, and a combination of these markers with CEA seems to be a more reasonable alternative.

Glucose

In 2013, Park *et al*[10], who were looking for potential cyst fluid markers for pancreatic mucinous cysts, published, for the first time, that glucose levels were significantly lower in mucinous cysts when compared to nonmucinous cysts (5 *vs* 82 mg/dL, P = 0.002). The best performance for glucose was observed by using a cut-off of 66 mg/dL, with a sensitivity, specificity, and diagnostic accuracy of 94%, 64%, and 84%, respectively. With this threshold, glucose had an accuracy similar to that of CEA > 192 ng/mL (84% *vs* 77%). Particularly for serous cystic neoplasms, glucose levels were significantly higher when compared to other cyst types (98 mg/dL *vs* 7 mg/dL, P = 0.0001). The diagnostic yield for the differentiation of serous cystic neoplasms at the same cut-off of 66 mg/dL had a sensitivity of 88%, a specificity of 89%, and a diagnostic accuracy of 89%. The same group validated these findings with a larger cohort two years later[11]. Sixty-five pancreatic cyst fluid samples with histological correlation were analyzed. Median glucose levels were once again lower in mucinous

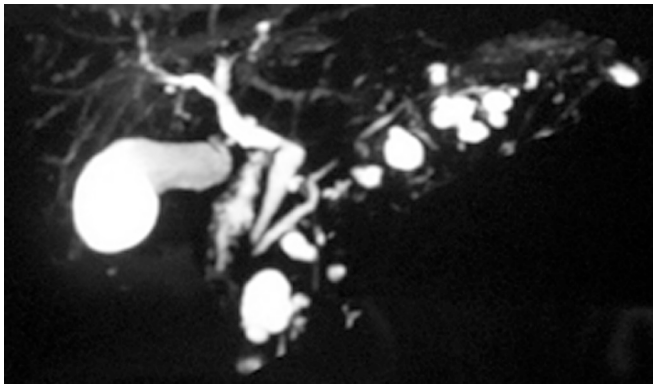

Figure 2 Branch duct—intraductal papillary mucinous neoplasms. Magnetic resonance cholangiopancreatography demonstrating a nondilated main pancreatic duct with multiple cystic dilated side branch ducts.

cysts (20 mg/dL *vs* 78 mg/dL, $P < 0.0001$). In this new study, the sensitivity and specificity for the definition of mucinous cysts at a glucose cut-off of ≤ 50 mg/dL were 88% and 78%, respectively. The standard CEA cut-off of 192 ng/mL had a sensitivity and specificity of 73% and 89%, respectively. However, the combination of both markers did not improve the diagnostic accuracy when compared to glucose or CEA alone. Recently, a well-designed study conducted by Carr *et al*[12] compared the cyst fluid glucose and CEA levels in samples from 153 patients with pathologically confirmed diagnoses. Median glucose levels were lower in mucinous cysts (19 *vs* 96 mg/dL, $P < 0.0001$). With the same threshold of ≤ 50 mg/dL, glucose had a sensitivity of 92%, a specificity of 87%, and a diagnostic accuracy of 90% in diagnosing mucinous cysts. All median glucose levels for mucinous cysts fell below 50 mg/dL. In comparison, a CEA threshold of > 192 ng/mL had a sensitivity of 58%, a specificity of 96%, and a diagnostic accuracy of 69% for mucinous cysts. Combining glucose and CEA for differentiating pancreatic mucinous cysts had a sensitivity of 95%, a specificity of 85%, and a diagnostic accuracy of 93% ($P = 0.03$). However, like CEA, cyst fluid glucose was unable to diagnose malignant disease. These studies have demonstrated that cyst fluid glucose performs similar to or even better than CEA in differentiating mucinous from nonmucinous cysts. Unlike CEA, glucose measurement is simple, rapid, inexpensive, reproducible, and requires only a few drops of cyst fluid.

In our initial experiment comparing cyst fluid glucose and CEA levels in 115 patients, glucose levels were < 50 mg/dL in 33 of 36 (91.6%) samples whose CEA levels were suggestive of mucinous pancreatic cysts at ≥ 192 ng/mL (Table 2). When CEA levels were < 5 ng/mL, suggestive of serous cystic neoplasms, glucose levels were ≥ 50 mg/dL in 48 of 51 (94.1%) samples (Table 3). Our median glucose levels in cysts whose CEA levels were ≥ 192 ng/mL and < 5 ng/mL were 5.5 mg/dL, and 98 mg/dL, respectively. The median glucose levels were 5 mg/dL in two studies evaluating mucinous cystic lesions[10,11]. On the other hand, the median glucose levels ranged between 86 and 103 mg/dL in studies evaluating serous cystic lesions[10-12]. Our findings are completely in line with the literature. Regardless these findings have not been compared to surgical pathology, they could demonstrate an almost perfect correlation between specific glucose and CEA thresholds for different types of PCLs (data not published).

CONCLUSION

PCLs have the potential to be malignant, and imaging, cytology, and cyst fluid CEA have demonstrated inadequate abilities for accurate diagnosis. In this context, glucose has emerged as a useful cyst fluid marker for distinguishing between mucinous and nonmucinous cysts with accuracy similar to or even better than CEA. Indeed, the initial results are promising, and more high-quality multicenter studies must reproduce these findings to corroborate cyst fluid glucose for routine use in the differential diagnosis of these lesions.

Table 2 Comparison between cyst fluid carcinoembryonic antigen and glucose levels, using a carcinoembryonic antigen cut-off suggestive of mucinous cystic neoplasms

Glucose levelsCEA levels	< 50 mg/dL	≥ 50 mg/dL	Total
≥ 192 ng/mL	33	3	36[a]
< 192 ng/mL	25	54	79
Total	58	57	115

CEA: Carcinoembryonic antigen;
[a]$P < 0.0001$.

Table 3 Comparison between cyst fluid carcinoembryonic antigen and glucose levels, using a carcinoembryonic antigen cut-off suggestive of serous cystic neoplasms

Glucose levelsCEA levels	< 50 mg/dL	≥ 50 mg/dL	Total
≥ 5 ng/mL	55	9	64[a]
< 5 ng/mL	3	48	51
Total	58	57	115

CEA: Carcinoembryonic antigen;
[a]$P < 0.0001$.

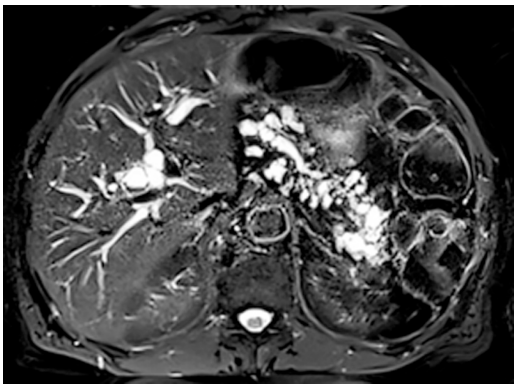

Figure 3 Mixed-intraductal papillary mucinous neoplasms. The main pancreatic duct is markedly dilated in the pancreatic head with multiple dilated side branches throughout the pancreas.

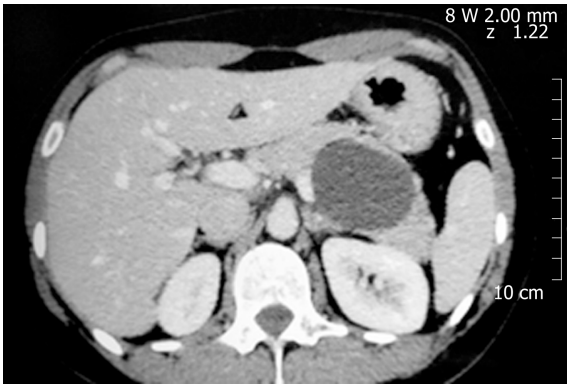

Figure 4 Mucinous cystic neoplasm. An unilocular cyst with thin walls and homogeneous content on computed tomography in the pancreatic body.

REFERENCES

1 **de Jong K**, Nio CY, Hermans JJ, Dijkgraaf MG, Gouma DJ, van Eijck CH, van Heel E, Klass G, Fockens

P, Bruno MJ. High prevalence of pancreatic cysts detected by screening magnetic resonance imaging examinations. *Clin Gastroenterol Hepatol* 2010; **8**: 806-811 [PMID: 20621679 DOI: 10.1016/j.cgh.2010.05.017]

2 **Zhang XM**, Mitchell DG, Dohke M, Holland GA, Parker L. Pancreatic cysts: Depiction on single-shot fast spin-echo MR images. *Radiology* 2002; **223**: 547-553 [PMID: 11997566 DOI: 10.1148/radiol.2232010815]

3 **Allen PJ**, D'Angelica M, Gonen M, Jaques DP, Coit DG, Jarnagin WR, DeMatteo R, Fong Y, Blumgart LH, Brennan MF. A selective approach to the resection of cystic lesions of the pancreas: Results from 539 consecutive patients. *Ann Surg* 2006; **244**: 572-582 [PMID: 16998366 DOI: 10.1097/01.sla.0000237652.84466.54]

4 **Fernández-del Castillo C**, Targarona J, Thayer SP, Rattner DW, Brugge WR, Warshaw AL. Incidental pancreatic cysts: Clinicopathologic characteristics and comparison with symptomatic patients. *Arch Surg* 2003; **138**: 427-3; discussion 433-4 [PMID: 12686529 DOI: 10.1001/archsurg.138.4.427]

5 **Kimura W**, Nagai H, Kuroda A, Muto T, Esaki Y. Analysis of small cystic lesions of the pancreas. *Int J Pancreatol* 1995; **18**: 197-206 [PMID: 8708390]

6 European Study Group on Cystic Tumours of the Pancreas. European evidence-based guidelines on pancreatic cystic neoplasms. *Gut* 2018; **67**: 789-804 [PMID: 29574408 DOI: 10.1136/gutjnl-2018-316027]

7 **Ardengh JC**, Lopes CV, de Lima-Filho ER, Kemp R, Dos Santos JS. Impact of endoscopic ultrasound-guided fine-needle aspiration on incidental pancreatic cysts. A prospective study. *Scand J Gastroenterol* 2014; **49**: 114-120 [PMID: 24188361 DOI: 10.3109/00365521.2013.854830]

8 **Tanaka M**, Fernández-del Castillo C, Adsay V, Chari S, Falconi M, Jang JY, Kimura W, Levy P, Pitman MB, Schmidt CM, Shimizu M, Wolfgang CL, Yamaguchi K, Yamao K; International Association of Pancreatology. International consensus guidelines 2012 for the management of IPMN and MCN of the pancreas. *Pancreatology* 2012; **12**: 183-197 [PMID: 22687371 DOI: 10.1016/j.pan.2012.04.004]

9 **Fernández-Esparrach G**, Ginès A. The problem of an incidental uniloculated cyst. *Minerva Med* 2014; **105**: 437-445 [PMID: 24867189]

10 **Park WG**, Wu M, Bowen R, Zheng M, Fitch WL, Pai RK, Wodziak D, Visser BC, Poultsides GA, Norton JA, Banerjee S, Chen AM, Friedland S, Scott BA, Pasricha PJ, Lowe AW, Peltz G. Metabolomic-derived novel cyst fluid biomarkers for pancreatic cysts: Glucose and kynurenine. *Gastrointest Endosc* 2013; **78**: 295-302.e2 [PMID: 23566642 DOI: 10.1016/j.gie.2013.02.037]

11 **Zikos T**, Pham K, Bowen R, Chen AM, Banerjee S, Friedland S, Dua MM, Norton JA, Poultsides GA, Visser BC, Park WG. Cyst Fluid Glucose is Rapidly Feasible and Accurate in Diagnosing Mucinous Pancreatic Cysts. *Am J Gastroenterol* 2015; **110**: 909-914 [PMID: 25986360 DOI: 10.1038/ajg.2015.148]

12 **Carr RA**, Yip-Schneider MT, Simpson RE, Dolejs S, Schneider JG, Wu H, Ceppa EP, Park W, Schmidt CM. Pancreatic cyst fluid glucose: Rapid, inexpensive, and accurate diagnosis of mucinous pancreatic cysts. *Surgery* 2018; **163**: 600-605 [PMID: 29241991 DOI: 10.1016/j.surg.2017.09.051]

13 **Jeffrey RB**. Imaging Pancreatic Cysts with CT and MRI. *Dig Dis Sci* 2017; **62**: 1787-1795 [PMID: 28220262 DOI: 10.1007/s10620-017-4501-6]

14 **Nougaret S**, Mannelli L, Pierredon MA, Schembri V, Guiu B. Cystic pancreatic lesions: From increased diagnosis rate to new dilemmas. *Diagn Interv Imaging* 2016; **97**: 1275-1285 [PMID: 27840080 DOI: 10.1016/j.diii.2016.08.017]

15 **Kadiyala V**, Lee LS. Endosonography in the diagnosis and management of pancreatic cysts. *World J Gastrointest Endosc* 2015; **7**: 213-223 [PMID: 25789091 DOI: 10.4253/wjge.v7.i3.213]

16 **Sahani DV**, Kambadakone A, Macari M, Takahashi N, Chari S, Fernandez-del Castillo C. Diagnosis and management of cystic pancreatic lesions. *AJR Am J Roentgenol* 2013; **200**: 343-354 [PMID: 23345356 DOI: 10.2214/AJR.12.8862]

17 **Sainani NI**, Saokar A, Deshpande V, Fernández-del Castillo C, Hahn P, Sahani DV. Comparative performance of MDCT and MRI with MR cholangiopancreatography in characterizing small pancreatic cysts. *AJR Am J Roentgenol* 2009; **193**: 722-731 [PMID: 19696285 DOI: 10.2214/AJR.08.1253]

18 **Visser BC**, Yeh BM, Qayyum A, Way LW, McCulloch CE, Coakley FV. Characterization of cystic pancreatic masses: Relative accuracy of CT and MRI. *AJR Am J Roentgenol* 2007; **189**: 648-656 [PMID: 17715113 DOI: 10.2214/AJR.07.2365]

19 **Ahmad NA**, Kochman ML, Brensinger C, Brugge WR, Faigel DO, Gress FG, Kimmey MB, Nickl NJ, Savides TJ, Wallace MB, Wiersema MJ, Ginsberg GG. Interobserver agreement among endosonographers for the diagnosis of neoplastic versus non-neoplastic pancreatic cystic lesions. *Gastrointest Endosc* 2003; **58**: 59-64 [PMID: 12838222 DOI: 10.1067/mge.2003.298]

20 **Wang QX**, Xiao J, Orange M, Zhang H, Zhu YQ. EUS-Guided FNA for Diagnosis of Pancreatic Cystic Lesions: A Meta-Analysis. *Cell Physiol Biochem* 2015; **36**: 1197-1209 [PMID: 26138881 DOI: 10.1159/000430290]

21 **Thornton GD**, McPhail MJ, Nayagam S, Hewitt MJ, Vlavianos P, Monahan KJ. Endoscopic ultrasound guided fine needle aspiration for the diagnosis of pancreatic cystic neoplasms: A meta-analysis. *Pancreatology* 2013; **13**: 48-57 [PMID: 23395570 DOI: 10.1016/j.pan.2012.11.313]

22 **Brugge WR**, Lewandrowski K, Lee-Lewandrowski E, Centeno BA, Szydlo T, Regan S, del Castillo CF, Warshaw AL. Diagnosis of pancreatic cystic neoplasms: A report of the cooperative pancreatic cyst study. *Gastroenterology* 2004; **126**: 1330-1336 [PMID: 15131794 DOI: 10.1053/j.gastro.2004.02.013]

23 **Gaddam S**, Ge PS, Keach JW, Mullady D, Fukami N, Edmundowicz SA, Azar RR, Shah RJ, Murad FM, Kushnir VM, Watson RR, Ghassemi KF, Sedarat A, Komanduri S, Jaiyeola DM, Brauer BC, Yen RD, Amateau SK, Hosford L, Hollander T, Donahue TR, Schulick RD, Edil BH, McCarter M, Gajdos C, Attwell A, Muthusamy VR, Early DS, Wani S. Suboptimal accuracy of carcinoembryonic antigen in differentiation of mucinous and nonmucinous pancreatic cysts: Results of a large multicenter study. *Gastrointest Endosc* 2015; **82**: 1060-1069 [PMID: 26077458 DOI: 10.1016/j.gie.2015.04.040]

24 **Park WG**, Mascarenhas R, Palaez-Luna M, Smyrk TC, O'Kane D, Clain JE, Levy MJ, Pearson RK, Petersen BT, Topazian MD, Vege SS, Chari ST. Diagnostic performance of cyst fluid carcinoembryonic antigen and amylase in histologically confirmed pancreatic cysts. *Pancreas* 2011; **40**: 42-45 [PMID: 20966811 DOI: 10.1097/MPA.0b013e3181f69f36]

25 **Linder JD**, Geenen JE, Catalano MF. Cyst fluid analysis obtained by EUS-guided FNA in the evaluation of discrete cystic neoplasms of the pancreas: A prospective single-center experience. *Gastrointest Endosc* 2006; **64**: 697-702 [PMID: 17055859 DOI: 10.1016/j.gie.2006.01.070]

26 **van der Waaij LA**, van Dullemen HM, Porte RJ. Cyst fluid analysis in the differential diagnosis of pancreatic cystic lesions: A pooled analysis. *Gastrointest Endosc* 2005; **62**: 383-389 [PMID: 16111956 DOI: 10.1016/S0016-5107(05)01581-6]

27 **Frossard JL**, Amouyal P, Amouyal G, Palazzo L, Amaris J, Soldan M, Giostra E, Spahr L, Hadengue A, Fabre M. Performance of endosonography-guided fine needle aspiration and biopsy in the diagnosis of pancreatic cystic lesions. *Am J Gastroenterol* 2003; **98**: 1516-1524 [PMID: 12873573 DOI: 10.1111/j.1572-0241.2003.07530.x]

28 **Oh SH**, Lee JK, Lee KT, Lee KH, Woo YS, Noh DH. The Combination of Cyst Fluid Carcinoembryonic Antigen, Cytology and Viscosity Increases the Diagnostic Accuracy of Mucinous Pancreatic Cysts. *Gut Liver* 2017; **11**: 283-289 [PMID: 27609484 DOI: 10.5009/gnl15650]

29 **Yoon WJ**, Daglilar ES, Mino-Kenudson M, Morales-Oyarvide V, Pitman MB, Brugge WR. Characterization of epithelial subtypes of intraductal papillary mucinous neoplasm of the pancreas with endoscopic ultrasound and cyst fluid analysis. *Endoscopy* 2014; **46**: 1071-1077 [PMID: 25208034 DOI: 10.1055/s-0034-1377629]

30 **Ngamruengphong S**, Bartel MJ, Raimondo M. Cyst carcinoembryonic antigen in differentiating pancreatic cysts: A meta-analysis. *Dig Liver Dis* 2013; **45**: 920-926 [PMID: 23790480 DOI: 10.1016/j.dld.2013.05.002]

31 **Cizginer S**, Turner BG, Bilge AR, Karaca C, Pitman MB, Brugge WR. Cyst fluid carcinoembryonic antigen is an accurate diagnostic marker of pancreatic mucinous cysts. *Pancreas* 2011; **40**: 1024-1028 [PMID: 21775920 DOI: 10.1097/MPA.0b013e31821bd62f]

32 **Boot C**. A review of pancreatic cyst fluid analysis in the differential diagnosis of pancreatic cyst lesions. *Ann Clin Biochem* 2014; **51**: 151-166 [PMID: 24097809 DOI: 10.1177/0004563213503819]

33 **Guo X**, Zhan X, Li Z. Molecular Analyses of Aspirated Cystic Fluid for the Differential Diagnosis of Cystic Lesions of the Pancreas: A Systematic Review and Meta-Analysis. *Gastroenterol Res Pract* 2016; **2016**: 3546085 [PMID: 26819604 DOI: 10.1155/2016/3546085]

34 **Lee JH**, Kim Y, Choi JW, Kim YS. KRAS, GNAS, and RNF43 mutations in intraductal papillary mucinous neoplasm of the pancreas: A meta-analysis. *Springerplus* 2016; **5**: 1172 [PMID: 27512631 DOI: 10.1186/s40064-016-2847-4]

35 **Springer S**, Wang Y, Dal Molin M, Masica DL, Jiao Y, Kinde I, Blackford A, Raman SP, Wolfgang CL, Tomita T, Niknafs N, Douville C, Ptak J, Dobbyn L, Allen PJ, Klimstra DS, Schattner MA, Schmidt CM, Yip-Schneider M, Cummings OW, Brand RE, Zeh HJ, Singhi AD, Scarpa A, Salvia R, Malleo G, Zamboni G, Falconi M, Jang JY, Kim SW, Kwon W, Hong SM, Song KB, Kim SC, Swan N, Murphy J, Geoghegan J, Brugge W, Fernandez-Del Castillo C, Mino-Kenudson M, Schulick R, Edil BH, Adsay V, Paulino J, van Hooft J, Yachida S, Nara S, Hiraoka N, Yamao K, Hijioka S, van der Merwe S, Goggins M, Canto MI, Ahuja N, Hirose K, Makary M, Weiss MJ, Cameron J, Pittman M, Eshleman JR, Diaz LA, Papadopoulos N, Kinzler KW, Karchin R, Hruban RH, Vogelstein B, Lennon AM. A combination of molecular markers and clinical features improve the classification of pancreatic cysts. *Gastroenterology* 2015; **149**: 1501-1510 [PMID: 26253305 DOI: 10.1053/j.gastro.2015.07.041]

World Journal of Gastroenterology

Submit a Manuscript: https://www.f6publishing.com

World J Gastroenterol 2019 May 21; 25(19): 2279-2293

DOI: 10.3748/wjg.v25.i19.2279

ISSN 1007-9327 (print) ISSN 2219-2840 (online)

REVIEW

Mechanisms of hepatocellular carcinoma progression

Olorunseun O Ogunwobi, Trisheena Harricharran, Jeannette Huaman, Anna Galuza, Oluwatoyin Odumuwagun, Yin Tan, Grace X Ma, Minhhuyen T Nguyen

ORCID number: Olorunseun O Ogunwobi (0000-0003-3388-2137); Trisheena Harricharran (0000-0002-6300-3247); Jeannette Huaman (0000-0002-7832-6903); Anna Galuza (0000-0002-5401-5158); Oluwatoyin Odumuwagun (0000-0002-0776-3444); Yin Tan (0000-0001-6280-6403); Grace Ma (0000-0002-3619-0550); Minhhuyen T Nguyen (0000-0002-2112-282X).

Author contributions: All authors contributed intellectually to this manuscript. Ogunwobi OO conceived, designed, revised, edited, and approved the final version of the manuscript.

Conflict-of-interest statement: Ogunwobi OO, Tan Y and Ma GX are supported by the National Cancer Institute grant number U54 CA221704(5). Ogunwobi OO is a Co-Founder of NucleoBio, Inc, a City University of New York biotechnology start-up company.

Manuscript source: Invited manuscript

Olorunseun O Ogunwobi, Trisheena Harricharran, Jeannette Huaman, Anna Galuza, Oluwatoyin Odumuwagun, Department of Biological Sciences, Hunter College of The City University of New York, New York, NY 10065, United States

Olorunseun O Ogunwobi, Trisheena Harricharran, Jeannette Huaman, The Graduate Center Departments of Biology and Biochemistry, The City University of New York, New York, NY 10016, United States

Olorunseun O Ogunwobi, Trisheena Harricharran, Joan and Sanford I. Weill Department of Medicine, Weill Cornell Medicine, Cornell University, New York, NY 10065, United States

Olorunseun O Ogunwobi, Trisheena Harricharran, Jeannette Huaman, Anna Galuza, Oluwatoyin Odumuwagun, Hunter College Center for Cancer Health Disparities Research (CCHDR), New York, NY 10065, United States

Yin Tan, Grace X Ma, Center for Asian Health, School of Medicine, Temple University, Philadelphia, PA 19140, United States

Minhhuyen T Nguyen, Department of Medicine, Fox Chase Cancer Center, Philadelphia, PA 19111, United States

Corresponding author: Olorunseun O Ogunwobi, MBBS, MSc, PhD, Associate Professor, Department of Biological Sciences, Hunter College of The City University of New York, 695 Park Ave, New York, NY 10065, United States. ogunwobi@genectr.hunter.cuny.edu
Telephone: +1-212-896-0447

Abstract

Hepatocellular carcinoma (HCC) is the most common primary malignancy of the liver. It is the second leading cause of cancer-related deaths worldwide, with a very poor prognosis. In the United States, there has been only minimal improvement in the prognosis for HCC patients over the past 15 years. Details of the molecular mechanisms and other mechanisms of HCC progression remain unclear. Consequently, there is an urgent need for better understanding of these mechanisms. HCC is often diagnosed at advanced stages, and most patients will therefore need systemic therapy, with sorafenib being the most common at the present time. However, sorafenib therapy only minimally enhances patient survival. This review provides a summary of some of the known mechanisms that either cause HCC or contribute to its progression. Included in this review are the roles of viral hepatitis, non-viral hepatitis, chronic alcohol intake, genetic predisposition and congenital abnormalities, toxic exposures, and autoimmune diseases of the liver. Well-established molecular mechanisms of HCC progression such as epithelial-mesenchymal transition, tumor-stromal interactions and the

Received: March 8, 2019
Peer-review started: March 8, 2019
First decision: March 20, 2019
Revised: March 27, 2019
Accepted: April 10, 2019
Article in press: April 10, 2019
Published online: May 21, 2019

P-Reviewer: Guo K, Huang YQ, Sun XY
S-Editor: Ma RY
L-Editor: Filipodia
E-Editor: Ma YJ

tumor microenvironment, cancer stem cells, and senescence bypass are also discussed. Additionally, we discuss the roles of circulating tumor cells, immunomodulation, and neural regulation as potential new mechanisms of HCC progression. A better understanding of these mechanisms could have implications for the development of novel and more effective therapeutic and prognostic strategies, which are critically needed.

Key words: Hepatocellular carcinoma; Viral/non-viral hepatitis; Alcohol consumption; Epithelial-mesenchymal transition; Tumor-stromal interactions; Tumor microenvironment; Cancer stem cells; Circulating tumor cells; Immunomodulation; Neural regulation

Core tip: The overall prognosis for hepatocellular carcinoma patients remains poor, as there has only been minimal improvement over the past 15 years. Details of the mechanisms of hepatocellular carcinoma progression remain unclear. This review discusses a summary of both well-established and newly proposed mechanisms of hepatocellular carcinoma progression. A better understanding of these mechanisms is critical to the development of novel and more effective therapeutic strategies likely to improve hepatocellular carcinoma patient outcomes.

Citation: Ogunwobi OO, Harricharran T, Huaman J, Galuza A, Odumuwagun O, Tan Y, Ma GX, Nguyen MT. Mechanisms of hepatocellular carcinoma progression. *World J Gastroenterol* 2019; 25(19): 2279-2293
URL: https://www.wjgnet.com/1007-9327/full/v25/i19/2279.htm
DOI: https://dx.doi.org/10.3748/wjg.v25.i19.2279

INTRODUCTION

Hepatocellular carcinoma (HCC) is the most common primary liver cancer comprising 75%-85% of cases of liver cancer[1]. It is the sixth most common cancer and the second leading cause of cancer deaths worldwide[1]. The incidence of HCC in the United States has been increasing over the past two decades[1-3]. While the overall prognosis for HCC patients in the United States has improved somewhat in the past 15 years, it still remains poor. In fact, in the United States, the 2-year survival for HCC is less than 50% and 5-year survival is only 10%[4].

In Asia, chronic hepatitis B virus (HBV) infection is the primary cause of HCC. While in the Western world, chronic hepatitis C virus (HCV), alcoholic cirrhosis and non-alcoholic steatohepatitis (NASH) are the main causes[5]. Other known risk factors of HCC include heavy alcohol consumption, nonalcoholic fatty liver disease, consumption of aflatoxins, obesity, type 2 diabetes and tobacco smoking[6,7].

Early diagnosis and effective treatment of HCC remain a challenge. While some patients can be symptomatic, including symptoms such as right upper abdominal quadrant pain, anorexia, early satiety, weight loss, obstructive jaundice, fever, watery diarrhea, lethargy, and bone pain (from metastases)[6,7], most patients remain asymptomatic, and clinical presentation occurs at advanced stages of the disease.

If detected very early, HCC can actually be cured with an excellent long-term prognosis[7], where the principal treatment options would be surgical resection or liver transplantation if the patient is a suitable transplant candidate[8]. However, for the vast majority of HCC patients, their cancer is detected at an advanced stage where surgical cure is no longer an option[7]. Most patients will therefore need chemotherapy, which works by destroying cancer cells and inhibiting the proliferation of new cancer cells *via* the use of chemical agents. Sorafenib, a small multi-tyrosine kinase inhibitor that blocks Raf kinase, vascular endothelial growth factor (VEGF), and platelet-derived growth factor (PDGF) receptor activities, is the most commonly used chemotherapeutic agent to treat HCC[4]. Although a targeted chemotherapeutic agent, its use has been shown to minimally enhance patient survival[9] by only about 7-10 months[10]. Other drugs such as sunitinib, brivanib, and other angiogenic inhibitors are currently still under development and hold promise in targeting the extensive angiogenic network that is present in the liver[11,12]. Additional

multi-kinase inhibitors recently approved for HCC treatment include regorafenib (for secondary treatment after sorafenib), as well as levatinib (another first-line drug to treat HCC besides sorafenib). However, neither provide much more additional benefit than sorafenib treatment[13,14]. As such, better treatment options are still needed.

To address this unmet need, researchers are trying to identify different mechanisms that may be involved in HCC progression to find alternative therapeutic strategies[8]. There have been various signaling pathways and molecules implicated in HCC progression. Some of these will be discussed in this review article and are summarized in Figure 1.

MECHANISMS OF ETIOLOGY

Several risk factors have been implicated in the development and progression of HCC, notably chronic viral hepatitis, non-viral hepatitis, chronic alcohol intake, certain disease states (obesity and diabetes), and consumption of toxin-contaminated staples[15]. The epidemiologic distribution of these risk factors varies according to geographic location and host-specific factors.

Viral hepatitis

HBV and HCV are major causes of viral hepatitis that lead to the development of cirrhosis and HCC. The pathogenesis of HBV-induced HCC is thought to involve several mechanisms, including HBV-DNA integration into host genetic machinery, DNA methylation, oxidative stress, and HBx protein[16]. The risk of developing HCC has been shown to be proportional to HBV-DNA level in liver cells. HBV gains entry into liver cells through a receptor mediated pathway. Chronic illness results from persistence of the virus in the host cells *via* various mechanisms that include infection of immune defense control centers, viral inhibition of antigen presentation, selective immune suppression, down-regulation of viral gene expression, and viral mutations that functionally incapacitate virus-specific T cells from recognizing HBV antigen[17]. Immune response and inflammatory reactions induce cytokine and chemokine mobilization, causing oxidative stress. This, in turn, promotes constant activation of several genes that cause cirrhosis, including TERT, MLL4, RARβ, CCNE1, Cyclin A2, FN1, ROCK1, SENP5, ANGPT1, PDGF receptor, calcium signaling-related genes, ribosomal protein genes, epidermal growth factor receptor (commonly known as EGFR), and mevalonate kinase carboxypeptidase[15].

HBV and HCV viral proteins may be involved in hijacking the cellular machinery. Viral attack can also directly cause cirrhotic tissue development through the release of proinflammatory cytokines (*e.g.*, interleukin (IL)6, tumor necrosis factor (TNF)-α, IL1 and IL18)[18].

HCV hijacks host cellular machinery to increase cellular proliferation, steatosis, inflammatory processes, mitochondrial dysfunction, insulin resistance, all leading to oxidative stress, genetic instability and DNA damage with cirrhosis and HCC as a likely outcome[19].

HCC risk drastically increases at the cirrhotic liver stage, suggesting a close association.

The corresponding interplay of inflammatory responses, gene activation, and viral clearance suppression creates a conditioned environment that promotes cellular mutations leading to HCC.

Non-viral hepatitis

Even though viral hepatitis from HBV and HCV are strongly associated with liver cancer, there are non-viral risk factors that can induce the development of HCC[20]. Diabetes mellitus, alcohol abuse, cardiovascular disease, liver inflammation, obesity, dyslipidemia and non-alcoholic fatty liver disease (NAFLD) are some other major contributors to HCC development.

Accumulation of iron in the liver of NASH and HCC patients[21,22] is correlated with progression of fibrosis and HCC[23]. In this context, a possible tumor biomarker may be serum ferritin rather than iron. However, because there is no exact correlation between iron inside the liver and iron in the blood, it is difficult to clarify the pathological features of ferritin on the poor prognosis of non-viral HCC (nvHCC)[24]. Results of a cohort study of 93 patients with nvHCC, 62 of whom had alcohol abuse problems, showed an increase in ferritin level in non-diabetics[24]. However, further research needs to be done to assess the correlation between the impacts of alcohol and ferritin on NAFLD[24].

On the other hand, HCC is associated with obesity. Obesity impairs metabolism, induces inflammation and is an etiological factor for NAFLD, steatosis, NASH, hepatic fibrosis, cirrhosis, and ultimately HCC. Caused partly by a sedentary lifestyle

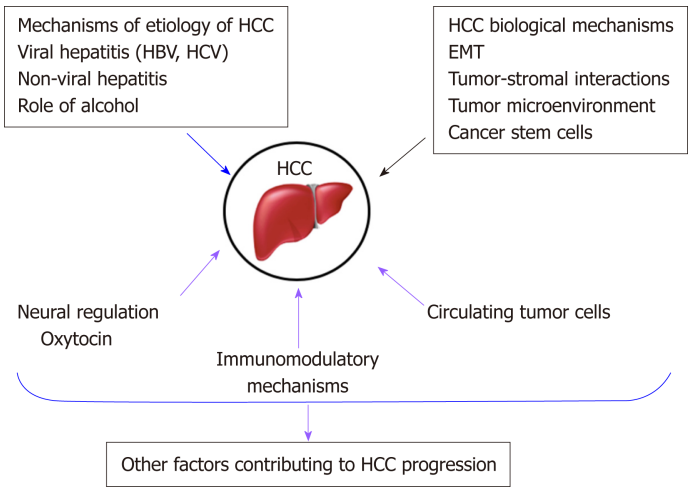

Figure 1 Summary of the HCC progression mechanisms discussed in this review. HCC: Hepatocellular carcinoma; HBV: Hepatitis B virus; HCV: Hepatitis C virus.

and obesity, impaired lipid metabolism and deregulation of energy equilibrium in the liver contributes to the correlation between type 2 diabetes and NAFLD. In fact, several studies have shown that high BMI, waist circumference, and type II diabetes mellitus are associated with higher risks of liver cancer[25,26]. They have also suggested that the association may vary depending on the status of viral hepatitis infection[25]. Conversely, NAFLD provides the metabolic environment to induce insulin resistance[27], a known etiological factor for HCC.

Role of alcohol

Chronic alcohol intake is detrimental to our health. It leads to liver cirrhosis, and subsequently HCC. Alcoholic liver disease is one of the leading causes of HCC[28]. According to case studies from all over the world, alcohol abuse is related to up to 2-fold increased risk of HCC[29]. Moreover, studies performed on mice fed an alcohol diet have shown exacerbation of inflammation, epithelial-mesenchymal transition (EMT) and fibrosis, and consequent progression to HCC[28].

Pure ethanol does not directly cause inflammation and liver damage, however, toxic by-products of alcohol catabolism such as accumulation of acetaldehyde and free radicals can influence oxidative stress, apoptotic cell death, necrosis and necroptosis[29]. Reactive oxygen species (ROS) generation is the result of increased inflammatory cytokine secretion caused by constant inflammatory pathways[19]. ROS-induced DNA damage, genomic vulnerability of hepatocytes and T-lymphocyte suppression contribute to HCC development[19].

Also, alcohol catabolism impacts several steps of lipid metabolism, which leads to liver steatosis and inhibition of fatty acid oxidation[29].

Reversibility of gene expression *via* epigenetic alteration is an important biological phenomenon that often plays a role in tumorigenesis. Epigenetic mechanisms affected by excessive alcohol consumption lead to altered DNA methylation and acetylation. For instance, altered acetylation is associated with hepatic steatosis alcohol-induced HCC[29]. Overexpression of *c-Met* and hepatocyte growth factor is directly associated with promoter hypomethylation in circulating tumor cells (CTCs) of HCC in a syngeneic BALB/c mouse tumor model[30].

Moreover, alcohol abuse is associated with HCC *via* impaired metabolism, such as accumulation of acetaldehyde, hypomethylation, lack of antioxidants and retinoic acid, together with inflammation, oxidative stress, hypoxia and genetic instability[28].

Other mechanisms of progression to cirrhosis and HCC

In addition to the role of viral hepatitis and alcohol in the development of HCC, other possible risk factors include genetic predisposition and congenital abnormalities, toxic exposures (aflatoxin or arsenic contaminated food), and autoimmune diseases of the liver.

Several congenital abnormalities have been shown to predispose patients to liver cirrhosis and HCC. These include hereditary tyrosinemia, Wilson's disease, alpha-1-antitrypsin deficiency, and hemochromatosis[31].

The pathogenesis of aflatoxin B1 (AFB1) - induced HCC includes several mechanisms, including the formation of mutagenic and carcinogenic intermediates and adducts. Aflatoxins are released from food contaminated by the fungi, *Aspergillus*

flavus and *Aspergillus parasiticus*. A series of chemical transformations occur that result in the conversion of AFB1 to established mutagenic or carcinogenic compounds: aflatoxin-B1 → aflatoxin B1-8,9 exo-epoxide → 8,9-dihydroxy-8-(N7) guanyl-9-hydroxy aflatoxin B1 adduct → aflatoxin B1 formaminopyrimidine adduct. These adducts and intermediates can also directly induce a mutation at codon 249 of the p53 tumor suppressor gene. This replaces arginine with serine, a change that reverses the tumor suppressing ability of the gene. There are reports that suggest that AFB1 acts synergistically[32] with HBV to induce HCC. Additive interactions have also been reported[33].

In a systematic review, Tansel *et al*[34] demonstrated a relationship between increased risk of developing HCC in patients with liver cirrhosis as a result of autoimmune hepatitis (AIH). The risk of liver cirrhosis from AIH was found to be lower than that of liver cirrhosis secondary to HBV and HCV infection or primary biliary cholangitis. Nevertheless, the risk of liver cirrhosis and HCC from AIH is clinically significant.

ESTABLISHED BIOLOGICAL MECHANISMS OF HCC PROGRESSION

There are several established biological mechanisms involved in the progression of HCC. These include EMT, tumor-stromal interactions, tumor microenvironment, cancer stem cells, and dysregulation of microRNAs and well-known signaling pathways[35,36]. Some of these are discussed below.

EMT

EMT is a biological process that occurs normally during development and wound healing, but is hijacked by cancer cells. During this process, epithelial cells, which are normally attached to a basement membrane and closely adhered to one another, lose their cell adhesive properties and become migratory in nature[37-39]. This endowed mesenchymal behavior permits the successful migration of cells, which if usurped by cancer cells, can promote their dissemination and spread throughout the body.

EMT has been recognized by many in the field to be important for cancer progression[40,41]. In HCC, there have been several reports of EMT effectors such as cadherins, fibronectin, vimentin, and integrins, being altered to permit a more mesenchymal phenotype. Furthermore, transcription factors promoting EMT, including Snail, Slug, Twist and Zeb, are also upregulated during HCC progression[42,43]. Additionally, there have been a number of studies on exosomes, microRNAs, long noncoding RNAs, and regulatory signaling pathways that have been associated with EMT and demonstrate consequences in HCC progression[30,41,44-49]. This is indicative of the important role that EMT plays in HCC progression. The molecular mechanisms of EMT may have diagnostic, prognostic, and therapeutic implications in HCC.

Tumor-stromal interactions and role of the tumor microenvironment

Metastasis is the most common cause of cancer-related deaths[30,50]. Worldwide, HCC is a leading cause of death from cancer[51]. However, the molecular mechanisms of HCC and metastasis are still being clarified[50].

Tumor development and malignant progression can be promoted by a constantly changing extracellular environment that is impacted by microenvironmental stimuli, immune cell cooperation, and inflammatory signals. There is communication between hepatic tumor cells and non-tumor stroma. The non-tumor stroma consists of components of the extracellular matrix (ECM) such as non-malignant fibroblasts, immune and endothelial cells, collectively known as the peri-tumoral microenvironment[52]. Major alterations to the hepatic microenvironment and cells in chronic liver disease influence cancer development[53]. For example, a hypoxic microenvironment in primary HCC is strongly associated with progression and angiogenesis. The consequent enhanced blood supply in the tumor mediates growth formation and metastasis[54].

According to previous studies, tumor cells cross-talk with the abnormal microenvironment, ECM, inflammatory cytokines, chemokines and upregulated growth factors, contributing to increased angiogenesis[55,56]. Although the molecular mechanisms of tumor-stromal interactions are still being clarified, existing evidence show an accumulation of hepatic stellate cells (HSCs), triggered by hypoxia-induced platelet-derived growth factor-BB (PDGF-BB), and proliferation in the tumor stroma, as well as an increase in VEGF-A expression in HSCs leads to HCC angiogenesis[54].

Interactions between normal tumor-suppressive microenvironment and hepatic

stellate cells and normal liver fibroblasts have been reported[53]. One of the major factors in liver fibrosis and cirrhosis is activated HSCs[53]. The important paracrine interactions between activated HSCs and hepatocytes impact HCC proliferation and metastasis[57-59]. HSCs (also known as peri-sinusoidal cells), one of the components of the cellular tumor microenvironment in HCC, are responsible for collagen synthesis in the liver[51]. As liver damage occurs, activated HSCs accumulate in the ECM and induce hepatic fibrosis and hepatocarcinogenesis[51].

The exact molecular mechanisms of interactions between non-tumor stromal constituents (specifically macrophages) and hepatic cancer cells are unclear. Studies in mice have shown induced macrophage infiltration of alternatively activated phenotype M2 pro-tumor monocyte-derived macrophages into tumors developed in the chronically damaged livers of mice injected with carbon tetrachloride (CCl_4) for 7 weeks[52]. Therefore, an inflamed liver background is favorably associated with increased cancer development[52].

Cancer stem cells in HCC

Liver lineage studies have uncovered four maturational levels of cells that allow the liver to strike a perfect balance between cell gain and cell loss. These include mature hepatocytes, oval cells, bone marrow cells and hepato-pancreas stem cells[60]. These different levels of stem cells integrate to respond to loss of liver cells in the body in several ways, and are thus implicated in liver cirrhosis and HCC.

The cancer stem cell (CSC) theory has been proposed as an explanatory mechanism of HCC metastasis, progression and aggressiveness. CSCs, like regular stem cells, have self-renewing features and are capable of differentiating into tumor cells of varying phenotypes and through several pathways, partly accounting for the heterogeneous clinical presentation of HCC[61]. Previous research has successfully demonstrated that liver cells are directly involved in hepatocarcinogenesis[62], and transformation of these cells may give rise to CSCs. Some reports also suggest that cancer cells in HCC develop from dedifferentiation of mature hepatocytes rather than from uncontrolled proliferation of liver stem cells[63], with intrinsic factors (genetics, autoimmune diseases) contributing, and extrinsic factors (HBV, HCV, alcohol, AFB1) accounting for 70%-90% of the transformation of small hepatocyte-like progenitor cells to cancer cells of HCC[64]. Nevertheless, the correlation between stem-cell division and cancer risk cannot distinguish the effect of intrinsic factors from that of extrinsic factors.

Stem cells originating from the bone marrow, known as bone marrow-derived stem cells, have been demonstrated to be involved in the progression of HCC. Yavorkovsky *et al*[65] observed the biomarkers when liver trauma simulating HCC was induced with allyl alcohol and demonstrated that only bone marrow-derived stem cells were activated to respond to the trauma.

Stem cells originating from the canal of Hering (oval cells) are mobilized in chronic liver injury[66]. Oval cell biomarkers include γ-glutamyl transpeptidase, glutathione-S-transferase, OV6, α-fetoprotein, neural cell adhesion molecule 1, and chromogranin A[67]. The normal compensatory mechanisms that mobilize stem cells during liver injury are altered in HCC in such a way that promotes progression of the carcinogenic process.

Various models are being used to explain cancer development and intra-tumoral heterogeneity in HCC. These include CSCs, cancer cell plasticity and the clonal evolution model, to mention a few[68]. While the majority of heterogeneous tumor cells stay inactive[69], a small subgroup comprised of CSCs and cancer initiating cells, facilitate tumor development and growth[70-72]. Phenotypic plasticity of cancer cells, which allows conversion from cancer stem cell to non-CSC and vice versa, is one of the proposed mechanisms that may be responsible for the intra-tumoral heterogeneity found in solid tumors[73]. According to previous studies, underlying molecular mechanisms of EMT and CSCs were found to be associated with a high risk for poor prognosis of cancer patients[68].

During normal development, EMT plays a crucial role in organogenesis[74]. At the time of early embryogenesis, through EMT, cell-cell adhesive epithelial cells undergo trans-differentiation and become mobile mesenchymal cells that can migrate, and invade into neighboring tissues and have increased resistance to apoptosis[73-75]. On the other hand, mesenchymal cells can transform back to epithelial cells *via* the process of mesenchymal-to-epithelial transition, or MET. These reprogramming processes emphasize the epithelial cell plasticity[73] facilitating metastasis to distant and local anatomical sites *via* increased invasive and migratory functions[68,73,74].

The CSC hypothesis in cancer remains controversial. While some studies have demonstrated the CSC hypothesis in brain, skin, and colon cancers, others have suggested that tumor-initiating cells (TICs, CSC-like cells) exist instead of CSCs in other cancer types[69,76]. Some studies have demonstrated that HCC arises from either

TICs or hepatocytes. According to previous research based on drug-treated HCC patients, TICs are the main trigger of tumor development and progression[61]. However, the exact origin of TICs is still not completely understood.

Liver CSCs (LCSCs) have many analogous characteristics to normal liver stem/progenitor cells. In addition to self-renewal and tumorigenesis abilities, LCSCs have been implicated in therapeutic drug resistance and relapse in patients[77]. Long-term inflammatory microenvironment, caused by HBV or HCV, chronic alcohol consumption or NASH, and progression of HCC[35] highly contribute to reprogramming of non-CSC into CSCs[78] and the acquisition of CSC-like properties by non-CSCs through carcinogenic dedifferentiation[79].

Identification of tumor - specific biomarkers and discovery of molecular mechanisms are crucial to establish effective therapeutic and early detection strategies for cancer[60,80]. Through the work of several investigators, we are now familiar with some of the putative surface markers for liver CSCs, including epithelial cell adhesion molecule (EpCAM)[81], CD90[82], CD133[83], CD44[84], and CD13[85]. However, there is still uncertainty as to which cell surface markers best identify CSCs in different cancers.

Therapeutic approaches involving inhibitor targeting of signaling pathways, such as Wnt, hedgehog (Hh), TGF-β and Notch signaling, have been shown to diminish LCSC self-reprogramming, metastasis and tumor proliferation[60]. Moreover, drugs designed to modulate cross-talk between CSCs and cancer cells and the tumor microenvironment may have success in inhibiting tumor growth[60]. Other efforts to target LCSC markers and epigenetic modulators could produce promising results.

OTHER MECHANISMS OF HCC PROGRESSION

Another established mechanism of HCC progression is senescence bypass. The liver cells have powerful regenerative abilities. Progenitor cells rapidly divide to restore the balance offset by tissue loss. However, these cells reach a Hayflick limit, a point where cell division is permanently arrested after a number of divisions. The cells are said to exhibit replicative senescence. Replicative senescence can be due to (1) shortening of telomeres in the absence of telomerase, thereby halting cell division; (2) telomeric-independent oncogene activation; and (3) elevated ROS. Telomere shortening triggers the DNA damage response, which is thought to activate several signaling pathways, including the p53-p21pRB pathway, bringing replication to a halt. Non-telomeric senescence utilizes both ATM/Chk/p53 and p16-pRB pathways. Oncogene-induced senescence is closely associated with DNA hyper-replication that succeeds oncogenic activation. Several oncogenic pathways have been reported to be involved in triggering oncogene-induced senescence, including activated Ras, c-myc or Wnt/β-catenin[86,87]. Given the tumor suppressing tendency of cell senescence, bypassing it can result in the proliferation of genetically mutated cells, further DNA instability and propagation of HCC. Researchers have been exploring cell senescence induction as a potential strategy in cancer therapeutics.

Nuclear factor kappa-light-chain-enhancer of activated B cells (NF-kB) plays a critical role in how cells respond to stressful stimuli, including infections and ultraviolet radiation[88]. Inflammatory responses mediated by the NF-kB signaling pathway have been reported to be involved in perpetuating the malignant state. NF-kB activation suppresses apoptosis[89], activates EMT[90], represses maspin (a metastasis suppressor gene)[91], and targets VEGF and other angiogenic factors required in forming new blood vessels that supply HCC[90].

There has been considerable advancement in understanding the fundamental epigenetic mechanisms in gene expression, which is now allowing for the development of novel insights into chronic liver disease epigenetic control[92]. For example, loss of DNA methylation has been pointed to as potential diagnostic markers in HCC progression. Some studies have also suggested that non-coding RNAs (ncRNAs) such as microRNAs (miRNAs), small non-coding RNAs (sncRNAs), long non-coding RNAs (lncRNAs), RNA interference (RNAi), small interfering RNAs (siRNAs), and piwi-interacting RNAs (piRNAs), could serve as therapeutic strategies for HCC[93,94]. Several preclinical studies have shown that significant tumor suppression can be achieved by modulating ncRNAs[93,94].

Other interesting factors that have been shown to correlate with HCC patient prognosis are molecular stratification and mutational signatures[95,96]. There are different classes of liver cancer based on varying molecular features and cell of origin[96]. It has been shown that each stratification has a different implication on patient prognosis[95-97]. For example, proliferative subclasses result in a more aggressive phenotype and poorer patient outcomes[97].

In terms of mutational signature, there are several genetic alterations that are

promising for therapeutic interventions. For instance, approximately 15% of HCCs harbor amplifications at 11q13 and 6p21[95]. Currently, a better understanding of how molecular stratification and mutational signatures affect HCC progression is still needed before they can be used as therapeutic strategies or biomarkers in a clinical setting.

CTCs in HCC

There is increasing evidence that CTCs play an important role in HCC progression. CTCs are considered an intermediate stage of metastasis. They are cancer cells that have dissociated from the primary tumor, enter circulation, and may subsequently form metastatic lesions[98,99]. There is strong interest in studying CTC biology to understand their molecular mechanisms and how they affect metastasis. Moreover, CTCs have clinical applications, such as diagnostic applications circumventing the need for invasive tissue biopsies[100].

As illustrated in Figure 2, a considerable amount of data has been and can be gathered through the study of CTCs in HCC. Through isolation, characterization and correlation of CTCs with pathological features, as well as disease stage, researchers have shown that a greater CTC count in patient blood is associated with poorer HCC prognosis[53,101-106]. As there is a current lack of reliable biomarkers for the early, non-invasive detection of HCC, a few studies have demonstrated the potential feasibility of using CTCs as a possible diagnostic marker[104,107-110]. Although CTCs are found in very low numbers in the blood[110,111], the advent of new single-cell sequencing technologies and methods to successfully expand CTCs in long-term cultures has enabled their molecular profiling and characterization[104,110,112-115], hence making CTCs promising diagnostic biomarkers in HCC.

IMMUNOMODULATORY MECHANISMS IN HCC

Additionally, several immune mechanisms have been observed to be dysregulated during HCC progression[116]. For instance, HCC is a cancer arising against the backdrop of an inflammatory state in the liver. HBV, HCV, and many of the other etiological factors discussed earlier in this article give rise to chronic inflammation. In turn, this leads to the production of inhibitory cytokines such as IL-10 and transforming growth factor beta (TGFβ), which dampen the immune response and favor tumor growth[117-119]. During HCC progression, regulatory T cells and myeloid-derived suppressor cells are also recruited to the tumor site as a result of these cytokine secretions, adding to the already immunosuppressive environment[116,118,120]. Lastly, it has been found that several checkpoint inhibitor receptors such as CTLA4 and PD-1 are commonly upregulated in immune cells in the HCC setting. With more checkpoint inhibitor receptors being expressed on these immune cells, they are unable to become active and counterattack tumor cells for clearance from the body[119,121,122].

Ironically, a fundamental characteristic of the liver may also permit tumorigenesis. The liver is immunologically tolerant. This is because the liver is in constant contact with microbiota from the gut and therefore needs to have a tolerant immune response so that it does not become hyperactivated[116,119]. This, in conjunction with the supplementary immunosuppressive mechanisms that develop during HCC progression, enable tumors to grow. This irony makes exploration of immunotherapy for HCC a challenging but potentially exciting prospect to consider.

Indeed, several studies have shown that immune checkpoint inhibitors have had some efficacy in preclinical and early stage clinical trials of HCC. Additionally, the fact that sorafenib, the current first line treatment for advanced HCC, has been noted to exhibit some immunomodulatory effects, seems to suggest the potential efficacy of immunotherapeutic strategies in HCC[122-125].

NEURAL REGULATION OF HCC

Tumor cells and the cells in the tumor microenvironment are affected by stress physiology[126]. Neuroeffector molecules can reach the tumor microenvironment *via* the circulatory system or nerve fibers. During threatening or stressful life circumstances, there is an activation of the sympathetic nervous system, which mediates fightorflight stress responses. The hypothalamus-pituitary-adrenal axis is responsible for mediating withdrawal responses from more profound and overwhelming threats. The neurotransmitter norepinephrine is released by the sympathetic nervous system nerve fibers, while the major stress hormone cortisol is released into the blood by the adrenal gland upon hypothalamus-pituitary-adrenal

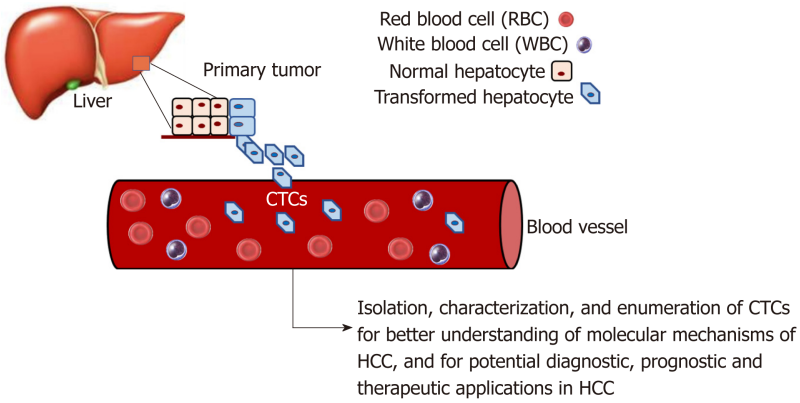

Figure 2 Use of circulating tumor cells as a non-invasive means to study HCC progression. CTCs: Circulating tumor cells; HCC: Hepatocellular carcinoma.

activation[126]. Cortisol is secreted by the adrenal glands. However, its secretion is regulated by the pituitary gland. Under conditions of severe psychological stress, corticotropin-releasing factor upregulates the secretion of adrenocorticotropic hormone by the pituitary gland. The adrenocorticotropic hormone in turn upregulates the secretion of cortisol[127]. Cortisol can reach the tumor microenvironment *via* circulating blood, while norepinephrine can do so by being released from nerve fibers (carried by blood vessels), which are recruited in larger amounts by some tumors when these tumors secrete nerve growth factors. Cortisol and norepinephrine binding to the intracellular glucocorticoid receptor (located within the cell) or the beta adrenergic receptor (located on the cell surface) can trigger cellular responses[126].

It has long been recognized that psychosocial conditions affect the progression of some cancers[126]. In fact, epidemiological studies have shown that there is an accelerated progression of various cancers among patients with high stress levels or low social support[126]. While the relationship between stress and cancer development is not fully understood, some studies have shown that psychological stress causes abnormal immune responses, which are associated with cancer pathogenesis[128,129]. Cortisol release has been linked to the development and progression of, and survival from various cancers[130-134]. Cortisol inhibits immune responses, which allow cancer cells to evade the immune system[127,134].

Prostate cancer patients have also been shown to have high cortisol levels compared to low risk individuals[131], and breast cancer patients were reported to have high serum cortisol levels, which can be downregulated by emotional support[135].

Serum levels of cortisol have been shown to be higher in HCC patients than in healthy individuals[134]. Studies by Wu and colleagues have shown that exposing HCC cell cultures to cortisol represses p53 expression by upregulating expression of the p53 suppressor Bcl2L12. This suggests that cortisol is a factor that plays a role in the development of HCC[134]. Consequently, it has been suggested that cortisol may be a therapeutic target in HCC treatment[134].

Oxytocin is a neuropeptide hormone produced by hypothalamic neurons and has multiple roles in the central nervous system. While oxytocin is best known for its role in the female reproductive system (milk ejection), further research has shown that oxytocin also plays important roles in complex social behaviors, including stress and trust, anxiety, social interaction and bonding, and parental care, as well as in neuropsychiatric disorders linked to such social behaviors[136,137]. Oxytocin and its receptor have more recently been shown to play roles in some cancers[138-142].

Cortisol has also been linked to some functions of oxytocin[140]. Some studies have shown that higher oxytocin levels and increased social support (a known prognostic player in cancer) are associated with diminished effects of stress. In a study by Mankorious and colleagues, it was shown that there is a cross-talk network between oxytocin and cortisol at the molecular level, where the carcinogenic effect of cortisol was reversed by oxytocin *via* autophagy in human ovarian cancer cells *in vitro*[140].

It is known that the effects of oxytocin in cancer may depend on cell type, hormone concentration, its interactions with other hormones in the microenvironment, and the location of its receptor on the cell membrane[137]. Unpublished work from our laboratory analyzing data from sequenced HCC and pancreatic cancer cases in the TCGA dataset showed that genetic alterations in the oxytocin and oxytocin receptor genes were associated with lower median months of overall survival. It would be interesting to determine whether there could be an interaction between oxytocin and

cortisol, which could be involved in a potential neural regulation of HCC as well as other gastrointestinal cancers.

CONCLUSION

There has been minimal improvement in the prognosis for HCC patients over the past two decades. The detailed molecular mechanisms of HCC progression remain unclear, and there is an urgent need to better understand the mechanisms underlying HCC progression so as to develop novel and effective therapeutic strategies and reliable prognostic biomarkers. Further, a better understanding of mechanisms of HCC development can further aid efforts at developing effective preventative strategies. This review provides a summary of some of the mechanisms of HCC etiology, and some of the well-established as well as a few recently proposed mechanisms of HCC progression.

REFERENCES

1 **Bray F**, Ferlay J, Soerjomataram I, Siegel RL, Torre LA, Jemal A. Global cancer statistics 2018: GLOBOCAN estimates of incidence and mortality worldwide for 36 cancers in 185 countries. *CA Cancer J Clin* 2018; **68**: 394-424 [PMID: 30207593 DOI: 10.3322/caac.21492]

2 **Siegel RL**, Miller KD, Jemal A. Cancer Statistics, 2017. *CA Cancer J Clin* 2017; **67**: 7-30 [PMID: 28055103 DOI: 10.3322/caac.21387]

3 **Ghouri YA**, Mian I, Rowe JH. Review of hepatocellular carcinoma: Epidemiology, etiology, and carcinogenesis. *J Carcinog* 2017; **16**: 1 [PMID: 28694740 DOI: 10.4103/jcar.JCar_9_16]

4 **Golabi P**, Fazel S, Otgonsuren M, Sayiner M, Locklear CT, Younossi ZM. Mortality assessment of patients with hepatocellular carcinoma according to underlying disease and treatment modalities. *Medicine (Baltimore)* 2017; **96**: e5904 [PMID: 28248853 DOI: 10.1097/MD.0000000000005904]

5 **Medavaram S**, Zhang Y. Emerging therapies in advanced hepatocellular carcinoma. *Exp Hematol Oncol* 2018; **7**: 17 [PMID: 30087805 DOI: 10.1186/s40164-018-0109-6]

6 **Siegel RL**, Miller KD, Jemal A. Cancer statistics, 2018. *CA Cancer J Clin* 2018; **68**: 7-30 [PMID: 29313949 DOI: 10.3322/caac.21442]

7 **Dimitroulis D**, Damaskos C, Valsami S, Davakis S, Garmpis N, Spartalis E, Athanasiou A, Moris D, Sakellariou S, Kykalos S, Tsourouflis G, Garmpi A, Delladetsima I, Kontzoglou K, Kouraklis G. From diagnosis to treatment of hepatocellular carcinoma: An epidemic problem for both developed and developing world. *World J Gastroenterol* 2017; **23**: 5282-5294 [PMID: 28839428 DOI: 10.3748/wjg.v23.i29.5282]

8 **Daher S**, Massarwa M, Benson AA, Khoury T. Current and Future Treatment of Hepatocellular Carcinoma: An Updated Comprehensive Review. *J Clin Transl Hepatol* 2018; **6**: 69-78 [PMID: 29607307 DOI: 10.14218/JCTH.2017.00031]

9 **Ikeda M**, Morizane C, Ueno M, Okusaka T, Ishii H, Furuse J. Chemotherapy for hepatocellular carcinoma: current status and future perspectives. *Jpn J Clin Oncol* 2018; **48**: 103-114 [PMID: 29253194 DOI: 10.1093/jjco/hyx180]

10 **Keating GM**. Sorafenib: A Review in Hepatocellular Carcinoma. *Target Oncol* 2017; **12**: 243-253 [PMID: 28299600 DOI: 10.1007/s11523-017-0484-7]

11 **Sanz-Cameno P**, Trapero-Marugán M, Chaparro M, Jones EA, Moreno-Otero R. Angiogenesis: from chronic liver inflammation to hepatocellular carcinoma. *J Oncol* 2010; **2010**: 272170 [PMID: 20592752 DOI: 10.1155/2010/272170]

12 **Sampat KR**, O'Neil B. Antiangiogenic therapies for advanced hepatocellular carcinoma. *Oncologist* 2013; **18**: 430-438 [PMID: 23576483 DOI: 10.1634/theoncologist.2012-0388]

13 **Personeni N**, Pressiani T, Santoro A, Rimassa L. Regorafenib in hepatocellular carcinoma: latest evidence and clinical implications. *Drugs Context* 2018; **7**: 212533 [PMID: 30002715 DOI: 10.7573/dic.212533]

14 **Spallanzani A**, Orsi G, Andrikou K, Gelsomino F, Rimini M, Riggi L, Cascinu S. Lenvatinib as a therapy for unresectable hepatocellular carcinoma. *Expert Rev Anticancer Ther* 2018; **18**: 1069-1076 [PMID: 30220234 DOI: 10.1080/14737140.2018.1524297]

15 **Dhanasekaran R**, Bandoh S, Roberts LR. Molecular pathogenesis of hepatocellular carcinoma and impact of therapeutic advances. *F1000Res* 2016; 5 [PMID: 27239288 DOI: 10.12688/f1000research.6946.1]

16 **Tarocchi M**, Polvani S, Marroncini G, Galli A. Molecular mechanism of hepatitis B virus-induced hepatocarcinogenesis. *World J Gastroenterol* 2014; **20**: 11630-11640 [PMID: 25206269 DOI: 10.3748/wjg.v20.i33.11630]

17 **Ortega-Prieto AM**, Dorner M. Immune Evasion Strategies during Chronic Hepatitis B and C Virus Infection. *Vaccines (Basel)* 2017; 5 [PMID: 28862649 DOI: 10.3390/vaccines5030024]

18 **Ramakrishna G**, Rastogi A, Trehanpati N, Sen B, Khosla R, Sarin SK. From cirrhosis to hepatocellular carcinoma: new molecular insights on inflammation and cellular senescence. *Liver Cancer* 2013; **2**: 367-383 [PMID: 24400224 DOI: 10.1159/000343852]

19 **Bartosch B**, Thimme R, Blum HE, Zoulim F. Hepatitis C virus-induced hepatocarcinogenesis. *J Hepatol* 2009; **51**: 810-820 [PMID: 19545926 DOI: 10.1016/j.jhep.2009.05.008]

20 **Alzahrani B**, Iseli TJ, Hebbard LW. Non-viral causes of liver cancer: does obesity led inflammation play a role? *Cancer Lett* 2014; **345**: 223-229 [PMID: 24007864 DOI: 10.1016/j.canlet.2013.08.036]

21 **Sorrentino P**, D'Angelo S, Ferbo U, Micheli P, Bracigliano A, Vecchione R. Liver iron excess in patients with hepatocellular carcinoma developed on non-alcoholic steato-hepatitis. *J Hepatol* 2009; **50**: 351-357 [PMID: 19070395 DOI: 10.1016/j.jhep.2008.09.011]

22 **Hann HW**, Kim CY, London WT, Blumberg BS. Increased serum ferritin in chronic liver disease: a risk factor for primary hepatocellular carcinoma. *Int J Cancer* 1989; **43**: 376-379 [PMID: 2538399]

23 **Asare GA**, Bronz M, Naidoo V, Kew MC. Synergistic interaction between excess hepatic iron and alcohol ingestion in hepatic mutagenesis. *Toxicology* 2008; **254**: 11-18 [PMID: 18852013 DOI:

10.1016/j.tox.2008.08.024]
24 **Siriwardana RC**, Niriella MA, Dassanayake A, Ediriweera D, Gunetilleke B, Sivasundaram T, de Silva J. Association of Serum Ferritin with Diabetes and Alcohol in Patients with Non-Viral Liver Disease-Related Hepatocellular Carcinoma. *Liver Cancer* 2017; **6**: 307-312 [PMID: 29234634 DOI: 10.1159/000477266]
25 **Campbell PT**, Newton CC, Freedman ND, Koshiol J, Alavanja MC, Beane Freeman LE, Buring JE, Chan AT, Chong DQ, Datta M, Gaudet MM, Gaziano JM, Giovannucci EL, Graubard BI, Hollenbeck AR, King L, Lee IM, Linet MS, Palmer JR, Petrick JL, Poynter JN, Purdue MP, Robien K, Rosenberg L, Sahasrabuddhe VV, Schairer C, Sesso HD, Sigurdson AJ, Stevens VL, Wactawski-Wende J, Zeleniuch-Jacquotte A, Renehan AG, McGlynn KA. Body Mass Index, Waist Circumference, Diabetes, and Risk of Liver Cancer for U.S. Adults. *Cancer Res* 2016; **76**: 6076-6083 [PMID: 27742674 DOI: 10.1158/0008-5472.CAN-16-0787]
26 **Wei L**, Li N, Wang G, Feng X, Lyu Z, Li X, Wen Y, Chen Y, Chen H, Chen S, Wu S, Dai M, He J. Waist Circumference Might Be a Predictor of Primary Liver Cancer: A Population-Based Cohort Study. *Front Oncol* 2018; **8**: 607 [PMID: 30631750 DOI: 10.3389/fonc.2018.00607]
27 **Hu M**, Phan F, Bourron O, Ferré P, Foufelle F. Steatosis and NASH in type 2 diabetes. *Biochimie* 2017; **143**: 37-41 [PMID: 29097281 DOI: 10.1016/j.biochi.2017.10.019]
28 **Yan G**, Wang X, Sun C, Zheng X, Wei H, Tian Z, Sun R. Chronic Alcohol Consumption Promotes Diethylnitrosamine-Induced Hepatocarcinogenesis via Immune Disturbances. *Sci Rep* 2017; **7**: 2567 [PMID: 28566719 DOI: 10.1038/s41598-017-02887-7]
29 **Ramadori P**, Cubero FJ, Liedtke C, Trautwein C, Nevzorova YA. Alcohol and Hepatocellular Carcinoma: Adding Fuel to the Flame. *Cancers (Basel)* 2017; **9** [PMID: 28946672 DOI: 10.3390/cancers9100130]
30 **Ogunwobi OO**, Puszyk W, Dong HJ, Liu C. Epigenetic upregulation of HGF and c-Met drives metastasis in hepatocellular carcinoma. *PLoS One* 2013; **8**: e63765 [PMID: 23723997 DOI: 10.1371/journal.pone.0063765]
31 **Singh AK**, Kumar R, Pandey AK. Hepatocellular Carcinoma: Causes, Mechanism of Progression and Biomarkers. *Curr Chem Genom Transl Med* 2018; **12**: 9-26 [PMID: 30069430 DOI: 10.2174/2213988501812010009]
32 **Kew MC**. Aflatoxins as a cause of hepatocellular carcinoma. *J Gastrointestin Liver Dis* 2013; **22**: 305-310 [PMID: 24078988]
33 **Wu HC**, Santella R. The role of aflatoxins in hepatocellular carcinoma. *Hepat Mon* 2012; **12**: e7238 [PMID: 23162603 DOI: 10.5812/hepatmon.7238]
34 **Tansel A**, Katz LH, El-Serag HB, Thrift AP, Parepally M, Shakhatreh MH, Kanwal F. Incidence and Determinants of Hepatocellular Carcinoma in Autoimmune Hepatitis: A Systematic Review and Meta-analysis. *Clin Gastroenterol Hepatol* 2017; **15**: 1207-1217.e4 [PMID: 28215616 DOI: 10.1016/j.cgh.2017.02.006]
35 **Llovet JM**, Zucman-Rossi J, Pikarsky E, Sangro B, Schwartz M, Sherman M, Gores G. Hepatocellular carcinoma. *Nat Rev Dis Primers* 2016; **2**: 16018 [PMID: 27158749 DOI: 10.1038/nrdp.2016.18]
36 **Llovet JM**, Montal R, Sia D, Finn RS. Molecular therapies and precision medicine for hepatocellular carcinoma. *Nat Rev Clin Oncol* 2018; **15**: 599-616 [PMID: 30061739 DOI: 10.1038/s41571-018-0073-4]
37 **Brabletz T**, Kalluri R, Nieto MA, Weinberg RA. EMT in cancer. *Nat Rev Cancer* 2018; **18**: 128-134 [PMID: 29326430 DOI: 10.1038/nrc.2017.118]
38 **Kalluri R**, Weinberg RA. The basics of epithelial-mesenchymal transition. *J Clin Invest* 2009; **119**: 1420-1428 [PMID: 19487818 DOI: 10.1172/JCI39104]
39 **Lamouille S**, Xu J, Derynck R. Molecular mechanisms of epithelial-mesenchymal transition. *Nat Rev Mol Cell Biol* 2014; **15**: 178-196 [PMID: 24556840 DOI: 10.1038/nrm3758]
40 **Ye X**, Weinberg RA. Epithelial-Mesenchymal Plasticity: A Central Regulator of Cancer Progression. *Trends Cell Biol* 2015; **25**: 675-686 [PMID: 26437589 DOI: 10.1016/j.tcb.2015.07.012]
41 **Huaman J**, Bach C, Ilboudo A, Ogunwobi OO, Liu C. Epithelial-to-Mesenchymal Transition in Hepatocellular Carcinoma. Liu C. *Precision Molecular Pathology of Liver Cancer*. Cham: Springer International Publishing 2018; 131-152
42 **Puisieux A**, Brabletz T, Caramel J. Oncogenic roles of EMT-inducing transcription factors. *Nat Cell Biol* 2014; **16**: 488-494 [PMID: 24875735 DOI: 10.1038/ncb2976]
43 **Tiwari N**, Gheldof A, Tatari M, Christofori G. EMT as the ultimate survival mechanism of cancer cells. *Semin Cancer Biol* 2012; **22**: 194-207 [PMID: 22406545 DOI: 10.1016/j.semcancer.2012.02.013]
44 **Chen L**, Guo P, He Y, Chen Z, Chen L, Luo Y, Qi L, Liu Y, Wu Q, Cui Y, Fang F, Zhang X, Song T, Guo H. HCC-derived exosomes elicit HCC progression and recurrence by epithelial-mesenchymal transition through MAPK/ERK signalling pathway. *Cell Death Dis* 2018; **9**: 513 [PMID: 29725020 DOI: 10.1038/s41419-018-0534-9]
45 **Long L**, Xiang H, Liu J, Zhang Z, Sun L. ZEB1 mediates doxorubicin (Dox) resistance and mesenchymal characteristics of hepatocarcinoma cells. *Exp Mol Pathol* 2019; **106**: 116-122 [PMID: 30615851 DOI: 10.1016/j.yexmp.2019.01.001]
46 **Qu W**, Wen X, Su K, Gou W. MiR-552 promotes the proliferation, migration and EMT of hepatocellular carcinoma cells by inhibiting AJAP1 expression. *J Cell Mol Med* 2019; **23**: 1541-1552 [PMID: 30597727 DOI: 10.1111/jcmm.14062]
47 **Shi C**, Chen Y, Chen Y, Yang Y, Bing W, Qi J. $CD4^+$ $CD25^+$ regulatory T cells promote hepatocellular carcinoma invasion via TGF-β1-induced epithelial-mesenchymal transition. *Onco Targets Ther* 2018; **12**: 279-289 [PMID: 30643426 DOI: 10.2147/OTT.S172417]
48 **Xia C**, Zhang XY, Liu W, Ju M, Ju Y, Bu YZ, Wang W, Shao H. LINC00857 contributes to hepatocellular carcinoma malignancy via enhancing epithelial-mesenchymal transition. *J Cell Biochem* 2018 [PMID: 30506763 DOI: 10.1002/jcb.28074]
49 **Zhang B**, Shi D, Zhang X, Liang G, Liu W, Qiao S. FK866 inhibits the epithelial-mesenchymal transition of hepatocarcinoma MHCC97-H cells. *Oncol Lett* 2018; **16**: 7231-7238 [PMID: 30546461 DOI: 10.3892/ol.2018.9541]
50 **Das DK**, Durojaiye V, Ilboudo A, Naidoo MK, Ogunwobi O. A "Patient-Like" Orthotopic Syngeneic Mouse Model of Hepatocellular Carcinoma Metastasis. *J Vis Exp* 2015; e52858 [PMID: 26555484 DOI: 10.3791/52858]
51 **Yang JD**, Nakamura I, Roberts LR. The tumor microenvironment in hepatocellular carcinoma: current status and therapeutic targets. *Semin Cancer Biol* 2011; **21**: 35-43 [PMID: 20946957 DOI: 10.1016/j.semcancer.2010.10.007]
52 **Delire B**, Henriet P, Lemoine P, Leclercq IA, Stärkel P. Chronic liver injury promotes hepatocarcinoma cell seeding and growth, associated with infiltration by macrophages. *Cancer Sci* 2018; **109**: 2141-2152

[PMID: 29727510 DOI: 10.1111/cas.13628]
53 **Affo S**, Yu LX, Schwabe RF. The Role of Cancer-Associated Fibroblasts and Fibrosis in Liver Cancer. *Annu Rev Pathol* 2017; **12**: 153-186 [PMID: 27959632 DOI: 10.1146/annurev-pathol-052016-100322]
54 **Lu Y**, Lin N, Chen Z, Xu R. Hypoxia-induced secretion of platelet-derived growth factor-BB by hepatocellular carcinoma cells increases activated hepatic stellate cell proliferation, migration and expression of vascular endothelial growth factor-A. *Mol Med Rep* 2015; **11**: 691-697 [PMID: 25333351 DOI: 10.3892/mmr.2014.2689]
55 **Galiè M**, Sorrentino C, Montani M, Micossi L, Di Carlo E, D'Antuono T, Calderan L, Marzola P, Benati D, Merigo F, Orlando F, Smorlesi A, Marchini C, Amici A, Sbarbati A. Mammary carcinoma provides highly tumourigenic and invasive reactive stromal cells. *Carcinogenesis* 2005; **26**: 1868-1878 [PMID: 15975963 DOI: 10.1093/carcin/bgi158]
56 **Hernandez-Gea V**, Toffanin S, Friedman SL, Llovet JM. Role of the microenvironment in the pathogenesis and treatment of hepatocellular carcinoma. *Gastroenterology* 2013; **144**: 512-527 [PMID: 23313965 DOI: 10.1053/j.gastro.2013.01.002]
57 **Friedman SL**. Mechanisms of hepatic fibrogenesis. *Gastroenterology* 2008; **134**: 1655-1669 [PMID: 18471545 DOI: 10.1053/j.gastro.2008.03.003]
58 **Amann T**, Bataille F, Spruss T, Mühlbauer M, Gäbele E, Schölmerich J, Kiefer P, Bosserhoff AK, Hellerbrand C. Activated hepatic stellate cells promote tumorigenicity of hepatocellular carcinoma. *Cancer Sci* 2009; **100**: 646-653 [PMID: 19175606 DOI: 10.1111/j.1349-7006.2009.01087.x]
59 **Faouzi S**, Lepreux S, Bedin C, Dubuisson L, Balabaud C, Bioulac-Sage P, Desmoulière A, Rosenbaum J. Activation of cultured rat hepatic stellate cells by tumoral hepatocytes. *Lab Invest* 1999; **79**: 485-493 [PMID: 10212001]
60 **Wang N**, Wang S, Li MY, Hu BG, Liu LP, Yang SL, Yang S, Gong Z, Lai PBS, Chen GG. Cancer stem cells in hepatocellular carcinoma: an overview and promising therapeutic strategies. *Ther Adv Med Oncol* 2018; **10**: 1758835918816287 [PMID: 30622654 DOI: 10.1177/1758835918816287]
61 **Fransvea E**, Paradiso A, Antonaci S, Giannelli G. HCC heterogeneity: molecular pathogenesis and clinical implications. *Cell Oncol* 2009; **31**: 227-233 [PMID: 19478390 DOI: 10.3233/CLO-2009-0473]
62 **Williams GM**, Gebhardt R, Sirma H, Stenbäck F. Non-linearity of neoplastic conversion induced in rat liver by low exposures to diethylnitrosamine. *Carcinogenesis* 1993; **14**: 2149-2156 [PMID: 8106178]
63 **Bralet MP**, Pichard V, Ferry N. Demonstration of direct lineage between hepatocytes and hepatocellular carcinoma in diethylnitrosamine-treated rats. *Hepatology* 2002; **36**: 623-630 [PMID: 12198654 DOI: 10.1053/jhep.2002.35540]
64 **Wu S**, Powers S, Zhu W, Hannun YA. Substantial contribution of extrinsic risk factors to cancer development. *Nature* 2016; **529**: 43-47 [PMID: 26675728 DOI: 10.1038/nature16166]
65 **Yavorkovsky L**, Lai E, Ilic Z, Sell S. Participation of small intraportal stem cells in the restitutive response of the liver to periportal necrosis induced by allyl alcohol. *Hepatology* 1995; **21**: 1702-1712 [PMID: 7539398]
66 **Zhang Y**, Bai XF, Huang CX. Hepatic stem cells: existence and origin. *World J Gastroenterol* 2003; **9**: 201-204 [PMID: 12532431]
67 **Mikhail S**, He AR. Liver cancer stem cells. *Int J Hepatol* 2011; **2011**: 486954 [PMID: 21994859 DOI: 10.4061/2011/486954]
68 **Jayachandran A**, Dhungel B, Steel JC. Epithelial-to-mesenchymal plasticity of cancer stem cells: therapeutic targets in hepatocellular carcinoma. *J Hematol Oncol* 2016; **9**: 74 [PMID: 27578206 DOI: 10.1186/s13045-016-0307-9]
69 **Machida K**. Existence of cancer stem cells in hepatocellular carcinoma: myth or reality? *Hepatol Int* 2017; **11**: 143-147 [PMID: 27990610 DOI: 10.1007/s12072-016-9777-7]
70 **Jordan CT**, Guzman ML, Noble M. Cancer stem cells. *N Engl J Med* 2006; **355**: 1253-1261 [PMID: 16990388 DOI: 10.1056/NEJMra061808]
71 **Bonnet D**, Dick JE. Human acute myeloid leukemia is organized as a hierarchy that originates from a primitive hematopoietic cell. *Nat Med* 1997; **3**: 730-737 [PMID: 9212098]
72 **Lapidot T**, Sirard C, Vormoor J, Murdoch B, Hoang T, Caceres-Cortes J, Minden M, Paterson B, Caligiuri MA, Dick JE. A cell initiating human acute myeloid leukaemia after transplantation into SCID mice. *Nature* 1994; **367**: 645-648 [PMID: 7509044 DOI: 10.1038/367645a0]
73 **Cabrera MC**, Hollingsworth RE, Hurt EM. Cancer stem cell plasticity and tumor hierarchy. *World J Stem Cells* 2015; **7**: 27-36 [PMID: 25621103 DOI: 10.4252/wjsc.v7.i1.27]
74 **Pattabiraman DR**, Weinberg RA. Tackling the cancer stem cells - what challenges do they pose? *Nat Rev Drug Discov* 2014; **13**: 497-512 [PMID: 24981363 DOI: 10.1038/nrd4253]
75 **Thiery JP**. Epithelial-mesenchymal transitions in tumour progression. *Nat Rev Cancer* 2002; **2**: 442-454 [PMID: 12189386 DOI: 10.1038/nrc822]
76 **Wang T**, Shigdar S, Gantier MP, Hou Y, Wang L, Li Y, Shamaileh HA, Yin W, Zhou SF, Zhao X, Duan W. Cancer stem cell targeted therapy: progress amid controversies. *Oncotarget* 2015; **6**: 44191-44206 [PMID: 26496035 DOI: 10.18632/oncotarget.6176]
77 **Vu NB**, Nguyen TT, Tran LC, Do CD, Nguyen BH, Phan NK, Pham PV. Doxorubicin and 5-fluorouracil resistant hepatic cancer cells demonstrate stem-like properties. *Cytotechnology* 2013; **65**: 491-503 [PMID: 23104270 DOI: 10.1007/s10616-012-9511-9]
78 **Rao S**, Zaidi S, Banerjee J, Jogunoori W, Sebastian R, Mishra B, Nguyen BN, Wu RC, White J, Deng C, Amdur R, Li S, Mishra L. Transforming growth factor-β in liver cancer stem cells and regeneration. *Hepatol Commun* 2017; **1**: 477-493 [PMID: 29404474 DOI: 10.1002/hep4.1062]
79 **Nio K**, Yamashita T, Kaneko S. The evolving concept of liver cancer stem cells. *Mol Cancer* 2017; **16**: 4 [PMID: 28137313 DOI: 10.1186/s12943-016-0572-9]
80 **Yoon SK**. The biology of cancer stem cells and its clinical implication in hepatocellular carcinoma. *Gut Liver* 2012; **6**: 29-40 [PMID: 22375168 DOI: 10.5009/gnl.2012.6.1.29]
81 **Yamashita T**, Ji J, Budhu A, Forgues M, Yang W, Wang HY, Jia H, Ye Q, Qin LX, Wauthier E, Reid LM, Minato H, Honda M, Kaneko S, Tang ZY, Wang XW. EpCAM-positive hepatocellular carcinoma cells are tumor-initiating cells with stem/progenitor cell features. *Gastroenterology* 2009; **136**: 1012-1024 [PMID: 19150350 DOI: 10.1053/j.gastro.2008.12.004]
82 **Yang ZF**, Ho DW, Ng MN, Lau CK, Yu WC, Ngai P, Chu PW, Lam CT, Poon RT, Fan ST. Significance of CD90+ cancer stem cells in human liver cancer. *Cancer Cell* 2008; **13**: 153-166 [PMID: 18242515 DOI: 10.1016/j.ccr.2008.01.013]
83 **Ma S**, Chan KW, Hu L, Lee TK, Wo JY, Ng IO, Zheng BJ, Guan XY. Identification and characterization of tumorigenic liver cancer stem/progenitor cells. *Gastroenterology* 2007; **132**: 2542-2556 [PMID:

17570225 DOI: 10.1053/j.gastro.2007.04.025]
84 **Zhu Z**, Hao X, Yan M, Yao M, Ge C, Gu J, Li J. Cancer stem/progenitor cells are highly enriched in CD133+CD44+ population in hepatocellular carcinoma. *Int J Cancer* 2010; **126**: 2067-2078 [PMID: 19711346 DOI: 10.1002/ijc.24868]
85 **Haraguchi N**, Ishii H, Mimori K, Tanaka F, Ohkuma M, Kim HM, Akita H, Takiuchi D, Hatano H, Nagano H, Barnard GF, Doki Y, Mori M. CD13 is a therapeutic target in human liver cancer stem cells. *J Clin Invest* 2010; **120**: 3326-3339 [PMID: 20697159 DOI: 10.1172/JCI42550]
86 **Merle P**, Trepo C. Molecular mechanisms underlying hepatocellular carcinoma. *Viruses* 2009; **1**: 852-872 [PMID: 21994573 DOI: 10.3390/v1030852]
87 **Di Micco R**, Fumagalli M, Cicalese A, Piccinin S, Gasparini P, Luise C, Schurra C, Garre' M, Nuciforo PG, Bensimon A, Maestro R, Pelicci PG, d'Adda di Fagagna F. Oncogene-induced senescence is a DNA damage response triggered by DNA hyper-replication. *Nature* 2006; **444**: 638-642 [PMID: 17136094 DOI: 10.1038/nature05327]
88 **Naugler WE**, Karin M. NF-kappaB and cancer-identifying targets and mechanisms. *Curr Opin Genet Dev* 2008; **18**: 19-26 [PMID: 18440219 DOI: 10.1016/j.gde.2008.01.020]
89 **Van Antwerp DJ**, Martin SJ, Kafri T, Green DR, Verma IM. Suppression of TNF-alpha-induced apoptosis by NF-kappaB. *Science* 1996; **274**: 787-789 [PMID: 8864120]
90 **Bassères DS**, Baldwin AS. Nuclear factor-kappaB and inhibitor of kappaB kinase pathways in oncogenic initiation and progression. *Oncogene* 2006; **25**: 6817-6830 [PMID: 17072330 DOI: 10.1038/sj.onc.1209942]
91 **Luo JL**, Tan W, Ricono JM, Korchynskyi O, Zhang M, Gonias SL, Cheresh DA, Karin M. Nuclear cytokine-activated IKKalpha controls prostate cancer metastasis by repressing Maspin. *Nature* 2007; **446**: 690-694 [PMID: 17377533 DOI: 10.1038/nature05656]
92 **Hardy T**, Mann DA. Epigenetics in liver disease: from biology to therapeutics. *Gut* 2016; **65**: 1895-1905 [PMID: 27624887 DOI: 10.1136/gutjnl-2015-311292]
93 **Xiao Z**, Shen J, Zhang L, Li M, Hu W, Cho C. Therapeutic targeting of noncoding RNAs in hepatocellular carcinoma: Recent progress and future prospects. *Oncol Lett* 2018; **15**: 3395-3402 [PMID: 29467864 DOI: 10.3892/ol.2018.7758]
94 **Peng L**, Yuan XQ, Zhang CY, Peng JY, Zhang YQ, Pan X, Li GC. The emergence of long non-coding RNAs in hepatocellular carcinoma: an update. *J Cancer* 2018; **9**: 2549-2558 [PMID: 30026854 DOI: 10.7150/jca.24560]
95 **Sia D**, Villanueva A, Friedman SL, Llovet JM. Liver Cancer Cell of Origin, Molecular Class, and Effects on Patient Prognosis. *Gastroenterology* 2017; **152**: 745-761 [PMID: 28043904 DOI: 10.1053/j.gastro.2016.11.048]
96 **Letouzé E**, Shinde J, Renault V, Couchy G, Blanc JF, Tubacher E, Bayard Q, Bacq D, Meyer V, Semhoun J, Bioulac-Sage P, Prévôt S, Azoulay D, Paradis V, Imbeaud S, Deleuze JF, Zucman-Rossi J. Mutational signatures reveal the dynamic interplay of risk factors and cellular processes during liver tumorigenesis. *Nat Commun* 2017; **8**: 1315 [PMID: 29101368 DOI: 10.1038/s41467-017-01358-x]
97 **Hagel M**, Miduturu C, Sheets M, Rubin N, Weng W, Stransky N, Bifulco N, Kim JL, Hodous B, Brooijmans N, Shutes A, Winter C, Lengauer C, Kohl NE, Guzi T. First Selective Small Molecule Inhibitor of FGFR4 for the Treatment of Hepatocellular Carcinomas with an Activated FGFR4 Signaling Pathway. *Cancer Discov* 2015; **5**: 424-437 [PMID: 25776529 DOI: 10.1158/2159-8290.CD-14-1029]
98 **Micalizzi DS**, Maheswaran S, Haber DA. A conduit to metastasis: circulating tumor cell biology. *Genes Dev* 2017; **31**: 1827-1840 [PMID: 29051388 DOI: 10.1101/gad.305805.117]
99 **Gallerani G**, Fici P, Fabbri F. Circulating Tumor Cells: Back to the Future. *Front Oncol* 2017; **6**: 275 [PMID: 28123996 DOI: 10.3389/fonc.2016.00275]
100 **van de Stolpe A**, Pantel K, Sleijfer S, Terstappen LW, den Toonder JM. Circulating tumor cell isolation and diagnostics: toward routine clinical use. *Cancer Res* 2011; **71**: 5955-5960 [PMID: 21896640 DOI: 10.1158/0008-5472.CAN-11-1254]
101 **Pantel K**, Brakenhoff RH, Brandt B. Detection, clinical relevance and specific biological properties of disseminating tumour cells. *Nat Rev Cancer* 2008; **8**: 329-340 [PMID: 18404148 DOI: 10.1038/nrc2375]
102 **Fan JL**, Yang YF, Yuan CH, Chen H, Wang FB. Circulating Tumor Cells for Predicting the Prognostic of Patients with Hepatocellular Carcinoma: A Meta Analysis. *Cell Physiol Biochem* 2015; **37**: 629-640 [PMID: 26344495 DOI: 10.1159/000430382]
103 **Li J**, Han X, Yu X, Xu Z, Yang G, Liu B, Xiu P. Clinical applications of liquid biopsy as prognostic and predictive biomarkers in hepatocellular carcinoma: circulating tumor cells and circulating tumor DNA. *J Exp Clin Cancer Res* 2018; **37**: 213 [PMID: 30176913 DOI: 10.1186/s13046-018-0893-1]
104 **Okajima W**, Komatsu S, Ichikawa D, Miyamae M, Ohashi T, Imamura T, Kiuchi J, Nishibeppu K, Arita T, Konishi H, Shiozaki A, Morimura R, Ikoma H, Okamoto K, Otsuji E. Liquid biopsy in patients with hepatocellular carcinoma: Circulating tumor cells and cell-free nucleic acids. *World J Gastroenterol* 2017; **23**: 5650-5668 [PMID: 28883691 DOI: 10.3748/wjg.v23.i31.5650]
105 **Schulze K**, Gasch C, Staufer K, Nashan B, Lohse AW, Pantel K, Riethdorf S, Wege H. Presence of EpCAM-positive circulating tumor cells as biomarker for systemic disease strongly correlates to survival in patients with hepatocellular carcinoma. *Int J Cancer* 2013; **133**: 2165-2171 [PMID: 23616258 DOI: 10.1002/ijc.28230]
106 **von Felden J**, Schulze K, Krech T, Ewald F, Nashan B, Pantel K, Lohse AW, Riethdorf S, Wege H. Circulating tumor cells as liquid biomarker for high HCC recurrence risk after curative liver resection. *Oncotarget* 2017; **8**: 89978-89987 [PMID: 29163804 DOI: 10.18632/oncotarget.21208]
107 **Guo W**, Sun YF, Shen MN, Ma XL, Wu J, Zhang CY, Zhou Y, Xu Y, Hu B, Zhang M, Wang G, Chen WQ, Guo L, Lu RQ, Zhou CH, Zhang X, Shi YH, Qiu SJ, Pan BS, Cao Y, Zhou J, Yang XR, Fan J. Circulating Tumor Cells with Stem-Like Phenotypes for Diagnosis, Prognosis, and Therapeutic Response Evaluation in Hepatocellular Carcinoma. *Clin Cancer Res* 2018; **24**: 2203-2213 [PMID: 29374055 DOI: 10.1158/1078-0432.CCR-17-1753]
108 **Qi LN**, Xiang BD, Wu FX, Ye JZ, Zhong JH, Wang YY, Chen YY, Chen ZS, Ma L, Chen J, Gong WF, Han ZG, Lu Y, Shang JJ, Li LQ. Circulating Tumor Cells Undergoing EMT Provide a Metric for Diagnosis and Prognosis of Patients with Hepatocellular Carcinoma. *Cancer Res* 2018; **78**: 4731-4744 [PMID: 29915159 DOI: 10.1158/0008-5472.CAN-17-2459]
109 **Sun C**, Liao W, Deng Z, Li E, Feng Q, Lei J, Yuan R, Zou S, Mao Y, Shao J, Wu L, Zhang C. The diagnostic value of assays for circulating tumor cells in hepatocellular carcinoma: A meta-analysis. *Medicine (Baltimore)* 2017; **96**: e7513 [PMID: 28723763 DOI: 10.1097/MD.0000000000007513]
110 **Yin CQ**, Yuan CH, Qu Z, Guan Q, Chen H, Wang FB. Liquid Biopsy of Hepatocellular Carcinoma:

Circulating Tumor-Derived Biomarkers. *Dis Markers* 2016; **2016**: 1427849 [PMID: 27403030 DOI: 10.1155/2016/1427849]
111 **Alvarez Cubero MJ**, Lorente JA, Robles-Fernandez I, Rodriguez-Martinez A, Puche JL, Serrano MJ. Circulating Tumor Cells: Markers and Methodologies for Enrichment and Detection. *Methods Mol Biol* 2017; **1634**: 283-303 [PMID: 28819860 DOI: 10.1007/978-1-4939-7144-2_24]
112 **D'Avola D**, Villacorta-Martin C, Martins-Filho SN, Craig A, Labgaa I, von Felden J, Kimaada A, Bonaccorso A, Tabrizian P, Hartmann BM, Sebra R, Schwartz M, Villanueva A. High-density single cell mRNA sequencing to characterize circulating tumor cells in hepatocellular carcinoma. *Sci Rep* 2018; **8**: 11570 [PMID: 30068984 DOI: 10.1038/s41598-018-30047-y]
113 **Chen J**, Cao SW, Cai Z, Zheng L, Wang Q. Epithelial-mesenchymal transition phenotypes of circulating tumor cells correlate with the clinical stages and cancer metastasis in hepatocellular carcinoma patients. *Cancer Biomark* 2017; **20**: 487-498 [PMID: 28869439 DOI: 10.3233/CBM-170315]
114 **Li YM**, Xu SC, Li J, Han KQ, Pi HF, Zheng L, Zuo GH, Huang XB, Li HY, Zhao HZ, Yu ZP, Zhou Z, Liang P. Epithelial-mesenchymal transition markers expressed in circulating tumor cells in hepatocellular carcinoma patients with different stages of disease. *Cell Death Dis* 2013; **4**: e831 [PMID: 24091674 DOI: 10.1038/cddis.2013.347]
115 **Vona G**, Estepa L, Béroud C, Damotte D, Capron F, Nalpas B, Mineur A, Franco D, Lacour B, Pol S, Bréchot C, Paterlini-Bréchot P. Impact of cytomorphological detection of circulating tumor cells in patients with liver cancer. *Hepatology* 2004; **39**: 792-797 [PMID: 14999698 DOI: 10.1002/hep.20091]
116 **Lee S**, Loecher M, Iyer R. Immunomodulation in hepatocellular cancer. *J Gastrointest Oncol* 2018; **9**: 208-219 [PMID: 29564186 DOI: 10.21037/jgo.2017.06.08]
117 **Makarova-Rusher OV**, Medina-Echeverz J, Duffy AG, Greten TF. The yin and yang of evasion and immune activation in HCC. *J Hepatol* 2015; **62**: 1420-1429 [PMID: 25733155 DOI: 10.1016/j.jhep.2015.02.038]
118 **Nishida N**, Kudo M. Immunological Microenvironment of Hepatocellular Carcinoma and Its Clinical Implication. *Oncology* 2017; **92** Suppl 1: 40-49 [PMID: 27764823 DOI: 10.1159/000451015]
119 **Sachdeva M**, Chawla YK, Arora SK. Immunology of hepatocellular carcinoma. *World J Hepatol* 2015; **7**: 2080-2090 [PMID: 26301050 DOI: 10.4254/wjh.v7.i17.2080]
120 **Zhao F**, Korangy F, Greten TF. Cellular immune suppressor mechanisms in patients with hepatocellular carcinoma. *Dig Dis* 2012; **30**: 477-482 [PMID: 23108303 DOI: 10.1159/000341695]
121 **Wellenstein MD**, de Visser KE. Cancer-Cell-Intrinsic Mechanisms Shaping the Tumor Immune Landscape. *Immunity* 2018; **48**: 399-416 [PMID: 29562192 DOI: 10.1016/j.immuni.2018.03.004]
122 **Lugade AA**, Kalathil S, Miller A, Iyer R, Thanavala Y. High immunosuppressive burden in advanced hepatocellular carcinoma patients: Can effector functions be restored? *Oncoimmunology* 2013; **2**: e24679 [PMID: 24073364 DOI: 10.4161/onci.24679]
123 **Greten TF**, Sangro B. Targets for immunotherapy of liver cancer. *J Hepatol* 2017 [PMID: 28923358 DOI: 10.1016/j.jhep.2017.09.007]
124 **Lin YY**, Tan CT, Chen CW, Ou DL, Cheng AL, Hsu C. Immunomodulatory Effects of Current Targeted Therapies on Hepatocellular Carcinoma: Implication for the Future of Immunotherapy. *Semin Liver Dis* 2018; **38**: 379-388 [PMID: 30357775 DOI: 10.1055/s-0038-1673621]
125 **Mukaida N**, Nakamoto Y. Emergence of immunotherapy as a novel way to treat hepatocellular carcinoma. *World J Gastroenterol* 2018; **24**: 1839-1858 [PMID: 29740200 DOI: 10.3748/wjg.v24.i17.1839]
126 **Cole SW**. New challenges in psycho-oncology: Neural regulation of the cancer genome. *Psychooncology* 2018; **27**: 2305-2309 [PMID: 30022563 DOI: 10.1002/pon.4838]
127 **Dong T**, Zhi L, Bhayana B, Wu MX. Cortisol-induced immune suppression by a blockade of lymphocyte egress in traumatic brain injury. *J Neuroinflammation* 2016; **13**: 197 [PMID: 27561600 DOI: 10.1186/s12974-016-0663-y]
128 **Lang MJ**, David V, Giese-Davis J. The Age Conundrum: A Scoping Review of Younger Age or Adolescent and Young Adult as a Risk Factor for Clinical Distress, Depression, or Anxiety in Cancer. *J Adolesc Young Adult Oncol* 2015; **4**: 157-173 [PMID: 26697266 DOI: 10.1089/jayao.2015.0005]
129 **Idris SZ**, Hassan N, Lee LJ, Md Noor S, Osman R, Abdul-Jalil M, Nordin AJ, Abdullah M. Increased regulatory T cells in acute lymphoblastic leukemia patients. *Hematology* 2015; **20**: 523-529 [PMID: 26119924 DOI: 10.1179/1607845415Y.0000000025]
130 **Sephton SE**, Lush E, Dedert EA, Floyd AR, Rebholz WN, Dhabhar FS, Spiegel D, Salmon P. Diurnal cortisol rhythm as a predictor of lung cancer survival. *Brain Behav Immun* 2013; **30** Suppl: S163-S170 [PMID: 22884416 DOI: 10.1016/j.bbi.2012.07.019]
131 **Fabre B**, Grosman H, Gonzalez D, Machulsky NF, Repetto EM, Mesch V, Lopez MA, Mazza O, Berg G. Prostate Cancer, High Cortisol Levels and Complex Hormonal Interaction. *Asian Pac J Cancer Prev* 2016; **17**: 3167-3171 [PMID: 27509946]
132 **Moreno-Smith M**, Lutgendorf SK, Sood AK. Impact of stress on cancer metastasis. *Future Oncol* 2010; **6**: 1863-1881 [PMID: 21142861 DOI: 10.2217/fon.10.142]
133 **Schrepf A**, Thaker PH, Goodheart MJ, Bender D, Slavich GM, Dahmoush L, Penedo F, DeGeest K, Mendez L, Lubaroff DM, Cole SW, Sood AK, Lutgendorf SK. Diurnal cortisol and survival in epithelial ovarian cancer. *Psychoneuroendocrinology* 2015; **53**: 256-267 [PMID: 25647344 DOI: 10.1016/j.psyneuen.2015.01.010]
134 **Wu W**, Liu S, Liang Y, Zhou Z, Bian W, Liu X. Stress Hormone Cortisol Enhances Bcl2 Like-12 Expression to Inhibit p53 in Hepatocellular Carcinoma Cells. *Dig Dis Sci* 2017; **62**: 3495-3500 [PMID: 29043595 DOI: 10.1007/s10620-017-4798-1]
135 **Webster S**, Chandrasekaran S, Vijayaragavan R, Sethu G. Impact of Emotional Support on Serum Cortisol in Breast Cancer Patients. *Indian J Palliat Care* 2016; **22**: 141-149 [PMID: 27162424 DOI: 10.4103/0973-1075.179607]
136 **Scerbo MJ**, Gerdes JM. Bonding With β-Cells-A Role for Oxytocin in Glucose Handling. *Diabetes* 2017; **66**: 256-257 [PMID: 28108604 DOI: 10.2337/dbi16-0053]
137 **Lerman B**, Harricharran T, Ogunwobi OO. Oxytocin and cancer: An emerging link. *World J Clin Oncol* 2018; **9**: 74-82 [PMID: 30254962 DOI: 10.5306/wjco.v9.i5.74]
138 **Cassoni P**, Sapino A, Fortunati N, Munaron L, Chini B, Bussolati G. Oxytocin inhibits the proliferation of MDA-MB231 human breast-cancer cells via cyclic adenosine monophosphate and protein kinase A. *Int J Cancer* 1997; **72**: 340-344 [PMID: 9219843]
139 **Xu H**, Fu S, Chen Q, Gu M, Zhou J, Liu C, Chen Y, Wang Z. The function of oxytocin: a potential biomarker for prostate cancer diagnosis and promoter of prostate cancer. *Oncotarget* 2017; **8**: 31215-31226 [PMID: 28415720 DOI: 10.18632/oncotarget.16107]

140 **Mankarious A**, Dave F, Pados G, Tsolakidis D, Gidron Y, Pang Y, Thomas P, Hall M, Karteris E. The pro-social neurohormone oxytocin reverses the actions of the stress hormone cortisol in human ovarian carcinoma cells in vitro. *Int J Oncol* 2016; **48**: 1805-1814 [PMID: 26935408 DOI: 10.3892/ijo.2016.3410]
141 **Lindblad M**, García Rodríguez LA, Chandanos E, Lagergren J. Hormone replacement therapy and risks of oesophageal and gastric adenocarcinomas. *Br J Cancer* 2006; **94**: 136-141 [PMID: 16404367 DOI: 10.1038/sj.bjc.6602906]
142 **Skinner HG**, Michaud DS, Colditz GA, Giovannucci EL, Stampfer MJ, Willett WC, Fuchs CS. Parity, reproductive factors, and the risk of pancreatic cancer in women. *Cancer Epidemiol Biomarkers Prev* 2003; **12**: 433-438 [PMID: 12750238]

World Journal of Gastroenterology

Submit a Manuscript: https://www.f6publishing.com

World J Gastroenterol 2019 May 21; 25(19): 2294-2307

DOI: 10.3748/wjg.v25.i19.2294

ISSN 1007-9327 (print) ISSN 2219-2840 (online)

MINIREVIEWS

Congenital peritoneal encapsulation: A review and novel classification system

Aneesh Dave, James McMahon, Assad Zahid

ORCID number: Aneesh Dave (0000-0002-9128-7048); James McMahon (0000-0002-2656-0466); Assad Zahid (0000-0002-4401-416X).

Author contributions: All authors equally contributed to this paper with conception and design of the study, literature review and analysis, drafting and critical revision and editing, and final approval of the final version.

Conflict-of-interest statement: No potential conflicts of interest.

Received: February 15, 2019
Peer-review started: February 17, 2019
First decision: March 14, 2019
Revised: March 23, 2019
Accepted: March 29, 2019
Article in press: March 30, 2019
Published online: May 21, 2019

P-Reviewer: Jun C, Szilagyi A
S-Editor: Yan JP
L-Editor: A
E-Editor: Ma YJ

Aneesh Dave, James McMahon, Assad Zahid, Department of Colorectal Surgery, Royal Prince Alfred Hospital, Camperdown 2050, New South Wales, Australia

Aneesh Dave, Assad Zahid, Sydney Medical School, Edward Ford Building, the University of Sydney, Camperdown 2006, New South Wales, Australia

Corresponding author: Assad Zahid, BSc, MBBS, MPhil, Surgeon, Department of Colorectal Surgery, Royal Prince Alfred Hospital, Missenden Road, PO Box 4270, Camperdown 2050, New South Wales, Australia. assad.zahid@nhs.net
Telephone: +61-295156111

Abstract

Congenital peritoneal encapsulation (CPE) is a very rare, congenital condition characterised by the presence of an accessory peritoneal membrane which encases a variable extent of the small bowel. It is unclear how CPE develops, however it is currently understood to be a result of an aberrant adhesion in the peritoneal lining of the physiological hernia in foetal mid-gut development. The condition was first described in 1868, and subsequently there have been only 45 case reports of the phenomenon. No formal, systematised review of CPE has yet been performed, meaning the condition remains poorly understood, underdiagnosed and mismanaged. Diagnosis of CPE remains clinical with important adjuncts provided by imaging and diagnostic laparoscopy. Two thirds of patients present with abdominal pain, likely secondary to sub-acute bowel obstruction. A fixed, asymmetrical distension of the abdomen and differential consistency on abdominal palpation are more specific clinical features present in approximately 10% of cases. CPE is virtually undetectable on plain imaging, and is only detected on 40% of patients with computed tomography scan. Most patients will undergo diagnostic laparotomy to confirm the diagnosis. Management of CPE includes both medical management of the critically-unstable patient and surgical laparotomy, partial peritonectomy and adhesiolysis. Prognosis following prompt surgical treatment is excellent, with a majority of patients being symptom free at follow up. This review summarises the current literature on the aetiology, diagnosis and treatment of this rare disease. We also introduce a novel classification system for encapsulating bowel diseases, which may distinguish CPE from the commoner, more morbid conditions of abdominal cocoon and encapsulating peritoneal sclerosis.

Key words: Congenital; Encapsulation; Peritoneum; Cocoon; Sclerosis

Core tip: Congenital peritoneal encapsulation (CPE) is a very rare congenital disorder characterised by the presence of an accessory peritoneal membrane surrounding the entirety of the small intestine. Though not fully understood, it is thought to arise due to an aberrant peritoneal adhesion during foetal mid-gut development. It is a rare but important cause of undifferentiated abdominal pain and sub-acute small bowel obstruction. We present a comprehensive review of CPE including an international epidemiological focus, diagnosis and treatment. We also describe a novel classification system for encapsulating bowel diseases.

Citation: Dave A, McMahon J, Zahid A. Congenital peritoneal encapsulation: A review and novel classification system. *World J Gastroenterol* 2019; 25(19): 2294-2307
URL: https://www.wjgnet.com/1007-9327/full/v25/i19/2294.htm
DOI: https://dx.doi.org/10.3748/wjg.v25.i19.2294

INTRODUCTION

Congenital peritoneal encapsulation (CPE) is a very rare, congenital malformation of the gastro-intestinal tract. It is characterised by the presence of an accessory peritoneal membrane which covers a variable extent of the small bowel. This in turn creates an accessory extra-peritoneal sac in which the bowel is contained. The membrane is morphologically and histologically identical to peritoneum. The condition is often asymptomatic, detected incidentally during routine imaging or surgery and even in posthumous dissection. However, CPE also remains a rare but important cause of recurrent, undifferentiated abdominal pain and sub-acute small bowel obstruction. The condition was first described by Cleland[1] in 1868 as a 'secondary sac bounded by omentum and meso-colon, and communicating with the general sac by means of a small aperture'. Since this time, it has been described in less than fifty cases. To our knowledge, there has been no prior definitive, systematised review of CPE, and therefore the condition has remained poorly understood, underdiagnosed and mismanaged. This review attempts to integrate all the literature available to provide an understanding of the aetiology, pathology, diagnosis and management of this rare and unusual condition. In addition, we provide a novel classification system for encapsulating bowel diseases, which categorises CPE and the similar phenomena of abdominal cocoon and encapsulating peritoneal sclerosis (EPS) in a histo-morphological manner.

METHODS

An electronic, systematic search of the literature was performed using several databases, including Medline, PubMED, Scopus and Google Scholar (Figure 1). The search was not limited by English language restriction or by date of publication. The following search terms were used as keywords: "Peritoneal Encapsulation", "Congenital Peritoneal Encapsulation" and "Abdominal Cocoon". The electronic search was augmented by means of manual searches of the reference lists of the selected publications. Article titles and abstracts were reviewed independently by two investigators for relevance to CPE. A significant volume of the literature reported cases of the more common abdominal cocoon or EPS, and these were excluded. Most cases of CPE could be identified and included through the abstract alone. If further clarification was required, clinical information, histopathology and photographs were used to determine cases. Full manuscripts of articles were read thoroughly and independently by two investigators, and information was extracted, including age, sex, past medical history, clinical information, diagnostic studies, management, histopathology and follow-up status. In two case reports[2,3] full articles could not be found either by contacting the journal or the relevant authors. In these cases, the abstracts alone were used to gather information. In total, 42 reports[1-42] describing 45 separate cases of CPE were found and collated. Table 1 demonstrates the key demographic and clinical information obtained from the cases.

Table 1 Patient demographics and key clinical characteristics

Case	Ref.	Year	Country	Age	Sex	Clinical Features	Tests	Manage-ment	Other
1	McMahon *et al*[23]	2018	Australia	20	M	Intermittent abdominal pain, distension	CT	Surgical resection of sac	Symptom free recovery
2	Wolski *et al*[41]	2017	Poland	12	M	Abdominal pain for 1 wk	XR, US	Surgical resection of sac	Post-operative complication of adhesion SBO
3	Griffith *et al*[13]	2017	United Kingdom	12	M	Abdominal pain and vomiting for 1 wk	XR, US	Surgical resection of sac	Gangrenous acalculous cholecystitis
4	Arumugam *et al*[6]	2017	India	22	F	Small bowel obstruction, assymetric distension	CT	Surgical resection of sac	
5	Zoulamoglou *et al*[42]	2016	Greece	28	F	Intermittent abdominal pain for 1 yr, asymmetric distension	XR, CT	Surgical resection of sac	
6	Teixeira *et al*[36]	2015	Portugal	25	M	Small bowel obstruction. Fixed, assymetrical distension	XR, CT	Surgical resection of sac	
7	Stewart *et al*[35]	2014	Australia	16	M	Intermittent, chronic abdominal pain	XR, US	Surgical resection of sac	
8	Wani *et al*[40]	2013	India	28	M	Generalised, intermittent abdominal pain	XR, CT, labs	Surgical resection of sac	
9	Naidoo *et al*[26]	2013	India	40	M	Stab wound	XR, fluoro, CT	Surgical resection of sac	Stabbing injury
10	Mitrousias *et al*[24]	2012	Greece	78	F	3 d of abdominal pain	XR, CT, labs	Surgical resection of sac	Helical pattern on CT
11	Shamsuddin *et al*[30]	2012	Pakistan	16	F	Small bowel obstruction	XR	Failed conservative. Surgical resection.	Excellent recovery
12	Ince *et al*[15]	2012	Turkey	71	M	Small bowel obstruction	XR, US, CT	Ileocaecal resection	
13	Al-Taan *et al*[5]	2010	United Kingdom	82	M	Asympto-matic		Surgical resection of tumour and sac	Bowel cancer
14	Kumara *et al*[17]	2009	Sri Lanka	44	F	Cushing's syndrome secondary to right adrenal tumour	CT	Surgical resection of tumour and sac	Adrenal tumour
15	Sherigar *et al*[31]	2007	United Kingdom	85	F	Small bowel obstruction	XR, CT	Surgical resection of sac	Patient died from chest sepsis
16	Basu *et al*[9]	2006	India	21	F	Distension, peritonism	XR, US, labs	Resection of sac, appendix, lavage	7 yr follow up
17	Chew *et al*[11]	2006	Singapore	38	M	Small bowel obstruction	XR, CT	Surgical resection of sac	

18	Shioya *et al*[32]	2005	Japan	34	M	Small bowel obstruction, right inguinal hernia	XR, labs	Surgical resection of sac	Excellent recovery
19	Okobia *et al*[2]	2001	Nigeria	15	F	Abdominal pain			
20	Mordehai *et al*[25]	2001	Israel	14	F	Abdominal pain, vomiting, weight loss	XR, US	Surgical resection of sac	Post-operative ileus
21	Naraynsingh *et al*[27]	2001	West Indies	64	M	Abdominal pain, fixed asymmetrical distension, differential palpation		Surgical resection of sac	
22	Lee *et al*[19]	2000	South Korea	22	F	Abdominal pain, distension	XR, CT, labs	Failed conservative management. Surgical resection of sac	Excellent recovery
23	Kyaw *et al*[18]	1998	Singapore	11	M	Abdominal pain for 5 d, soft mass left flank	US, CT	Surgical resection of sac	Hydrone-phrosis
24	Casas *et al*[10]	1998	Spain	43	M	Intermittent abdominal pain for 6 mo	XR, fluoro, US, CT	Surgical resection of sac	Hydrone-phrosis. Asympto-matic at 14 mo
25	Constantinides *et al*[12]	1998	Italy	49	F	Found at autopsy. Intermittent, severe abdominal pain during life.			
26	Adedeji *et al*[4]	1994	United Kingdom	40	M	Abdominal pain, peritonism for 1 d	XR, labs	Surgical resection of sac	
27	Tsunoda *et al*[38]	1993	Japan	52	M	Small bowel obstruction, central abdominal mass	XR, US, CT	Surgical resection of sac	Asympto-matic at 8 mo
28	Silva *et al*[34]	1992	Japan	29	M	Intermittent abdominal pain, scaphoid abdomen	XR, fluoro, CT, labs	Surgical resection of sac	Patient died due to gangrenous small bowel
29	Awasthi *et al*[8]	1991	India	16	F	Abdominal pain for 9 mo, distension	XR, fluoro	Surgical resection of sac	Discharged day 6 with resolution of symptoms.
30	Arora *et al*[3]	1989	India		F	Abdominal pain			Colorectal cancer
31	Askew *et al*[7]	1988	United Kingdom		M	Incidental finding during surgery			
32	Walsh *et al*[39]	1988	Ireland	82	M	Small bowel obstruction	XR		
33	Huddy *et al*[14]	1988	United Kingdom	56	M	Intermittent abdominal pain	XR	Surgical resection of sac	
34	Lifschitz *et al*[22]	1987	Ciskei	66	M	Abdominal pain, vomiting, distension for 3 wk	XR, labs	Surgical resection of sac	

35	Jamieson *et al*[16]	1985	United Kingdom			Incidental finding during laparotomy		Surgical resection of sac	Colorectal cancer
36	Sieck *et al*[33]	1983	Saudi Arabia	14	F	Nausea, vomiting, distension for 3 mo	XR, fluoro, labs	Surgical resection of sac	Patient had breast cancer
37	Sieck *et al*[33]	1983	Saudi Arabia	65	F	Intermittent pelvic pain, fever, abdominal distension for 5 yr		Surgical resection of sac	
38	Sayfan *et al*[29]	1979	Israel	12	F	Abdominal pain, vomiting for 1 d	XR, labs	Surgical resection of sac	Excellent recovery. Discharged day 7
39	Lewin *et al*[20]	1970	United States	66	M	Post-mortem examination. Patient died of acute myocardial infarct.			
40	Thorlaksen *et al*[37]	1953	Canada	57	M	Diarrhoea, abdominal pain for several years	XR, labs	Initial conservative management successful.	
41	Thorlaksen *et al*[37]	1953	Canada	53	M	Incidental finding in asymptomatic patient	XR, labs	Surgical resection of sac	Car accident, intra-abdominal haemmor-hage
42	Thorlaksen *et al*[37]	1953	Canada	64	M	Epigastric pain, constipation for 2 yr	XR, labs	Surgical resection of sac	
43	Papez *et al*[28]	1932	United States	61	M	Cadaveric dissection			
44	Lickley *et al*[21]	1907	United Kingdom	52	M	Autopsy. Asympto-matic during life			
45	Cleland *et al*[1]	1868	Ireland			Cadaveric dissection			

XR: X-Ray; CT: Computed tomography; US: Ultrasound scan; Fluoro: Fluoroscopic imaging; Labs: Laboratory investigations.

AETIOLOGY

The cause of CPE remains poorly understood, however it likely develops at the time the foetal mid-gut herniates into the umbilical cord at 8-10 wk gestation. The most widely accepted aetiology is attributed to Papez[28], who postulates that it is caused by an aberrant peritoneal adhesion between the linings of the physiological umbilical hernia and the caudal duodenum. Within the cord, the mid-gut is encased by peritoneum which lines the hernia walls like a sack. The neck of this sac is thus intimately adjacent to the caudal duodenum. If an adhesion forms between these peritoneal layers, significant traction forces are placed on the peritoneum which lines the mid-gut at the time the hernia is reduced. This may cause it to peel off and surround the small bowel as an extra-peritoneal accessory sac. This theory successfully explains the morphological resemblance of the membrane to peritoneum and its extra-peritoneal location.

A competing theory by Thorlakson *et al*[37] suggests that CPE may develop due to an abnormality in the reduction of the physiological hernia. The proximal limb of the hernia (which forms jejunum and ileum) is usually reduced first, naturally occupying the lower left of the abdomen. This causes the dorsal mesentery to be pushed to the left. Following this, the distal limb reduces and passes cranially to lie just caudal the liver. Instead, if the distal limb were to reduce first and inappropriately occupy the lower left quadrant, the proximal limb would be forced more caudally and toward the

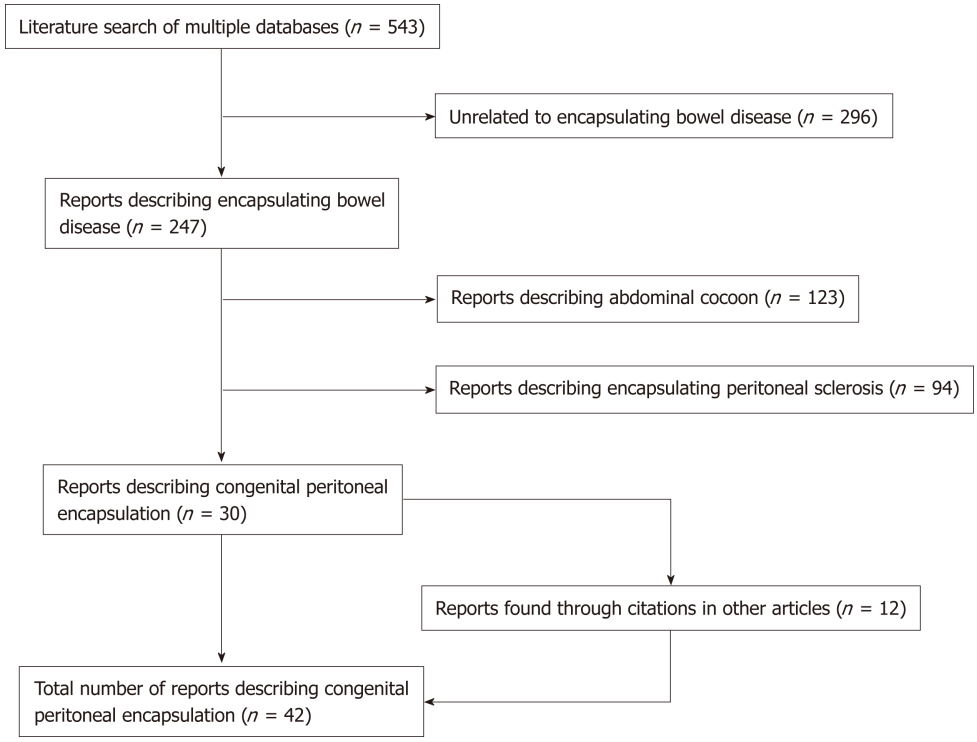

Figure 1 Literature search.

right. The distal limb would then attempt a migration toward the right iliac fossa, and in doing so its dorsal mesentery would cover the entirety of the proximal limb, thereby forming the peritoneal sac over the mid-gut. However, if this were the case, it would be expected that there would be significant mesenteric abnormalities such as mal-position and mal-rotation, which are not always associated with CPE.

EPIDEMIOLOGY

Given the rarity of the condition, the incidence and prevalence of CPE is difficult to quantify. However, CPE does not appear to have any predilection toward particular ethnicities. Table 2 demonstrates the geographic distribution of cases. 42% of cases were reported from Europe, with the most common countries being United Kingdom (*n* = 8), Israel (*n* = 2)[25,29], Greece (*n* = 2)[24,42] and Ireland (*n* = 2)[1,39]. India has the second highest number of cases after the United Kingdom, with six in total[3,6,8,9,26,40]. The mean age of patients at the time of diagnosis was 40.8 (range 11-85 years). Interestingly, there is a 5:3 male predominance. The mean age of diagnosis for males and females was 46 and 32 respectively. This reflects a differential pattern of presentation between genders. Females are diagnosed earlier, with a majority presenting prior to 30 years. In contrast, males display a bi-modal age distribution, with peak presentations occurring in the 20-30 years and 60-70 year period. Medical co-morbidities of patients were documented in some reports, however it is unclear whether these are causally linked to CPE. Three patients had a diagnosis of co-morbid cancer. Two of these patients had gastro-intestinal cancer[5,16] and one of the breast[33]. One patient had an incomplete situs inversus and congenital epigastric hernia[15] and two patients had co-morbid inguinal hernia[11,32].

CLASSIFICATION OF ENCAPSULATING BOWEL DISEASES

Classification system

CPE is one type of a collection of conditions which are characterised by encapsulation of the bowel. We introduce a novel classification system which aims to distinguish CPE from the similar, yet discrete, conditions of abdominal cocoon and EPS (Figure 2). Abdominal cocoon and EPS were first described over 100 years ago by Owtschinnikow[43] and have been aptly reviewed by Danford *et al*[44]. These are acquired conditions which are characterised by a thick fibro-collagenous encasing of

Table 2 Geographical distribution of cases

Country	Case number
United Kingdom	8
India	6
Canada	3
Japan	3
Australia	2
Greece	2
Ireland	2
Israel	2
Saudi Arabia	2
Singapore	2
United States	2
Ciskei	1
Italy	1
South Korea	1
Nigeria	1
Pakistan	1
Poland	1
Portugal	1
Spain	1
Sri Lanka	1
Turkey	1
West Indies	1

the small and large bowel. As such, they have a different aetiology, pathogenesis, and management to CPE. EPS describes cases of the disease that have known associations or aetiological factors, such as abdominal trauma and peritoneal dialysis. Abdominal cocoon, a term first used by Foo *et al*[45] in 1976, describes idiopathic cases of this disease with no known aetiological factors. We also introduce a novel, broader term, "Fibrotic Peritoneal Encapsulation (FPE)" or FPE, to denote the entire spectrum of these diseases, both primary and secondary. This term adequately describes both the morphology and histopathology of this disease, differentiating it from CPE.

Fibrotic peritoneal encapsulation

A robust discussion of FPE, both primary and secondary, is outside the scope of this review, and has been reported elsewhere[44,46-49]. However key differences between fibrotic encapsulating bowel diseases and CPE should be noted as part of forming a differential diagnosis. These are highlighted in Table 3. Firstly FPE is an acquired condition which is far more common than CPE. In most cases, there is a known secondary cause for the disease[44]. The most common of these is peritoneal dialysis[50], in which the annual incidence of FPE varies from 0.14%-2.5%[51,52]. Other causative factors include local irritant factors (abdominal trauma[53], abdominal surgery[54], peritoneal shunts[55], peritoneal tuberculosis[56], peritoneal foreign body[57], intra-peritoneal chemotherapy[58]) and systemic factors (beta blocking agents[59], methotrexate[60], cirrhosis[61], Systemic Lupus Erythematosus[62], malignancy, sarcoidosis[63]). FPE is considered to be an inflammatory process, which leads to scarring and fibrosis of the peritoneal membranes through a process of cytokine and cell-mediated inflammation[64]. Furthermore, FPE tends to be significantly more symptomatic and morbid compared to CPE. Following commencement of peritoneal dialysis, an estimated 20% of patients will develop FPE at 8 years[50]. Patients tend to present with bowel obstruction, and long-standing intermittent abdominal pain. 29% of patients with FPE require emergency surgery at the time of presentation[65], and the mortality at one year is as high as 50%[66]. The morphological and histological pathology is the most definitive differentiating factor of FPE. Morphologically, FPE appears as a thick, firm, fibrotic membrane. It is separate from the peritoneum, but may have significant adhesions to the peritoneum and other surrounding structures. Histologically, FPE is characterised by dense fibro-connective tissue proliferation, chronic inflammatory cell infiltration and dilated lymphatics. This differs to CPE, which is histologically identical to peritoneum, and displays no inflammatory

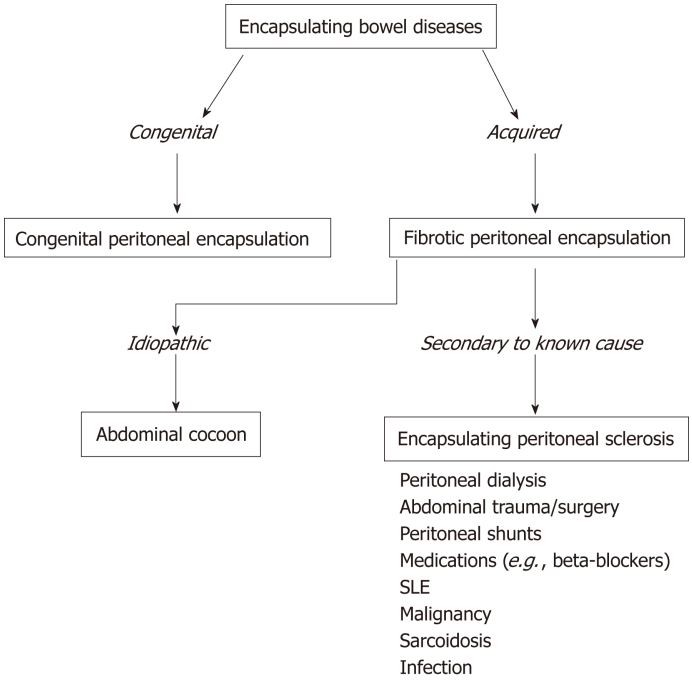

Figure 2 Classification system for encapsulating bowel diseases. SLE: Systemic lupus erythematosus.

component.

Abdominal cocoon

Abdominal Cocoon, also called idiopathic FPE, was first described by Foo *et al*[45] in 1978 as a form of FPE where no established cause can be identified. Foo's case series reported on three adolescent girls who presented with bowel obstruction and were found to have thick, fibrotic peritoneal membranes at laparotomy. Since that time, approximately 75 case reports of abdominal cocoon have been reported, and have been summarised by Akbulut[67]. The disease is most prevalent in India, China and Turkey and has no obvious gender or age distribution. Though historically abdominal cocoon was thought to affect adolescent girls, more recent studies have shown that it tends to occur mainly in equatorial areas and may be twice as common in males. It has been suggested abdominal cocoon may be caused by 'subclinical peritonitis'[45], possibly as a result of retrograde menstruation, with a complex interplay with superimposed viral infections, salpingitis and cell mediated tissue damage[68]. This, of course, fails to explain its preponderance in males. Other studies have suggested that perhaps developmental disorders, vascular anomalies or omental hypoplasia[69] may be the basis of the disease.

DIAGNOSIS

Clinical presentation

The diagnosis of CPE remains clinical, though confirmation may be obtained through diagnostic imaging and laparotomy. There is no defining gold-standard for diagnosis of CPE and this means the condition may be underdiagnosed. A proposed diagnostic algorithm is provided in Figure 3, which highlights the key clinical, radiographic and pathological features of CPE.

Symptoms associated with a presentation of CPE very likely reflect the development of an acute or sub-acute small bowel obstruction, with abdominal pain, tenderness, nausea and vomiting being the predominant clinical features. Abdominal pain is the most common cause for presentation in CPE, with 66% (n = 30) of patients reporting sudden or chronic. In these patients, 53% (n = 16) reported similar symptoms in the preceding 12 mo, usually with decreased severity. This implies that CPE may be a cause for undifferentiated, intermittent chronic abdominal pain, and diagnosis is generally delayed. Hence, CPE should be suspected in patients presenting with these symptoms. Many patients also described nausea, vomiting and constipation associated with the onset of abdominal pain. On abdominal examination, abdominal tenderness was described in 58% of patients (n = 26), usually in the peri-

Table 3 Key differences between congenital peritoneal encapsulation and fibrotic peritoneal encapsulation

	Congenital peritoneal encapsulation	Fibrotic peritoneal encapsulation
Aetiology		
Cause	Congenital	Acquired
Trigger		Primary/Idiopathic (abdominal cocoon) or secondary (encapsulating peritoneal sclerosis)
Epidemiology		
Incidence	45 cases	Idiopathic: 184 cases Secondary: Based on cause
Age (yr, range)	40.8 (11-85)	34.7 (7-87)
Sex (M:F)	5:3	2:1
Geographical Geography	Europe, Sub-continental Asia	Equatorial regions
Pathology		
Morphology	Identical to peritoneum. Thin, semi-transparent, vascularised, soft.	Similar to scar tissue. Thick, white, firm, fibrotic.
Histopathology	Identical to peritoneum. Mesothelial lining, fibro-connective tissue.	Dense fibro-connective tissue proliferation, chronic inflammatory cell infiltration and dilated lymphatics
Manage-ment		
Treatment	Peritonectomy, adhesiolysis	Corticosteroids, tamoxifen, peritonectomy
Prognosis	Excellent. Near complete resolution of symptoms.	Up to 50% mortality at 1 yr following diagnosis.

umbilical area. Peritoneal irritation (defined as one or more of involuntary guarding, rigidity or rebound tenderness) was described in 27% (n = 12) of cases. Abdominal distension was reported in 40% (n = 18) of cases, and seven cases described bowel sounds as being "high pitched", "exaggerated: or "hyper-active". One case described acute compression of the abdominal aorta due to CPE, resulting in extensive small bowel necrosis and death[34].

Two unique clinical features of CPE have been described, which may be more specific and aid a more prompt diagnosis. A fixed, asymmetrical distension of the abdomen was reported in 16% (n = 7) of cases. The distension was considered fixed if it was noted not to vary with peristaltic activity, and likely represents the fixed position of the bowel which is trapped within the accessory membrane. Secondly, a differential consistency of the abdominal wall to palpation has been described in several cases of CPE. It is thought that areas of the bowel which are covered by the membrane tend to be fixed, flat and firm, whilst areas which are outside of the membrane are distended and soft (as in small bowel obstruction).

In seven cases, CPE was found incidentally during surgery in asymptomatic patients. These patients were undergoing abdominal surgery for other reasons: namely, colorectal cancer[5,16], obstructive jaundice[7], right adrenal tumour[17], penetrating stab wound injury[26], tubo-ovarian abscess[33] and intra-abdominal haemorrhage[37]. Four cases of CPE were diagnosed at autopsy in patients who had no reported abdominal symptoms or complaints during life[1,20,21,28].

Imaging

Though the diagnosis of CPE remains clinical, a variety of imaging modalities may be used to aid in diagnosis. Importantly, these modalities may also screen medically unstable patients for complications of small bowel obstruction, including perforation, haemorrhage and ischemia. The use of plain X-ray has been reported in 30 cases. The majority of films showed signs of small bowel obstruction, with 56% (n = 17) reporting central, dilated loops of small bowel and 33% (n = 7) reporting air fluid levels. Two cases reported the presence of hydronephrosis[10,18]. It should be noted that 23% (n = 7) of cases reported no abnormality on plain films, and hence this modality alone cannot be reliably used to diagnose CPE. The use of contrast with X-Ray was used in 10 studies to better visualise CPE. The majority of fluoroscopic cases demonstrated non-specific features of small bowel obstruction. However, three cases demonstrated a concertina or serpentiform pattern of small bowel arrangement[26,33,36]. This sign occurs when the small bowel is packed tightly on to itself in layers within the accessory sac, such that is resembles a coiled snake or concertina. This sign is more specific to CPE, and if found it should warrant further imaging.

Fifteen reports documented the use of computed tomography (CT). Only 40% (n = 6) of these cases reported radiological evidence of a membranous capsule

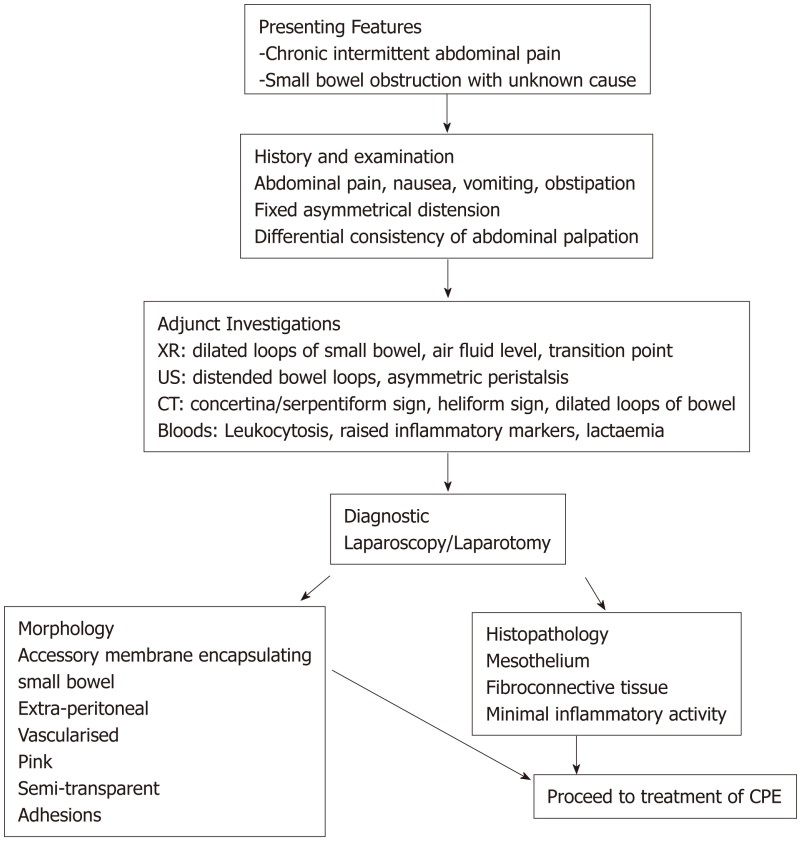

Figure 3 Diagnostic algorithm for congenital peritoneal encapsulation. XR: X-ray; CT: Computed tomography; US: Ultrasound scan; CPE: Congenital peritoneal encapsulation.

surrounding the bowel, as seen in Figure 4. Hence, CT scanning may not have the resolution to visualise the accessory sac in all cases, and should remain only an adjunct to a clinical diagnosis. Other features commonly reported in CT scans include dilated loops of bowel in 46% of cases (n = 7), and fluid collection in 12% of cases (n = 2). Mitrousias *et al*[24] described a novel helical pattern of small bowel within the membranous sac on 3D volume rendered imaging. Ultrasonography has also been used in nine cases, of which four reported no significant abnormalities. Other findings included small bowel dilation, ascites[25], hydronephrosis[10] and gall bladder distension[9].

It is clear that imaging is neither sensitive nor specific in identifying cases of CPE. It should therefore be used only as an adjunct to aid in the diagnosis of CPE. Imaging does, however, maintain an important role in determining the presence and severity of complications in medically unwell patients, such as acute bowel obstruction, perforation, ischaemia and bleeding.

Laboratory investigations

No specific laboratory studies exist for aiding in the diagnosis of CPE. Routine blood tests were reported in 13 studies. In six of these, leucocytosis or raised inflammatory markers were noted. In the remaining seven cases, all blood tests were within normal ranges.

ANATOMICAL PATHOLOGY

A majority of CPE cases are diagnosed at the time of direct visual inspection during diagnostic laparotomy or laparoscopy, as seen in Figure 5. 69% (n = 31) of cases described the accessory sac in CPE as morphologically similar to that of peritoneum. This is consistent with Papez's theory of CPE as an accessory peritoneal membrane derived from the umbilical hernia. The membrane is typically semi-transparent, vascularised and thin. This contrasts markedly with the thick, white, fibrotic capsule in FPE. The extent of encapsulation of the small bowel in CPE was reported in most cases. 25 cases reported the sac encasing the entirety of the small bowel. The sac typically starts at the duodeno-jujenal junction, to a point within approximately 10-40

Figure 4 Computed tomography scan (coronal view) of patient with congenital peritoneal encapsulation.

cm of the ileo-caecal junction. Four cases described the accessory sac as covering only a small part of the ileum. In cases of small bowel obstruction, the transition point was typically found at the proximal opening of the accessory membrane.

HISTOPATHOLOGY

Histopathology was reported in only 14 of the 42 cases. Four of these cases reported histopathological findings consistent with normal peritoneal tissue. In two of these reports, there were features suggestive of active inflammation. Fibrosis (n = 2), fibrous tissue (n = 3), fibro-connective tissue (n = 1) and fibrovascular tissue (n = 1) were reported in 7 cases. Two of these cases also reported the presence of mesothelial cells. The remaining histopathological reports included non-specific chronic inflammatory changes, membranous and elastic bundles and an isolated report of mesothelium.

MANAGEMENT AND PROGNOSIS

Treatment of CPE can be conservative, medical or surgical. Conservative management has only been described in a single case of CPE, which was asymptomatic and diagnosed incidentally on routine imaging. The patient remained well and required no further medical management. Medical management generally involves the resuscitation, stabilisation and treatment of the unstable patient with CPE. This is likely due to acute small bowel obstruction and the potential complications associated with this, including perforation, ischaemia, necrosis and haemorrhage. A majority of patients that were hospitalised with CPE were fasted and received nasogastric decompression, intravenous fluid therapy, intravenous anti-biotics and intravenous proton pump inhibitors.

Surgical management consists of exploratory laparotomy, peritonectomy, adhesiolysis and enterolysis. Excision of the sac is usually performed from along its attachments proximally and distally. This has generally been described as a straightforward procedure, devoid of major intra-operative hazards, likely because the accessory sac is extra-peritoneal. Most importantly, adhesions at the neck of the sac must be carefully resected to ensure complete release of the bowel and prevent bowel obstruction and ischaemia post-operatively. In our experience[23], the most difficult part of the procedure is at the time of releasing the proximal neck of the sac. It may lie adjacent to the duodeno-jejunal flexure, and is hence in close proximity to the superior mesenteric vasculature. Care should be taken in this step to ensure the vessels remain undamaged, whilst ensuring complete resection o the sac and any associated adhesions.

Prognosis following prompt surgical management of CPE is excellent. 14 cases reported excellent post-operative recovery with no complications. Length of hospital stay was recorded in 8 cases, with an average of 13 d, and a range of 6-33 d. Very few papers have reported on long term follow up of patients, with the longest being 7 years of symptom free survival[9]. Two patients died during the initial hospital admission: One patient died due to sepsis secondary to a chest infection[31], and the other died due to extensive bowel necrosis[34]. This latter patient was noted to have extensive gangrenous small bowel at the time of initial laparotomy, presumably due to acute bowel obstruction and compression of the abdominal aorta. On re-look

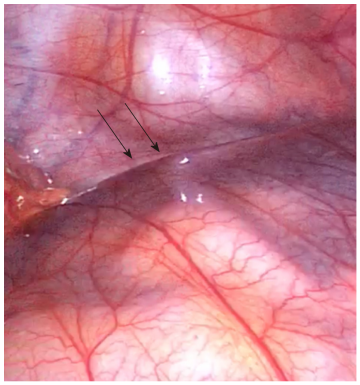

Figure 5 Accessory peritoneal membrane, with attachment to posterior body wall (arrow).

laparotomy after 24 h, the patient went into cardiac arrest and died. Other complications that have been reported with CPE include post-operative ileus[25], bowel obstruction secondary to adhesions[41], biliary fistula[37] and duodenal ulceration requiring resection[37].

CONCLUSION

CPE is a very rare, congenital condition which has been described in less than fifty cases in the literature. For this reason, it remains poorly understood, underdiagnosed and mismanaged. It is an important consideration in patients with long-standing, undifferentiated, intermittent abdominal pain, and these patients should be investigated appropriately. More rarely, patients can develop acute bowel obstruction due to CPE, and warrant hospitalisation, medical stabilisation and emergency surgical procedures. The diagnosis remains clinical, with several unique clinical findings of CPE including a fixed, asymmetrical abdomen being specific indicators of the disease. Adjuncts such as plain imaging, fluoroscopy, CT scanning and ultrasound may also be used in conjunction to aid in diagnosis. Ultimately, most patients undergo diagnostic laparotomy and excision of the accessory peritoneal layer, which results in an excellent prognosis. It is yet unclear what causes CPE, and further work is required to elucidate this as it may provide insights in better identifying patients at risk, and treating them accordingly.

REFERENCES

1 **Cleland**. On an Abnormal Arrangement of the Peritoneum, with Remarks on the Development of the Mesocolon.. *West Afr J Med* 1868; 201-206 [PMID: 17230753]
2 **Okobia MN**, Osime U, Evbuomwan I. Congenital peritoneal encapsulation of small intestine: A case report. *West Afr J Med* 2001; **20**: 279-281 [PMID: 11922170]
3 **Arora PK**, Narang R, Sethna KS, Gupta D. Peritoneal encapsulation of small bowel--(a case report). *J Postgrad Med* 1989; **35**: 219-221 [PMID: 2641523]
4 **Adedeji OA**, McAdam WA. Small bowel obstruction due to encapsulation and abnormal artery. *Postgrad Med J* 1994; **70**: 132-133 [PMID: 8170887 DOI: 10.1136/pgmj.70.820.132]
5 **Al-Taan OS**, Evans MD, Shami JA. An asymptomatic case of peritoneal encapsulation: Case report and review of the literature. *Cases J* 2010; **3**: 13 [PMID: 20150981 DOI: 10.1186/1757-1626-3-13]
6 **Arumugam PK**, Dalal AK. Peritoneal encapsulation - an unexpected cause of acute intestinal obstruction. *J Visc Surg* 2017; **154**: 303-305 [PMID: 28688775 DOI: 10.1016/j.jviscsurg.2017.06.001]
7 **Askew G**, Sykes PA. Encapsulated small bowel: An anatomical curiosity explained. *J R Coll Surg Edinb* 1988; **33**: 224 [PMID: 3221346]
8 **Awasthi S**, Saraswat VA, Kapoor VK. Peritoneal encapsulation of the small bowel: A rare cause of intestinal obstruction. *Am J Gastroenterol* 1991; **86**: 383 [PMID: 1998328 DOI: 10.3109/00365529108996507]
9 **Basu A**, Gupta A, Biswas S. An interesting case of a left paraduodenal hernia with peritoneal encapsulation presenting as acute intestinal obstruction. *Hellenic J Surg* 2014; **86**: 109 [DOI: 10.1007/s13126-014-0108-y]
10 **Casas JD**, Mariscal A, Martínez N. Peritoneal encapsulation: CT appearance. *AJR Am J Roentgenol* 1998; **171**: 1017-1019 [PMID: 9762988 DOI: 10.2214/ajr.171.4.9762988]
11 **Chew MH**, Sophian Hadi I, Chan G, Ong HS, Wong WK. A problem encapsulated: The rare peritoneal encapsulation syndrome. *Singapore Med J* 2006; **47**: 808-810 [PMID: 16924364]
12 **Costantinides F**, Di Nunno N, Bernasconi P, Jonjic N, Melato M. A new type of peritoneal encapsulation of the small bowel. *Am J Surg Pathol* 1998; **22**: 1297-1298 [PMID: 9777993 DOI: 10.1097/00000478-199810000-00018]
13 **Griffith D**, Boal M, Rogers T. Peritoneal encapsulation; a rare cause of bowel obstruction. *Ann R Coll*

Surg Engl 2017; **99**: e11-e12 [PMID: 27502346 DOI: 10.1308/rcsann.2016.0264]
14 **Huddy SP**, Bailey ME. Small bowel obstruction due to peritoneal encapsulation. *Br J Surg* 1988; **75**: 262 [PMID: 3349335 DOI: 10.1002/bjs.1800750325]
15 **Ince V**, Dirican A, Yilmaz M, Barut B, Ersan V, Yilmaz S. Peritoneal encapsulation in a patient with incomplete situs inversus. *J Coll Physicians Surg Pak* 2012; **22**: 659-660 [PMID: 23058152]
16 **Jamieson NV**. An anatomical curiosity. *Ann R Coll Surg Engl* 1985; **67**: 237 [PMID: 4037634 DOI: 10.1097/00000658-198506000-00018]
17 **Kumara TL**, Kollure SK. A case of peritoneal encapsulation syndrome. *Ceylon Med J* 2009; **54**: 17-18 [PMID: 19391451 DOI: 10.4038/cmj.v54i1.468]
18 **Kyaw K**. Left mesocolic hernia or peritoneal encapsulation?--a case report. *Singapore Med J* 1998; **39**: 30-31 [PMID: 9557102]
19 **Lee S**, Kim JC, Yun SS, Choi SH, Lim KW. A Case of Small Bowel Obstruction due to Peritoneal Encapsulation. *Korean J Gastroenterol* 2000; **35**: 122-125
20 **Lewin K**, McCarthy LJ. Peritoneal encapsulation of the small intestine. *Gastroenterology* 1970; **59**: 270-272 [PMID: 5448203]
21 **Lickley JD**, Cameron J. Note on a Case of Abnormal Disposition of the Peritoneum. *J Anat Physiol* 1906; **41**: 88-90 [PMID: 17232714 DOI: 10.1002/ar.1090010503]
22 **Lifschitz O**, Tiu J, Sumeruk RA. Peritoneal encapsulation of small intestine. A case report. *S Afr Med J* 1987; **71**: 452 [PMID: 3563796]
23 **McMahon J**, Dave A, Zahid A, Austin K. Peritoneal encapsulation as a cause of chronic recurrent abdominal pain in a young male. *J Surg Case Rep* 2018; **2018**: rjy033 [PMID: 29593863 DOI: 10.1093/jscr/rjy033]
24 **Mitrousias V**, Alexiou E, Katsanas A, Batzalexis K, Germanos S. The helix sign in the peritoneal encapsulation syndrome: A new sign in a rare cause of bowel obstruction? *J Gastrointestin Liver Dis* 2015; **24**: 144 [PMID: 26114169 DOI: 10.15403/jgld.2014.1121.242.hlx]
25 **Mordehai J**, Kleiner O, Kirshtein B, Barki Y, Mares AJ. Peritoneal encapsulation: A rare cause of bowel obstruction in children. *J Pediatr Surg* 2001; **36**: 1059-1061 [PMID: 11431778 DOI: 10.1053/jpsu.2001.24746]
26 **Naidoo K**, Mewa Kinoo S, Singh B. Small Bowel Injury in Peritoneal Encapsulation following Penetrating Abdominal Trauma. *Case Rep Surg* 2013; **2013**: 379464 [PMID: 23533912 DOI: 10.1155/2013/379464]
27 **Naraynsingh V**, Maharaj D, Singh M, Ramdass MJ. Peritoneal encapsulation: A preoperative diagnosis is possible. *Postgrad Med J* 2001; **77**: 725-726 [PMID: 11677284 DOI: 10.1136/pmj.77.913.725]
28 **Papez JW**. A rare intestinal anomaly of embryonic origin. *Anat Rec* 1932; **54**: 197-198 [DOI: 10.1002/ar.1090540209]
29 **Sayfan J**, Adam YG, Reif R. Peritoneal encapsulation in childhood. Case report, embryologic analysis, and review of literature. *Am J Surg* 1979; **138**: 725-727 [PMID: 495863 DOI: 10.1016/0002-9610(79)90359-3]
30 **Shamsuddin S**, Bilal M, Rehman B, Najeeb E, Faisal S. Peritoneal encapsulation presenting as small bowel obstruction in a 16 year old girl. *J Ayub Med Coll Abbottabad* 2012; **24**: 215 [PMID: 24669659]
31 **Sherigar JM**, McFall B, Wali J. Peritoneal encapsulation: Presenting as small bowel obstruction in an elderly woman. *Ulster Med J* 2007; **76**: 42-44 [PMID: 17288307 DOI: 10.1620/tjem.169.345]
32 **Shioya T**, Shibuya T, Tokunaga A, Matsumoto K. Intestinal obstruction due to peritoneal encapsulation of the small bowel: Report of a case. *Nihon Gekakei Rengo Gakkaishi (J Japanese Coll Surg)* 2005; **30**: 625-628 [DOI: 10.4030/jjcs1979.30.4_625]
33 **Sieck JO**, Cowgill R, Larkworthy W. Peritoneal encapsulation and abdominal cocoon. Case reports and a review of the literature. *Gastroenterology* 1983; **84**: 1597-1601 [PMID: 6840491]
34 **Silva MB**, Connolly MM, Burford-Foggs A, Flinn WR. Acute aortic occlusion as a result of extrinsic compression from peritoneal encapsulation. *J Vasc Surg* 1992; **16**: 286-289 [PMID: 1495152 DOI: 10.1016/0741-5214(92)90120-W]
35 **Stewart D**, Rampersad R, King SK. Peritoneal encapsulation as a cause for recurrent abdominal pain in a 16-year-old male. *ANZ J Surg* 2017; **87**: 414-415 [PMID: 25387831 DOI: 10.1111/ans.12907]
36 **Teixeira D**, Costa V, Costa P, Alpoim C, Correia P. Congenital peritoneal encapsulation. *World J Gastrointest Surg* 2015; **7**: 174-177 [PMID: 26328038 DOI: 10.4240/wjgs.v7.i8.174]
37 **THORLAKSON PH**, MONIE IW, THORLAKSON TK. Anomalous peritoneal encapsulation of the small intestine; a report of three cases. *Br J Surg* 1953; **40**: 490-493 [PMID: 13042117 DOI: 10.1002/bjs.18004016317]
38 **Tsunoda T**, Mochinaga N, Eto T, Furui J, Tomioka T, Takahara H. Sclerosing encapsulating peritonitis combined with peritoneal encapsulation. *Arch Surg* 1993; **128**: 353-355 [PMID: 8442696 DOI: 10.1001/archsurg.1993.01420150113021]
39 **Walsh TN**, Russell J. Peritoneal encapsulation of the small bowel. *Br J Surg* 1988; **75**: 1148 [PMID: 3208055 DOI: 10.1002/bjs.1800751134]
40 **Wani I**, Wani K, Wani M, Bhat G, Shah M. Peritoneal encapsulation, left paraduodenal hernia with retroperitonealization of inferior mesenteric vein leading to triple obstruction. *Int J Case Rep Images* 2013; **4**: 169-174 [DOI: 10.5348/ijcri-2013-03-287-CR-8]
41 **Wolski M**, Żerańska M, Piotrowska A, Pomorska K, Kamiński A. Congenital peritoneal encapsulation – A cause of intestinal strangulation in a child. *J Pediatr Surg Case Rep* 2017; **21**: 4-6 [DOI: 10.1016/j.epsc.2017.03.010]
42 **Zoulamoglou M**, Flessas I, Zarokosta M, Piperos T, Kalles V, Tsiaousis I, Kaklamanos I, Sgantzos M, Mariolis-Sapsakos T. Congenital peritoneal encapsulation of the small intestine: A rare case report. *Int J Surg Case Rep* 2016; **27**: 28-31 [PMID: 27522401 DOI: 10.1016/j.ijscr.2016.07.046]
43 **Owtschinnikow P**. Peritonitis chronica fibrosa incapsulata. *Arch für Klin Chir* 1907; **83**: 623-634
44 **Danford CJ**, Lin SC, Smith MP, Wolf JL. Encapsulating peritoneal sclerosis. *World J Gastroenterol* 2018; **24**: 3101-3111 [PMID: 30065556 DOI: 10.3748/wjg.v24.i28.3101]
45 **Foo KT**, Ng KC, Rauff A, Foong WC, Sinniah R. Unusual small intestinal obstruction in adolescent girls: The abdominal cocoon. *Br J Surg* 1978; **65**: 427-430 [PMID: 656764 DOI: 10.1002/bjs.1800650617]
46 **Moinuddin Z**, Summers A, Van Dellen D, Augustine T, Herrick SE. Encapsulating peritoneal sclerosis-a rare but devastating peritoneal disease. *Front Physiol* 2015; **5**: 470 [PMID: 25601836 DOI: 10.3389/fphys.2014.00470]
47 **Kawaguchi Y**, Kawanishi H, Mujais S, Topley N, Oreopoulos DG. Encapsulating peritoneal sclerosis: Definition, etiology, diagnosis, and treatment. International Society for Peritoneal Dialysis Ad Hoc

Committee on Ultrafiltration Management in Peritoneal Dialysis. *Perit Dial Int* 2000; **20** Suppl 4: S43-S55 [PMID: 11098928]
48 **Brown MC**, Simpson K, Kerssens JJ, Mactier RA; Scottish Renal Registry. Encapsulating peritoneal sclerosis in the new millennium: A national cohort study. *Clin J Am Soc Nephrol* 2009; **4**: 1222-1229 [PMID: 19541815 DOI: 10.2215/CJN.01260209]
49 **Korte MR**, Sampimon DE, Betjes MG, Krediet RT. Encapsulating peritoneal sclerosis: The state of affairs. *Nat Rev Nephrol* 2011; **7**: 528-538 [PMID: 21808281 DOI: 10.1038/nrneph.2011.93]
50 **Brown EA**, Bargman J, van Biesen W, Chang MY, Finkelstein FO, Hurst H, Johnson DW, Kawanishi H, Lambie M, de Moraes TP, Morelle J, Woodrow G. Length of Time on Peritoneal Dialysis and Encapsulating Peritoneal Sclerosis - Position Paper for ISPD: 2017 Update. *Perit Dial Int* 2017; **37**: 362-374 [PMID: 28676507 DOI: 10.3747/pdi.2017.00018]
51 **Kawanishi H**, Moriishi M. Epidemiology of encapsulating peritoneal sclerosis in Japan. *Perit Dial Int* 2005; **25** Suppl 4: S14-S18 [PMID: 16300268 DOI: 10.1002/nau.1021]
52 **Betjes MG**, Habib SM, Boeschoten EW, Hemke AC, Struijk DG, Westerhuis R, Abrahams AC, Korte MR. Significant Decreasing Incidence of Encapsulating Peritoneal Sclerosis in the Dutch Population of Peritoneal Dialysis Patients. *Perit Dial Int* 2017; **37**: 230-234 [PMID: 28360369 DOI: 10.3747/pdi.2016.00109]
53 **Kaur S**, Doley RP, Chabbhra M, Kapoor R, Wig J. Post trauma abdominal cocoon. *Int J Surg Case Rep* 2015; **7C**: 64-65 [PMID: 25590647 DOI: 10.1016/j.ijscr.2014.10.081]
54 **Kaman L**, Iqbal J, Thenozhi S. Sclerosing encapsulating peritonitis: complication of laparoscopic cholecystectomy. *J Laparoendosc Adv Surg Tech A* 2010; **20**: 253-255 [PMID: 20374014 DOI: 10.1089/lap.2010.0024]
55 **Sigaroudinia MO**, Baillie C, Ahmed S, Mallucci C. Sclerosing encapsulating peritonitis--a rare complication of ventriculoperitoneal shunts. *J Pediatr Surg* 2008; **43**: E31-E33 [PMID: 18485933 DOI: 10.1016/j.jpedsurg.2008.01.019]
56 **Sharma V**, Mandavdhare HS, Rana SS, Singh H, Kumar A, Gupta R. Role of conservative management in tubercular abdominal cocoon: A case series. *Infection* 2017; **45**: 601-606 [PMID: 28341896 DOI: 10.1007/s15010-017-1012-5]
57 **Árnadóttir M, Jónasson JG, Indridason ÓS**. Encapsulating peritoneal sclerosis following a peritoneal foreign body reaction to Dacron fibres-a case report. *NDT Plus* 2011; **4**: 107-109 [PMID: 25984126 DOI: 10.1093/ndtplus/sfq202]
58 **Takebayashi K**, Sonoda H, Shimizu T, Ohta H, Ishida M, Mekata E, Endo Y, Tani T, Tani M. Successful surgical approach for a patient with encapsulating peritoneal sclerosis after hyperthermic intraperitoneal chemotherapy: A case report and literature review. *BMC Surg* 2014; **14**: 57 [PMID: 25160862 DOI: 10.1186/1471-2482-14-57]
59 **Eltringham WK**, Espiner HJ, Windsor CW, Griffiths DA, Davies JD, Baddeley H, Read AE, Blunt RJ. Sclerosing peritonitis due to practolol: A report on 9 cases and their surgical management. *Br J Surg* 1977; **64**: 229-235 [PMID: 856375 DOI: 10.1002/bjs.1800640402]
60 **Sachdev A**, Usatoff V, Thaow C. Sclerosing encapsulating peritonitis and methotrexate. *Aust N Z J Obstet Gynaecol* 2006; **46**: 58-59 [PMID: 16441697 DOI: 10.1111/j.1479-828X.2006.00517.x]
61 **Wakabayashi H**, Okano K, Suzuki Y. Clinical challenges and images in GI. Image 2. Perforative peritonitis on sclerosing encapsulating peritonitis (abdominal cocoon) in a patient with alcoholic liver cirrhosis. *Gastroenterology* 2007; **132**: 854, 1210 [PMID: 17383416 DOI: 10.1053/j.gastro.2007.01.060]
62 **Pepels MJ**, Peters FP, Mebis JJ, Ceelen TL, Hoofwijk AG, Erdkamp FL. Sclerosing peritonitis: An unusual cause of ascites in a patient with systemic lupus erythematosus. *Neth J Med* 2006; **64**: 346-349 [PMID: 17057274 DOI: 10.1089/jwh.2006.15.977]
63 **Ngô Y**, Messing B, Marteau P, Nouël O, Pasquiou A, Lavergne A, Rambaud JC. Peritoneal sarcoidosis. An unrecognized cause of sclerosing peritonitis. *Dig Dis Sci* 1992; **37**: 1776-1780 [PMID: 1425080 DOI: 10.1007/BF01299875]
64 **Lambie MR**, Chess J, Summers AM, Williams PF, Topley N, Davies SJ; GLOBAL Fluid Study Investigators. Peritoneal inflammation precedes encapsulating peritoneal sclerosis: Results from the GLOBAL Fluid Study. *Nephrol Dial Transplant* 2016; **31**: 480-486 [PMID: 26908833 DOI: 10.1093/ndt/gfv440]
65 **Li N**, Zhu W, Li Y, Gong J, Gu L, Li M, Cao L, Li J. Surgical treatment and perioperative management of idiopathic abdominal cocoon: Single-center review of 65 cases. *World J Surg* 2014; **38**: 1860-1867 [PMID: 24519587 DOI: 10.1007/s00268-014-2458-6]
66 **Balasubramaniam G**, Brown EA, Davenport A, Cairns H, Cooper B, Fan SL, Farrington K, Gallagher H, Harnett P, Krausze S, Steddon S. The Pan-Thames EPS study: Treatment and outcomes of encapsulating peritoneal sclerosis. *Nephrol Dial Transplant* 2009; **24**: 3209-3215 [PMID: 19211652 DOI: 10.1093/ndt/gfp008]
67 **Akbulut S**. Accurate definition and management of idiopathic sclerosing encapsulating peritonitis. *World J Gastroenterol* 2015; **21**: 675-687 [PMID: 25593498 DOI: 10.3748/wjg.v21.i2.675]
68 **Narayanan R**, Bhargava BN, Kabra SG, Sangal BC. Idiopathic sclerosing encapsulating peritonitis. *Lancet* 1989; **2**: 127-129 [PMID: 2567895 DOI: 10.1016/S0140-6736(89)90183-9]
69 **Xu P**, Chen LH, Li YM. Idiopathic sclerosing encapsulating peritonitis (or abdominal cocoon): A report of 5 cases. *World J Gastroenterol* 2007; **13**: 3649-3651 [PMID: 17659721 DOI: 10.3748/wjg.v13.i26.3649]

World Journal of Gastroenterology

Submit a Manuscript: https://www.f6publishing.com

World J Gastroenterol 2019 May 21; 25(19): 2308-2314

DOI: 10.3748/wjg.v25.i19.2308

ISSN 1007-9327 (print) ISSN 2219-2840 (online)

MINIREVIEWS

Autoimmune hepatitis and IgG4-related disease

Kosuke Minaga, Tomohiro Watanabe, Hobyung Chung, Masatoshi Kudo

ORCID number: Kosuke Minaga (0000-0001-5407-7925); Tomohiro Watanabe (0000-0001-7781-6305); Hobyung Chung (0000-0003-1112-6533); Masatoshi Kudo (0000-0002-4102-3474).

Author contributions: Minaga K and Watanabe T wrote the manuscript draft and prepared the table. Chung H and Kudo M assisted in writing the manuscript and reviewed the final version.

Manuscript source: Invited manuscript

Received: March 8, 2019
Peer-review started: March 8, 2019
First decision: April 11, 2019
Revised: April 13, 2019
Accepted: April 19, 2019
Article in press: April 20, 2019
Published online: May 21, 2019

P-Reviewer: Aguilera A, Gao RP, Kahraman A
S-Editor: Ma RY
L-Editor: A
E-Editor: Ma YJ

Kosuke Minaga, Tomohiro Watanabe, Masatoshi Kudo, Department of Gastroenterology and Hepatology, Kindai University Faculty of Medicine, Osaka-Sayama, Osaka 589-8511, Japan

Hobyung Chung, Department of Gastroenterology and Hepatology, Kobe City General Hospital, Chuo-ku, Kobe 650-0047, Japan

Corresponding author: Tomohiro Watanabe, MD, PhD, Associate Professor, Department of Gastroenterology and Hepatology, Kindai University Faculty of Medicine, 377-2 Ohno-Higashi, Osaka-Sayama, Osaka 589-8511, Japan. tomohiro@med.kindai.ac.jp
Telephone: +81-72-3660221
Fax: +81-72-3672880

Abstract

IgG4-related disease (IgG4-RD) is a chronic-fibroinflammatory disorder affecting a wide range of organs. Elevation of serum IgG4 concentrations and abundant infiltration of IgG4-expressing plasma cells are key diagnostic features of this autoimmune disease. Although common organ involvement of IgG4-RD includes the salivary glands, pancreas, and bile duct, hepatic involvement is less well established. Recently, five studies identified a subtype of autoimmune hepatitis (AIH), called IgG4-associated AIH (IgG4-AIH). IgG4-AIH is diagnosed based on significant accumulation of IgG4-expressing plasmacytes in the liver in patients who met the diagnostic criteria for classical AIH. Although four of the five reports regarded IgG4-AIH based on hepatic accumulation of IgG4-positive cells alone, one report diagnosed IgG4-AIH based on both hepatic accumulation of IgG4-positive cells and elevated serum concentrations of IgG4. IgG4-AIH diagnosed based on the latter criteria may be a hepatic manifestation of IgG4-RD whereas IgG4-AIH diagnosed based on the former criteria may be a subtype of AIH. In this review article, we summarize and discuss clinicopathological features of IgG4-AIH.

Key words: Autoimmune hepatitis; IgG4; IgG4-related disease; IgG4-associated autoimmune hepatitis

Core tip: IgG4-associated autoimmune hepatitis (IgG4-AIH) is a new disease entity characterized by the accumulation of IgG4-expressing plasma cells in the liver. Recent studies diagnosed IgG4-AIH based on hepatic accumulation of IgG4$^+$ cells alone or in combination with elevated serum concentrations of IgG4. Further studies are required to determine whether IgG4-AIH is a subtype of AIH or a hepatic manifestation of IgG4-related disease.

Citation: Minaga K, Watanabe T, Chung H, Kudo M. Autoimmune hepatitis and IgG4-related disease. *World J Gastroenterol* 2019; 25(19): 2308-2314
URL: https://www.wjgnet.com/1007-9327/full/v25/i19/2308.htm
DOI: https://dx.doi.org/10.3748/wjg.v25.i19.2308

INTRODUCTION

Emergence and establishment of IgG4-related disease (IgG4-RD) has dramatically changed our view of autoimmune disorders involving the pancreas and biliary tract[1,2]. Autoimmune pancreatitis (AIP) is classified into type 1 AIP and type 2 AIP, with the former type being regarded as a pancreatic manifestation of systemic IgG4-RD[3]. Moreover, a subtype of IgG4-RD preferentially affecting the biliary tract is now called as IgG4-related sclerosing cholangitis (IgG4-SC)[4]. IgG4-RD is a new disease entity characterized by elevated concentrations of serum IgG4 and infiltration of IgG4-expressing plasma cells in the affected organs. In addition to enhanced IgG4 antibody responses, many patients with IgG4-RD exhibit multiple organ involvement[5]. Clinicopathological analysis showed that IgG4-RD can occur in almost all the organs in the body, however, this disorder preferentially affects the pancreas, salivary glands, biliary tract, kidney, and lung[5].

Although type 1 AIP and IgG4-SC are recognized as pancreatic and biliary tract manifestations of systemic IgG4-RD[1-4], the hepatic involvement of this autoimmune disorder remains poorly understood[6]. Five studies including ours, have proposed a novel disease entity called IgG4-associated autoimmune hepatitis (IgG4-AIH)[7-11]. In this review article, we try to clarify clinical characteristics of IgG4-AIH by comparison with the characteristics of classical AIH. Furthermore, we discuss whether IgG4-AIH should be considered as a subtype of AIH or as hepatic involvement of systemic IgG4-RD.

HEPATIC INVOLVEMENT OF IGG4-RELATED DISEASE

Umemura *et al*[12] were the first to perform clinicopathological analysis of hepatic manifestations in IgG4-RD. They examined liver biopsy specimens obtained from 17 patients with AIP. Elevation of serum aspartate aminotransaminase (AST) and/or alanine aminotransaminase (ALT) was noted in 59% of AIP patients, whereas elevation of serum alkaline phosphatase (ALP) and/or gamma-glutamyl transferase (γGTP) was noted in 100%. Elevation of serum concentrations of IgG4, IgG, and anti-nuclear antibody (ANA) were seen in 94%, 65%, and 47%, respectively. Thus, AIP patients analyzed in this study shared biochemical and immunological abnormalities with AIH patients in terms of elevations of liver enzymes, IgG, and ANA[13-15]. A wide variety of histological findings, including portal inflammation (35%), interface hepatitis (24%), lobular hepatitis (29%), bile duct damage (59%), and canalicular cholestasis (53%) were observed in the livers of patients with AIP[12]. These pathological findings strongly indicate that around 20-30% patients with AIP exhibit pathological findings similar to classical AIH since portal inflammation, interface hepatitis, and lobular hepatitis are detected in most cases of AIH[13-15].

Infiltration of IgG4-expressing plasma cells in the liver was confirmed in 47% of patients with AIP, but not in those with classical AIH, primary biliary cholangitis (PBC), or primary sclerosing cholangitis (PSC) when more than 5 positive cells [/high powered field, (HPF)] was defined as positive[12]. The numbers of hepatic IgG4-expressing plasma cells were positively correlated to serum concentrations of IgG4 and the presence of bile duct thickness, suggesting that, in this study, patients with IgG4-RD involving both the pancreas (AIP) and the biliary tract (IgG4-SC) exhibit accumulation of IgG4-expressing plasma cells in the liver. These seminal studies by Umemura *et al*[12] provide evidence that a significant proportion of patients with AIP exhibit laboratory and pathological findings akin to classical AIH. At present, it remains unknown whether AIH-like liver lesions observed in patients with AIP are regarded as hepatic manifestation of IgG4-RD.

Another type of hepatic manifestation of IgG4-RD is hepatic inflammatory pseudotumor. Hepatic pseudotumors are classified into two types; fibrohistiocytic and lymphoplasmacytic[16]. Massive infiltration of IgG4-expressing plasma cells accompanied by obliterative phlebitis, one of the characteristic pathological findings in IgG4-RD[1,2], was seen in the lymphoplasmacytic type of hepatic pseudotumor.

Based on these pathological findings, Zen *et al*[16] proposed that the lymphoplasmacytic type of hepatic pseudotumor is a hepatic manifestation of IgG4-RD. However, detailed examinations of clinical characteristics, including serum IgG4 concentrations are lacking in this study in which 16 cases of hepatic pseudotumors were enrolled. Taken together, recent studies provide evidence that AIH-like lesions and hepatic pseudotumors might occur as hepatic involvement of systemic IgG4-RD.

IGG4-AIH AND CLASSICAL AUTOIMMUNE HEPATITIS

The first case of IgG4-AIH was reported by Umemura *et al*[17] in 2007. Serum levels of ALT, ALP, γGTP, IgG, and IgG4 were markedly elevated in this case. Interface hepatitis, lobular hepatitis, and rosette formation were seen in the liver biopsy specimens. This case met the diagnostic criteria for AIH proposed by the International Autoimmune Hepatitis Group (IAIHG)[18] and was diagnosed as AIH. On the other hand, this case was atypical with regard to classical AIH in that abundant infiltration of IgG4-expressing plasma cells in the portal tract and a marked elevation of serum IgG4 concentrations were observed. Based on enhanced IgG4 antibody responses, the authors proposed a new disease entity called IgG4-AIH[17]. Following this case report, five groups, including ours, tried to identify and characterize IgG4-AIH in patients who met the diagnostic criteria for AIH (Table 1)[7-11].

CLINICAL CHARACTERISTICS OF IGG4-AIH

We reviewed five reports addressing the incidence, laboratory and pathological findings, and efficacy of glucocorticoid treatment in IgG4-AIH[7-11] (Table 1).

Diagnostic criteria and proportion of IgG4-AIH

Chung *et al*[7] were the first to examine the incidence of IgG4-AIH in patients with classical AIH. They examined 26 AIH patients who met the diagnostic criteria proposed by the IAIHG. They defined IgG4-AIH when more than 5 IgG4-expressing plasma cells (/HPF) were detected in the portal tracts. According to this criteria, 9 of the 26 AIH patients were diagnosed with IgG4-AIH[7]. In another study conducted in India, 10 of the 40 AIH patients were diagnosed as IgG4-AIH based on the Chung's criteria[7,9]. In subsequent three studies, IgG4-AIH was defined when more than 10 IgG4-expressing plasma cells were detected in the liver[8,10,11]. In one study, the presence of the overlap syndrome with IgG4-AIH in combination with PSC or PBC was reported[10]. Although the proportion of IgG4-AIH was highly variable (from 3.3 % to 34.6%) probably due to the difference of the diagnostic criteria[7-11], it was clear that a unique type of AIH characterized by significant infiltration of IgG4-expressing plasma cells exists in patients with formerly diagnosed AIH. Moreover, Aydemir *et al*[11] reported that 6 out of 40 children with AIH were regarded as IgG4-AIH. Collectively, these five reports successfully identified a subtype of AIH, called IgG4-AIH, based on significant infiltration of IgG4-expressing plasma cells in the liver.

Nakanuma *et al*[19,20] proposed new diagnostic criteria for IgG4-AIH with reference to systemic IgG4-RD. According to the Nakanuma's criteria, IgG4-AIH is characterized by elevated concentrations of serum IgG4 and infiltration of IgG4-expressing plasma cells in the liver (> or = 10 cells /HPF). Although Umemura's study fully meets this strict criteria[8], the other four studies do not satisfy this criteria[7,9-11]. Application of this new criteria for the diagnosis might make IgG4-AIH an extremely rare disease entity since only three cases have met this criteria[19]. Given the fact the Nakanuma's criteria is proposed based on the well-established criteria for IgG4-RD, application of this criteria might be useful for the diagnosis of IgG4-AIH as hepatic involvement of systemic IgG4-RD. However, it remains to be determined whether IgG4-AIH occurs as a subtype of classical AIH or hepatic involvement of IgG4-RD.

Liver enzyme abnormality

Regarding liver enzyme abnormality, one study described that mean AST level in the IgG4-AIH group was significantly higher than in the classical AIH group whereas the differences of mean ALT, ALP and total bilirubin levels were not significant between the two groups[9]. In the remaining four reports[7,8,10,11], serum levels of hepatobiliary enzymes such as AST, ALT, ALP, and γGTP were comparable between IgG4-AIH and classical AIH (IgG4-non-associated AIH). Thus, blood biochemical examinations do not distinguish IgG4-AIH and IgG4-non-associated AIH in most cases.

Table 1 Autoimmune hepatitis and IgG4-associated autoimmune hepatitis

Ref.	Chunget al[7]	Umemuraet al[8]	Amarapurkar et al[9]	Canivetet al[10]	Aydemir et al[11]
Country	Japan	Japan	India	France	Turkey
Number of AIH	26 adults	60 adults	40 adults	28 adults	40 children
Number of IgG4-AIH	9 (34.6%)	2 (3.3 %)	10 (25.0%)	7 (25.0%)	6 (15.0%)
Diagnostic criteria for IgG4-AIH	> 5 $IgG4^+$ cells/HPF	> 10 $IgG4^+$ cells/HPF	> 5 $IgG4^+$ cells/HPF	> 10 $IgG4^+$ cells/HPF	> 10 $IgG4^+$ cells/HPF
Laboratory findings *vs* cAIH					
ALT	No difference	No difference	No difference	No difference	No difference
ALP	No difference	No difference	No difference	No difference	NA
γGTP	No difference	NA	NA	No difference	No difference
IgG	Higher	No difference	NA	Higher	No difference
IgG4	No difference	Higher	Higher	NA	NA
Presence of ANA	No difference	No difference	NA	No difference	NA
Detection rate of pathological findings *vs* cAIH					
Portal inflammation	No difference	No difference	NA	NA	No difference
Interface hepatitis	No difference	Higher	NA	NA	No difference
Lobular hepatitis	Higher	Higher	NA	NA	NA
Plasma cell infiltration	Higher	Higher	NA	NA	No difference
Eosinophil infiltration	Not detected	No difference	NA	NA	No difference
Rosette formation	Higher	Higher	NA	No difference	No difference
Bile duct damage	No difference	Lower	NA	NA	NA
Degree of Fibrosis *vs* cAIH	No difference	NA	No difference	No difference	No difference
IAIHG score *vs* cAIH	Higher	No difference	No difference	NA	No difference
ALT normalization time after PSL therapy *vs* cAIH	Shorter	NA	NA	NA	Shorter

cAIH: Classical autoimmune hepatitis; HPF: High-powered field; NA: Not available; IAIHG: International autoimmune hepatitis group; PSL: Prednisolone.

Serum immunological findings

HLA DR-3 and DR-4 serotypes are associated with classical AIH[13-15]. Umemura *et al*. showed that one of two patients with IgG4-AIH was positive for HLA-DR4[8]. The HLA status was not examined in the other four studies[7,9-11]. Thus, it remains unknown whether HLA typing is useful to differentiate between IgG4-AIH and classical AIH.

Elevated levels of serum IgG and ANA titers are hallmarks of AIH[13-15]. No difference was seen in serum levels of ANA titers in these two types of AIH[7,8,10]. In contrast, serum concentrations of IgG were significantly higher in patients with IgG4-associated AIH than in those with IgG4-non-associated AIH in two studies[7,10].

Serum concentrations of IgG4 were measured in three studies[7-9]. Serum concentrations of IgG4 were comparable between the two types of AIH in one study[7] whereas patients with IgG4-AIH exhibited a marked elevation of this Ig subtype as compared with those with IgG4-non-associated AIH in the other two studies[8,9]. At present, the reasons accounting for the discrepancy between Chung's and Umemura's studies remain unknown. One plausible explanation is that IgG4-AIH defined by Chung *et al*[7] might be a different disease to that identified by Umemura *et al*[8] Considering the fact that Umemura's cases of IgG4-AIH meet the strict diagnostic criteria[19], IgG4-AIH defined by Umemura *et al*[8] might be a hepatic manifestation of systemic IgG4-RD rather than a subtype of AIH. On the contrary, IgG4-AIH defined by Chung *et al*. might be a subtype of AIH characterized by moderately increased IgG4 responses in the liver, but not in the serum.

Pathological findings

In Umemura's study[8], both of the patients with IgG4-AIH exhibited portal inflammation, interface hepatitis, lobular hepatitis, plasma cell infiltration, and rosette formation whereas neither presented with bile duct damage. Consistent with this

report, the incidence of lobular hepatitis, plasma cell infiltration, and rosette formation was higher in patients with IgG4-AIH than in those with IgG4-non-associated AIH[7]. Moreover, the degree of portal inflammation was more severe in patients with IgG4-AIH than in those with IgG4-non-associated AIH[7]. Thus, adult patients with IgG4-AIH appear to exhibit a more severe pathology than those with IgG4-non-associated AIH although the degree of fibrosis was comparable between the two disorders. In contrast to these studies in adult AIH patients, the degree of chronic inflammation in children did not show a significant difference between IgG4-associated AIH and IgG4-non-associated AIH as judged by the grade of portal inflammation, interface hepatitis, rosette formation, and fibrosis[11].

As for the type of immune cells characterizing IgG4-AIH, a marked infiltration of $CD3^+$ T cells, $CD20^+$ B cells, IgG^+ cells and $CD38^+$ plasma cells was seen in the liver of patients with IgG4-AIH as compared with that of patients with IgG4-non-associated AIH[7]. Abundant infiltration of these adaptive immune cells, especially plasma cells, leads us to speculate that enhanced IgG4 antibody responses can be partially explained by an increased accumulation of plasma cells in the liver and that moderately increased IgG4 antibody responses (5-10 cells/HPF) may be an epiphenomenon associated with increased accumulation of plasma cells[7,19]. However, infiltration of IgG1-expressing plasma cells was comparable in the liver between IgG4-AIH and IgG4-non-associated AIH in Chung's study[7]. Therefore, selective enhancement of IgG4 antibody responses might be also induced even in cases exhibiting normal serum IgG4 concentrations and moderately increased accumulation of IgG4-expressing plasma cells in the liver. In this regard, there is no doubt that selective enhancement in IgG4 antibody responses are actually induced in IgG4-AIH patients who met the strict criteria proposed by Nakanuma *et al*[8,19].

Sensitivity to glucocorticoid and azathioprine

Glucocorticoid treatment is the first line of treatment for both AIH[13-15] and IgG4-RD[1-4]. Sensitivity to glucocorticoids was investigated in IgG4-AIH and IgG4-non-associated AIH through assessment of ALT normalization time. The proportions of patients showing normalization of ALT were comparable between IgG4-AIH and IgG4-non-associated AIH at 1 or 2 years after the initiation of glucocorticoid treatment[9,10]. In contrast, the ALT normalization time after the glucocorticoid treatment was shorter in patients with IgG4-AIH than in those with IgG4-non-associated AIH in two studies[7,11]. Thus, accumulation of IgG4-expressing plasma cells in the liver might be a surrogate marker for the prediction of glucocorticoid treatment. Patients with IgG4-AIH were treated with glucocorticoid followed by the maintenance therapy with azathioprine[9-11]. The response rates to azathioprine at the maintenance phase were comparable between IgG4-AIH and IgG4-non-associated AIH.

IGG4-AIH AS A SUBTYPE OF AIH OR AS A HEPATIC MANIFESTATION OF IGG4-RD

One major question arising from the previous studies summarized above[7-11] is whether IgG4-AIH is a subtype of classical AIH or a hepatic manifestation of systemic IgG4-RD. Since all of these studies identified and characterized IgG4-AIH among patients with classical AIH, AIH is likely to be classified into IgG4-AIH and IgG4-non-associated AIH. Given the fact that IgG4-AIH is diagnosed based on the presence of IgG4-expressing plasma cells in the liver, it is possible that immune responses necessary for IgG4 antibody class switch recombination underlie the immuno-pathogenesis of IgG4-AIH. Extensive immuno-histochemical analysis by Chung *et al*. showed that the numbers of $CD3^+$ T cells, $CD20^+$ B cells, and $CD38^+$ plasma cells in the liver were greater in patients with IgG4-AIH than in those with IgG4-non-associated AIH[7]. The results of this study strongly suggest that adaptive immune responses might be involved in the immuno-pathogenesis of IgG4-AIH and that enhanced IgG4 responses in the liver might be secondary and as a result of activation of adaptive immune cells. However, hepatic immune cell populations or profiles of cytokines leading to enhanced IgG4 antibody responses have been poorly clarified.

IgG4-RD is characterized by multiple organ involvement and a unique form of fibrosis called storiform fibrosis[1,2]. Although systemic IgG4-RD preferentially affects the salivary glands, pancreas, biliary tract, and kidneys [1,2], hepatic involvement is less well characterized[6]. Neither multiple organ involvement nor the presence of storiform fibrosis had been examined in patients with IgG4-AIH when these five studies were published[7-11]. Lack of multiple organ involvement as well as storiform fibrosis supports the idea that IgG4-AIH is a subtype of classical AIH rather than

hepatic manifestation of IgG4-RD. However, it is too early to recognize IgG4-AIH as a subtype of classical AIH as a case with co-occurrence of IgG4-SC and IgG4-AIH has been reported[21]. Moreover, metachronous development of IgG4-SC and IgG4-related AIP was observed in two cases that had been formerly diagnosed as IgG4-AIH[19]. These two cases of IgG4-AIH bearing other organ involvement and elevated serum concentrations of IgG4 are considered to exhibit AIH lesions as hepatic involvement of systemic IgG4-RD. Thus, IgG4-AIH can occur as hepatic involvement of systemic IgG4-RD if accumulation of IgG4-expressing plasma cells in the liver is accompanied by a marked elevation of serum IgG4 concentrations. Therefore, it is strongly suggested that IgG4-AIH identified in the previous five studies is categorized into two types[7-11]; a subtype of AIH characterized by moderately enhanced IgG4 responses in the liver alone[7] and a hepatic manifestation of IgG4-RD sharing pathological finding with AIH and exhibiting systemic enhanced IgG4 responses[8,19].

Another important question that needs to be addressed is the clinicopathological difference between IgG4-AIH and IgG4-hepatopathy, both of which can arise from systemic IgG4-RD[8,12,19]. Although IgG4-hepatopathy and IgG4-AIH share key pathological findings such as portal inflammation, interface hepatitis, and lobular hepatitis, the former disease frequently presents with bile duct damage and eosinophilic infiltration, compared to the latter[8,12,19]. Thus, careful pathological examinations might be useful in discriminating between these two disorders.

Much progress has been made in the immuno-pathogenesis of IgG4-RD in terms of autoantigens and pathogenic cell types. Laminin 511, Annexin A11, and galectin 3 are identified as target autoantigens in IgG4-RD[22-24]. Plasmacytoid dendritic cells (pDCs) producing both IFN-α and IL-33 play crucial roles in murine experimental AIP and human IgG4-related AIP[2,25,26]. Examination of serum antibody titers against the autoantigens listed above and analysis of pDC activation in the liver may be useful in determining whether IgG4-AIH occurs as a hepatic manifestation of IgG4-RD.

CONCLUSION

Recent clinicopathological analysis identified IgG4-AIH as a subtype of AIH. Confirmation of hepatic accumulation of IgG4-expressing plasma cells is absolutely required for the diagnosis of IgG4-AIH on the condition that the patient meets the diagnostic criteria for AIH. IgG4-AIH can occur not only in adults but also in children. Previous studies with a limited number of patients have indicated that IgG4-AIH and IgG4-non-associated AIH share laboratory findings, pathological findings, and sensitivity to glucocorticoids. However, accumulation of IgG4-expressing plasma cells was only detected in IgG4-AIH. It should be noted, however, that ALT normalization time after the glucocorticoid treatment might be shorter in IgG4-AIH than in IgG4-non-associated AIH[7,11]. Thus, significant infiltration of IgG4-expressing plasma cells in the liver may be useful as a biomarker for the prediction of the efficacy of glucocorticoid in AIH. One important issue that needs to be addressed in future studies is whether IgG4-AIH is a subtype of AIH or a hepatic manifestation of IgG4-RD. Establishment of IgG4-AIH as a new disease entity awaits characterization of clinicopathological findings and immune responses in accumulated cases with IgG4-AIH.

REFERENCES

1 **Stone JH**, Zen Y, Deshpande V. IgG4-related disease. *N Engl J Med* 2012; **366**: 539-551 [PMID: 22316447 DOI: 10.1056/NEJMra1104650]

2 **Watanabe T**, Minaga K, Kamata K, Kudo M, Strober W. Mechanistic Insights into Autoimmune Pancreatitis and IgG4-Related Disease. *Trends Immunol* 2018; **39**: 874-889 [PMID: 30401468 DOI: 10.1016/j.it.2018.09.005]

3 **Kamisawa T**, Chari ST, Lerch MM, Kim MH, Gress TM, Shimosegawa T. Recent advances in autoimmune pancreatitis: type 1 and type 2. *Gut* 2013; **62**: 1373-1380 [PMID: 23749606 DOI: 10.1136/gutjnl-2012-304224]

4 **Nakazawa T**, Naitoh I, Hayashi K, Miyabe K, Simizu S, Joh T. Diagnosis of IgG4-related sclerosing cholangitis. *World J Gastroenterol* 2013; **19**: 7661-7670 [PMID: 24282356 DOI: 10.3748/wjg.v19.i43.7661]

5 **Brito-Zerón P**, Ramos-Casals M, Bosch X, Stone JH. The clinical spectrum of IgG4-related disease. *Autoimmun Rev* 2014; **13**: 1203-1210 [PMID: 25151972 DOI: 10.1016/j.autrev.2014.08.013]

6 **Joshi D**, Webster GJ. Biliary and hepatic involvement in IgG4-related disease. *Aliment Pharmacol Ther* 2014; **40**: 1251-1261 [PMID: 25312536 DOI: 10.1111/apt.12988]

7 **Chung H**, Watanabe T, Kudo M, Maenishi O, Wakatsuki Y, Chiba T. Identification and characterization of IgG4-associated autoimmune hepatitis. *Liver Int* 2010; **30**: 222-231 [PMID: 19650840 DOI: 10.1111/j.1478-3231.2009.02092.x]

8 **Umemura T**, Zen Y, Hamano H, Joshita S, Ichijo T, Yoshizawa K, Kiyosawa K, Ota M, Kawa S,

Nakanuma Y, Tanaka E. Clinical significance of immunoglobulin G4-associated autoimmune hepatitis. *J Gastroenterol* 2011; **46** Suppl 1: 48-55 [PMID: 20862498 DOI: 10.1007/s00535-010-0323-4]
9 **Amarapurkar AD**, Amarapurkar DN. Immunoglobulin IgG4 and autoimmune hepatitis. *Trop Gastroenterol* 2015; **36**: 112-117 [PMID: 26710480]
10 **Canivet CM**, Anty R, Patouraux S, Saint-Paul MC, Lebeaupin C, Gual P, Duclos-Vallee JC, Tran A. Immunoglobulin G4-associated autoimmune hepatitis may be found in Western countries. *Dig Liver Dis* 2016; **48**: 302-308 [PMID: 26553036 DOI: 10.1016/j.dld.2015.10.005]
11 **Aydemir Y**, Akcoren Z, Demir H, Saltik Temizel IN, Ozen H, Yuce A. Clinical and histopathological features of immunoglobulin G4-associated autoimmune hepatitis in children. *J Gastroenterol Hepatol* 2019; **34**: 742-746 [PMID: 30378176 DOI: 10.1111/jgh.14525]
12 **Umemura T**, Zen Y, Hamano H, Kawa S, Nakanuma Y, Kiyosawa K. Immunoglobin G4-hepatopathy: association of immunoglobin G4-bearing plasma cells in liver with autoimmune pancreatitis. *Hepatology* 2007; **46**: 463-471 [PMID: 17634963 DOI: 10.1002/hep.21700]
13 **Heneghan MA**, Yeoman AD, Verma S, Smith AD, Longhi MS. Autoimmune hepatitis. *Lancet* 2013; **382**: 1433-1444 [PMID: 23768844 DOI: 10.1016/S0140-6736(12)62163-1]
14 **Czaja AJ**, Manns MP. Advances in the diagnosis, pathogenesis, and management of autoimmune hepatitis. *Gastroenterology* 2010; **139**: 58-72.e4 [PMID: 20451521 DOI: 10.1053/j.gastro.2010.04.053]
15 **Krawitt EL**. Autoimmune hepatitis. *N Engl J Med* 2006; **354**: 54-66 [PMID: 16394302 DOI: 10.1056/NEJMra050408]
16 **Zen Y**, Fujii T, Sato Y, Masuda S, Nakanuma Y. Pathological classification of hepatic inflammatory pseudotumor with respect to IgG4-related disease. *Mod Pathol* 2007; **20**: 884-894 [PMID: 17571078 DOI: 10.1038/modpathol.3800836]
17 **Umemura T**, Zen Y, Hamano H, Ichijo T, Kawa S, Nakanuma Y, Kiyosawa K. IgG4 associated autoimmune hepatitis: a differential diagnosis for classical autoimmune hepatitis. *Gut* 2007; **56**: 1471-1472 [PMID: 17504944 DOI: 10.1136/gut.2007.122283]
18 **Alvarez F**, Berg PA, Bianchi FB, Bianchi L, Burroughs AK, Cancado EL, Chapman RW, Cooksley WG, Czaja AJ, Desmet VJ, Donaldson PT, Eddleston AL, Fainboim L, Heathcote J, Homberg JC, Hoofnagle JH, Kakumu S, Krawitt EL, Mackay IR, MacSween RN, Maddrey WC, Manns MP, McFarlane IG, Meyer zum Büschenfelde KH, Zeniya M. International Autoimmune Hepatitis Group Report: review of criteria for diagnosis of autoimmune hepatitis. *J Hepatol* 1999; **31**: 929-938 [PMID: 10580593]
19 **Nakanuma Y**, Ishizu Y, Zen Y, Harada K, Umemura T. Histopathology of IgG4-Related Autoimmune Hepatitis and IgG4-Related Hepatopathy in IgG4-Related Disease. *Semin Liver Dis* 2016; **36**: 229-241 [PMID: 27466793 DOI: 10.1055/s-0036-1584320]
20 **Kamisawa T**, Okazaki K. Diagnosis and Treatment of IgG4-Related Disease. *Curr Top Microbiol Immunol* 2017; **401**: 19-33 [PMID: 28197739 DOI: 10.1007/82_2016_36]
21 **Li H**, Sun L, Brigstock DR, Qi L, Gao R. IgG4-related sclerosing cholangitis overlapping with autoimmune hepatitis: Report of a case. *Pathol Res Pract* 2017; **213**: 565-569 [PMID: 28238541 DOI: 10.1016/j.prp.2017.01.024]
22 **Shiokawa M**, Kodama Y, Sekiguchi K, Kuwada T, Tomono T, Kuriyama K, Yamazaki H, Morita T, Marui S, Sogabe Y, Kakiuchi N, Matsumori T, Mima A, Nishikawa Y, Ueda T, Tsuda M, Yamauchi Y, Sakuma Y, Maruno T, Uza N, Tsuruyama T, Mimori T, Seno H, Chiba T. Laminin 511 is a target antigen in autoimmune pancreatitis. *Sci Transl Med* 2018; **10** [PMID: 30089633 DOI: 10.1126/scitranslmed.aaq0997]
23 **Hubers LM**, Vos H, Schuurman AR, Erken R, Oude Elferink RP, Burgering B, van de Graaf SFJ, Beuers U. Annexin A11 is targeted by IgG4 and IgG1 autoantibodies in IgG4-related disease. *Gut* 2018; **67**: 728-735 [PMID: 28765476 DOI: 10.1136/gutjnl-2017-314548]
24 **Perugino CA**, AlSalem SB, Mattoo H, Della-Torre E, Mahajan V, Ganesh G, Allard-Chamard H, Wallace Z, Montesi SB, Kreuzer J, Haas W, Stone JH, Pillai S. Identification of galectin-3 as an autoantigen in patients with IgG_4-related disease. *J Allergy Clin Immunol* 2019; **143**: 736-745.e6 [PMID: 29852256 DOI: 10.1016/j.jaci.2018.05.011]
25 **Watanabe T**, Yamashita K, Arai Y, Minaga K, Kamata K, Nagai T, Komeda Y, Takenaka M, Hagiwara S, Ida H, Sakurai T, Nishida N, Strober W, Kudo M. Chronic Fibro-Inflammatory Responses in Autoimmune Pancreatitis Depend on IFN-α and IL-33 Produced by Plasmacytoid Dendritic Cells. *J Immunol* 2017; **198**: 3886-3896 [PMID: 28373582 DOI: 10.4049/jimmunol.1700060]
26 **Arai Y**, Yamashita K, Kuriyama K, Shiokawa M, Kodama Y, Sakurai T, Mizugishi K, Uchida K, Kadowaki N, Takaori-Kondo A, Kudo M, Okazaki K, Strober W, Chiba T, Watanabe T. Plasmacytoid Dendritic Cell Activation and IFN-α Production Are Prominent Features of Murine Autoimmune Pancreatitis and Human IgG4-Related Autoimmune Pancreatitis. *J Immunol* 2015; **195**: 3033-3044 [PMID: 26297761 DOI: 10.4049/jimmunol.1500971]

World Journal of Gastroenterology

Submit a Manuscript: https://www.f6publishing.com

World J Gastroenterol 2019 May 21; 25(19): 2315-2326

DOI: 10.3748/wjg.v25.i19.2315

ISSN 1007-9327 (print) ISSN 2219-2840 (online)

ORIGINAL ARTICLE

Basic Study

Electroacupuncture at ST36 modulates gastric motility *via* vagovagal and sympathetic reflexes in rats

Meng-Jiang Lu, Zhi Yu, Yan He, Yin Yin, Bin Xu

ORCID number: Meng-Jiang Lu (0000000186354659); Zhi Yu (0000000291792618); Yan He (0000-0002-9718-6483); Bin Xu (0000000340063009); Yin Yin (0000-0003-0516-7494).

Author contributions: Yu Z and Lu MJ contributed equally to this work; Yu Z and Xu B conceived and designed the experiments; Lu MJ performed the experiments and wrote the paper; Yan H and Yin Y performed the experiments; Lu MJ and Yu Z analyzed the data; all authors read and approved the final version of the article to be published.

Supported by the National Natural Science Foundation of China, No. 81373749; No. 81574071, and No. 81673883.

Institutional review board statement: The study was reviewed and approved by the Institutional Review Board of the Nanjing University of Chinese Medicine.

Institutional animal care and use committee statement: All experimental manipulations were undertaken in accordance with the Guide for the Care and Use of Laboratory Animals (National Institutes of Health), and the study was approved by the Institutional Animal Care and Use Committee of Nanjing University of Chinese Medicine (No. 201805A017).

Conflict-of-interest statement: The authors declare that there are no conflicts of interest to disclose.

Meng-Jiang Lu, Zhi Yu, Yan He, Yin Yin, Bin Xu, Key Laboratory of Acupuncture and Medicine Research of Ministry of Education, Nanjing University of Chinese Medicine, Nanjing 210023, Jiangsu Province, China

Corresponding author: Bin Xu, PhD, Professor, Key Laboratory of Integrated Acupuncture and Drugs, Nanjing University of Chinese Medicine, No. 138, Xianlin Road, Nanjing 210023, Jiangsu Province, China. xubin@njucm.edu.cn
Telephone: +86-132-5529-1963

Abstract

BACKGROUND

Electroacupuncture (EA) at ST36 can significantly improve gastrointestinal symptoms, especially in promoting gastrointestinal motility. The automatic nervous system plays a main role in EA, but few studies exist on how vagovagal and sympathetic reflexes affect EA to regulate gastrointestinal motility.

AIM

To study the role of vagovagal and sympathetic reflexes in EA at ST36, as well as the associated receptor subtypes that are involved.

METHODS

Gastric motility was measured with a manometric balloon placed in the gastric antrum area in anesthetized animals. The peripheral nervous discharge was measured using a platinum electrode hooking the vagus or greater splanchnic nerve, and the central nervous discharge was measured with a glass microelectrode in the dorsal motor nucleus of the vagus (DMV). The effects and mechanisms of EA at ST36 were explored in male Sprague-Dawley rats which were divided in to a control group, vagotomy group, sympathectomy group, and microinjection group [including an artificial cerebrospinal fluid group, glutamate (L-Glu) group, and γ-aminobutyric acid (GABA) group] and in genetically modified male mice [β1β2 receptor-knockout (β1β2$^{-/-}$) mice, M2M3 receptor-knockout (M2M3$^{-/-}$) mice, and wild-type control mice].

RESULTS

EA at ST36 promoted gastric motility during 30-120 s. During EA, both vagus and sympathetic nerve discharges increased, with a much higher frequency of vagus nerve discharge than sympathetic discharge. The gastric motility mediated by EA at ST36 was interdicted by vagotomy. However, gastric motility mediated by EA at ST36 was increased during 0-120 s by sympathectomy, which eliminated the delay effect of EA during 0-30 s, but it was lower than the control group during

Data sharing statement: No additional unpublished data are available.

ARRIVE guidelines statement: The authors have read the ARRIVE guidelines, and the manuscript was prepared and revised according to the ARRIVE guidelines.

Manuscript source: Unsolicited manuscript

Received: February 28, 2019
Peer-review started: March 1, 2019
First decision: April 4, 2019
Revised: April 22, 2019
Accepted: May 3, 2019
Article in press: May 3, 2019
Published online: May 21, 2019

P-Reviewer: Caboclo JF, De Quadros LG, Mohamed SY
S-Editor: Yan JP
L-Editor: Wang TQ
E-Editor: Ma YJ

30-120 s. Using gene knockout mice and their wild-type controls to explore the receptor mechanisms, we found that EA at ST36 decreased gastric motility in M2/3$^{-/-}$ mice, and promoted gastric motility in β1/2$^{-/-}$ mice. Extracellular recordings showed that EA at ST36 increased spikes of the DMV. Microinjection of L-Glu into the DMV increased gastric motility, while EA at ST36 decreased gastric motility during 0-60 s, and promoted gastric motility during 60-120 s. Injection of GABA reduced or increased gastric motility, and reduced the promoting gastric motility effect of EA at ST36.

CONCLUSION
These data suggest that EA at ST36 modulates gastric motility *via* vagovagal and sympathetic reflexes mediated through M2/3 and β1/2 receptors, respectively. Sympathetic nerve activity mediated through β1/2 receptors is associated with an early delay in modulation of gastric motility by EA at ST36.

Key words: Gastric motility; Electroacupuncture; Vagovagal reflex; Sympathetic nerve; Rats

Core tip: In this study, we measured intragastric pressure to observe the effect of electroacupuncture (EA) at ST36 on gastric motility at different time intervals. The role of the peripheral autonomic nervous system in EA was determined using the vagus nerve and splanchnic nerve severance model, as well as by detecting peripheral autonomic nerve discharge. M2/3 and β1/2 receptor knockout mouse models were further used to identify autonomic receptor subtypes specifically involved in the regulation of gastric motility. Finally, we studied the role of brainstem neurocircuits during EA at ST36 by detecting the dorsal motor nucleus of the vagus (DMV) neuron discharge and the effect of microinjection of γ-aminobutyric acid and glutamate to the DMV. Using these approaches, the role of vagovagal and sympathetic reflexes in regulating gastric motility by EA at ST36 was determined.

Citation: Lu MJ, Yu Z, He Y, Yin Y, Xu B. Electroacupuncture at ST36 modulates gastric motility *via* vagovagal and sympathetic reflexes in rats. *World J Gastroenterol* 2019; 25(19): 2315-2326
URL: https://www.wjgnet.com/1007-9327/full/v25/i19/2315.htm
DOI: https://dx.doi.org/10.3748/wjg.v25.i19.2315

INTRODUCTION

Extrinsic neural inputs originating in the central nervous system (CNS) provide modulation of gastric motility, especially in the upper gastrointestinal tract. In particular, brainstem vagovagal parasympathetic neurocircuits have the most prominent role in the CNS-mediated control of upper gastrointestinal tract motility[1]. Vagovagal neurocircuits comprise the nucleus tractus solitarius (NTS), the dorsal motor nucleus of the vagus (DMV), and the nucleus ambiguous. The DMV is the nuclei of origin of vagal motor fibers. The efferent fibers from the DMV form synaptic contacts with postganglionic neurons located in the target organ which modulate gastric motility.

Gastric dysmotility is a common symptom of gastrointestinal diseases such as functional dyspepsia and diabetic gastroparesis. Although cisapride and domperidone can promote gastric motility in patients with insufficient gastric motility, adverse cardiac reactions are often reported in the clinic[2-5]. Electroacupuncture (EA) is widely used in clinical practice due to its safety, high efficacy, and low toxicity. Studies have shown that EA at ST36 can significantly improve gastrointestinal symptoms, especially in promoting gastrointestinal motility[6-9]. However, the mechanism underlying its efficacy remain exploring. Most studies have shown that EA at ST36 is closely related to vagus nerve activity, especially the dorsal vagal complex of the neural pathway[10-13].

In this study, we measured intragastric pressure to observe the effect of EA at ST36 on gastric motility at different time intervals. The role of the peripheral autonomic

nervous system in EA was determined using the vagus nerve and splanchnic nerve severance model, as well as by detecting peripheral autonomic nerve discharge. M2/3 and β1/2 receptor knockout mouse models were further used to identify autonomic receptor subtypes specifically involved in the regulation of gastric motility. Finally, we studied the role of brainstem neurocircuits during EA at ST36 by detecting DMV neuron discharge and the effect of microinjection of γ-aminobutyric acid (GABA) and glutamate (L-Glu) to the DMV. Using these approaches, the role of vagovagal and sympathetic reflexes in regulating gastric motility by EA at ST36 was determined.

MATERIALS AND METHODS

Animals

Male Sprague-Dawley rats weighing 250-300 g (Model Animal Research Center of Nanjing Medical University, China) were divided into a control group, sham surgery group, vagotomy group, sympathectomy group, and microinjection group (including an artificial cerebrospinal fluid group, GABA group, and L-Glu group). M2/3$^{-/-}$ mice (M2/3$^{-/-}$, D2; 129-Chrm2^{tml} Chrm3^{tml}, D0407, Kumamoto University, Japan), β1/2$^{-/-}$mice (β1/2$^{-/-}$; Adrb1^{tmlBkk}Adrb2^{tmlBkk}/J, J003810, donated by the Jackson Laboratory, United States), and their wild-type mice (male, 20-25 g; Model Animal Research Center of Nanjing Medical University, China) were applied. Gene knockout in mice was verified by PCR.

All animals were housed under controlled environmental conditions (22 °C, 40%-60% relative humidity, 12/12 h light/dark cycle) and were given free access to water and food. All animals were allowed 1 week of feeding adaptation. All experimental manipulations were undertaken in accordance with the Principles of Laboratory Animal Care and the Guide for the Care and Use of Laboratory Animals, published by the National Science Council, China.

Drugs

Animals were anaesthetized with urethane (U2500; Sigma, St. Louis, MO, United States). L-Glu (G1251-100G; Sigma), GABA (A2129-10G; Sigma), artificial cerebrospinal fluid (R22153; Yuan Ye Biological Co., Ltd., Shanghai, China), and Pontamine sky blue (24410; Sigma) were administered *via* microinjection prior to surgery. Penicillin (2011; Shandong Shengwang Pharmaceutical Co., Ltd., Shandong, China) was administered after surgery. The concentrations and doses of the drugs were as follows: urethane (20%; 0.8 g/kg for rats and 5 mL/kg for mice), L-Glu (0.1 mol/L, 0.2 μL), GABA (0.1 mol/L, 0.2 μL), artificial cerebrospinal fluid (0.2 μL), penicillin (0.2 mL/d of 800 IU penicillin in 5 mL saline per rat, intramuscular), and Pontamine sky blue (1% dissolved in 0.5 mol/L sodium acetate).

Assessment of gastric motility

Experimental animals were fasted for 12 h and were free to drink. A small skin incision (length: 5-8 mm in rats, 2-3 mm in mice) was made below the xiphoid process, then a small balloon made of flexible rubber (about 2 mm in diameter for rats and 1 mm in diameter for mice) was inserted into the duodenum and placed in the antrum of the stomach. The small balloon was connected to a polyethylene tube filled with 0.05-0.1 mL of warm water. The pressure in the balloon was further analyzed using a transducer (YP201; Chengdu Instrument Factory) and a physiological signal collection system (RM6240; Chengdu Instrument Factory). Baseline intragastric pressure was maintained at 0.1 Kpa, and the experimental animals were maintained at a temperature of 37 ± 0.5 °C with an electric heating pad.

Surgery

For vagotomy, rats were fasted for 24 h before surgery and anesthetized with urethane. The skin was prepared with iodophor disinfection. A small skin incision was introduced along the midline of the abdomen, and the stomach and subphrenic surface of the animal were exposed. The distal and proximal ventral gastric vagus branches were separated and cut. After surgery, penicillin was injected for 3 d to prevent infection. The rats were fed liquid food within 3 d after surgery. After 5 d, the rats were used in the experiment. For sympathectomy, preoperative preparation was the same as for vagotomy. Between the left iliac horn and the lumbar muscle, the left greater splanchnic nerve was separated and cut. Postoperative treatment was the same as that for vagotomy.

Parasympathetic and sympathetic nerve discharge

Vagus nerve discharge: Rats were anesthetized with urethane, a small skin incision was made in the midline of the abdomen, and the left vagus nerve was separated as

for vagotomy. The nerve was hooked with the positive electrode, and the surrounding tissue was hooked with the reference electrode.

Sympathetic nerve discharge: Rats were anesthetized with urethane, a small skin incision was made in the midline of the abdomen, and the left greater splanchnic nerve was separated as for sympathectomy. The nerve was hooked with the positive electrode, and the surrounding tissue was hooked with the reference electrode. Nerve discharge was recorded using a preamplifier (NL100, CED, United Kindom) and a Micro1401-3 bioelectric module (NL125NL126, CED, United Kindom) connected to a biosignal acquisition and analysis system (Microl 1401-3, CED, United Kindom). The signal filtering was 10-1000 Hz, sampling frequency was 20000Hz, and amplification was 1000 times. The data were recorded with Spike2 software.

Localization, microinjection, and nerve discharge of the dorsal motor nucleus of the vagus nerve

Rats were anesthetized with 20% urethane (8 mL/kg) and placed in a prone position on a brain stereotaxic instrument maintained at a temperature of 37 °C using an electric heating pad. The head was fixed with an ear rod and rat head clip. After removing the cranial fur, a longitudinal incision was made in the middle of the head, the subcutaneous tissue was separated and the skull was clearly exposed, and the anterior fontanelle and posterior fontanelle were adjusted to the same horizontal line. The vagus dorsal motor nucleus was determined according to the brain localization map of Paxinos and Watson for rats (coordinate: AP 13.2 mm, RL 0.5 mm, H 8 mm)[14].

For microinjection of the rostral part DMV, a small hole (about 2 mm diameter) was drilled into the skull using an electric bone drill. A customized injection cannula (a stainless steel catheter with an outer diameter of 0.7 mm, inner diameter of 0.4 mm, and length of 10 mm) was inserted through the hole, and zinc phosphate cement was used to seal the hole. After surgery, penicillin was injected for 3 d to prevent infection. The rats were fed liquid food within 3 d after surgery. After 5 d, the rats were used in the experiment. Thereafter, the rats received artificial cerebrospinal fluid (0.1 mol/L, 0.2 μL), L-Glu (0.1 mol/L, 0.2 μL), and GABA (0.1 mol/L, 0.2 μL) *via* the microinjection catheter. The rats were divided into three groups depending on the drug they received.

To measure nerve discharge of the DMV, a glass microelectrode (0.5 mol/L sodium acetate electrolyte filled with 1% Pontamine sky blue) was passed through a microinjection thruster to reach the DMV nerve (coordinate: AP 13.2 mm, RL 0.5 mm, H 8 mm), and its extracellular nerve discharge was recorded. When spontaneous neuronal discharge appeared, neuronal discharge before EA (1 min), during EA (2 min), and after EA (1 min) was recorded. After completion of the recording, the next intervention was performed after the baseline returned to the pre-EA level.

The tissue recording site was localized after each recording of nerve discharge. A digital DC stabilized power stimulator was used to pass reverse direct current (10 μA, 20 min) to the microelectrode, and Pontamine sky blue was passed through the microelectrophoresis mode to the tip of the electrode.

Dissected brains were soaked in 4% paraformaldehyde solution. Thick sections (40-60 μm) of brain tissue were used to observe the location of the Pontamine sky blue marker under a light microscope. The location of the dye marker was compared with the position of the vagus nerve dorsal motor nucleus based on Paxinos and Watson rat brain location to determine the accuracy of vagus dorsal motor nucleus recording localization.

EA stimulation

ST36 (Zusanli) is located in the posterolateral aspect of the knee joint, about 5 mm below the capitulum fibulae; the stimulation method was EA stimulation, and the needle was connected to Han's EA instrument (LH402A; Beijing Huawei Technologies Co., Ltd.). The stimulating intensity was 2 mA, frequency was 2/15 Hz, and stimulation time was 2 min.

Statistical analysis

Discharge data were collected using the amplifier and biosignal acquisition device, and recorded and analyzed using the Spike2 software. The recorded intragastric pressure data were analyzed with a physiological signal collection system. The change in discharge frequency or percentage change in gastric motility was compared between during and before EA. An absolute value of change in discharge frequency ≥ 20% was regarded as an effective excitation or inhibition effect, and an absolute value of gastric motility change ≥ 5% was regarded as effective excitation or inhibition. The following effect formula (1) was used to indicate the change in percentage:

Percentage change = [(DreEA-PreEA)/PreEA] × 100% (1)

Data were analyzed with SPSS 23.0 software and GraphPad Prism 6.0. All data are expressed as the mean ± standard deviation. Any two groups were compared using independent sample *t*-tests, and one-way analysis of variance was used for more than two groups. $P < 0.05$ indicated statistical significance.

RESULTS

Effect of EA at ST36 on gastric movement and peripheral autonomic discharge

In order to understand the effect of EA at ST36 on gastric motility, we monitored changes in intragastric pressure during EA for 120 s. We observed that there was no significant change in intragastric pressure at 0-30 s during EA ($P > 0.05$), and the intragastric pressure was significantly increased from 30-60 s ($P < 0.05$, Figure 1A). Simultaneously, we examined discharge of the vagus nerve and the greater visceral nerve during EA. The discharge frequency during EA was significantly increased compared to the pre-EA frequency, and the vagus nerve discharge frequency was significantly higher than that of the greater visceral nerve ($P < 0.05$, Figure 1C). These findings suggest that the vagus nerve and the greater visceral nerve are both affected by EA at ST36, with the vagus nerve affected to a greater degree.

Effect of EA at ST36 on gastric motility in different nerve transection groups

In order to further understand the role of the vagus nerve and the greater visceral nerve in gastric movement related to EA at ST36, we observed changes in intragastric pressure in different neurotomy groups. Compared with the normal control group, the intragastric pressure during EA in the vagus nerve transection group was significantly reduced. During EA at 0-30 s, the intragastric pressure of the greater visceral nerve transection group was significantly increased ($P < 0.05$, Figure 2). These results suggest that the promotion of gastric motility caused by EA at ST36 is related to vagus nerve activation, and the delayed aspect of this effect (no significant change in intragastric pressure at 0-30 s) depends mainly on activation of the greater visceral nerve.

Effect of EA at ST36 on gastric motility in M2/3$^{-/-}$ and β1/2$^{-/-}$ mice

To further study the effects of different receptor subtypes of the vagus nerve and the greater visceral nerve on gastric movement induced by EA at ST36, we measured associated changes in intragastric pressure in different receptor knockout mouse models. Compared with wild-type B6 mice, EA at ST36 inhibited gastric movement in M2/3$^{-/-}$ mice. At 0-30 s, the intragastric pressure of β1/2$^{-/-}$ mice was significantly increased by EA at ST36 ($P < 0.05$, Figure 3). These results suggest that the effect of EA at ST36 on gastric motility depends on the vagus nerve M2/3 receptor. The delayed function of this effect is mainly dependent on activation of the greater visceral nerve β1/2 receptor.

Effect of EA at ST36 on the discharge of neurons in the dorsal motor nucleus of the vagus nerve

In order to further understand the mechanism of the vagus nerve circuit in EA at ST36, we measured neuronal discharge in the DMV nerve during EA at ST36. Seventy percent of the 47 neurons recorded showed excitatory responses to EA at ST36, and the frequency of neuronal discharge during EA was significantly higher than that before EA ($P < 0.05$, Figure 4).

Effect of microinjection of L-Glu and GABA into the DMV on gastric motility

Studies have shown that L-Glu and GABA play an important role in the brainstem vagus nerve circuit. In order to clarify the effect of L-Glu and GABA on gastric motility regulation in the DMV, we microinjected L-Glu and GABA into the DMV to detect changes in intragastric pressure between 60 s before injection and 60 s after injection. Microinjection of L-Glu significantly increased intragastric pressure in the DMV compared with the artificial cerebrospinal fluid control group, while microinjection of GABA produced both excitatory and inhibitory effects ($P < 0.05$, Figure 5).

Effect of EA at ST36 on gastric movement after microinjection of L-Glu and GABA in the DMV

In order to clarify transmitter regulation during EA at ST36 in the brainstem vagus nerve circuit, we measured the effect of EA at ST36 on gastric motility after microinjection of L-Glu and GABA into the DMV. Compared with the control group, the effect of EA at ST36 was significantly reduced after injection of GABA. During EA

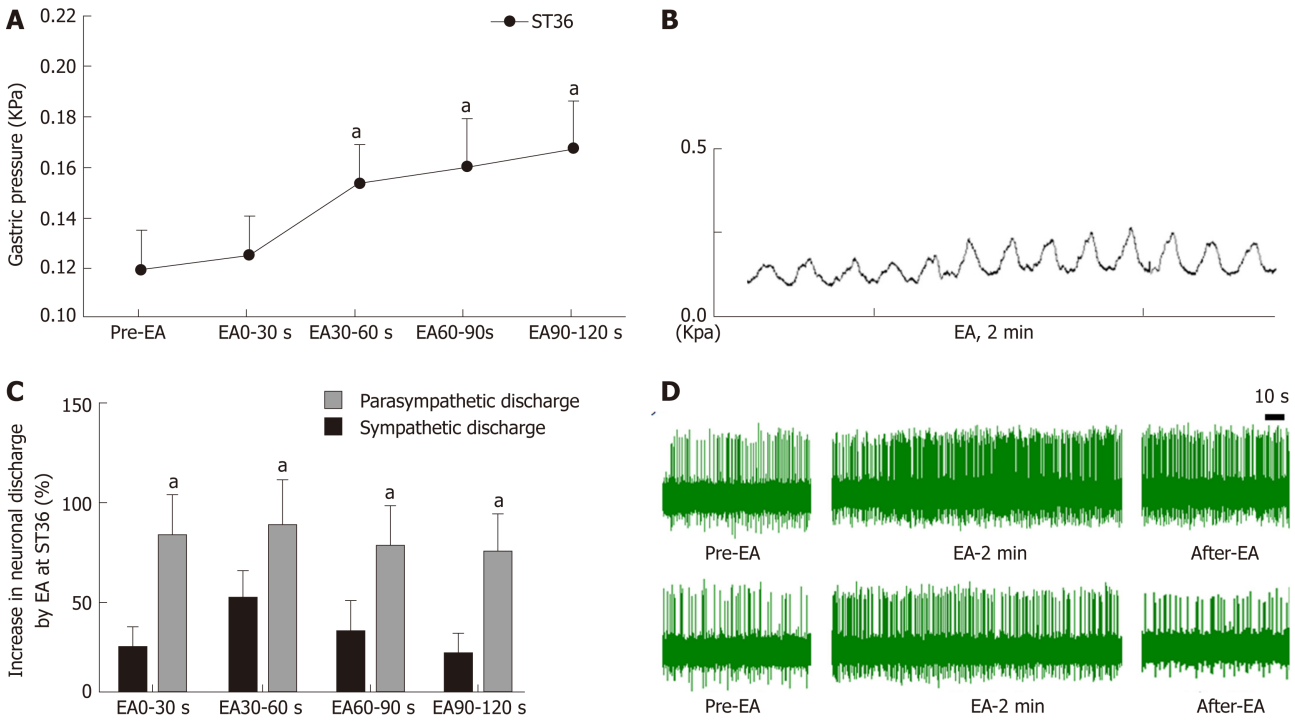

Figure 1 Effect of electroacupuncture at ST36 on gastric motility and vagus and sympathetic discharge. A: Effect of electroacupuncture (EA) at ST36 on intragastric pressure; $^{a}P < 0.05$ compared with pre-EA intragastric pressure; B: Waveform of gastric motility by EA at ST36; C: Percent change in discharge of the vagus nerve and greater splanchnic nerve induced by EA at ST36; $^{a}P < 0.05$ compared with sympathetic nerve discharge during the same time interval; D: Waveform of vagus nerve discharge (upper panel) and greater splanchnic nerve discharge (lower panel). EA: Electroacupuncture.

0-60 s, the gastric motility was inhibited after injection of L-Glu ($P < 0.05$, Figure 6). These results suggest that both GABA and L-Glu are involved in the brainstem vagus nerve circuit of EA at ST36.

DISCUSSION

Along with the rapid pace of life and changes in dietary habits, the incidence of gastrointestinal dysfunction is increasing, with abdominal distension, abdominal pain, nausea, and vomiting being the main symptoms. Many patients also experience these symptoms due to gastric dysmotility. Acupuncture therapy is widely used to treat gastrointestinal diseases because of its low side effect profile and good curative effect, and ST36 is the most frequently used acupoint for the treatment of gastrointestinal dysfunction. Previous studies have shown that acupuncture at ST36 regulates gastrointestinal motility mainly *via* the autonomic nervous system[15-17]. However, there is no clear study on how the vagus nerve and sympathetic nerves participate in regulation, and what role the brainstem neural circuit plays.

Current research has found that acupuncture of the lower limbs can cause excitability of the vagus nerve, thereby increasing gastric motility[18,19]. However, the vagus nerve is not exclusively involved in regulation of gastric motility during acupuncture at ST36. Our study found that the time period during which EA at ST36 started to take effect was 30 s after stimulation onset, and that gastric movement did not change significantly during the first 0-30 s (Figure 1). We also examined vagus nerve and greater splanchnic nerve activity during EA. Neuronal discharge of the vagus nerve and the splanchnic nerve was significantly increased compared with the time period before EA (Figure 2), while the frequency of vagus nerve discharge was significantly higher than that of the greater splanchnic nerve (Figure 3). These data suggest that the vagus nerve and sympathetic nerve are involved in EA regulation, and that the vagus nerve may play a major role in increasing gastric motility.

To further clarify the autonomic nervous system mechanisms involved in gastric motility regulation, we observed changes in gastric motility after transecting the vagus nerve and greater splanchnic nerve. We found that after the vagus nerve was transected, the gastric motility-promoting effect of EA at ST36 was essentially abolished. When the greater splanchnic nerve was transected, the delayed effect of EA at ST36 disappeared (Figure 2). Therefore, EA at ST36 can increase gastric movement

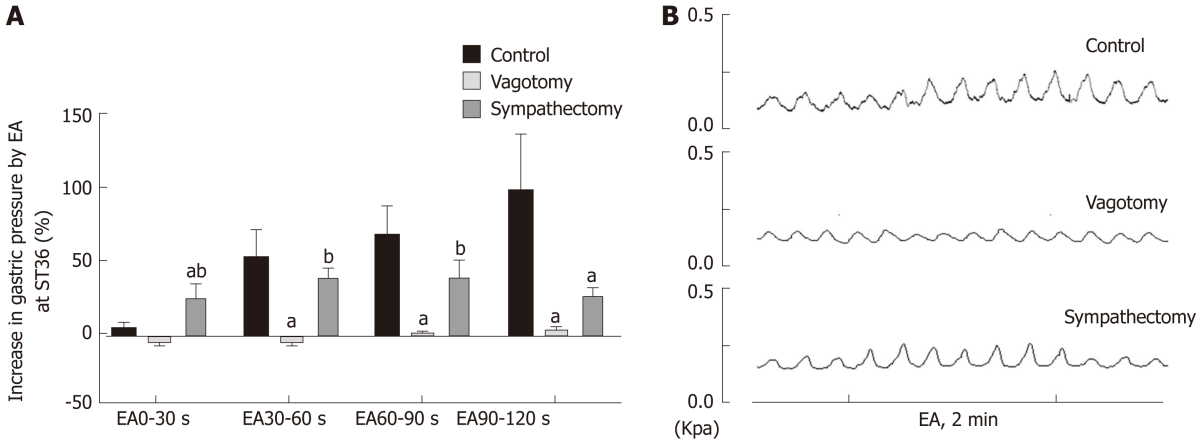

Figure 2 Effect of electroacupuncture at ST36 on gastric motility in different surgical model groups. A: Percentage change of gastric motility in the control group, vagus nerve transection group, and splanchnic nerve transection group; [a]$P < 0.05$ compared with the control group during the same time period, [b]$P < 0.05$ compared with the vagus nerve transection group during the same time period; B: Waveforms of gastric motility in the control group, vagus nerve transection group, and splanchnic nerve transection group. EA: Electroacupuncture.

via the vagus nerve, and this effect is delayed due to involvement of sympathetic nerves.

The vagus nerve and sympathetic nervous system regulate gastric motility together[20]. The vagus nerve neural circuit involves the brainstem vagus nerve neural circuit and the vagus nerve efferent fibers, which are transmitted *via* posterior membrane receptors of the gastric wall, with different receptors having different regulatory roles[21]. Studies have shown that when the vagus nerve releases the excitatory neurotransmitter acetylcholine, it mainly acts through two major receptor systems of the postsynaptic membrane, the nicotinic receptor (N) and muscarinic receptor (M), to promote gastric motility[22]. When the vagus nerve releases inhibitory neuronal NANC transmitter, it inhibits gastric motility. Five subtypes of M receptors exist[23], with M2M3 being the primary receptors distributed in the gastrointestinal smooth muscle[24]. Sympathetic nerves release norepinephrine and adrenaline through the branch of the spinal cord that innervates the gastric segment *via* the communicating branch, anterior ganglia, and the posterior ganglia. These transmitters act on postsynaptic β and α2 receptors, thereby inhibiting smooth muscle contraction and decreasing gastric motility.

As stated, EA regulates gastrointestinal motility *via* the vagus and sympathetic nerves. Studies have shown that injection of the M receptor blocker atropine can inhibit the gastric motility-promoting effect of EA at LI11 (Quchi)[25], and the injection of the beta blocker propranolol can abrogate the inhibition of jejunal motility[26]. However, due to a poor specificity of the blockers, the specific receptor subtype(s) through which these effects are mediated is not clearly known. Our study found that compared with wild-type mice, the delayed effect of EA at ST36 disappeared in $\beta1/2^{-/-}$ mice, and gastric motility increased significantly during the 0-30 s period. EA at ST36 in $M2/3^{-/-}$ mice decreased gastric motility. These observations demonstrate that EA at ST36 acts through efferent vagus nerve activation of postsynaptic M2M3 receptors to promote gastric motility, while sympathetic activation of β1β2 receptors underlies the early delayed gastric motility response. Interestingly, EA at ST36 inhibited gastric motility in M2M3 receptor knockout mice.

Since the vagus nerve plays an important role in promoting gastric motility by EA at ST36, we focused on the effect of EA at ST36 on the vagus nerve neural circuit. We found that the brainstem vagus nerve neural circuit plays an important role in regulating gastric motility, including the solitary tract nucleus, the vagus nerve dorsal motor nucleus, and the nucleus ambiguus. The sensory afferent transmits the mechanical and chemical signals of the stomach to the solitary tract nucleus[27] through L-Glu; these signals are then transmitted to the DMV or the high-grade center *via* L-Glu, GABA, and catecholamines, and the DMV transmits the signal through the efferent vagus nerve. The main neurotransmitters involved are L-Glu and GABA[28]. L-Glu is a common excitatory neurotransmitter in the brain and its receptors include both ionotropic L-Glu receptors and metabotropic L-Glu receptors. Studies have found that microinjection of L-Glu into the DMV produces different effects. Sun *et al*[29] injected L-Glu into the right DMV and NTS to induce inhibition of gastric motility; Cruz *et al*[30] found that injecting L-Glu into the rostrum of the DMV promoted gastric motility, while injecting L-Glu into the tail of the DMV induced inhibition of gastric

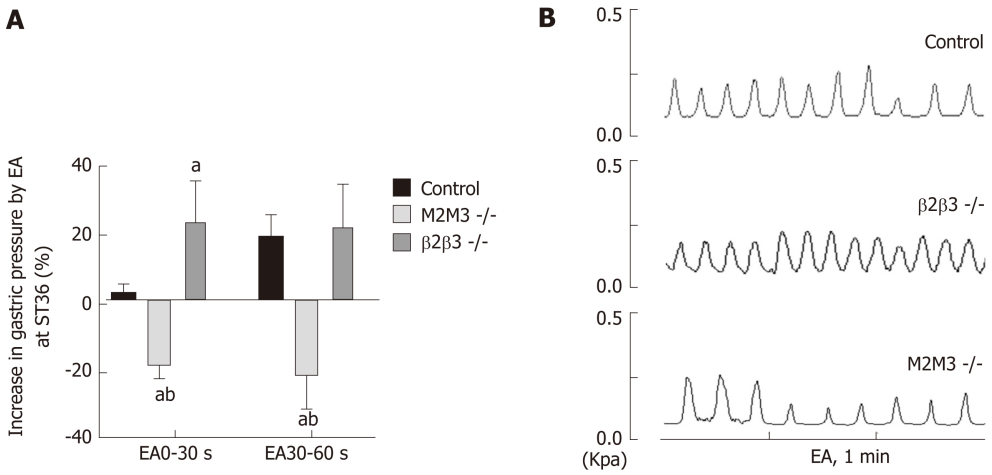

Figure 3 Effect of electroacupuncture at ST36 on gastric motility in mouse receptor knockout models. A: Effect of electroacupuncture (EA) at ST36 on gastric motility in wild-type mice, β1/β2 knockout mice, and M2/M3 knockout mice; [a]$P < 0.05$ compared with the control group during the same time period, [b]$P < 0.05$ compared with the β1/2$^{-/-}$ group during the same time period; B: Waveform of gastric movement induced by EA at ST36 in wild-type mice, β1/2 knockout mice, and M2/3 knockout mice. EA: Electroacupuncture.

motility. These effects can be blocked by transecting the vagus nerve.

GABA is the major inhibitory amino acid in the brain, with three major receptor types and multiple receptor subtypes. Browning *et al*[31] believe that glutamatergic neurons between the NTS and DMV do not affect the regulation of gastric motility. On the contrary, GABAergic neurons are important for the regulation of gastric motility; Pearson *et al*[32] found that the brainstem neural circuit that regulates the gastric antrum involves GABAergic transmission. Multiple studies have shown that GABAergic synaptic input in the solitary tract nucleus inhibits the efferent vagus nerve which regulates the upper digestive tract, thereby affecting gastric function[33].

Studies have shown that EA can affect the brainstem, as supported by imaging and c-fos immunopositive expression[34,35], and have also shown that the solitary nucleus is involved in acupuncture regulation of the gastrointestinal tract[36,37]. Our study found that injecting L-Glu into the rostrum of the DMV promotes gastric motility, while injecting GABA produces both inhibitory and stimulatory effects. To examine whether EA at ST36 involves the brainstem vagus nerve neuronal circuit, we examined the neuronal discharge of the DMV. Compared to baseline spontaneous discharge, EA at ST36 can significantly excite DMV neurons. To study the involvement of L-Glu and GABA in the EA process, we performed EA at ST36 along with the injection of L-Glu and GABA, respectively, into the DMV. Gastric motility decreased during the first 0-60 s after injecting L-Glu followed by EA; the motility-promoting effect of EA showed a significant decline after the injection of GABA. These observations suggest that both L-Glu and GABA are involved in the brainstem nerve circuit of EA at ST36 that regulates gastric motility. GABA in the DMV antagonized the effect of EA at ST36.

In conclusion, our findings show that EA at ST36 mainly regulates gastric movement through the DMV vagovagal reflex circuit by L-Glu and GABA. While M2M3 receptors play a major role in mediating the vagus nerve efferent effect on gastric motility, the involvement of the sympathetic nervous system and β1β2 receptors may be the cause of delayed initiation of gastric motility. The vagus-sympathetic circuit is involved in the neural circuit that regulates gastric movement by EA at ST36.

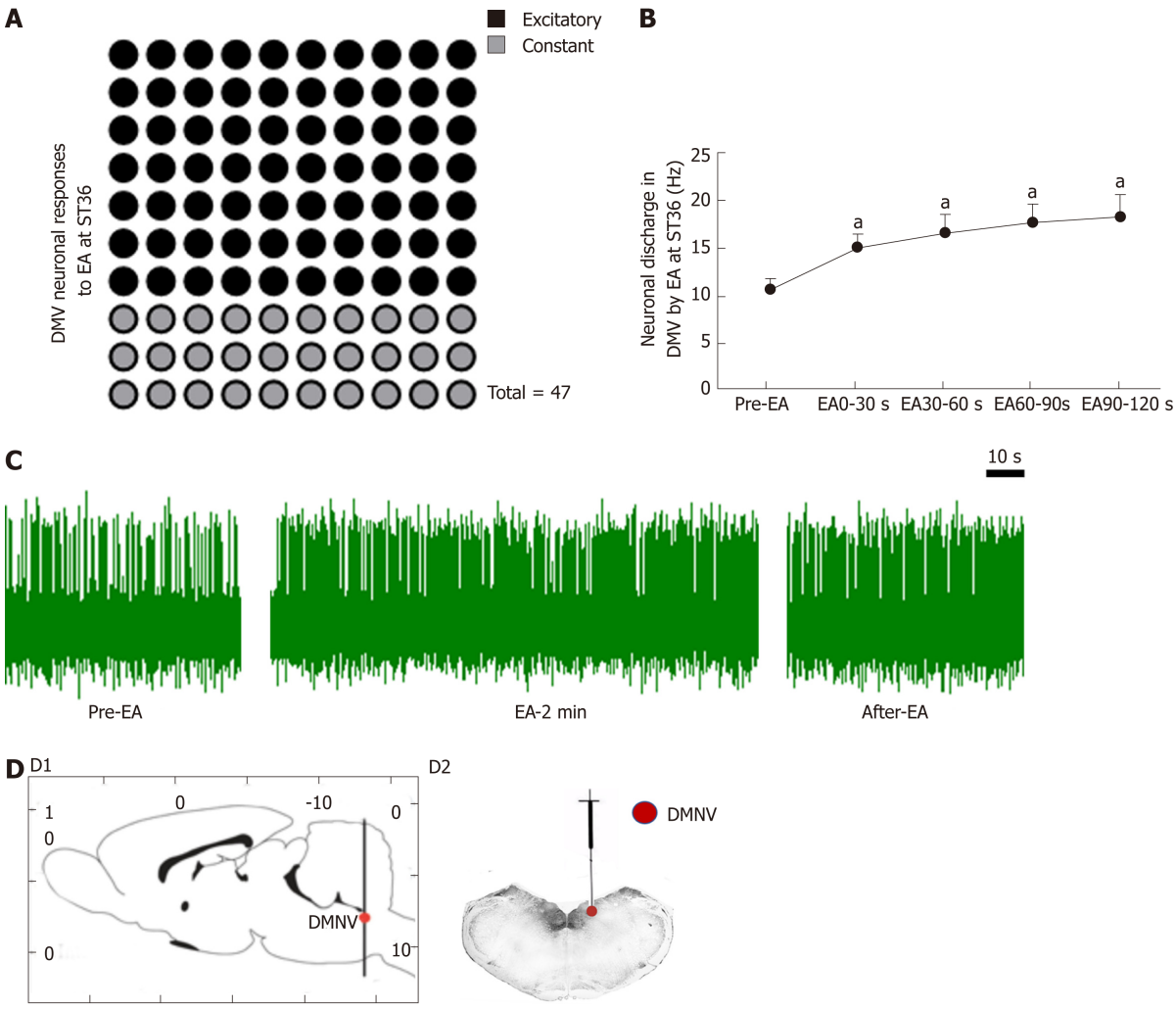

Figure 4 Effect of electroacupuncture at ST36 on neurons in the dorsal motor nucleus of the vagus nerve. A: Number of dorsal motor nucleus of the vagus nerve (DMV) neuron responses during electroacupuncture (EA) at ST36; B: Discharge frequency of DMV neurons; $^{a}P < 0.05$ compared with pre-EA; C: Waveform of DMV neuron discharge by EA at ST36; D: Location of the DMV (D1-D2, location of the DMV; D2, location of injected Pontamine sky blue in the DMV). EA: Electroacupuncture; DMV: Dorsal motor nucleus of the vagus nerve.

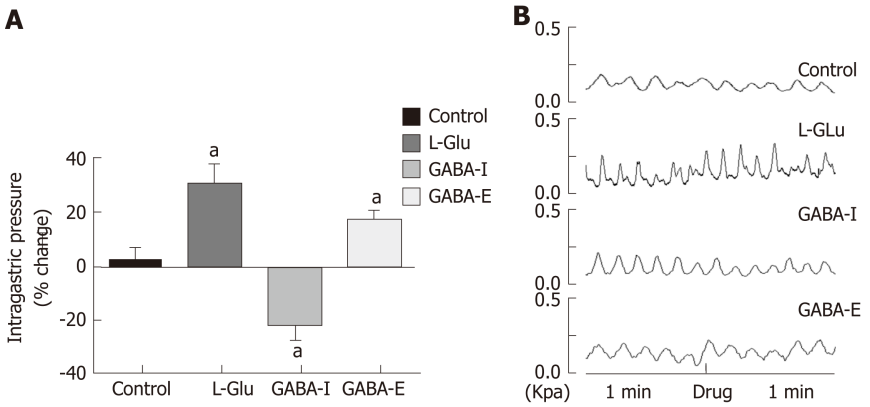

Figure 5 Gastric motility changes after dorsal motor nucleus of the vagus nerve microinjection of different amino acids. A: Percentage change of gastric motility after microinjection of artificial cerebrospinal fluid, glutamic acid, or γ-aminobutyric acid (GABA) into dorsal motor nucleus of the vagus nerve (DMV) (GABA-I is the inhibitory effect group, and GABA-E is the excitatory effect group); $^{a}P < 0.05$ compared with the control group; B: Waveform of gastric movement changes after microinjection of artificial cerebrospinal fluid, glutamic acid, and GABA into the DMV. GABA: γ-aminobutyric acid; DMV: Dorsal motor nucleus of the vagus nerve; L-Glu: Glutamate.

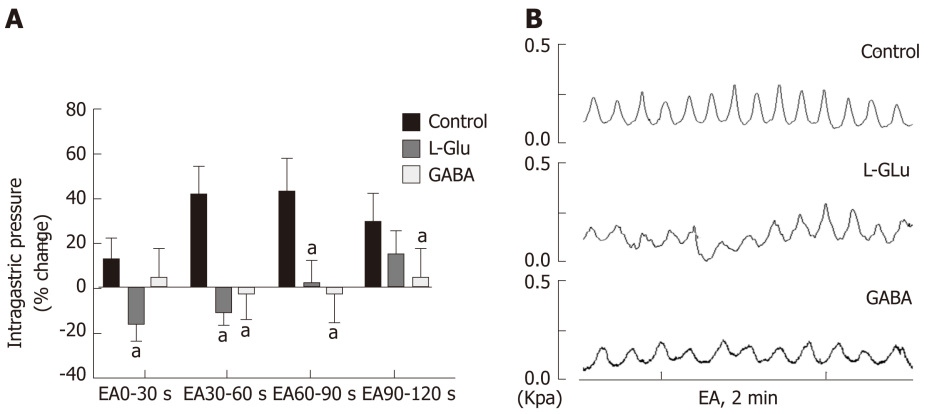

Figure 6 Effect of electroacupuncture at ST36 on gastric motility after microinjection of different amino acids. A: Percentage change of gastric movement by electroacupuncture (EA) at ST36 after microinjection of artificial cerebrospinal fluid, GABA, or glutamic acid to the dorsal motor nucleus of the vagus nerve; $^{a}P < 0.05$ compared with the control group; B: Waveform of gastric motility induced by EA at ST36 after microinjection of artificial cerebrospinal fluid, γ-aminobutyric acid, or glutamic acid into the DMV. EA: Electroacupuncture; GABA: γ-aminobutyric acid; DMV: Dorsal motor nucleus of the vagus nerve; L-Glu: Glutamate.

ARTICLE HIGHLIGHTS

Research background

Electroacupuncture (EA) at ST36 can significantly improve gastrointestinal symptoms, especially in promoting gastrointestinal motility. The automatic nervous system plays a main role in EA at ST36, but few studies exist on how vagovagal and sympathetic reflexes affect EA in regulating gastrointestinal motility.

Research motivation

This study aimed to investigate the mechanism of the automatic nervous system in promoting gastrointestinal motility by EA at ST36. The results obtained may be used to explain the mechanism of EA in regulating gastrointestinal motility. Furthermore, it may provide a reference to neurostimulation therapy.

Research objectives

The objective of this study was to determine the role of vagovagal and sympathetic reflexes in EA at ST36, as well as the associated receptor subtypes that are involved. The results obtained may be used to explain the mechanism of EA in regulating gastrointestinal motility. Furthermore, it may provide a reference to neurostimulation therapy.

Research methods

Gastric motility was measured with a manometric balloon in anesthetized animals. The peripheral nervous activity was measured with a platinum electrode hooking the vagus or greater splanchnic nerve, and the central nervous activity was measured with a glass microelectrode in the DMV. The effects and mechanisms of EA at ST36 were explored in male Sprague-Dawley rats which were divided into a control group, vagotomy group, sympathectomy group, and microinjection group [including an artificial cerebrospinal fluid group, glutamate (L-Glu) group, and γ-aminobutyric acid (GABA) group] and in genetically modified male mice [β1β2 receptor-knockout ($\beta1\beta2^{-/-}$) mice, M2M3 receptor-knockout ($M2M3^{-/-}$) mice, and wild-type control mice].

Research results

EA at ST36 promoted gastric motility during 30-120 s. During EA, the vagus nerve activity was much higher than sympathetic activity. The gastric motility mediated by EA at ST36 was interdicted by vagotomy. However, the delay effect of EA during 0-30 s was eliminated by sympathectomy. EA at ST36 decreased gastric motility in $M2/3^{-/-}$ mice and promoted gastric motility in $\beta1/2^{-/-}$ mice. Extracellular recordings showed that EA at ST36 increased spikes of the dorsal motor nucleus of the vagus (DMV). Microinjection of L-Glu into the DMV increased gastric motility, while EA at ST36 decreased gastric motility during 0-60s, and promoted gastric motility during 60-120 s. Injection of GABA reduced or increased gastric motility, and reduced the gastric motility-promoting effect of EA at ST36.

Research conclusions

EA at ST36 modulates gastric motility *via* vagovagal and sympathetic reflexes mediated through M2/3 and β1/2 receptors, respectively. Sympathetic nerve activity mediated through β1/2 receptors is associated with an early delay in the modulation of gastric motility by EA at ST36. GABA and L-Glu in the DMV are involved in regulating gastric motility by EA at ST36.

Research perspectives

The results prove that both vagal and sympathetic reflexes are involved in regulating gastric

motility by EA at ST36. Future studies should investigate specific transcutaneous stimulation which can regulate gastric motility accurately.

REFERENCES

1 **Travagli RA**, Hermann GE, Browning KN, Rogers RC. Brainstem circuits regulating gastric function. *Annu Rev Physiol* 2006; **68**: 279-305 [PMID: 16460274 DOI: 10.1146/annurev.physiol.68.040504.094635]
2 **Kyrmizakis DE**, Chimona TS, Kanoupakis EM, Papadakis CE, Velegrakis GA, Helidonis ES. QT prolongation and torsades de pointes associated with concurrent use of cisapride and erythromycin. *Am J Otolaryngol* 2002; **23**: 303-307 [PMID: 12239699 DOI: 10.1053/ajot.2002.124543]
3 **Rochoy M**, Auffret M, Béné J, Gautier S; Réseau français des centres régionaux de pharmacovigilance. [Antiemetics and cardiac effects potentially linked to prolongation of the QT interval: Case/non-case analysis in the national pharmacovigilance database]. *Rev Epidemiol Sante Publique* 2017; **65**: 1-8 [PMID: 27988172 DOI: 10.1016/j.respe.2016.06.335]
4 **Ehrenpreis ED**, Roginsky G, Alexoff A, Smith DG. Domperidone is Commonly Prescribed With QT-Interacting Drugs: Review of a Community-based Practice and a Postmarketing Adverse Drug Event Reporting Database. *J Clin Gastroenterol* 2017; **51**: 56-62 [PMID: 27182647 DOI: 10.1097/MCG.0000000000000543]
5 **Giudicessi JR**, Ackerman MJ, Camilleri M. Cardiovascular safety of prokinetic agents: A focus on drug-induced arrhythmias. *Neurogastroenterol Motil* 2018; **30**: e13302 [PMID: 29441683 DOI: 10.1111/nmo.13302]
6 **Xu S**, Hou X, Zha H, Gao Z, Zhang Y, Chen JD. Electroacupuncture accelerates solid gastric emptying and improves dyspeptic symptoms in patients with functional dyspepsia. *Dig Dis Sci* 2006; **51**: 2154-2159 [PMID: 17082991 DOI: 10.1007/s10620-006-9412-x]
7 **Chen JDZ**, Ni M, Yin J. Electroacupuncture treatments for gut motility disorders. *Neurogastroenterol Motil* 2018; **30**: e13393 [PMID: 29906324 DOI: 10.1111/nmo.13393]
8 **Zhang Z**, Wang C, Li Q, Zhang M, Zhao H, Dong L, Wang G, Jin Y. Electroacupuncture at ST36 accelerates the recovery of gastrointestinal motility after colorectal surgery: A randomised controlled trial. *Acupunct Med* 2014; **32**: 223-226 [PMID: 24739815 DOI: 10.1136/acupmed-2013-010490]
9 **Jin Y**, Zhao Q, Zhou K, Jing X, Yu X, Fang J, Liu Z, Zhu B. Acupuncture for Functional Dyspepsia: A Single Blinded, Randomized, Controlled Trial. *Evid Based Complement Alternat Med* 2015; **2015**: 904926 [PMID: 26294930 DOI: 10.1155/2015/904926]
10 **Song GQ**, Sun Y, Liu LS, Pasricha PJ, Chen JD. T1332 Electroacupuncture Improves Impaired Gastric Accommodation and Vagal Activity in a Novel Rodent Model of Functional Dyspepsia. *Gastroenterology* 2008; **134**: A533-A533 [DOI: 10.1016/S0016-5085(08)62488-9]
11 **Imai K**, Ariga H, Takahashi T. Electroacupuncture improves imbalance of autonomic function under restraint stress in conscious rats. *Am J Chin Med* 2009; **37**: 45-55 [PMID: 19222111 DOI: 10.1142/S0192415X0900662X]
12 **Zhang S**, Li S, Liu Y, Ye F, Yin J, Foreman RD, Wang D, Chen JDZ. Electroacupuncture via chronically implanted electrodes improves gastric dysmotility mediated by autonomic-cholinergic mechanisms in a rodent model of functional dyspepsia. *Neurogastroenterol Motil* 2018; **30**: e13381 [PMID: 29856090 DOI: 10.1111/nmo.13381]
13 **Wang H**, Liu WJ, Shen GM, Zhang MT, Huang S, He Y. Neural mechanism of gastric motility regulation by electroacupuncture at RN12 and BL21: A paraventricular hypothalamic nucleus-dorsal vagal complex-vagus nerve-gastric channel pathway. *World J Gastroenterol* 2015; **21**: 13480-13489 [PMID: 26730159 DOI: 10.3748/wjg.v21.i48.13480]
14 **Paxinos G**, Watson C. *The Rat Brain in Stereotaxic Coordinates*. London: Academic Press 2007;
15 **Liu JH**, Yan J, Yi SX, Chang XR, Lin YP, Hu JM. Effects of electroacupuncture on gastric myoelectric activity and substance P in the dorsal vagal complex of rats. *Neurosci Lett* 2004; **356**: 99-102 [PMID: 14746873 DOI: 10.1016/j.neulet.2003.11.044]
16 **Li YQ**, Zhu B, Rong PJ, Ben H, Li YH. Neural mechanism of acupuncture-modulated gastric motility. *World J Gastroenterol* 2007; **13**: 709-716 [PMID: 17278193 DOI: 10.3748/wjg.v13.i5.709]
17 **Noguchi E**. Mechanism of reflex regulation of the gastroduodenal function by acupuncture. *Evid Based Complement Alternat Med* 2008; **5**: 251-256 [PMID: 18830456 DOI: 10.1093/ecam/nem077]
18 **Yu Z**, Xia YB, Lu MX, Lin J, Yu WJ, Xu B. [Influence of electroacupuncture stimulation of "tianshu" (ST 25), "quchi" (LI 11) and "shangjuxu" (ST 37) and their pairs on gastric motility in the rat]. *Zhen Ci Yan Jiu* 2013; **38**: 40-47 [PMID: 23650799]
19 **Sato A**, Sato Y, Suzuki A, Uchida S. Neural mechanisms of the reflex inhibition and excitation of gastric motility elicited by acupuncture-like stimulation in anesthetized rats. *Neurosci Res* 1993; **18**: 53-62 [PMID: 8134020 DOI: 10.1016/0168-0102(93)90105-Y]
20 **Smirnov VM**, Lychkova AE. Synergism of sympathetic and parasympathetic systems in the regulation of gastric motility. *Bull Exp Biol Med* 2002; **134**: 12-14 [PMID: 12459856 DOI: 10.1023/A:1020683916599]
21 **Browning KN**, Travagli RA. Plasticity of vagal brainstem circuits in the control of gastric function. *Neurogastroenterol Motil* 2010; **22**: 1154-1163 [PMID: 20804520 DOI: 10.1111/j.1365-2982.2010.01592.x]
22 **Armstrong DM**, Manley L, Haycock JW, Hersh LB. Co-localization of choline acetyltransferase and tyrosine hydroxylase within neurons of the dorsal motor nucleus of the vagus. *J Chem Neuroanat* 1990; **3**: 133-140 [PMID: 1971179 DOI: 10.1016/S0027-5107(97)00031-6]
23 **Tobin G**, Giglio D, Lundgren O. Muscarinic receptor subtypes in the alimentary tract. *J Physiol Pharmacol* 2009; **60**: 3-21 [PMID: 19439804]
24 **Lin S**, Kajimura M, Takeuchi K, Kodaira M, Hanai H, Kaneko E. Expression of muscarinic receptor subtypes in rat gastric smooth muscle: Effect of M3 selective antagonist on gastric motility and emptying. *Dig Dis Sci* 1997; **42**: 907-914 [PMID: 9149041 DOI: 10.1023/A:1018808329603]
25 **Hu X**, Yuan M, Yin Y, Wang Y, Li Y, Zhang N, Sun X, Yu Z, Xu B. Electroacupuncture at LI11 promotes jejunal motility via the parasympathetic pathway. *BMC Complement Altern Med* 2017; **17**: 329 [PMID: 28637453 DOI: 10.1186/s12906-017-1826-9]
26 **Yu Z**, Zhang N, Lu CX, Pang TT, Wang KY, Jiang JF, Zhu B, Xu B. Electroacupuncture at ST25 inhibits jejunal motility: Role of sympathetic pathways and TRPV1. *World J Gastroenterol* 2016; **22**: 1834-1843 [PMID: 26855542 DOI: 10.3748/wjg.v22.i5.1834]

27 **Browning KN**, Travagli RA. Central nervous system control of gastrointestinal motility and secretion and modulation of gastrointestinal functions. *Compr Physiol* 2014; **4**: 1339-1368 [PMID: 25428846 DOI: 10.1002/cphy.c130055]

28 **Babic T**, Browning KN, Travagli RA. Differential organization of excitatory and inhibitory synapses within the rat dorsal vagal complex. *Am J Physiol Gastrointest Liver Physiol* 2011; **300**: G21-G32 [PMID: 20947702 DOI: 10.1152/ajpgi.00363.2010]

29 **Sun HZ**, Zhao SZ, Cui XY, Ai HB. Hindbrain Effects of L-Glutamate on Gastric Motility in Rats. *Gastroenterology Res* 2009; **2**: 43-47 [PMID: 27956950 DOI: 10.4021/gr2009.02.1274]

30 **Cruz MT**, Murphy EC, Sahibzada N, Verbalis JG, Gillis RA. A reevaluation of the effects of stimulation of the dorsal motor nucleus of the vagus on gastric motility in the rat. *Am J Physiol Regul Integr Comp Physiol* 2007; **292**: R291-R307 [PMID: 16990483 DOI: 10.1152/ajpregu.00863.2005]

31 **Pearson RJ**, Gatti PJ, Sahibzada N, Massari VJ, Gillis RA. Ultrastructural evidence for selective GABAergic innervation of CNS vagal projections to the antrum of the rat. *Auton Neurosci* 2011; **160**: 21-26 [PMID: 21112817 DOI: 10.1016/j.autneu.2010.10.010]

32 **Andresen MC**, Kunze DL. Nucleus tractus solitarius--gateway to neural circulatory control. *Annu Rev Physiol* 1994; **56**: 93-116 [PMID: 7912060 DOI: 10.1146/annurev.ph.56.030194.000521]

33 **Iwa M**, Tateiwa M, Sakita M, Fujimiya M, Takahashi T. Anatomical evidence of regional specific effects of acupuncture on gastric motor function in rats. *Auton Neurosci* 2007; **137**: 67-76 [PMID: 17884736 DOI: 10.1016/j.autneu.2007.08.001]

34 **Zeng F**, Lan L, Tang Y, Liu M, Liu X, Song W, Li Y, Qin W, Sun J, Yu S, Gao X, Tian J, Liang F. Cerebral responses to puncturing at different acupoints for treating meal-related functional dyspepsia. *Neurogastroenterol Motil* 2015; **27**: 559-568 [PMID: 25693969 DOI: 10.1111/nmo.12532]

35 **Huang Z**, Liu N, Zhong S, Lu J, Zhang N. [The role of nucleus tractus solitarii (NTS) in acupuncture inhibition of visceral-somatic reflex (VSR)]. *Zhen Ci Yan Jiu* 1991; **16**: 43-47 [PMID: 1873901]

36 **He JF**, Yan J, Li JS, Liu JH, Wang C, Chang XR, Qu YT. Neuron discharge and c-Fos expression in the nucleus of the solitary tract following electroacupuncture at acupoints of the Yangming Stomach Meridian of Foot. *J Acupunct Meridian Stud* 2013; **6**: 82-88 [PMID: 23591003 DOI: 10.1016/j.jams.2012.12.002]

37 **Peng L**, Liu M, Chang X, Yang Z, Yi S, Yan J, Peng Y. Role of the nucleus tractus solitarii in the protection of pre-moxibustion on gastric mucosal lesions. *Neural Regen Res* 2014; **9**: 198-204 [PMID: 25206801 DOI: 10.4103/1673-5374.125350]

World Journal of Gastroenterology

Submit a Manuscript: https://www.f6publishing.com

World J Gastroenterol 2019 May 21; 25(19): 2327-2337

DOI: 10.3748/wjg.v25.i19.2327

ISSN 1007-9327 (print) ISSN 2219-2840 (online)

ORIGINAL ARTICLE

Case Control Study

Risk factors for progression to acute-on-chronic liver failure during severe acute exacerbation of chronic hepatitis B virus infection

Ling Yuan, Bai-Mei Zeng, Lu-Lu Liu, Yi Ren, Yan-Qing Yang, Jun Chu, Ying Li, Fang-Wan Yang, Yi-Huai He, Shi-De Lin

ORCID number: Ling Yuan (0000-0003-3457-8604); Bai-Mei Zeng (0000-0003-4313-8686); Lu-Lu Liu (0000-0003-1286-7632); Yi Ren (0000-0001-5770-0460); Yan-Qing Yang (0000-0002-9985-8677); Jun Chu (0000-0002-8106-6305); Ying Li (0000-0001-5793-5104); Fang-Wan Yang (0000-0002-8227-7577); Yi-Huai He (0000-0002-8639-3436); Shi-De Lin (0000-0001-8803-4069).

Author contributions: Yuan L and Zeng BM contributed equally to this work; Yuan L, Zeng BM, Liu LL, Ren Y, Chu J, Yang YQ, and Lin SD performed the research; Yuan L and Zeng BM wrote the manuscript; He YH, Yang FW, Li Ying, and Lin SD performed the biostatistic analysis; Zeng BM, Liu LL, Ren Y, Chu J, Yang YQ, and Lin SD analyzed the data; all authors discussed the results and commented on the manuscript.

Supported by the National Natural Science Foundation of China, No. 81460124 and No. 81860114.

Institutional review board statement: This study was approved by the Institutional Review Board of Affiliated Hospital of Zunyi Medical University, Guizhou Province, China.

Informed consent statement: All patients were informed of the use of their data in writing for clinical research purposes and accepted.

Conflict-of-interest statement: The authors declare that they have no conflicts of interest in this study.

Ling Yuan, Bai-Mei Zeng, Yan-Qing Yang, Jun Chu, Ying Li, Fang-Wan Yang, Yi-Huai He, Shi-De Lin, Department of Infectious Diseases, Affiliated Hospital of Zunyi Medical University, Zunyi 563003, Guizhou Province, China

Lu-Lu Liu, Department of Gastroenterology, Jiangsu Province Hospital, Pukou Branch, Nanjing 210000, Jiangsu Province, China

Yi Ren, Department of Respiratory Medicine, the Fifth People's Hospital of Chongqing, Chongqing 400062, China

Corresponding author: Shi-De Lin, MD, Chief Doctor, Occupational Physician, Professor, Department of Infectious Diseases, Affiliated Hospital of Zunyi Medical University, 201 Dalian street, Zunyi 563003, Guizhou Province, China. linshide6@zmc.edu.cn
Telephone: +86-851-28609183
Fax: +86-851-28609183

Abstract

BACKGROUND

Acute exacerbation in patients with chronic hepatitis B virus (HBV) infection results in different severities of liver injury. The risk factors related to progression to hepatic decompensation (HD) and acute-on-chronic liver failure (ACLF) in patients with severe acute exacerbation (SAE) of chronic HBV infection remain unknown.

AIM

To identify risk factors related to progression to HD and ACLF in compensated patients with SAE of chronic HBV infection.

METHODS

The baseline characteristics of 164 patients with SAE of chronic HBV infection were retrospectively reviewed. Independent risk factors associated with progression to HD and ACLF were identified. The predictive values of our previously established prediction model in patients with acute exacerbation (AE model) and the model for end-stage liver disease (MELD) score in predicting the development of ACLF were evaluated.

RESULTS

Among 164 patients with SAE, 83 (50.6%) had compensated liver cirrhosis (LC), 43 had progression to HD without ACLF, and 29 had progression to ACLF within

Manuscript source: Unsolicited manuscript

Received: February 14, 2019
Peer-review started: February 17, 2019
First decision: March 20, 2019
Revised: March 29, 2019
Accepted: April 19, 2019
Article in press: April 20, 2019
Published online: May 21, 2019

P-Reviewer: Bouare N, Farshadpour F, Sagnelli C
S-Editor: Yan JP
L-Editor: Wang TQ
E-Editor: Ma YJ

28 d after admission. Independent risk factors associated with progression to HD were LC and low alanine aminotransferase. Independent risk factors for progression to ACLF were LC, high MELD score, high aspartate aminotransferase (AST) levels, and low prothrombin activity (PTA). The area under the receiver operating characteristic of the AE model [0.844, 95% confidence interval (CI): 0.779-0.896] was significantly higher than that of MELD score (0.690, 95%CI: 0.613-0.760, $P < 0.05$) in predicting the development of ACLF.

CONCLUSION
In patients with SAE of chronic HBV infection, LC is an independent risk factor for progression to both HD and ACLF. High MELD score, high AST, and low PTA are associated with progression to ACLF. The AE model is a better predictor of ACLF development in patients with SAE than MELD score.

Key words: Acute-on-chronic liver failure; Chronic hepatitis B; Hepatic decompensation; Liver cirrhosis; Risk factors; Severe acute exacerbation

Core tip: The risk factors related to progression in patients with severe acute exacerbation (SAE) of chronic hepatitis B virus (HBV) infection remain unknown. This is the largest study to identify the risk factors related to progression to hepatic decompensation (HD) and acute-on-chronic liver failure (ACLF) in compensated patients with SAE of chronic HBV infection. We found that liver cirrhosis is an independent risk factor for progression to both HD and ACLF. High model for end-stage liver disease score, high aspartate aminotransferase, and low prothrombin activity are associated with progression to ACLF.

Citation: Yuan L, Zeng BM, Liu LL, Ren Y, Yang YQ, Chu J, Li Y, Yang FW, He YH, Lin SD. Risk factors for progression to acute-on-chronic liver failure during severe acute exacerbation of chronic hepatitis B virus infection. *World J Gastroenterol* 2019; 25(19): 2327-2337
URL: https://www.wjgnet.com/1007-9327/full/v25/i19/2327.htm
DOI: https://dx.doi.org/10.3748/wjg.v25.i19.2327

INTRODUCTION

In China, the majority of patients with end-stage liver diseases and liver disease-related death are caused by chronic hepatitis B virus (HBV) infection[1]. There are five phases in the natural history of chronic HBV infection, including hepatitis B e-antigen (HBeAg)-positive chronic HBV infection, HBeAg-positive chronic hepatitis B (CHB), HBeAg-negative chronic HBV infection, HBeAg-negative CHB, and hepatitis B surface antigen (HBsAg)-negative phase[2]. Hepatitis flares with different degrees of liver injury mostly occur in the HBeAg-positive CHB and HBeAg-negative CHB phases[3-5]. Acute exacerbation (AE) and severe AE (SAE) refer to the severe liver injury occurring in patients with chronic HBV infection during hepatitis flare[6,7]. AE of chronic HBV infection occurs in 40%-50% of HBeAg–positive patients and in 15%-30% of HBeAg-negative CHB patients[8-10]. Patients with AE or SAE eventually progress to hepatic decompensation (HD) and acute-on-chronic liver failure (ACLF) if their liver injury deteriorates further.

In patients with chronic HBV infection, HD manifesting as ascites, esophagogastric variceal bleeding (EVB), or hepatic encephalopathy is a significant stage during progression from AE to liver failure[11,12]. Once progressed to HD, the liver function of patients with AE or SAE becomes more unstable and undergoes more rapid deterioration to ACLF following intrahepatic or extrahepatic insults[13,14]. Despite improved clinical management, the mortality of patients with ACLF ranges from 50%-80% without liver transplantation[15]. It has been recognized that early diagnosis and treatment play an important role in survival of patients with ACLF; in earlier stages, intensive treatment may be effective in impeding disease progression[15,16]. Therefore, it is imperative to find the risk factors related to deterioration of HD and ACLF in patients with AE and SAE.

Several studies have been conducted to determine these risk factors. However, most of these studies have included patients with diverse etiologies and degrees of liver injury, with understandably inconsistent results[8,17-18]. It is therefore challenging to identify common factors related to disease progression in patients with high heterogeneity in terms of severity and cause. In a previous study, we assessed risk factors in patients with AE of chronic HBV infection, wherein AE was defined as alanine transaminase (ALT) > 5 × upper limits of normal (ULN), total bilirubin (TBil) ≥ 5 × ULN, and prothrombin time activity (PTA) of 40%-60%. We found that baseline age, HBV DNA, and international normalized ratio (INR) levels were independent factors related to the development of ACLF[19]. Based on this study, we established an AE model to predict the progression to ACLF in patients with AE. Although patients with AE or SAE of chronic HBV infection show different degrees of liver injury, it remains to be elucidated whether the risk factors in progression to ACLF are similar among these patients. Therefore, in this study, we included patients with SAE as ALT > 10 × ULN, TBil ≥ 3 × ULN, and PTA of 40%-60% and aimed to identify the baseline risk factors associated with post-admission progression to HD or ACLF.

MATERIALS AND METHODS

Study cohort

The study subjects were patients with SAE admitted to the Department of Infectious Diseases, Affiliated Hospital of Zunyi Medical University between January 2011 and August 2018. Figure 1 shows the flow chart for the patient selection process. In all, 164 patients with SAE of chronic HBV infection were included. The remaining 42 patients were excluded from the study by the exclusion criteria, which included coexistence with drug-induced hepatitis, alcoholic liver disease, hyperthyroidism, pregnancy, hepatocellular carcinoma, or acute hepatitis A, C, or E. Patients who had decompensated liver cirrhosis (LC) or were previously diagnosed with decompensated LC were also excluded.

Diagnostic criteria for SAE and ACLF

SAE of chronic HBV infection was diagnosed on the basis of the criteria proposed by Tsubota *et al*[20] and Wong *et al*[21]. The criteria for SAE of chronic HBV infection were as follows: (1) Presence of HBsAg and HBV DNA for > 6 mo before hospitalization; (2) ALT > 10 × ULN (400 IU/L) and TBil ≥ 3 × ULN (51 μmol/L); and (3) PTA of 40%-60%. Further, ACLF was diagnosed as the recent development of jaundice (TBil ≥ 5 × ULN) and coagulopathy (PTA < 40% or INR ≥ 1.5), complicated within four weeks by ascites and/or encephalopathy in a patient with previously diagnosed or undiagnosed chronic liver disease[12]. Cirrhosis was diagnosed based on previous liver biopsy findings or a composite of clinical signs and laboratory test, endoscopy, radiology, and FibroScan (Echosens, Paris, France) results. HD was defined as the presence of one of the following: new onset of hepatic encephalopathy, EVB, or ascites[22].

Treatment schedule

After admission, all patients received standard conservative therapy. None of them received liver transplantation. The standard conservative therapy included bed rest, liver-protective treatment (glutathione, adenosylmethionine, and branched-chain amino acids), nutritional and energy supplements, intravenous plasma and albumin (ALB) infusions, water-electrolyte and acid-base equilibrium maintenance, and prevention and treatment of complications. All patients received antiviral therapy including lamivudine, entecavir, or telbivudine within 3 days of admission according to their HBV replication levels and patient willingness. Plasma exchange was administered to patients who had progression to ACLF.

Candidate predictor variables

Patient demographics, clinical and laboratory parameters, and imaging findings were retrospectively collected from computerized and paper medical records. Laboratory variables including aspartate transaminase (AST), ALT, TBil, ALB, prealbumin, cholinesterase (CHE), gamma-glutamyl transpeptidase, PTA, INR, white blood cell count, platelet (PLT), serum sodium (Na+), blood urea nitrogen (BUN), creatinine (Cr), and HBV DNA levels were obtained within 24 h of the first diagnosis. In addition, the model for end-stage liver disease (MELD) score was calculated according to the following formula: MELD score = 3.78 × ln[TBil (mg/dL)] + 11.2 × ln(INR) + 9.57 × ln[Cr (mg/dL)] + 6.43 × (constant for liver disease etiology = 0, if cholestatic or alcoholic, otherwise = 1). The AE model was calculated as R = -13.323 + 0.553 × log HBV DNA (copies/mL) + 3.631 × INR + 0.053 × age (years)[19].

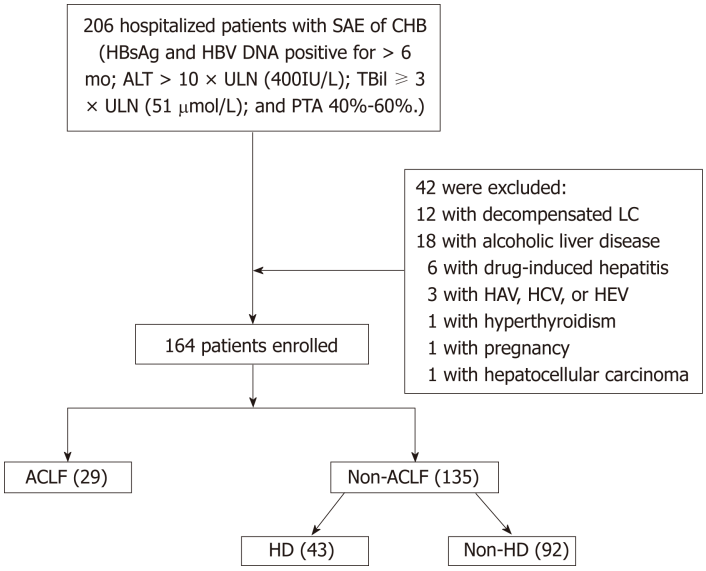

Figure 1 Outline of the screening and case selection protocol. ACLF: Acute-on-chronic liver failure; ALT: Alanine aminotransferase; CHB: Chronic hepatitis B; HAV: Hepatitis A virus; HBsAg: Hepatitis B surface antigen; HCV: Hepatitis C virus; HD: Hepatic decompensation; HEV: Hepatitis E virus; LC: Liver cirrhosis; PTA: Prothrombin activity; SAE: Severe acute exacerbation; TBil: Total bilirubin; ULN: Upper limit of normal.

Ethics statement

The protocol conformed to the provisions of the Declaration of Helsinki and was approved by the Human Ethical Committee of the Affiliated Hospital of Zunyi Medical University. All patients were informed of the use of their data in writing for clinical research purposes and accepted.

Statistical analysis

Statistical analyses were performed using SPSS version 19.0 (IBM Corp., Armonk, NY, United States) and MedCalc® 15.8 (MedCalc Software BVBA, Ostend, Belgium). Patient characteristics were compared between patients with and without HD or ACLF. $\chi 2$ tests, *t*-tests, and Mann–Whitney *U* tests were used for categorical variables, variables with normal distribution, and variables with a non-normal distribution, respectively. Univariate and multivariate analyses were performed using logistic regression analysis. The predictive values of our previously established AE model in patients with SAE and the MELD score were evaluated by the receiver operating characteristic (ROC) curve and the area under the ROC curve (AUROC). To identify the optimal cut-off point for each model, the Youden index was used. The cut-off sensitivity, specificity, positive predictive value (PPV), and negative predictive value (NPV) were calculated. $P < 0.05$ was considered statistically significant.

RESULTS

Patient characteristics

A total of 164 patients (mean age: 39.8 ± 11.1 years, 143 men and 21 women) were enrolled in the study. In all, 101 (61.6%) patients were HBeAg-positive and 83 (50.6%) had LC. Further, 43 (26.2%) patients had progression to HD without developing ACLF, and 29 (17.7%) patients had progression to ACLF within 28 d of admission. After admission of patients with SAE, the mean duration for development of HD and ACLF was 9.6 d (1-18 d) and 10.5 d (2-21 d), respectively. Thirteen (44.8%) patients with ACLF died during the 3 mo of follow-up. The other 92 patients (mean age: 36.6 ± 9.4 years, 82 men and 10 women) did not progress to HD or ACLF.

Difference in baseline characteristics between patients with and without post-admission progression to HD or ACLF

By comparing the baseline clinical characteristics and laboratory findings in patients with and without post-admission progression to HD, we found that among 43 patients who had progression to HD, 42 (97.7%) had LC on admission. However, among the 92 patients without progression to HD, only 20 (21.7%) had LC on admission. Further details on comparisons between baseline characteristics of patients

with and without post-admission progression to HD and ACLF can be found in Tables 1 and 2, respectively.

Risk factors related to the progression of HD in patients with SAE

Among 135 patients without progression to ACLF, 43 had progression to HD. Forty-two patients developed ascites and one patient developed EVB. As shown in Table 3, older age of patients; LC; lower serum levels of ALB, ALT, AST, CHE, PLT; and a higher serum level of BUN were found as the risk factors associated with post-admission HD in univariate logistic regression analysis. The independent risk factors associated with progressing to HD were LC and lower ALT level.

Risk factors related to the development of ACLF in patients with SAE

In the 29 patients who had progression to ACLF within 28 d after admission, 21 had LC on admission. As shown in Table 4, the risk factors associated with post-admission progression to ACLF were being complicated with LC, higher MELD score, higher serum levels of HBV DNA and AST, and lower serum level of PTA. The independent risk factors associated with progression to ACLF included higher MELD score, higher AST level, and lower PTA level.

Prediction of progression to ACLF in patients with SAE

To test the predictive value of the AE model in patients with SAE, we compared the ROC curve and AUROC of the AE model with those of the MELD score. As shown in Figure 2, the performance of the AE model [AUROC = 0.844, 95% confidence interval (CI): 0.779-0.896] was significantly better than that of the MELD score (AUROC = 0.690, 95%CI: 0.613-0.760, $P < 0.05$) in predicting the post-admission progression to ACLF. With a cut-off of -2.085, the AE model had a higher sensitivity (89.6%) and NPV (99.6%) than the MELD score at the cut-off value of 19.92 (55.2% and 89.3%, respectively). However, the specificity (62.2%) and PPV (33.8%) of the AE model were lower than those of the MELD score (80.2% and 38.1%, respectively).

DISCUSSION

The precipitating factors and pathogenesis of AE or SAE are different in patients with compensated liver diseases and decompensated LC[23,24]. Worsening of underlying chronic liver disease is the most common precipitating factor for AE or SAE in patients with compensated liver diseases[13]. However, in decompensated LC, the occurrence of AE or SAE and progression to liver failure are mostly triggered by complications including bacterial infection, renal function impairment, and gastrointestinal bleeding[25,26]. In this study, we excluded patients with SAE induced by other hepadnavirus infection and bacterial infection. We also excluded patients with decompensated LC; therefore, SAE in patients of this study mostly resulted from HBV reactivation. This group of patients exhibited similar clinical characteristics and pathogenesis of SAE[3], thus enabling the identification of common risk factors associated with progression to HD and ACLF. As far as we know, this is the largest study cohort in an investigation of this condition.

We included patients with SAE of chronic HBV infection with ALT > 10 × ULN, TBil ≥ 3 × ULN, and PTA of 40%-60%%. Forty-three (26.2%) patients had progression to HD and 29 (17.7%) patients had progression to ACLF within 28 d of admission. Therefore, the patients in this study had more serious liver injury than patients with AE as previously reported (only 7.59% of patients had progression to ACLF)[19]. We found that LC was an independent risk factor associated with progression to both HD and ACLF, while high MELD score, high AST, and low PTA were independent risk factors associated with progression to ACLF.

Several risk factors for post-admission development of ACLF in patients with SAE were different from those in patients with AE. In our previous study, LC was not an independent factor associated with the development of ACLF in patients with AE[19]. In this study, however, LC was an independent risk factor for post-admission progression of both HD and ACLF in patients with SAE. It is generally considered that in patients with chronic HBV infection, total liver injury consists of acute and chronic liver injury during AE or SAE[6,15]. Therefore, when the degree of acute liver injury reaches a certain limit, LC may be the determining factor for the outcomes during hepatitis flare. However, it is still unclear at what degree of acute liver injury the compensated LC may have a significant effect on the outcome of patients with chronic HBV infection. Contradictory results have been reported in previous studies, likely attributable to high heterogeneity in the degrees of liver injury and etiologies of study subjects[20,27-29]. Our results are the first to demonstrate that in patients with SAE of chronic HBV infection, compensated LC plays a determining role in the

Table 1 Baseline characteristics of patients with and without post-admission progression to hepatic decompensation

Variable	Total (*n* = 135)	Patients		*P*-value
		Without progression to HD (*n* = 92)	With progression to HD (*n* = 43)	
Males	120 (88.9)	82 (88.2)	38 (90.5)	0.777[1]
Age (yr)	39.1 ± 10.6	36.6 ± 9.4	44.6 ± 11.2	0.000[2]
LC	62 (45.9)	20 (21.7)	42 (97.7)	0.000[1]
HBeAg-positive	53 (39.3)	38 (40.9)	15 (35.7)	0.355[1]
log HBV DNA (copies/mL)	6.7 (5.6, 7.5)	6.9 (5.9, 7.5)	6.3 (4.2, 7.2)	0.044[3]
Na+ (mmol/L)	137.0 ± 2.9	136.9 ± 3.0	136.9 ± 2.8	0.927[2]
ALT (IU/L)	680.0 (421.0, 1191.0)	838.0 (495.5, 1333.5)	469.0 (265.5, 725.5)	0.000[3]
AST (IU/L)	592.0 (313.0, 980.0)	636.0 (369.0, 1212.5)	502.5 (268.5, 760.0)	0.022[3]
GGT (IU/L)	145.0 (108.0, 223.0)	145.0 (110.5, 221.5)	145.5 (94.5, 225.0)	0.845[3]
CHE (IU/L)	3.9 ± 1.5	4.3 ± 1.4	3.2 ± 1.4	0.000[2]
TBil (μmol/L)	174.1 (96.1, 288.7)	153.7 (93.9, 283.5)	160.7 (88.8, 250.5)	0.932[3]
ALB (g/L)	33.6 ± 4.9	34.4 ± 4.2	31.6 ± 5.2	0.001[2]
PA (mg/L)	48.0 (35.0, 69.0)	54.4 ± 25.4	49.4 ± 30.5	0.329[3]
BUN (mmol/L)	3.9 (3.0, 4.6)	3.8 (2.9, 4.4)	4.5(3.3, 4.4)	0.010[3]
Cr (μmol/L)	74.0 (67.0, 83.0)	74.0 (67.0, 84.0)	73.0 (66.3, 82.0)	0.557[3]
INR	1.46 ± 0.18	1.45 ± 0.18	1.47 ± 0.16	0.510[2]
PTA (%)	51.9 ± 5.5	51.6 ± 5.5	52.9 ± 5.5	0.208[2]
WBC (10^9/L)	5.2 (3.18, 6.7)	5.4 (3.9, 6.5)	4.7 (3.8, 7.5)	0.613[3]
PLT (10^9/L)	120.2 ± 49.1	128.9 ± 49.5	100.9 ± 42.8	0.002[2]
MELD	17.5 ± 3.8	17.5 ± 3.9	17.3 ± 3.7	0.830[2]

Data are presented as the mean ± SD, *n* (%), or median (interquartile range).
[1]Chi-square test results;
[2]*t*-test results;
[3]*U* test results. *P*-value: Patients with post-admission progression to hepatic decompensation *vs* patients without post-admission progression. ALT: Alanine aminotransferase; AST: Aspartate aminotransferase; BUN: Urea nitrogen; CHE: Cholinesterase; Cr: Creatinine; GGT: Glutamine transpeptidase; HBeAg: Hepatitis B e-antigen; HD: Hepatic decompensation; INR: International standardization ratio; LC: Liver cirrhosis; MELD: Model for end-stage liver disease; Na^+: Sodium; PA: Prealbumin; PLT: Platelet; PTA: Prothrombin activity; TBil: Total bilirubin; WBC: White blood cell.

development of both HD and ACLF.

Another differing result from our previous study in patients with AE was that HBV DNA was not an independent risk factor for progression to ACLF in patients with SAE of chronic HBV infection, although high HBV DNA level was one of the risk factors for progression to ACLF in the univariate analysis. Numerous studies have found that the occurrence of HCC and LC is closely correlated with high HBV DNA levels in patients with chronic HBV infection[30]. However, whether the short-term outcomes in patients with AE of chronic HBV infection are also influenced by HBV DNA levels remains unclear[20,21,31]. In patients with AE, it has been suggested that high HBV DNA levels might indicate an active immune attack of hepatocytes and ineffective inhibition of HBV DNA replication, resulting in prolonged liver injury, and patients may eventually progress to ACLF[3,32,33]. In a previous study, we found that HBV DNA was an independent risk factor for post-admission progression to ACLF in patients with AE[19]. Jeng *et al*[34] also found that in patients with AE, while TBil, PTA, and HBV DNA levels were risk factors, HBV DNA level was the only independent risk factor for HD. A high HBV DNA level of 1.55×10^9 copies/mL was predictive of HD. However, other studies found no relationship between baseline HBV DNA and AE severity or mortality of patients with AE[20,32,35,36]. Our results showing that HBV DNA played differing roles in the outcomes of patients with AE and SAE suggest that the influence of HBV DNA is dependent on the degree or stage of hepatitis flare. Patients with more severe liver injury are usually at a later stage during AE or SAE, as at this stage the deleterious role of HBV DNA may be masked by other risk factors. Hsu *et al* also found that in patients with SAE (defined as TBil level > 2 mg/dL and PT prolongation by more than 3 s, or with ascites/hepatic encephalopathy) of chronic HBV infection, the mortality of patients was mainly determined by the pronounced coagulopathy; only in patients with INR ≤ 1.7, HBV DNA level was the risk factor for mortality[17].

Table 2 Baseline characteristics of patients with and without post-admission progression to acute-on-chronic liver failure

Variable	Total (*n* = 164)	Patients		*P*-value
		Without progression to ACLF (*n* = 135)	With progression to ACLF (*n* = 29)	
Males	143 (87.2)	120 (88.9)	23 (79.3)	0.216[1]
Age (yr)	39.8 ± 10.1	39.1 ± 10.6	43.1 ± 11.1	0.066[2]
LC	83 (50.6)	62 (45.9)	21 (72.4)	0.013[1]
HBeAg-positive	101 (61.6)	82 (60.7)	19 (65.5)	0.679[1]
log HBV DNA (copies/mL)	6.7 (5.6, 7.5)	6.7 (5.5, 7.5)	7.1 (6.4, 7.7)	0.038[3]
Na+ (mmol/L)	137.0 ± 2.9	137.1 ± 2.7	137.7 ± 2.9	0.828[2]
ALT (IU/L)	724.5 (441.5, 1227.6)	680.0 (421.0, 1191.0)	833.0 (532.0, 1770.0)	0.056[3]
AST (IU/L)	628.0 (330.3, 1101.0)	592.0 (313.0, 980.0)	779.0 (426.5, 1411.0)	0.041[3]
GGT (IU/L)	139.5 (99.0, 210.8)	145.0 (108.0, 223.0)	111.0 (84.5, 162.5)	0.049[3]
CHE (IU/L)	4.0 ± 1.5	3.9 ± 1.5	4.1 ± 1.5	0.533[2]
TBil (μmol/L)	174.1 (96.1, 288.7)	155.1 (93.6, 272.9)	211.7 (147.3, 340.9)	0.038[3]
ALB (g/L)	33.5 ± 4.8	33.6 ± 4.8	33.3 ± 5.5	0.785[2]
PA (mg/L)	46.0 (31.3, 67.0)	48.0 (35.0, 69.0)	42.0 (26.5, 51.5)	0.041[3]
BUN (mmol/)	3.9 (3.0, 4.6)	3.9 (3.0, 4.6)	3.8 (3.2, 4.4)	0.923[3]
Cr (μmol/L)	73.0 (66.0, 82.0)	74.0 (67.0, 83.0)	71.0 (63.0, 77.5)	0.077[3]
INR	1.50 ± 0.21	1.46 ± 0.18	1.72 ± 0.24	0.000[2]
PTA (%)	51.1 (45.8, 55.8)	52.5 (48.1, 57.0)	44.0 (41.0, 47.8)	0.000[3]
WBC (10^9/L)	5.4 (3.9, 6.8)	5.2 (3.18, 6.7)	5.7 (4.4, 6.8)	0.207[3]
PLT (10^9/L)	118.9 ± 47.8	120.2 ± 49.1	112.5 ± 41.5	0.433[2]
MELD	17.9 ± 3.8	17.5 ± 3.8	19.8 ± 3.1	0.003[2]

Data are presented as the mean ± SD, *n* (%), or median (interquartile range).
[1]Chi-square test results;
[2]*t*-test results;
[3]*U* test results. *P*-value: Patients with post-admission progression to acute-on-chronic liver failure *vs* patients without post-admission progression. ACLF: Acute-on-chronic liver failure; ALT: Alanine aminotransferase; AST: Aspartate aminotransferase; BUN: Urea nitrogen; CHE: Cholinesterase; Cr: Creatinine; GGT: Glutamine transpeptidase; INR: International standardization ratio; LC: Liver cirrhosis; MELD: Model for end-stage liver disease; Na^+: Sodium; PA: Prealbumin; PLT: Platelet; PTA: Prothrombin activity; TBil: Total bilirubin; WBC: White blood cell.

Contrary to a higher HBV DNA level in patients who showed progression to ACLF, patients with progression of HD had a lower baseline HBV DNA level than those without progression to HD. Given that almost all patients with progression to HD had LC at baseline and previous studies have found that patients with LC had a lower HBV DNA level than those without[22], we considered that the high proportion of LC in patients with progression to HD resulted in a lower HBV DNA level than in those without progression to HD. Another interesting finding was that low ALT level was an independent risk factor for progression to HD. It is difficult to explain this result. ALT level reflects the degree of hepatocyte necrosis resulting from acute injury; further, we defined patients with SAE as having PTA between 40% and 60%, which reflects the total degree of liver injury. Therefore, low ALT levels in a patient may indicate a high degree of liver fibrosis. Our results suggest that the degree of liver fibrosis determines the development of HD in patients with compensated LC.

There is currently no predictive model for predicting the post-admission progression of ACLF in patients with SAE of chronic HBV infection. The MELD score is commonly used to assess liver disease severity[37]. It remains unknown whether the MELD score and AE model can predict the post-admission progression of ACLF in patients with SAE. In our study, although MELD score was a risk factor for progression to ACLF, the AUROC of MELD was < 0.7, indicating that the predictive value of MELD was low in patients with SAE. On the other hand, the AE model which did not include MELD score performed satisfactorily in predicting the occurrence of ACLF in patients with SAE of CHB. This result is difficult to explain. Because the AE model was established from patients with AE of chronic HBV infection, our result suggested that patients with AE and SAE had similar pathogenesis of progression to ACLF.

Our study was a retrospective, single-center study and has several limitations. First, we only studied patients' baseline clinical characteristics. We were not able to

Table 3 Univariate and multivariate analyses of risk factors associated with post-admission progression to hepatic decompensation

Variable	Univariate analysis				Multivariate analysis			
	B	OR	95%CI	*P*-value	β	OR	95%CI	*P*-value
Age	0.077	1.080	1.038-1.123	0.000				
HBV DNA	-0.276	0.759	0.587-0.981	0.035				
ALT	-0.002	0.998	0.997-0.999	0.000	-0.003	0.997	0.995-1.000	0.038
AST	-0.001	0.999	0.998-1.000	0.015				
CHE	-0.599	0.549	0.405-0.744	0.000				
ALB	-0.140	0.869	0.796-0.948	0.002				
BUN	0.238	1.268	1.029-1.563	0.026				
PLT	-0.014	0.986	0.977-0.995	0.003				
LC	5.019	151.2	19.6-1167.6	0.000	5.040	154.5	16.2-1469.0	0.000

CI: Confidence interval; OR: Odds ratio; ALB: Albumin; ALT: Alanine aminotransferase; AST: Aspartate aminotransferase; BUN: Urea nitrogen; CHE: Cholinesterase; HD: Hepatic decompensation; MELD: Model for end-stage liver disease; PLT: Platelet.

evaluate the predictive role of dynamic changes in HBV DNA as the short term changes in HBV DNA were not routinely measured in clinical practice. Although a few studies found that viral kinetics can predict the severity of AE in patients with CHB[32], a recent study showed that in patients with spontaneous SAE of CHB, either lamivudine or entecavir could induce a rapid decline of HBV viral load[38]. Second, the patients in this study were admitted from January 2011 to August 2018; although all patients received standard conservative therapy upon admission, the treatment methods may be different among the patients with SAE before admission. In addition, we did not detect HBV genotypes and HBV DNA mutation in most patients; therefore, we did not include these indicators in our study. To further elucidate the risk factors related to the development of ACLF in patients with SAE of chronic HBV infection, a prospective study involving more patients is needed.

Table 4 Univariate and multivariate analyses of risk factors associated with post-admission progression to acute-on-chronic liver failure

Variable	Univariate analysis				Multivariate analysis			
	B	OR	95%CI	*P*-value	β	OR	95%CI	*P*-value
MELD	0.161	1.175	1.049-1.315	0.005	0.184	1.202	1.033-1.398	0.017
HBV DNA	0.380	1.463	1.018-2.101	0.040				
AST	0.001	1.001	1.000-1.002	0.013	0.001	1.001	1.000-1.002	0.021
PTA	-0.252	0.777	0.704-0.858	0.000	-0.257	0.758	0.672-855	0.000
LC	1.128	3.091	1.280-7.465	0.012	2.125	8.369	2.389-29.322	0.001

ACLF: Acute-on-chronic liver failure; CI: Confidence interval; OR: Odds ratio; AST: Aspartate aminotransferase; LC: Liver cirrhosis; MELD: Model for end-stage liver disease; PTA: Prothrombin activity.

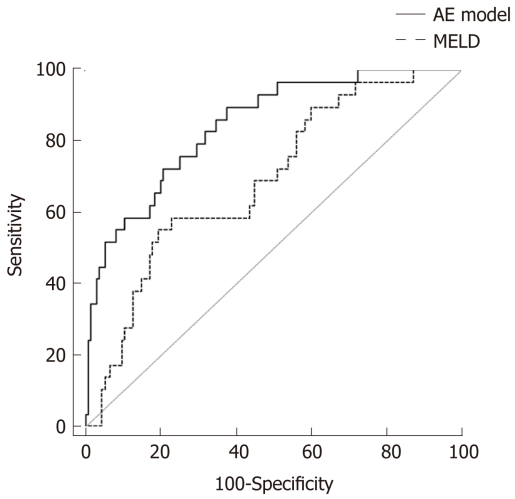

Figure 2 The area under the receiver operating characteristic curves of the AE model and model for end-stage liver disease for patients with severe acute exacerbation. AE model: The predictive model in the patients with acute exacerbation; MELD: Model for end-stage liver disease.

ARTICLE HIGHLIGHTS

Research background

The prognosis of patients with acute-on-chronic liver failure (ACLF) largely depends on early diagnosis and treatment. Patients with acute exacerbation (AE) or severe AE (SAE) of chronic hepatitis B virus (HBV) infection have a high tendency to further progress to hepatic decompensation (HD) and ACLF. Therefore, it is important to identify the risk factors for progression to HD and ACLF in patients with SAE of chronic HBV infection.

Research motivation

In a previous study, we have found that baseline age, HBV DNA, and international normalized ratio levels were independent factors associated with the development of ACLF in patients with AE of chronic HBV infection. Patients with AE or SAE have different degrees of liver injury, and it remains to be elucidated whether the risk factors for progression to ACLF are similar among these patients.

Research objectives

To identify risk factors related to progression to HD and ACLF in compensated patients with SAE of chronic HBV infection.

Research methods

The baseline characteristics of 164 patients with SAE of chronic HBV infection were retrospectively reviewed. Independent risk factors associated with progression to HD and ACLF were identified.

Research results

Independent risk factors associated with progression to HD were liver cirrhosis (LC) and low alanine aminotransferase (ALT). Independent risk factors for progression to ACLF were LC, high MELD score, high aspartate aminotransferase (AST) levels, and low prothrombin activity (PTA).

Research conclusions

Our results are the first to demonstrate that in patients with SAE of chronic HBV infection, compensated LC plays a determining role in the development of both HD and ACLF. High MELD score, high AST, and low PTA are associated with progression to ACLF.

Research perspectives

We found that liver cirrhosis is an independent risk factor for progression to both HD and ACLF. High model for end-stage liver disease score, high aspartate aminotransferase, and low prothrombin activity are associated with progression to ACLF.

REFERENCES

1 **Zhang S**, Wang F, Zhang Z. Current advances in the elimination of hepatitis B in China by 2030. *Front Med* 2017; **11**: 490-501 [PMID: 29170919 DOI: 10.1007/s11684-017-0598-4]
2 European Association for the Study of the Liver. Electronic address: easloffice@easloffice.eu.; European Association for the Study of the Liver. EASL 2017 Clinical Practice Guidelines on the management of hepatitis B virus infection. *J Hepatol* 2017; **67**: 370-398 [PMID: 28427875 DOI: 10.1016/j.jhep.2017.03.021]
3 **Chang ML**, Liaw YF. Hepatitis B flares in chronic hepatitis B: Pathogenesis, natural course, and management. *J Hepatol* 2014; **61**: 1407-1417 [PMID: 25178562 DOI: 10.1016/j.jhep.2014.08.033]
4 **Hoofnagle JH**. Reactivation of hepatitis B. *Hepatology* 2009; **49**: S156-S165 [PMID: 19399803 DOI: 10.1002/hep.22945]
5 **Kumar M**, Chauhan R, Gupta N, Hissar S, Sakhuja P, Sarin SK. Spontaneous increases in alanine aminotransferase levels in asymptomatic chronic hepatitis B virus-infected patients. *Gastroenterology* 2009; **136**: 1272-1280 [PMID: 19208347 DOI: 10.1053/j.gastro.2009.01.011]
6 **Wong VW**, Chan HL. Severe acute exacerbation of chronic hepatitis B: A unique presentation of a common disease. *J Gastroenterol Hepatol* 2009; **24**: 1179-1186 [PMID: 19682192 DOI: 10.1111/j.1440-1746.2009.05924.x]
7 **Tsai WL**, Sun WC, Cheng JS. Chronic Hepatitis B with Spontaneous Severe Acute Exacerbation. *Int J Mol Sci* 2015; **16**: 28126-28145 [PMID: 26703566 DOI: 10.3390/ijms161226087]
8 **Liaw YF**, Tai DI, Chu CM, Pao CC, Chen TJ. Acute exacerbation in chronic type B hepatitis: Comparison between HBeAg and antibody-positive patients. *Hepatology* 1987; **7**: 20-23 [PMID: 2433203 DOI: 10.1002/hep.1840070106]
9 **Liaw YF**, Chen JJ, Chen TJ. Acute exacerbation in patients with liver cirrhosis: A clinicopathological study. *Liver* 1990; **10**: 177-184 [PMID: 1696678 DOI: 10.1111/j.1600-0676.1990.tb00455.x]
10 **Fattovich G**, Brollo L, Alberti A, Realdi G, Pontisso P, Giustina G, Ruol A. Spontaneous reactivation of hepatitis B virus infection in patients with chronic type B hepatitis. *Liver* 1990; **10**: 141-146 [PMID: 2385155 DOI: 10.1111/j.1600-0676.1990.tb00449.x]
11 **Moreau R**, Jalan R, Gines P, Pavesi M, Angeli P, Cordoba J, Durand F, Gustot T, Saliba F, Domenicali M, Gerbes A, Wendon J, Alessandria C, Laleman W, Zeuzem S, Trebicka J, Bernardi M, Arroyo V; CANONIC Study Investigators of the EASL–CLIF Consortium. Acute-on-chronic liver failure is a distinct syndrome that develops in patients with acute decompensation of cirrhosis. *Gastroenterology* 2013; **144**: 1426-1437, 1437.e1-1437.e9 [PMID: 23474284 DOI: 10.1053/j.gastro.2013.02.042]
12 **Sarin SK**, Kedarisetty CK, Abbas Z, Amarapurkar D, Bihari C, Chan AC, Chawla YK, Dokmeci AK, Garg H, Ghazinyan H, Hamid S, Kim DJ, Komolmit P, Lata S, Lee GH, Lesmana LA, Mahtab M, Maiwall R, Moreau R, Ning Q, Pamecha V, Payawal DA, Rastogi A, Rahman S, Rela M, Saraya A, Samuel D, Saraswat V, Shah S, Shiha G, Sharma BC, Sharma MK, Sharma K, Butt AS, Tan SS, Vashishtha C, Wani ZA, Yuen MF, Yokosuka O; APASL ACLF Working Party. Acute-on-chronic liver failure: Consensus recommendations of the Asian Pacific Association for the Study of the Liver (APASL) 2014. *Hepatol Int* 2014; **8**: 453-471 [PMID: 26202751 DOI: 10.1007/s12072-014-9580-2]
13 **Wu T**, Li J, Shao L, Xin J, Jiang L, Zhou Q, Shi D, Jiang J, Sun S, Jin L, Ye P, Yang L, Lu Y, Li T, Huang J, Xu X, Chen J, Hao S, Chen Y, Xin S, Gao Z, Duan Z, Han T, Wang Y, Gan J, Feng T, Pan C, Chen Y, Li H, Huang Y, Xie Q, Lin S, Li L, Li J; Chinese Group on the Study of Severe Hepatitis B (COSSH). Development of diagnostic criteria and a prognostic score for hepatitis B virus-related acute-on-chronic liver failure. *Gut* 2018; **67**: 2181-2191 [PMID: 28928275 DOI: 10.1136/gutjnl-2017-314641]
14 **Gustot T**, Moreau R. Acute-on-chronic liver failure vs. traditional acute decompensation of cirrhosis. *J Hepatol* 2018; **69**: 1384-1393 [PMID: 30195459 DOI: 10.1016/j.jhep.2018.08.024]
15 **Nakayama N**, Uemura H, Uchida Y, Tomiya T, Ido A, Inoue K, Genda T, Takikawa Y, Sakaida I, Terai S, Yokosuka O, Shimizu M, Takikawa H, Mochida S. A multicenter pilot survey to clarify the clinical features of patients with acute-on-chronic liver failure in Japan. *Hepatol Res* 2018; **48**: 303-312 [PMID: 29341357 DOI: 10.1111/hepr.13064]
16 **Chen EQ**, Zeng F, Zhou LY, Tang H. Early warning and clinical outcome prediction of acute-on-chronic hepatitis B liver failure. *World J Gastroenterol* 2015; **21**: 11964-11973 [PMID: 26576085 DOI: 10.3748/wjg.v21.i42.11964]
17 **Hsu YC**, Wu CY, Chang CY, Tai CM, Tseng CH, Perng DS, Mo LR, Lin JT. Pretreatment viral DNA stratifies mortality risk in patients receiving antiviral therapy for severe acute exacerbation of chronic hepatitis B. *Antivir Ther* 2013; **18**: 221-228 [PMID: 23128388 DOI: 10.3851/IMP2435]
18 **Tsang SW**, Chan HL, Leung NW, Chau TN, Lai ST, Chan FK, Sung JJ. Lamivudine treatment for fulminant hepatic failure due to acute exacerbation of chronic hepatitis B infection. *Aliment Pharmacol Ther* 2001; **15**: 1737-1744 [PMID: 11683687 DOI: 10.1046/j.1365-2036.2001.01107.x]
19 **Ren Y**, Liu L, Li Y, Yang F, He Y, Zhu Y, Hu X, Lin S. Development and validation of a scoring system to predict progression to acute-on-chronic liver failure in patients with acute exacerbation of chronic hepatitis B. *Hepatol Res* 2018; **48**: 692-700 [PMID: 29336092 DOI: 10.1111/hepr.13062]
20 **Tsubota A**, Arase Y, Suzuki Y, Suzuki F, Sezaki H, Hosaka T, Akuta N, Someya T, Kobayashi M, Saitoh S, Ikeda K, Kumada H. Lamivudine monotherapy for spontaneous severe acute exacerbation of chronic hepatitis B. *J Gastroenterol Hepatol* 2005; **20**: 426-432 [PMID: 15740488 DOI: 10.1111/j.1440-1746.2004.03534.x]
21 **Wong VW**, Wong GL, Yiu KK, Chim AM, Chu SH, Chan HY, Sung JJ, Chan HL. Entecavir treatment in

patients with severe acute exacerbation of chronic hepatitis B. *J Hepatol* 2011; **54**: 236-242 [PMID: 21030105 DOI: 10.1016/j.jhep.2010.06.043]

22 **European Association for the Study of the Liver**. Electronic address: easloffice@easloffice.eu.; European Association for the Study of the Liver. EASL Clinical Practice Guidelines for the management of patients with decompensated cirrhosis. *J Hepatol* 2018; **69**: 406-460 [PMID: 29653741 DOI: 10.1016/j.jhep.2018.03.024]

23 **Mochida S**, Nakayama N, Ido A, Inoue K, Genda T, Takikawa Y, Sakaida I, Terai S, Yokosuka O, Shimizu M, Takikawa H. Proposed diagnostic criteria for acute-on-chronic liver failure in Japan. *Hepatol Res* 2018; **48**: 219-224 [PMID: 29361652 DOI: 10.1111/hepr.13066]

24 **Shi Y**, Yang Y, Hu Y, Wu W, Yang Q, Zheng M, Zhang S, Xu Z, Wu Y, Yan H, Chen Z. Acute-on-chronic liver failure precipitated by hepatic injury is distinct from that precipitated by extrahepatic insults. *Hepatology* 2015; **62**: 232-242 [PMID: 25800029 DOI: 10.1002/hep.27795]

25 **Fukui H**, Saito H, Ueno Y, Uto H, Obara K, Sakaida I, Shibuya A, Seike M, Nagoshi S, Segawa M, Tsubouchi H, Moriwaki H, Kato A, Hashimoto E, Michitaka K, Murawaki T, Sugano K, Watanabe M, Shimosegawa T. Evidence-based clinical practice guidelines for liver cirrhosis 2015. *J Gastroenterol* 2016; **51**: 629-650 [PMID: 27246107 DOI: 10.1007/s00535-016-1216-y]

26 **Clària J**, Stauber RE, Coenraad MJ, Moreau R, Jalan R, Pavesi M, Amorós À, Titos E, Alcaraz-Quiles J, Oettl K, Morales-Ruiz M, Angeli P, Domenicali M, Alessandria C, Gerbes A, Wendon J, Nevens F, Trebicka J, Laleman W, Saliba F, Welzel TM, Albillos A, Gustot T, Benten D, Durand F, Ginès P, Bernardi M, Arroyo V, Arroyo V. CANONIC Study Investigators of the EASL-CLIF Consortium and the European Foundation for the Study of Chronic Liver Failure (EF-CLIF). Systemic inflammation in decompensated cirrhosis: Characterization and role in acute-on-chronic liver failure. *Hepatology* 2016; **64**: 1249-1264 [PMID: 27483394 DOI: 10.1002/hep.28740]

27 **Zhang Q**, Han T, Li Y, Nie C, Liu H. Predictors of progression into acute-on-chronic liver failure from acute deterioration of pre-existing chronic liver disease. *Hepatol Res* 2016; **46**: 320-328 [PMID: 26234788 DOI: 10.1111/hepr.12567]

28 **Gao FY**, Liu Y, Li XS, Ye XQ, Sun L, Geng MF, Wang R, Liu HM, Zhou XB, Gu LL, Liu YM, Wan G, Wang XB. Score model for predicting acute-on-chronic liver failure risk in chronic hepatitis B. *World J Gastroenterol* 2015; **21**: 8373-8381 [PMID: 26217089 DOI: 10.3748/wjg.v21.i27.8373]

29 **Yuen MF**, Sablon E, Hui CK, Li TM, Yuan HJ, Wong DK, Doutreloigne J, Bogaerts V, Wong BC, Fan ST, Lai CL. Prognostic factors in severe exacerbation of chronic hepatitis B. *Clin Infect Dis* 2003; **36**: 979-984 [PMID: 12684909 DOI: 10.1086/374226]

30 **Terrault NA**, Lok ASF, McMahon BJ, Chang KM, Hwang JP, Jonas MM, Brown RS, Bzowej NH, Wong JB. Update on prevention, diagnosis, and treatment of chronic hepatitis B: AASLD 2018 hepatitis B guidance. *Hepatology* 2018; **67**: 1560-1599 [PMID: 29405329 DOI: 10.1002/hep.29800]

31 **Chen CH**, Lin CL, Hu TH, Hung CH, Tseng PL, Wang JH, Chang JY, Lu SN, Chien RN, Lee CM. Entecavir vs. lamivudine in chronic hepatitis B patients with severe acute exacerbation and hepatic decompensation. *J Hepatol* 2014; **60**: 1127-1134 [PMID: 24583247 DOI: 10.1016/j.jhep.2014.02.013]

32 **Mori N**, Suzuki F, Kawamura Y, Sezaki H, Hosaka T, Akuta N, Kobayashi M, Saito S, Suzuki Y, Arase Y, Ikeda K, Kobayashi M, Kumada H. Determinants of the clinical outcome of patients with severe acute exacerbation of chronic hepatitis B virus infection. *J Gastroenterol* 2012; **47**: 1022-1029 [PMID: 22370817 DOI: 10.1007/s00535-012-0561-8]

33 **Tsai SL**, Chen PJ, Lai MY, Yang PM, Sung JL, Huang JH, Hwang LH, Chang TH, Chen DS. Acute exacerbations of chronic type B hepatitis are accompanied by increased T cell responses to hepatitis B core and e antigens. Implications for hepatitis B e antigen seroconversion. *J Clin Invest* 1992; **89**: 87-96 [PMID: 1729285 DOI: 10.1172/JCI115590]

34 **Jeng WJ**, Sheen IS, Liaw YF. Hepatitis B virus DNA level predicts hepatic decompensation in patients with acute exacerbation of chronic hepatitis B. *Clin Gastroenterol Hepatol* 2010; **8**: 541-545 [PMID: 20298811 DOI: 10.1016/j.cgh.2010.02.023]

35 **Tsai WL**, Lo GH, Hsu PI, Lai KH, Lin CK, Chan HH, Chen WC, Cheng JS, Liu YC, Huang TS, Ger LP, Lin HH. Role of genotype and precore/basal core promoter mutations of hepatitis B virus in patients with chronic hepatitis B with acute exacerbation. *Scand J Gastroenterol* 2008; **43**: 196-201 [PMID: 18224565 DOI: 10.1080/00365520701745693]

36 **Chien RN**, Lin CH, Liaw YF. The effect of lamivudine therapy in hepatic decompensation during acute exacerbation of chronic hepatitis B. *J Hepatol* 2003; **38**: 322-327 [PMID: 12586298 DOI: 10.1097/00042737-200305000-00028]

37 **Singal AK**, Kamath PS. Model for End-stage Liver Disease. *J Clin Exp Hepatol* 2013; **3**: 50-60 [PMID: 25755471 DOI: 10.1016/j.jceh.2012.11.002]

38 **Lee TY**, Chen CY, Lia HC, Hsu YC, Yang SS. The ultra-short virological dynamics in response to entecavir or lamivudine during chronic hepatitis B with spontaneous severe acute exacerbation. *Antivir Ther* 2018; **23**: 77-85 [PMID: 28671553 DOI: 10.3851/IMP3183]

World Journal of Gastroenterology

Submit a Manuscript: https://www.f6publishing.com

World J Gastroenterol 2019 May 21; 25(19): 2338-2353

DOI: 10.3748/wjg.v25.i19.2338

ISSN 1007-9327 (print) ISSN 2219-2840 (online)

ORIGINAL ARTICLE

Retrospective Study

Role of D2 gastrectomy in gastric cancer with clinical para-aortic lymph node metastasis

Xiao-Hao Zheng, Wen Zhang, Lin Yang, Chun-Xia Du, Ning Li, Gu-Sheng Xing, Yan-Tao Tian, Yi-Bin Xie

ORCID number: Xiao-Hao Zheng (0000-0002-0282-1684); Wen Zhang (0000-0003-2594-5249); Lin Yang (0000-0002-4829-3119); Chun-Xia Du (0000-0003-3457-6377); Ning Li (0000-0002-7968-7364); Gu-Sheng Xing (0000-0002-7088-6973); Yan-Tao Tian (0000-0001-6479-7547); Yi-Bin Xie (0000-0002-0255-3018).

Author contributions: All authors helped to perform the research; Zheng XH and Xie YB contributed to study conception and design as well as manuscript writing; Zheng XH and Xing GS contributed to data collection; Zheng XH contributed to data analysis; Zheng XH, Zhang W, Yang L, Du CX, Li N, Tian YT, and Xie YB contributed to performing the treatment.

Supported by the CAMS Initiative for Innovative Medicine, No. 2016-I2M-1-007.

Institutional review board statement: This study was reviewed and approved by the Ethics Committee of CAMS.

Informed consent statement: The need for informed consent was waived because the analysis used anonymous clinical data that were obtained after each patient agreed to treatment by written consent.

Conflict-of-interest statement: All authors declare no conflicts of interest related to this article.

Data sharing statement: No additional data are available.

Xiao-Hao Zheng, Yan-Tao Tian, Yi-Bin Xie, Department of Pancreatic and Gastric Surgery, National Cancer Center/National Clinical Research Center for Cancer/Cancer Hospital, Chinese Academy of Medical Sciences and Peking Union Medical College, Beijing 100021, China

Wen Zhang, Lin Yang, Chun-Xia Du, Department of Medical Oncology, National Cancer Center/National Clinical Research Center for Cancer/Cancer Hospital, Chinese Academy of Medical Sciences and Peking Union Medical College, Beijing 100021, China

Ning Li, Department of Radiation Oncology, National Cancer Center/National Clinical Research Center for Cancer/Cancer Hospital, Chinese Academy of Medical Sciences and Peking Union Medical College, Beijing 100021, China

Gu-Sheng Xing, Department of Diagnostic Radiology, National Cancer Center/National Clinical Research Center for Cancer/Cancer Hospital, Chinese Academy of Medical Sciences and Peking Union Medical College, Beijing 100021, China

Corresponding author: Yi-Bin Xie, MD, Professor, Department of Pancreatic and Gastric Surgery, National Cancer Center/National Clinical Research Center for Cancer/Cancer Hospital, Chinese Academy of Medical Sciences and Peking Union Medical College, No. 17 Panjiayuannanli, Chaoyang District, Beijing 10021, China. yibinxie_2003@163.com
Telephone: +86-10-8778712

Abstract

BACKGROUND

Owing to the technical difficulty of pathological diagnosis, imaging is still the most commonly used method for clinical diagnosis of para-aortic lymph node metastasis (PALM) and evaluation of therapeutic effects in gastric cancer, which leads to inevitable false-positive findings in imaging. Patients with clinical PALM may have entirely different pathological stages (stage IV or not), which require completely different treatment strategies. There is no consensus on whether surgical intervention should be implemented for this group of patients. In particular, the value of D2 gastrectomy in a multidisciplinary treatment (MDT) approach for advanced gastric cancer with clinical PALM remains unknown.

AIM

To investigate the value of D2 gastrectomy in a MDT approach for gastric cancer patients with clinical PALM.

METHODS

In this real-world study, clinico-pathological data of all gastric cancer patients

Manuscript source: Unsolicited manuscript

Received: March 14, 2019
Peer-review started: March 14, 2019
First decision: March 27, 2019
Revised: April 17, 2019
Accepted: April 29, 2019
Article in press: April 29, 2019
Published online: May 21, 2019

P-Reviewer: Matowicka-Karna J, alebi Bezmin Abadi A, Tanabe S
S-Editor: Yan JP
L-Editor: Wang TQ
E-Editor: Ma YJ

treated at the Cancer Hospital, Chinese Academy of Medical Sciences between 2011 and 2016 were reviewed to identify those with clinically enlarged PALM. All the clinico-pathological data were prospectively documented in the patient medical record. For all the gastric cancer patients with advanced stage disease, especially those with suspicious distant metastasis, the treatment methods were determined by a multidisciplinary team.

RESULTS

In total, 48 of 7077 primary gastric cancer patients were diagnosed as having clinical PALM without other distant metastases. All 48 patients received chemotherapy as the initial treatment. Complete or partial response was observed in 39.6% (19/48) of patients in overall and 52.1% (25/48) of patients in the primary tumor. Complete response of PALM was observed in 50.0% (24/48) of patients. After chemotherapy, 45.8% (22/48) of patients received D2 gastrectomy, and 12.5% (6/48) of patients received additional radiotherapy. The postoperative major complication rate and mortality were 27.3% (6/22) and 4.5% (1/22), respectively. The median overall survival and progression-free survival of all the patients were 18.9 and 12.1 mo, respectively. The median overall survival of patients who underwent surgical resection or not was 50.7 and 12.8 mo, respectively. The 3-year and 5-year survival rates were 56.8% and 47.3%, respectively, for patients who underwent D2 resection. Limited PALM and complete response of PALM after chemotherapy were identified as favorable factors for D2 gastrectomy.

CONCLUSION

For gastric cancer patients with radiologically suspicious PALM that responds well to chemotherapy, D2 gastrectomy could be a safe and effective treatment and should be adopted in a MDT approach for gastric cancer with clinical PALM.

Key words: Gastric cancer; Para-aortic lymph node; Multidisciplinary; Gastrectomy; Conversion; Neoadjuvant

Core tip: The value of surgical resection in gastric cancer with radiologically overt para-aortic lymph node metastasis (PALM) is still not clear. Current controversial issues include the extent of resection (D1, D2, D2 + para-aortic lymph node metastasis dissection, or D3), surgical timing, and identification of optimal surgical candidates. This study confirmed the benefit of D2 gastrectomy after chemotherapy in select patients. Limited PALM at baseline and complete response of PALM after chemotherapy were proposed as criteria for selecting patients who will potentially benefit from D2 gastrectomy, which should be useful for future clinical trials.

Citation: Zheng XH, Zhang W, Yang L, Du CX, Li N, Xing GS, Tian YT, Xie YB. Role of D2 gastrectomy in gastric cancer with clinical para-aortic lymph node metastasis. *World J Gastroenterol* 2019; 25(19): 2338-2353
URL: https://www.wjgnet.com/1007-9327/full/v25/i19/2338.htm
DOI: https://dx.doi.org/10.3748/wjg.v25.i19.2338

INTRODUCTION

Gastric cancer is the fifth most common cancer and the third leading cause of mortality among all cancers worldwide. Gastric cancer with para-aortic lymph node metastasis (PALM) is considered a metastatic disease, and its prognosis remains poor after isolated surgical treatment. However, pathological diagnosis of enlarged para-aortic lymph nodes (PAN) is difficult. Certain methods, such as endoscopic ultrasound, B-ultrasound, or computed tomography (CT) guided fine needle aspiration, are theoretically feasible for pathological diagnosis of suspicious PALM. PAN biopsy is an invasive and technically difficult manipulation and thus is not typically used for clinical diagnosis of PALM in most institutes. In addition, positive

lymph nodes will disappear or shrink after preoperative treatment, which makes it difficult to re-biopsy the original nodes during follow-up. Despite the inevitable false-positive findings, imaging is still the most commonly used noninvasive method for clinical diagnosis of PALM and preoperative evaluation of therapeutic effects.

However, due to the fact that suspicious lymph node enlargement can be the result of inflammatory lymphadenopathy or malignancy, patients with radiologically overt PALM may have entirely different pathological stages (stage IV or not), which will require completely different treatment strategies. And the best clinical practice for patients with clinical PALM remains controversial for over ten years. Early this century, Sasako *et al*[1] conducted prophylactic D3 resection in advanced stage gastric cancer patients without radiologically overt PALM, and according to their results published in 2008, extended resection is not necessary. At the same time, through retrospective studies, other researchers have shown that D2 gastrectomy plus para-aortic lymph node dissection (PAND) might result in satisfactory outcomes in a highly select group of patients with PAN enlargement. Results reported by Tokunaga *et al*[2] and Roviello *et al*[3] in 2010 further complicate this issue. Both studies showed that even after extended D3 resection, the 5-year survival rates of patients with pathologically positive PAN were as low as 13.0% and 17.0%, respectively, not to mention the extremely high complication rate. Moreover, the phase III clinical trial REGATTA, in which patients with clinical PALM were enrolled, showed that chemotherapy alone was better than D1 gastrectomy followed by chemotherapy[4]. The above studies indicate that D1, D2 plus PAND, or D3 with adjuvant chemotherapy all failed to prolong the survival of patients with pathological PALM.

Recently, as preoperative chemotherapy was adopted into studies, Japanese oncologists reported an encouraging 5-year survival rate of 53% in gastric cancer with PALM treated by D2 gastrectomy with PAND after neoadjuvant chemotherapy. However, developing a safe and standard D2 plus PAND protocol after chemotherapy was challenging, and to date, only a few surgeons worldwide can perform it expertly. In addition, only 10% of patients who underwent D2 plus PAND had a pathologically positive PAN. Therefore, whether their method is the best solution for radiologically evident PALM is up for debate. Wang *et al*[5] considered patients with a good response to chemotherapy and PAN shrinkage to < 1.0 cm for D2 gastrectomy without PAND, and the surgery group had a non-inferior outcome compared with the Japanese results. More recently, several small studies have also reported improved survival through resection without metastasectomy after conversional chemotherapy. These results indicate that extensive resection might not be the only way to improve prognosis and D2 gastrectomy can provide a choice for select patients[6,7].

In our center, management of suspicious stage IV gastric cancer is determined by a multidisciplinary team. After conversional chemotherapy, the subsequent treatment method for patients with enlarged PAN prior to treatment is decided according to the response to chemotherapy. However, D3 or D2 resection plus PAND is not routinely recommended due to high morbidity and mortality. For those with enlarged PALM that cannot be controlled by chemotherapy, additional radiotherapy is recommended. In this study, we sought to determine the value of D2 gastrectomy in a multidisciplinary treatment approach for patients with clinical PALM based on data from this single center.

MATERIALS AND METHODS

Patients

In total, 7077 patients were diagnosed with gastric adenocarcinoma at the Cancer Hospital, Chinese Academy of Medical Sciences, from January 2011 to December 2016. We searched the clinico-pathological database for primary gastric adenocarcinoma patients with suspiciously enlarged lymph nodes in the para-aortic region documented in medical records prospectively. The inclusion criteria for this study were as follows: pathologically confirmed gastric adenocarcinoma with PAN enlargement; clinical T3-4 disease; no evidence of concurrent metastasis other than that in PAN, including distant hematogenous metastasis, distant lymph node metastasis, peritoneal metastasis and so on; esophageal invasion less than 3 cm; ECOG performance status of 0 or 1; sufficient oral intake and adequate organ function according to records at first visit; no previous malignancies; and pathologically confirmed HER2-negative gastric adenocarcinoma. In addition, patients who underwent reduction surgery or had positive lavage cytology were excluded, while palliative surgery to address severe uncontrollable complications during chemotherapy was allowed. This retrospective study was approved by the Ethics Committee of Cancer Institute and Hospital, Chinese Academy of Medical Sciences,

and the need for informed consent was waived.

Baseline evaluation

Contrast-enhanced thoracic/abdominal/pelvic CT, upper gastrointestinal tract endoscopy, and endoscopic ultrasonography (EUS) with or without positron emission tomography and CT (PET-CT) were conducted as the pretreatment workup. Both the clinical tumor stage (cT) and the clinical nodal stage (cN) were diagnosed *via* EUS and enhanced CT. Classification of TNM stage was defined according to the 8th edition of the American Joint Committee on Cancer Staging Manual. The clinical stage was evaluated by a multidisciplinary team based on all the radiological results.

The major criterion for clinical positive nodes on CT and EUS was solitary nodes ≥ 8 mm in minor diameter. The supplementary criteria for clinical PALM on EUS were as follows: echo-poor, roundish, or well-demarcated nodes. The supplementary criteria for clinical PALM on CT were as follows: Marked enhancement in the portal venous phase; cluster nodes regardless of the enhancement pattern; certain metastasis-associated enhancement patterns, such as central necrosis and heterogeneous enhancement; and highly clinically suspicious lymph nodes that did not satisfy the above criteria. The nodal size and anatomic location (station numbers) of all the suspicious lymph nodes were recorded. The lymph node station was classified using the fifteenth edition of the Japanese Classification of Gastric Carcinoma.

Chemotherapy and radiotherapy schedule

The chemotherapy regimens for this cohort of patients included S-1 plus oxaliplatin (SOX), docetaxel/oxaliplatin/S-1 (DOS), docetaxel/capecitabine/oxaliplatin (DOX), docetaxel/cisplatin/S-1 (DCS), capecitabine and oxaliplatin (XELOX), S-1 monotherapy, paclitaxel monotherapy, 5-fluorouracil (5-FU)/leucovorin (LV)/oxaliplatin (FOLFOX), irinotecan/5-FU/LV/oxaliplatin (FOLFOXIRI), and taxane/oxaliplatin.

Patients began receiving four cycles of adjuvant chemotherapy within 45 d after D2 gastrectomy, under the same regimen used preoperatively. For patients who were not suitable or unwilling to receive surgical resection, chemotherapy was continued. Second-line chemotherapy was administered when disease progression or recurrence was observed. Radiotherapy was not routinely recommended by the multidisciplinary team unless the presence of acute symptoms indicated a need for radiotherapy during chemotherapy or patients had an incomplete response (CR) of PALM after perioperative chemotherapy.

Tumor response and toxicity criteria

All the enrolled patients were treated with chemotherapy initially and then subjected to CT after every two cycles of chemotherapy for the first six cycles and every 2 mo thereafter. Patients were reevaluated by the multidisciplinary team, and after evaluation, D2 gastrectomy was recommended to patients who had responded well to treatment. Clinical response was evaluated using the Response Evaluation Criteria in Solid Tumors (RECIST) version 1.1, and the response of the primary tumor was assessed according to the fifteenth edition of the Japanese Classification of Gastric Carcinoma[8,9]. After chemotherapy, PAN disappearance or shrinkage to < 8 mm on CT was regarded as CR of PALM. Unless otherwise specified, all the diameters in this study refer to the short-axis diameter. The largest PAN was recorded as the index node, and the index nodes in the short axis is recorded as the index diameter. If all the enlarged lymph nodes disappeared in imaging, the index diameter was documented as a default value (5 mm) according to the RECIST 1.1. Two experienced radiologists were asked to evaluate the CT scans to document the overall response, response of the primary tumor, and the metastatic sites. Adverse events were assessed according to the National Cancer Institute's Common Terminology Criteria for Adverse Events v 4.0.

Follow-up

All the patients were followed *via* contrast-enhanced thoracic/abdominal/pelvic CT and blood testing every 3 mo for the first 3 years and every 6 mo thereafter.

Surgical procedure

Exploration and lavage cytology examination were carried out to exclude patients with other non-curable factors before gastrectomy. Distal, proximal, or total gastrectomy with D2 dissection was performed based on the tumor location. The PAN were not removed intentionally. The pathological response grading was based on the Mandard tumor grading system (TRG). Tumor staging and dissection range were in accordance with the eighth edition of the AJCC Cancer Staging Manual[10].

Postoperative complications were recorded according to the Clavien-Dindo classification.

Statistical analysis

The primary outcome was overall survival (OS, survival time from diagnosis to death from any cause), and the secondary outcome was progression-free survival (PFS, time from diagnosis to disease progression). Categorical data are presented as absolute and relative frequencies calculated using a chi-square test. Differences were determined by a Wilcoxon rank-sum test for non-normally distributed continuous variable (the short axis diameter of lymph nodes). We constructed violin plots of index diameter to analyze the index diameter distribution according to clinical factors. The Kaplan-Meier method was used to generate survival curves. All statistical tests were two-sided, and a *P*-value less than 0.05 was considered statistically significant. Analyses were performed using SAS software, version 9.4 (SAS Institute, Cary, NC, United States).

RESULTS

Patient characteristics

Between January 2011 and December 2016, 301 of 7077 gastric cancer patients were identified with PALM based on their medical history and were reevaluated by radiologists (Figure 1). A total of 209 patients were excluded because of a lack of concurrent PALM as the single non-curable factor. In addition, 19 patients with incomplete baseline information and 25 patients incompatible with the clinical inclusion criteria were also excluded. Finally, 48 patients with PALM as the single non-curable factor were included in this real-world study (Figure 1). Baseline information is shown in Table 1. The mean age at diagnosis was 57.2 years (range, 27-76 years), and male patients comprised the majority (81.3%). The common characteristics of the patients with radiological PAN enlargement were poor tumor differentiation and late tumor and nodal stage. In addition, major clinico-pathological characteristics were not significantly different between patients receiving or not receiving D2 gastrectomy.

Chemotherapy and adverse events

Of the 48 patients included, 17 were treated with SOX, 8 with DOS, 6 with DOX, 6 with DCS, 4 with XELOX, 2 with FOLFOX, 2 with taxane/oxaliplatin, and 3 with other regimens (S-1, paclitaxel monotherapy, or FOLFOXIRI). Among the 22 patients who underwent D2 gastrectomy after perioperative chemotherapy, 5 received DOS, 4 received SOX, 4 received DCS, 3 received XELOX, 2 received DOX, 2 received taxane/oxaliplatin, 1 received FOLFOX, and 1 received S-1 monotherapy. Following resection, 18 patients received adjuvant chemotherapy using the same regimen that was used preoperatively, and the other 4 patients did not receive adjuvant chemotherapy. Respectively, 6 and 8 patients among the patients who underwent D2 gastrectomy or not received less than six cycles of chemotherapy in total (Figure 1).

Adverse events associated with chemotherapy are listed in Table 2. The most frequent adverse events were anorexia (68.8%) and nausea (68.8%), most of which occurred at grade 1 or 2. Neutropenia was observed, with the most frequent adverse events being grade 3 or higher. One treatment-related death was reported in a patient who died of acute pulmonary embolism during the first cycle of initial chemotherapy.

Lymph node information and response assessment

Details related to lymph nodes at the first visit and at the time of best response during chemotherapy are listed in Table 3. The most common PAN station was No. 16b1 in 34 of 48 patients, followed by No. 16a2 (24/48). Overall, 27.1% (13/48) of patients had more than two para-aortic node stations involved. According to the RECIST 1.1 criteria, 26 patients had target lesions at baseline, while the other 22 patients had non-target lesions. The objective overall response rate in this group was 39.6% (19 of 48, Table 3). Response of the primary tumor was observed in 25 (52.1%) patients, and CR of metastatic sites was observed in 24 (50.0%) patients.

Surgical decision making

Violin plots of the distribution of the short axis diameter of the largest PAN distributed by whether the patient underwent D2 resection or not are shown in Figure 2A (baseline) and Figure 2C (after initial chemotherapy). Violin plots of the distribution of the short axis diameter of the largest PAN distributed by whether more than 2 PAN stations were involved or not are shown in Figure 2B (baseline) and Figure 2D (after initial chemotherapy). The distributions in both treatment groups and

Table 1 Characteristics of the patients at baseline

Variable	≥ 60 yr old	< 60 yr old
Gender		
Male	21 (91.3)	18 (72.0)
Female	2 (8.7)	7 (28.0)
Tumor location		
Lower	2 (8.7)	4 (16.0)
Middle	9 (39.1)	12 (48.0)
Upper	12 (52.2)	9 (36.0)
Clinical tumor stage		
T4	22 (95.7)	23 (92.0)
T3	1 (4.3)	2 (8.0)
Clinical nodal stage		
N2-3	18 (78.3)	21 (84.0)
N0-1	5 (21.7)	4 (16.0)
Macroscopic type		
4	4 (17.4)	3 (12.0)
1-3 or 5	19 (82.6)	22 (88.0)
Differentiation		
Poorly differentiated	18 (78.3)	23 (92.0)
Well differentiated	5 (21.7)	2 (8.0)
Performance status		
0	6 (26.1)	11 (44.0)
1	17 (73.9)	14 (56.0)

PAN stations significantly varied at baseline (chemotherapy *vs* chemotherapy plus D2 gastrectomy, $P = 0.01$, Figure 2A; PAN stations 1-2 *vs* 3-4, $P = 0.001$, Figure 2B) but were not significantly different after chemotherapy (chemotherapy *vs* chemotherapy plus D2 gastrectomy, $P = 0.29$, Figure 2C; PAN stations 1-2 *vs* 3-4, $P = 0.06$, Figure 2D). The correlation between CR of all clinical PALM and clinical characteristics is displayed in Table 4. The largest PAN in the short axis at baseline (≥15 mm *vs* < 15 mm), overall response (RECIST), and response of the primary lesion (JGCA) were correlated with CR of PALM. Considering the diameter of the index nodes, a CR was observed in 3 of 12 patients with PAN ≥ 15 mm (25%) and in 10 of 26 patients with PAN ≥ 10 mm (38.5%).

Of the 24 patients with CR of PALM, only 66.7% (16/24) achieved CR or partial response (PR) in the primary tumor. All 24 patients were recommended to receive surgical resection, and 14 patients with CR of PALM underwent D2 gastrectomy, while 8 patients with well-responded PALM also received D2 gastrectomy at the request of the patient. Among the 22 patients who received D2 gastrectomy, 2 exhibited CR, 5 exhibited PR, 2 exhibited stable disease (SD), 1 exhibited progressive disease (PD), and 12 were not evaluable considering the overall response; 2 exhibited CR, 12 exhibited PR, 7 exhibited SD, and 1 exhibited PD considering the response of the primary tumor. Among patients with an index node larger than 15 mm at the first visit, only 1 of 12 underwent D2 gastrectomy, and among patients with more than two PAN stations involved at baseline, only 1 of 13 underwent D2 gastrectomy.

In addition, six patients received radiotherapy as recommended by the multidisciplinary team in total. Among them, two patients received preoperative radiotherapy, three received adjuvant radiotherapy, and one received palliative radiotherapy.

Surgical outcomes

Lavage cytology was routinely performed, and positive lavage cytology was considered an incurable factor. Therefore, patients with positive cytology were excluded. For the 22 patients who ultimately underwent D2 gastrectomy, the median number of preoperative chemotherapy cycles was 4 [interquartile range (IQR), 3-5]. The median blood loss was 150 mL (IQR, 100-200 mL), and the median surgery time was 195 min (IQR, 170-214 min). Surgical and pathological data are listed in Table 5. Postoperative complications occurred in 27.3% (6/22) of patients, including abdominal infection (2/22), lymphatic fistula (1/22), pneumonia (1/22), anastomotic

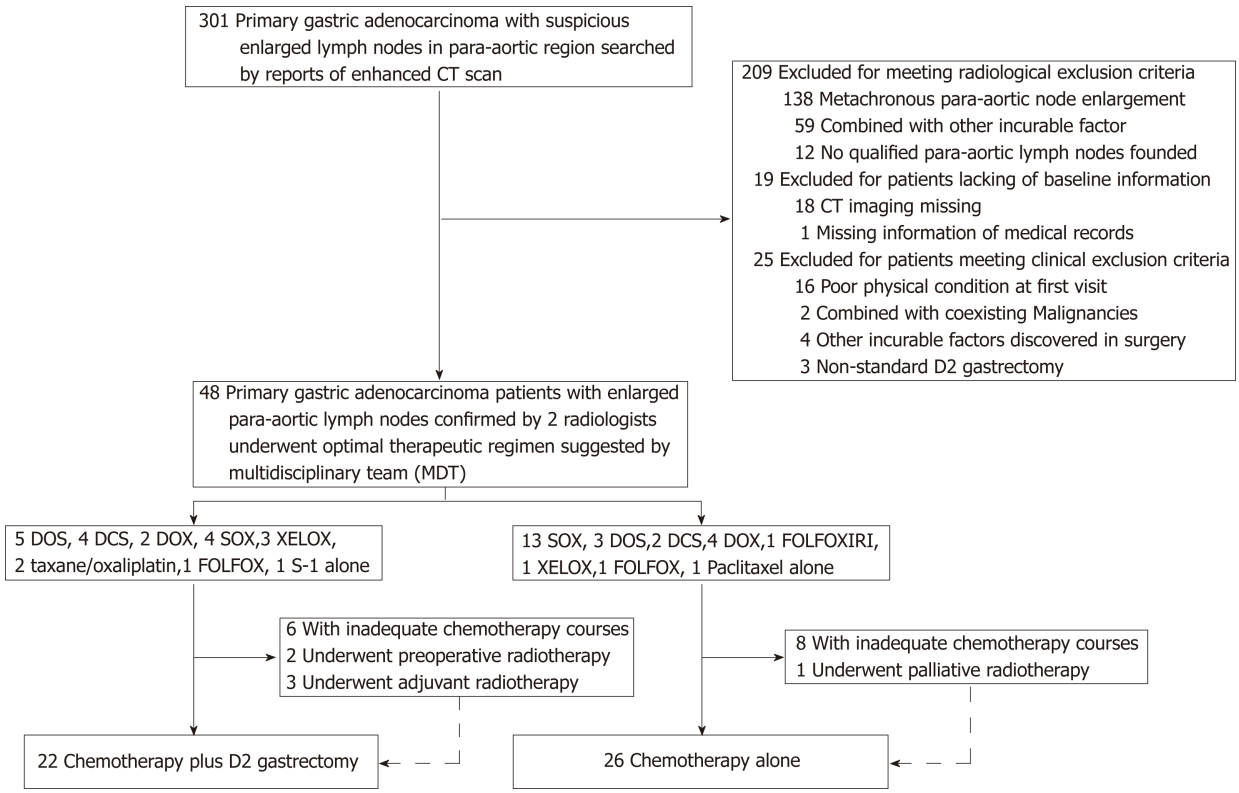

Figure 1 Flow chart. CT: Computed tomography; SOX: S-1 plus oxaliplatin; DOS: Docetaxel/oxaliplatin/S-1; DOX: Docetaxel/capecitabine/oxaliplatin; DCS: Docetaxel/cisplatin/S-1; XELOX: Capecitabine/oxaliplatin; FOLFOX: 5-fluorouracil/leucovorin/oxaliplatin; FOLFOXIRI: Irinotecan/5-fluorouracil/leucovorin/oxaliplatin.

leakage (1/22), and sudden cardiac death (1/22). One patient with a history of heart disease died of sudden cardiac death on postoperative day 28. Patients without CR of PALM were regarded as having an R1/R2 resection, and thus, R0 resection was achieved in 63.6% of patients. Three patients presented a pathological CR, and the pathological response rate was 68.2%.

Survival

Overall, 9 patients experienced recurrence after surgery during the follow-up period, with 7 patients experiencing recurrence within 1 year. The progressive sites included four cases of PAN recurrence, one case of hepatic metastasis, one case of peritoneal metastasis, and one case of malignant ascites. Two patients relapsed after 1 year, including one with lung recurrence and one with mediastinal lymph node metastasis. Distant lymph node metastasis was the most common site of recurrence and occurred in 55.6% (5/9) of cases.

Survival plots are presented in Figure 3. The median follow-up period was 16.2 months (range, 2.8-72.4 mo). The 3-year OS rate for all patients was 36.9% [95% confidence interval (CI): 21.2-52.6], the 3-year PFS rate of all patients was 27.6% (95%CI: 13.5-41.6), and the median OS and PFS were 18.9 and 12.1 mo, respectively (Figure 3A). The survival time of those who received D2 gastrectomy was much longer than that of patients who did not undergo gastrectomy (median OS: 50.7 mo *vs* 12.8 mo, $P = 0.0003$, Figure 3B; median PFS: 27.4 mo *vs* 7.8 mo, $P = 0.0002$, Figure 3C; 3-year survival rate: 56.8% (95%CI: 33.2-80.4) *vs* 19.0% (95%CI: 0.02-35.9)). The 5-year survival rate for the D2 gastrectomy patients reached 47.3% (95%CI: 21.4-73.3). The survival difference according to overall response was not significant (Figure 4D). However, according to the response of the primary tumor, the median OS of patients who responded well was significantly better than that of those who responded poorly (50.7 mo *vs* 11.5 mo, $P < 0.0001$, Figure 3E), and according to the response of PALM, the median OS of patients with CR of PALM was much better than that of patients without CR of PALM (50.7 mo *vs* 14.0 mo, $P = 0.0051$, Figure 3F). Differences in survival according to the index diameter (≥ 15 mm *vs* < 15 mm) and the stations involved (total PAN stations involved: > 2 *vs* 1-2) at baseline and the pathological response (Mandard TRG: 1-3 *vs* 4-5) were not significant in univariate analyses (data not shown).

Data of patients who survived more than 3 years are listed in Table 6. Among them, two underwent chemotherapy alone, while the other six received interventions *via* D2

Table 2 Adverse events of preoperative chemotherapy

Toxicity	Grade					Total	Grade ≥ 3 (%)
	1	2	3	4	5		
Diarrhea	4	2	2	0	0	8	4.2
Malaise	9	1	0	0	0	10	0.0
Anorexia	22	10	1	0	0	33	2.1
Nausea	20	11	2	0	0	33	4.2
Vomiting	6	4	0	0	0	10	0.0
Peripheral sensory neuropathy	13	4	0	0	0	17	0.0
Rash	1	0	1	0	0	2	2.1
Thromboembolic event	0	0	0	0	1	1	2.1
Anemia	11	2	3	0	0	16	6.3
Thrombocytopenia	7	6	4	1	0	18	10.4
Leukopenia	11	14	3	1	0	29	8.3
Neutropenia	7	5	9	4	0	25	27.1
Febrile neutropenia	4	0	0	0	0	4	0.0

gastrectomy. The surgical groups were characterized as having non-target PAN (short diameter < 15 mm), no more than two PAN stations involved at baseline, and CR of PALM after chemotherapy (range, 2-11 cycles) with or without the aid of radiotherapy (Table 6). One patient underwent D2 gastrectomy with an 11 mm left PAN (R1 resection) and received adjuvant radiotherapy to control the enlarged PAN. As a result, the suspicious PAN diminished dramatically, and the patient has been alive for 68 months after surgery without recurrence (Figure 4).

DISCUSSION

Chemotherapy is considered the primary choice for treatment of stage IV gastric cancer, but the prognosis remains poor. Surgery is not routinely recommended, except for palliative reasons. Under some conditions, treatment of clinical stage IV gastric cancer with a single incurable factor, such as PALM, positive lavage cytology, and sole liver metastasis, can be controversial. Unlike other incurable factors, PAN lesions are difficult for a biopsy, and the diagnosis and follow-up primarily depend on CT or PET-CT scanning. Thus, there is confusion concerning clinico-pathological issues in gastric cancer with suspicious PALM.

Currently, except PET-CT, clinical PALM is primarily diagnosed based on the enlarged diameter in the short axis of PAN[8,9]. In previously published studies, different enrollment criteria and distribution bias have compromised the comparability of results[11-15]. Although the current criteria for clinically positive lymph nodes on imaging examination, such as CT or EUS, are mainly based on lymph node measurement in the short axis[16-20], the cut-off value varies dramatically across different studies[12,21]. In this study, we selected a minimal axial diameter of 8 mm or greater as the main criterion for diagnosis of clinical lymph node metastasis, which is widely accepted in several studies and has shown a sensitivity and specificity of up to 85% and 95%, respectively[13-15,22]. In addition, the diameter of index nodes (equal to the largest clinically positive lymph nodes) was used to help us determine clinically positive PALM during treatment, because a change in the short diameter has been shown to be significantly correlated with pathological outcomes[23].

The incidence of metastases in the PAN was found to be only 8.5% in the JCOG 9501 trial, and thus, for the majority of gastric cancer patients without radiologically positive PALM, curative D2 surgery is adequate[1]. However, whether this method is suitable for patients with CR of PALM after chemotherapy remains unknown. In the present study, we defined PALM disappearance or shrinkage to < 8 mm in the short axis as clinical CR. Moreover, the survival of patients with clinical CR of PALM exhibited better survival than patients with positive PALM after chemotherapy. These results confirmed that CR of PALM was associated with a good prognosis and was a favorable factor for D2 resection. In addition, according to our results, a short axis < 8 mm can be chosen as the cut-off value for clinically negative PAN after chemotherapy, which is a stricter criterion than that in previous studies[5,8].

Table 3 Lymph node information at baseline and after chemotherapy

Variable	No. of patients (%)
At baselinePAN station involved number	
1-2	35 (72.9)
3-4	13 (27.1)
PAN station involved	
n16a1	8 (16.7)
n16a2	24 (50.0)
n16b1	34 (70.8)
n16b2	9 (18.8)
Clinical response after chemotherapy	
Overall (RECIST)	
Target lesions	
CR	2 (4.2)
PR	16 (33.3)
SD	6 (12.5)
PD	2 (4.2)
Non-target lesions only	
CR	1 (2.1)
Non-CR/Non-PD	19 (39.6)
PD	2 (4.2)
Primary lesions (JGCA)	
CR	3 (6.3)
PR	22 (45.8)
SD	19 (39.6)
PD	4 (8.3)
Metastatic lesions	
CR	24 (50.0)
Non-CR	24 (50.0)

PAN: Para-aortic node; CR: Complete response; PR: Partial response; SD: Stable disease; PD: Progressive disease; NE: Not evaluable; RECIST: Response Evaluation Criteria in Solid Tumors (version 1.1); JGCA: Japanese Gastric Cancer Association.

Current response evaluation criteria also lead to difficulties in response evaluation of gastric cancer patients with isolated PALM. In this study, 26 advanced gastric cancer patients with isolated PALM were absent from the classification of target lesions in RECIST 1.1, which regards primary tumors and lymph nodes < 15 mm as non-measurable[8]. After chemotherapy, 19 patients were considered inevaluable leading to a response rate of only 39.6%. We further analyzed the response by stratifying the primary tumor and PALM separately. The response of primary tumor was evaluated based on the 15th edition of the Japanese Classification of Gastric Carcinoma. While for PALM, we considered lymph node disappearance or shrinkage to < 8 mm as clinical CR after chemotherapy. Under the adjusted response evaluation system, we found that a good response of the primary tumor or CR of PALM was significantly correlated with better survival (Figure 3E and F).

Whether surgical resection is needed for stage IV gastric cancer remains controversial. PALM is classified as a relatively early type in stage IV gastric cancer, is associated with a lower tumor burden than other organ and peritoneal metastases[24], and could be considered as the most suitable type for surgery among all the types of stage IV gastric cancer[25,26]. In this group, the long-term OS of those who underwent D2 resection was much better than that of those who did not. The main reason was attributed to R0 resection and the difference in response to chemotherapy. Patients with a lower tumor burden or incurability *de novo*, which was characterized as a smaller tumor size, fewer metastatic lymph nodes, or fewer metastatic lymph node stations in gastric cancer with clinical PALM, are more prone to achieve CR of metastasis (Table 4); therefore, D2 gastrectomy was performed, resulting in a better prognosis. Kaito *et al*[27] found that involvement of a greater number of PAN stations was associated with a poorer prognosis. To date, most studies on surgical in-

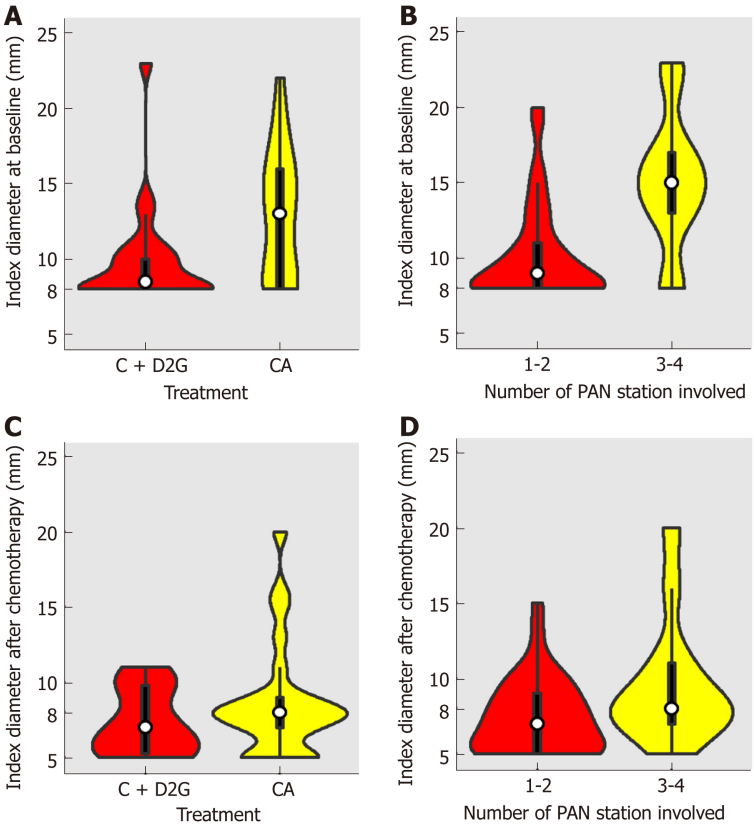

Figure 2 Violin plots of index diameter distribution of all patients. A: Violin plots of index diameter distribution at baseline of patients who underwent D2 resection or not; B: Violin plots of index diameter distribution at baseline of patients with involvement of more than two para-aortic lymph node stations or not; C: Violin plots of index diameter distribution of patients who underwent D2 resection or not after initial chemotherapy; D: Violin plots of index diameter distribution after initial chemotherapy of patients with involvement of more than two para-aortic lymph node stations or not. CA: Chemotherapy alone; C+D2G: Chemotherapy plus D2 gastrectomy; PAN: Para-aortic lymph node.

terventions in gastric cancer with clinical PALM have been limited to no more than two PAN stations (No. 16a2/16b1)[2,5,24,27-33]. Lymph node size was also found to be an independent prognostic factor for gastric cancer[21]. In the present study, we found that 58.3% (21/36) of patients with an index diameter less than 15 mm achieved CR after chemotherapy and then received surgical resection. We found confounding factors in both the station number and baseline lymph node size. Although patients with a higher metastatic burden, characterized as having a greater number of PAN stations involved and larger PAN size, did not show a significant impact on OS, they showed fewer chances of CR of PALM and fewer surgical decision made by the multidisciplinary team.

The extent of lymph node resection has long been a debated question. Japanese researchers tend to perform D2 resection plus PAND for advanced stage gastric cancer with overt PALM after chemotherapy; however, their results were not significantly better than those of the study that chose D2 gastrectomy. Many retrospective studies have reported a clinical benefit of curative D2 gastrectomy for patients with stage IV gastric cancer, who exhibited a CR of distant metastasis after chemotherapy without extensive resection[28,34,35].

We chose D2 resection as the surgical method for three reasons. First, no more than 10% of patients have radiologically occult metastasis in the para-aortic region, which indicates that D2 resection is adequate for most patients. Meanwhile, the most common recurrence site is para-aortic region even after PAND [27,30]. In this study, patients who underwent D2 surgery had a 22.7% lymph node recurrence rate, which is comparable to the 24.6%-30.0% lymph node recurrence rate of patients who underwent D2 gastrectomy plus PAND in previous studies. More importantly, the prognosis of pathologically positive patients was poor, therefore we did not think that PAND was necessary. Second, D3 or D2 plus PAND after chemotherapy has not been fully demonstrated in clinical studies, and is accompanied by a higher rate of morbidity and mortality even in the Japanese studies. Only a few gastrointestinal surgeons worldwide are experts at this complicated procedure[36-39]. Finally, with the development of radiotherapy, new techniques can provide excellent local control rates

Table 4 Demographic characteristics and response of para-aortic nodes

Variable	*n*	Response of PAN		*P*-value	Treatment		*P*-value
		Complete response	Residual tumor		With D2 resection	Without D2 resection	
Tumor location				0.5647			0.0931
Upper	21	10 (41.7)	11 (45.8)		7 (31.8)	14 (53.8)	
Middle	21	12 (50.0)	9 (37.5)		10 (45.5)	11 (42.3)	
Lower	6	2 (8.3)	4 (16.7)		5 (22.7)	1 (3.8)	
Clinical tumor stage				0.5510			0.4545
T3	3	2 (8.3)	1 (4.2)		2 (9.1)	1 (3.8)	
T4	45	22 (91.7)	23 (95.8)		20 (90.9)	25 (96.2)	
Clinical nodal stage				0.2673			0.1640
N0-1	9	6 (25.0)	3 (12.5)		6 (27.3)	3 (11.5)	
N2-3	39	18 (75.0)	21 (87.5)		16 (72.7)	23 (88.5)	
Macroscopic type				0.2199			0.5158
1-3 or 5	41	22 (91.7)	19 (79.2)		18 (81.8)	23 (88.5)	
4	7	2 (8.3)	5 (20.8)		4 (18.2)	3 (11.5)	
No. of PAN stations involved				0.1044			0.0012
1-2	35	20 (83.3)	15 (62.5)		21 (95.5)	14 (53.8)	
3-4	13	4 (16.7)	9 (37.5)		1 (4.5)	12 (46.2)	
Largest PAN in short-axis				0.0822			0.0899
< 10 mm	22	14 (58.3)	8 (33.3)		13 (59.1)	9 (34.6)	
≥ 10 mm	26	10 (41.7)	16 (66.7)		9 (40.9)	17 (65.4)	
Largest PAN in short-axis				0.0455			0.0026
< 15 mm	36	21 (87.5)	15 (62.5)		21 (95.5)	15 (57.7)	
≥ 15 mm	12	3 (12.5)	9 (37.5)		1 (4.5)	11 (42.3)	
Overall (RECIST)				0.0109			0.1405
CR + PR	19	10 (41.7)	9 (37.5)		7 (31.8)	12 (46.2)	
SD + PD	10	1 (4.2)	9 (37.5)		3 (13.6)	7 (26.9)	
NE	19	13 (54.2)	6 (25.0)		12 (54.5)	7 (26.9)	
Primary lesions (JGCA)				0.0431			0.1405
CR + PR	25	16 (66.7)	9 (37.5)		14 (63.6)	11 (42.3)	
SD + PD	23	8 (33.3)	15 (62.5)		8 (36.4)	15 (57.7)	

PAN: Para-aortic node; CR: Complete response; PR: Partial response; SD: Stable disease; PD: Progressive disease; NE: Not evaluable; RECIST: Response Evaluation Criteria in Solid Tumors (version 1.1); JGCA: Japanese Gastric Cancer Association.

to limit lymph node metastasis.

A similar phase II study conducted by Wang *et al*[5] also chose D2 resection as the surgical method and achieved an encouraging 1-year PFS rate of 47.8%, indicating non-inferior survival compared with neoadjuvant therapy plus extended dissection[31]. However, in our real-world study, the survival outcome was much more aggressive. The 3- and 5-year survival rates for patients who underwent D2 resection were 56.8% and 47.3%, respectively. In this study, the chemotherapy regimens and the compliance of perioperative chemotherapy varied. We think that the individualized chemotherapy regimens and the necessary radiotherapy targeted to each individual also contributed to the remarkable survival outcomes. In contrast, in some clinical trials, it is compulsory for patients to receive two or four cycles of chemotherapy regardless of whether it is the best timing[31,33,40,41].

Table 5 Surgical and pathological findings

Variable	Chemotherapy plus surgery
Residual tumor	
R0	14 (63.6)
R1-R2	8 (36.4)
Surgery approach	
Laparoscopy	8 (36.4)
Open	14 (63.6)
Extent of gastric resection	
Distal	11 (50.0)
Proximal	3 (13.6)
Total	7 (31.8)
Multiple organ resection	1 (4.5)
Macroscopic type	
1-3 or 5	18 (81.8)
4	4 (18.2)
Histological type	
Intestinal or mixed	11 (50.0)
Diffuse	11 (50.0)
Mandard grade	
1-2	2 (9.1)
3	13 (59.1)
4-5	7 (31.8)
Tumor depth	
ypT0	2 (9.1)
ypT1a	1 (4.5)
ypT1b	1 (4.5)
ypT2	1 (4.5)
ypT3	6 (27.3)
ypT4a	10 (45.5)
ypT4b	1 (4.5)
Lymph node metastases	
ypN0	7 (31.8)
ypN1	5 (22.7)
ypN2	2 (9.1)
ypN3a	5 (22.7)
ypN3b	3 (13.6)

Table 6 Long-term survivors (more than 3 years)

Therapy	PAN		Response			Survival			
	Target	SN	Overall	Primary	PAN	SR	OS	PFS	Status
C+S+C	NT	1	NE	PR	CR		65.1	65.1	Alive
C+S+C	NT	1	PR	PR	CR		72.4	72.4	Alive
C+S+C	NT	1	NE	PR	CR		62.1	62.1	Alive
C+S+C	NT	2	CR	CR	CR	L	52.8	16.8	Alive
C+S+CRT	NT	2	NE	SD	NN		70.1	70.1	Alive
C+S+CRT	NT	2	PR	PR	CR	PAN	50.7	16.2	Dead
C	T	3	CR	CR	CR	NA	37.8	20.9	Alive
C	T	3	PR	PR	NN	NA	36.3	36.3	Alive

C: Chemotherapy; S: D2 gastrectomy; CRT: Chemoradiotherapy; PAN: Para-aortic node; NT: Non-target lesions; SN: Para-aortic node station involved number; CR: Complete response; PR: Partial response; SD: Stable disease; PD: Progressive disease; NE: Not evaluable; NC: Non-complete response; SR:

Sites of recurrence; L: Lung; OS: Overall survival; PFS: Progression-free survival.

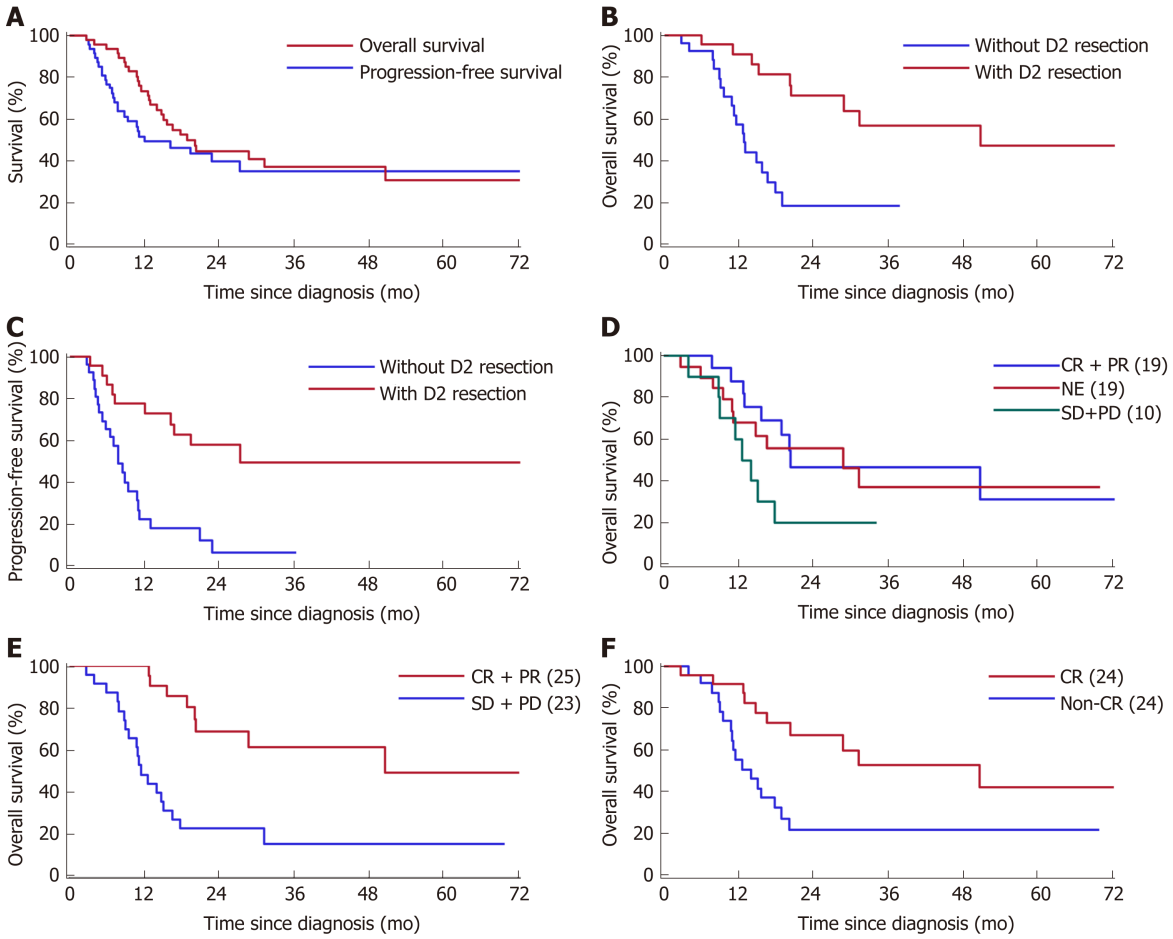

Figure 3 Kaplan-Meier curves for survival of the gastric cancer patients with clinically positive para-aortic node metastasis. A: Overall survival and progression-free survival of all patients; B: Overall survival of patients who underwent chemotherapy with or without D2 resection; C: Progression-free survival of patients who underwent chemotherapy with or without D2 resection; D: Overall survival of all patients assessed by overall response; E: Overall survival of all patients assessed by chemotherapy response of the primary tumor; F: Overall survival of all patients assessed by chemotherapy response of the metastatic para-aortic lymph node. CR: Complete response; PR: Partial response; SD: Stable disease; PD: Progressive disease; NE: Not evaluable.

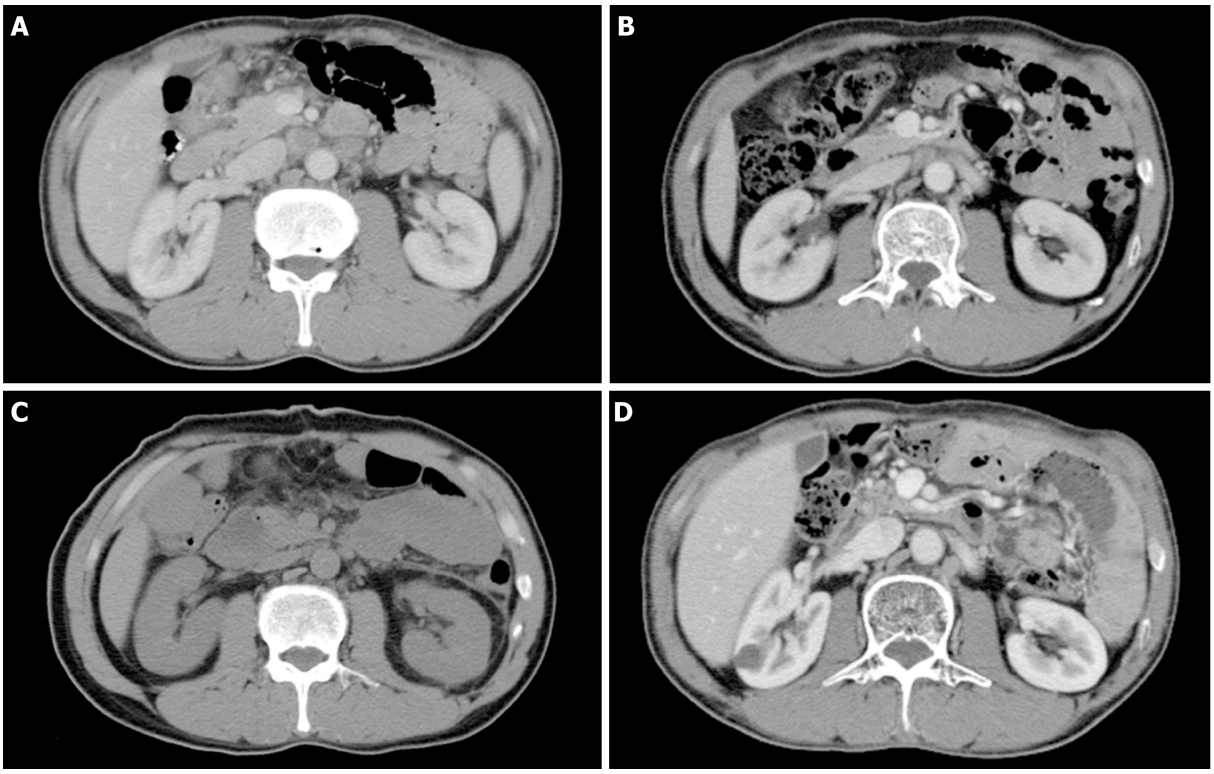

Figure 4 Computed tomography images of a gastric cancer patient with clinically positive para-aortic node metastasis who has survived for more than 70.1 mo. A: At baseline; B: Incomplete response of para-aortic lymph nodes after two cycles of preoperative chemotherapy (1.5 mo after initial treatment); C: After D2 gastrectomy (2.2 mo after initial treatment); D: Follow-up after adjuvant chemoradiotherapy (70.1 months after initial treatment).

ARTICLE HIGHLIGHTS

Research background

Para-aortic lymph node metastasis (PALM) is classified as stage IV gastric cancer with a dismal outcome after isolated surgical treatment. However, the treatment issues for patients with clinical para-aortic lymph node (PAN) enlargement are complex, as PAN enlargement can represent either inflammatory lymphadenopathy or malignant metastasis. In recent years, the role of surgery in multidisciplinary treatment (MDT) of gastric cancer with clinical PALM has been recognized. Nevertheless, the effect of D2 gastrectomy treatment has not yet been fully studied.

Research motivation

The benefit of addition of D2 gastrectomy to MDT and the unsettled clinico-pathological issues in gastric cancer with clinical PALM need to be discussed.

Research objectives

The present study aimed to determine whether D2 resection can be adopted for gastric cancer with radiologically overt PALM and to identify criteria of enrollment and response evaluation and find a best treatment strategy for this group of patients.

Research methods

We collected clinical and pathological data of gastric cancer patients with clinically positive PALM, including detailed information on PAN and clinical response. The short axis diameter of the largest PAN in every individual patient was recorded, and clinical response in the primary tumor and the metastatic sites was evaluated separately. Surgical decision making in accordance with the status of PALM after chemotherapy and survival data were documented.

Research results

D2 gastrectomy improved the prognosis of select patients, especially those with complete response (CR) of PALM. Patients with long-term survival were characterized as having limited PALM at baseline and CR of PALM after chemotherapy. For patients without CR of clinical PALM, radiotherapy may be considered as an option to complement D2 resection.

Research conclusions

Chemotherapy followed by D2 gastrectomy may be a promising strategy for treating select gastric cancer patients with radiologically suspicious PALM. Patients with limited PALM at baseline and CR of PALM after chemotherapy may be good candidates for D2 gastrectomy.

Large-scale, multicenter, randomized studies are needed to confirm the feasibility of addition of D2 gastrectomy to a practical MDT plan for patients with clinical PALM.

Research perspectives

Although we confirmed the benefit of D2 gastrectomy in gastric cancer patients with enlarged PALM, the problem of whether dissection of the para-aortic region is necessary remains unresolved. D2 gastrectomy has limitations as it greatly depends on good response of the metastatic lesions. Currently, a surgical strategy seems promising for gastric cancer with clinical PALM, but the best clinical practice should be identified in future research.

REFERENCES

1 **Sasako M**, Sano T, Yamamoto S, Kurokawa Y, Nashimoto A, Kurita A, Hiratsuka M, Tsujinaka T, Kinoshita T, Arai K, Yamamura Y, Okajima K; Japan Clinical Oncology Group. D2 lymphadenectomy alone or with para-aortic nodal dissection for gastric cancer. *N Engl J Med* 2008; **359**: 453-462 [PMID: 18669424 DOI: 10.1056/NEJMoa0707035]

2 **Tokunaga M**, Ohyama S, Hiki N, Fukunaga T, Aikou S, Yamaguchi T. Can superextended lymph node dissection be justified for gastric cancer with pathologically positive para-aortic lymph nodes? *Ann Surg Oncol* 2010; **17**: 2031-2036 [PMID: 20182811 DOI: 10.1245/s10434-010-0969-4]

3 **Roviello F**, Pedrazzani C, Marrelli D, Di Leo A, Caruso S, Giacopuzzi S, Corso G, de Manzoni G. Super-extended (D3) lymphadenectomy in advanced gastric cancer. *Eur J Surg Oncol* 2010; **36**: 439-446 [PMID: 20392590 DOI: 10.1016/j.ejso.2010.03.008]

4 **Fujitani K**, Yang HK, Mizusawa J, Kim YW, Terashima M, Han SU, Iwasaki Y, Hyung WJ, Takagane A, Park DJ, Yoshikawa T, Hahn S, Nakamura K, Park CH, Kurokawa Y, Bang YJ, Park BJ, Sasako M, Tsujinaka T; REGATTA study investigators. Gastrectomy plus chemotherapy versus chemotherapy alone for advanced gastric cancer with a single non-curable factor (REGATTA): A phase 3, randomised controlled trial. *Lancet Oncol* 2016; **17**: 309-318 [PMID: 26822397 DOI: 10.1016/S1470-2045(15)00553-7]

5 **Wang Y**, Yu YY, Li W, Feng Y, Hou J, Ji Y, Sun YH, Shen KT, Shen ZB, Qin XY, Liu TS. A phase II trial of Xeloda and oxaliplatin (XELOX) neo-adjuvant chemotherapy followed by surgery for advanced gastric cancer patients with para-aortic lymph node metastasis. *Cancer Chemother Pharmacol* 2014; **73**: 1155-1161 [PMID: 24748418 DOI: 10.1007/s00280-014-2449-1]

6 **Okabe H**, Ueda S, Obama K, Hosogi H, Sakai Y. Induction chemotherapy with S-1 plus cisplatin followed by surgery for treatment of gastric cancer with peritoneal dissemination. *Ann Surg Oncol* 2009; **16**: 3227-3236 [PMID: 19777180 DOI: 10.1245/s10434-009-0706-z]

7 **Beom SH**, Choi YY, Baek SE, Li SX, Lim JS, Son T, Kim HI, Cheong JH, Hyung WJ, Choi SH, Jung M, Kim HS, Jeung HC, Chung HC, Rha SY, Noh SH. Multidisciplinary treatment for patients with stage IV gastric cancer: The role of conversion surgery following chemotherapy. *BMC Cancer* 2018; **18**: 1116 [PMID: 30442107 DOI: 10.1186/s12885-018-4998-x]

8 **Schwartz LH**, Bogaerts J, Ford R, Shankar L, Therasse P, Gwyther S, Eisenhauer EA. Evaluation of lymph nodes with RECIST 1.1. *Eur J Cancer* 2009; **45**: 261-267 [PMID: 19091550 DOI: 10.1016/j.ejca.2008.10.028]

9 **Eisenhauer EA**, Therasse P, Bogaerts J, Schwartz LH, Sargent D, Ford R, Dancey J, Arbuck S, Gwyther S, Mooney M, Rubinstein L, Shankar L, Dodd L, Kaplan R, Lacombe D, Verweij J. New response evaluation criteria in solid tumours: Revised RECIST guideline (version 1.1). *Eur J Cancer* 2009; **45**: 228-247 [PMID: 19097774 DOI: 10.1016/j.ejca.2008.10.026]

10 **Amin MB**, Edge S, Greene F, Byrd DR, Brookland RK, Washington MK, Gershenwald JE, Compton CC, Hess KR, Sullivan DC, Jessup JM, Brierley JD, Gaspar LE, Schilsky RL, Balch CM, Winchester DP, Asare EA, Madera M, Gress DM, Meyer LR. AJCC Cancer Staging Manual. 8th ed. Springer International Publishing. 2017; XVII, 1032 [DOI: 10.1007/978-3-319-40618-3]

11 **Dorfman RE**, Alpern MB, Gross BH, Sandler MA. Upper abdominal lymph nodes: Criteria for normal size determined with CT. *Radiology* 1991; **180**: 319-322 [PMID: 2068292 DOI: 10.1148/radiology.180.2.2068292]

12 **Fukuya T**, Honda H, Hayashi T, Kaneko K, Tateshi Y, Ro T, Maehara Y, Tanaka M, Tsuneyoshi M, Masuda K. Lymph-node metastases: Efficacy for detection with helical CT in patients with gastric cancer. *Radiology* 1995; **197**: 705-711 [PMID: 7480743 DOI: 10.1148/radiology.197.3.7480743]

13 **Joo I**, Kim SH, Ahn SJ, Lee ES, Shin CI, Lee HJ, Yang HK. Preoperative tumor restaging and resectability assessment of gastric cancers after chemotherapy: Diagnostic accuracy of MDCT using new staging criteria. *Abdom Radiol (NY)* 2017; **42**: 2807-2815 [PMID: 28643135 DOI: 10.1007/s00261-017-1224-2]

14 **Marrelli D**, Mazzei MA, Pedrazzani C, Di Martino M, Vindigni C, Corso G, Morelli E, Volterrani L, Roviello F. High accuracy of multislices computed tomography (MSCT) for para-aortic lymph node metastases from gastric cancer: A prospective single-center study. *Ann Surg Oncol* 2011; **18**: 2265-2272 [PMID: 21267792 DOI: 10.1245/s10434-010-1541-y]

15 **Kwee RM**, Kwee TC. Imaging in assessing lymph node status in gastric cancer. *Gastric Cancer* 2009; **12**: 6-22 [PMID: 19390927 DOI: 10.1007/s10120-008-0492-5]

16 **Fairweather M**, Jajoo K, Sainani N, Bertagnolli MM, Wang J. Accuracy of EUS and CT imaging in preoperative gastric cancer staging. *J Surg Oncol* 2015; **111**: 1016-1020 [PMID: 25872753 DOI: 10.1002/jso.23919]

17 **Feng XY**, Wang W, Luo GY, Wu J, Zhou ZW, Li W, Sun XW, Li YF, Xu DZ, Guan YX, Chen S, Zhan YQ, Zhang XS, Xu GL, Zhang R, Chen YB. Comparison of endoscopic ultrasonography and multislice spiral computed tomography for the preoperative staging of gastric cancer - results of a single institution study of 610 Chinese patients. *PLoS One* 2013; **8**: e78846 [PMID: 24223855 DOI: 10.1371/journal.pone.0078846]

18 **Hwang SW**, Lee DH, Lee SH, Park YS, Hwang JH, Kim JW, Jung SH, Kim NY, Kim YH, Lee KH, Kim HH, Park DJ, Lee HS, Jung HC, Song IS. Preoperative staging of gastric cancer by endoscopic ultrasonography and multidetector-row computed tomography. *J Gastroenterol Hepatol* 2010; **25**: 512-518 [PMID: 20370729 DOI: 10.1111/j.1440-1746.2009.06106.x]

19 **Mehmedović A**, Mesihović R, Saray A, Vanis N. Gastric cancer staging: EUS and CT. *Med Arch* 2014; **68**: 34-36 [PMID: 24783909 DOI: 10.5455/medarh.2014.68.34-36]
20 **Mocellin S**, Marchet A, Nitti D. EUS for the staging of gastric cancer: A meta-analysis. *Gastrointest Endosc* 2011; **73**: 1122-1134 [PMID: 21444080 DOI: 10.1016/j.gie.2011.01.030]
21 **Tokunaga M**, Sugisawa N, Tanizawa Y, Bando E, Kawamura T, Terashima M. The impact of preoperative lymph node size on long-term outcome following curative gastrectomy for gastric cancer. *Ann Surg Oncol* 2013; **20**: 1598-1603 [PMID: 23117474 DOI: 10.1245/s10434-012-2699-2]
22 **De Manzoni G**, Marrelli D, Baiocchi GL, Morgagni P, Saragoni L, Degiuli M, Donini A, Fumagalli U, Mazzei MA, Pacelli F, Tomezzoli A, Berselli M, Catalano F, Di Leo A, Framarini M, Giacopuzzi S, Graziosi L, Marchet A, Marini M, Milandri C, Mura G, Orsenigo E, Quagliuolo V, Rausei S, Ricci R, Rosa F, Roviello G, Sansonetti A, Sgroi G, Tiberio GA, Verlato G, Vindigni C, Rosati R, Roviello F. The Italian Research Group for Gastric Cancer (GIRCG) guidelines for gastric cancer staging and treatment: 2015. *Gastric Cancer* 2017; **20**: 20-30 [PMID: 27255288 DOI: 10.1007/s10120-016-0615-3]
23 **Lee SM**, Kim SH, Lee JM, Im SA, Bang YJ, Kim WH, Kim MA, Yang HK, Lee HJ, Kang WJ, Han JK, Choi BI. Usefulness of CT volumetry for primary gastric lesions in predicting pathologic response to neoadjuvant chemotherapy in advanced gastric cancer. *Abdom Imaging* 2009; **34**: 430-440 [PMID: 18546037 DOI: 10.1007/s00261-008-9420-8]
24 **Park IH**, Kim SY, Kim YW, Ryu KW, Lee JH, Lee JS, Park YI, Kim NK, Park SR. Clinical characteristics and treatment outcomes of gastric cancer patients with isolated para-aortic lymph node involvement. *Cancer Chemother Pharmacol* 2011; **67**: 127-136 [PMID: 20221601 DOI: 10.1007/s00280-010-1296-y]
25 **Yoshida K**, Yamaguchi K, Okumura N, Tanahashi T, Kodera Y. Is conversion therapy possible in stage IV gastric cancer: The proposal of new biological categories of classification. *Gastric Cancer* 2016; **19**: 329-338 [PMID: 26643880 DOI: 10.1007/s10120-015-0575-z]
26 **Yamaguchi K**, Yoshida K, Tanaka Y, Matsuhashi N, Tanahashi T, Takahashi T. Conversion therapy for stage IV gastric cancer-the present and future. *Transl Gastroenterol Hepatol* 2016; **1**: 50 [PMID: 28138617 DOI: 10.21037/tgh.2016.05.12]
27 **Kaito A**, Kinoshita T, Tokunaga M, Sunagawa H, Watanabe M, Sugita S, Tonouchi A, Sato R, Abe I, Akimoto T. Prognostic Factors and Recurrence Pattern of Far-advanced Gastric Cancer with Pathologically-positive Para-aortic Lymph Nodes. *Anticancer Res* 2017; **37**: 3685-3692 [PMID: 28668861 DOI: 10.21873/anticanres.11740]
28 **Sato Y**, Ohnuma H, Nobuoka T, Hirakawa M, Sagawa T, Fujikawa K, Takahashi Y, Shinya M, Katsuki S, Takahashi M, Maeda M, Okagawa Y, Naoki U, Kikuch S, Okamoto K, Miyamoto H, Shimada M, Takemasa I, Kato J, Takayama T. Conversion therapy for inoperable advanced gastric cancer patients by docetaxel, cisplatin, and S-1 (DCS) chemotherapy: A multi-institutional retrospective study. *Gastric Cancer* 2017; **20**: 517-526 [PMID: 27553665 DOI: 10.1007/s10120-016-0633-1]
29 **Kodera Y**, Kobayashi D, Tanaka C, Fujiwara M. Gastric adenocarcinoma with para-aortic lymph node metastasis: A borderline resectable cancer? *Surg Today* 2015; **45**: 1082-1090 [PMID: 25366353 DOI: 10.1007/s00595-014-1067-1]
30 **Fujiwara Y**, Omori T, Demura K, Miyata H, Sugimura K, Ohue M, Kobayashi S, Takahashi H, Doki Y, Yano M. A Multidisciplinary Approach for Advanced Gastric Cancer with Paraaortic Lymph Node Metastasis. *Anticancer Res* 2015; **35**: 6739-6745 [PMID: 26637890 DOI: 10.1007/s00205-006-0014-8]
31 **Tsuburaya A**, Mizusawa J, Tanaka Y, Fukushima N, Nashimoto A, Sasako M; Stomach Cancer Study Group of the Japan Clinical Oncology Group. Neoadjuvant chemotherapy with S-1 and cisplatin followed by D2 gastrectomy with para-aortic lymph node dissection for gastric cancer with extensive lymph node metastasis. *Br J Surg* 2014; **101**: 653-660 [PMID: 24668391 DOI: 10.1002/bjs.9484]
32 **He Q**, Ma L, Li Y, Li G. A pilot study of an individualized comprehensive treatment for advanced gastric cancer with para-aortic lymph node metastasis. *BMC Gastroenterol* 2016; **16**: 8 [PMID: 26782354 DOI: 10.1186/s12876-016-0422-7]
33 **Ito S**, Sano T, Mizusawa J, Takahari D, Katayama H, Katai H, Kawashima Y, Kinoshita T, Terashima M, Nashimoto A, Nakamori M, Onaya H, Sasako M. A phase II study of preoperative chemotherapy with docetaxel, cisplatin, and S-1 followed by gastrectomy with D2 plus para-aortic lymph node dissection for gastric cancer with extensive lymph node metastasis: JCOG1002. *Gastric Cancer* 2017; **20**: 322-331 [PMID: 27299887 DOI: 10.1007/s10120-016-0619-z]
34 **Yamaguchi K**, Yoshida K, Tanahashi T, Takahashi T, Matsuhashi N, Tanaka Y, Tanabe K, Ohdan H. The long-term survival of stage IV gastric cancer patients with conversion therapy. *Gastric Cancer* 2018; **21**: 315-323 [PMID: 28616743 DOI: 10.1007/s10120-017-0738-1]
35 **Seo HS**, Song KY, Jung YJ, Park SM, Jeon HM, Kim W, Chin HM, Kim JJ, Kim SK, Chun KH, Kim JG, Lee JH, Lee HH, Kim DJ, Yoo HM, Kim CH, Kim EY, Park CH; Catholic Gastric Cancer Study Group (CGCSG). Radical Gastrectomy After Chemotherapy May Prolong Survival in Stage IV Gastric Cancer: A Korean Multi-institutional Analysis. *World J Surg* 2018; **42**: 3286-3293 [PMID: 29717344 DOI: 10.1007/s00268-018-4635-5]
36 **Günther K**, Horbach T, Merkel S, Meyer M, Schnell U, Klein P, Hohenberger W. D3 lymph node dissection in gastric cancer: Evaluation of postoperative mortality and complications. *Surg Today* 2000; **30**: 700-705 [PMID: 10955732 DOI: 10.1007/s005950070080]
37 **Bostanci EB**, Kayaalp C, Ozogul Y, Aydin C, Atalay F, Akoglu M. Comparison of complications after D2 and D3 dissection for gastric cancer. *Eur J Surg Oncol* 2004; **30**: 20-25 [PMID: 14736518 DOI: 10.1016/j.ejso.2003.10.008]
38 **Morita S**, Fukagawa T, Fujiwara H, Katai H. The clinical significance of para-aortic nodal dissection for advanced gastric cancer. *Eur J Surg Oncol* 2016; **42**: 1448-1454 [PMID: 26876636 DOI: 10.1016/j.ejso.2016.01.002]
39 **Tamura S**, Takeno A, Miki H. Lymph node dissection in curative gastrectomy for advanced gastric cancer. *Int J Surg Oncol* 2011; **2011**: 748745 [PMID: 22312521 DOI: 10.1155/2011/748745]
40 **Yoshikawa T**, Sasako M, Yamamoto S, Sano T, Imamura H, Fujitani K, Oshita H, Ito S, Kawashima Y, Fukushima N. Phase II study of neoadjuvant chemotherapy and extended surgery for locally advanced gastric cancer. *Br J Surg* 2009; **96**: 1015-1022 [PMID: 19644974 DOI: 10.1002/bjs.6665]
41 **Yoshikawa T**, Morita S, Tanabe K, Nishikawa K, Ito Y, Matsui T, Fujitani K, Kimura Y, Fujita J, Aoyama T, Hayashi T, Cho H, Tsuburaya A, Miyashita Y, Sakamoto J. Survival results of a randomised two-by-two factorial phase II trial comparing neoadjuvant chemotherapy with two and four courses of S-1 plus cisplatin (SC) and paclitaxel plus cisplatin (PC) followed by D2 gastrectomy for resectable advanced gastric cancer. *Eur J Cancer* 2016; **62**: 103-111 [PMID: 27244537 DOI: 10.1016/j.ejca.2016.04.012]

World Journal of Gastroenterology

Submit a Manuscript: https://www.f6publishing.com

World J Gastroenterol 2019 May 21; 25(19): 2354-2364

DOI: 10.3748/wjg.v25.i19.2354

ISSN 1007-9327 (print) ISSN 2219-2840 (online)

ORIGINAL ARTICLE

Observational Study

Combined evaluation of biomarkers as predictor of maintained remission in Crohn's disease

Elisa Sollelis, Régine Minet Quinard, Guillaume Bouguen, Marion Goutte, Félix Goutorbe, Damien Bouvier, Bruno Pereira, Gilles Bommelaer, Anthony Buisson

ORCID number: Elisa Sollelis (0000-0002-3647-5097); Régine Minet-Qunard (0000-0002-3426-3955); Guillaume Bouguen (0000-0002-7444-5905); Marion Goutte (0000-0001-7091-8157); Felix Goutorbe (0000-0002-5756-4574); Damien Bouvier (0000-0002-2707-4320); Bruno Pereira (0000-0001-6040-3192); Gilles Bommelaer (0000-0002-3248-2855); Anthony Buisson (0000-0002-6347-409X).

Author contributions: Buisson A is the guarantor of the article; Sollelis E and Buisson A contributed to study concept and design and writing of the article; Sollelis E, Bouguen G, Goutte M, Goutorbe F, Bouvier D, Pereira B, Bommelaer G and Buisson A contributed to substantial contribution to acquisition of data; Sollelis E, Quinard RM, Bouguen G, Goutte M, Goutorbe F, Bouvier D, Pereira B and Bommelaer G contributed to critical revision of the manuscript for important intellectual content; Sollelis E, Pereira B, Bommelaer G and Buisson A contributed to analysis and interpretation of data; Pereira B contributed to statistical analysis.

Institutional review board statement: The study was approved by local Ethics Committee (#2014/CE 72).

Informed consent statement: The study was performed in accordance with the Declaration of Helsinki, Good Clinical Practice and applicable regulatory

Elisa Sollelis, Marion Goutte, Gilles Bommelaer, Anthony Buisson, Inserm 3iHP, CHU Clermont-Ferrand, Service d'Hépato-Gastro Entérologie, Université Clermont Auvergne, Clermont-Ferrand F-63000, France

Elisa Sollelis, Marion Goutte, Gilles Bommelaer, Anthony Buisson, Inserm U1071, M2iSH, USC-INRA 2018, Université Clermont Auvergne, Clermont-Ferrand F-63000, France

Régine Minet Quinard, Damien Bouvier, Biochemistry laboratory, University Hospital G. Montpied, Clermont-Ferrand F-63000, France

Guillaume Bouguen, CHU Rennes, Univ Rennes, INSERM, CIC1414, Institut NUMECAN (Nutrition Metabolisms and Cancer), Rennes F-35000, France

Félix Goutorbe, Gastroenterology Department, Hospital of Bayonne, Bayonne F-64100, France

Bruno Pereira, Biostatistics Unit, DRCI, University Hospital, Clermont-Ferrand F-63000, France

Corresponding author: Anthony Buisson, MD, PhD, Associate Professor, Senior Lecturer, Gastroenterology Department,University Hospital Estaing, 1 place Aubrac, Clermont-Ferrand F-63100, France. a_buisson@hotmail.fr
Telephone: +33-473-750523
Fax: +33-473-750524

Abstract

BACKGROUND

The individual performances and the complementarity of Crohn's disease (CD) activity index (CDAI), C-reactive protein (CRP) and faecal calprotectin (Fcal) to monitor patients with CD remain poorly inves-tigated in the era of "tight control" and "treat to target" strategies.

AIM

To assess CDAI, CRP and Fcal variation, alone or combined, after 12 wk (W12) of anti-tumor necrosis factor (TNF) therapy to predict corticosteroids-free remission (CFREM = CDAI < 150, CRP < 2.9 mg/L and Fcal < 250 μg/g with no therapeutic intensification and no surgery) at W52.

METHODS

CD adult patients needing anti-TNF therapy with CDAI > 150 and either CRP > 2.9 mg/L or Fcal > 250 μg/g were prospectively enrolled.

RESULTS

Among the 40 included patients, 13 patients (32.5%) achieved CFREM at W52. In univariable analysis, CDAI < 150 at W12 (P = 0.012), CRP level < 2.9 mg/L at W12 (P = 0.001) and Fcal improvement at W12 (Fcal < 300 μg/g; or, for patients with initial Fcal < 300 μg/g, at least 50% decrease of Fcal or normalization of Fcal (< 100 μg/g) (P = 0.001) were predictive of CFREM at W52. Combined endpoint (CDAI < 150 and CRP ≤ 2.9 mg/L and FCal improvement) at W12 was the best predictor of CFREM at W52 with positive predictive value = 100.0% (100.0-100.0) and negative predictive value = 87.1% (75.3-98.9). In multivariable analysis, Fcal improvement at W12 [odd ratio (OR) = 45.1 (2.96-687.9); P = 0.03] was a better predictor of CFREM at W52 than CDAI < 150 [OR = 9.3 (0.36-237.1); P = 0.145] and CRP < 2.9 mg/L (0.77-278.0; P = 0.073).

CONCLUSION

The combined monitoring of CDAI, CRP and Fcal after anti-TNF induction therapy is able to predict favorable outcome within one year in patients with CD.

Key words: Biomarkers; Crohn's disease; Faecal calprotectin; Crohn's disease activity index; C-reactive protein; Tight control; Anti-tumor necrosis factor

Core tip: The CALM trial reported that a tight control of inflammation achieved better outcomes than conventional monitoring, but did not explore specifically the value of each biomarker. In this multicentre study, we investigated the performances of Crohn's disease (CD) activity index (CDAI), C-reactive protein (CRP) and faecal calprotectin (Fcal) variation, alone or combined, after 12 wk of anti-tumor necrosis factor (TNF) therapy to predict corticosteroids-free remission (CFREM) at one year, in CD patients treated with anti-TNF. We showed the complementarity of the variation of CDAI, CRP and Fcal after anti-TNF induction therapy, to predict CFREM at one year, and confirmed that Fcal was the most effective predictor among these three markers.

Citation: Sollelis E, Quinard RM, Bouguen G, Goutte M, Goutorbe F, Bouvier D, Pereira B, Bommelaer G, Buisson A. Combined evaluation of biomarkers as predictor of maintained remission in Crohn's disease. *World J Gastroenterol* 2019; 25(19): 2354-2364
URL: https://www.wjgnet.com/1007-9327/full/v25/i19/2354.htm
DOI: https://dx.doi.org/10.3748/wjg.v25.i19.2354

INTRODUCTION

Crohn's disease (CD) is a chronic and disabling disorder that can highly affect quality of life[1]. The natural history of CD can lead to cumulative bowel damage such as stricture, fistula or intestinal resection[2,3]. In this context, mucosal healing is recognized hitherto as the best therapeutic endpoint in patients with CD, as it is associated with sustained clinical remission, reduced rates of subsequent hospitalization and surgery[4]. In daily practice, this endpoint is limited by the potential risks[5] and the need of repeated endoscopic procedures, which is felt as a burden by patients with CD[6].

Faecal calprotectin (Fcal) is a well-accepted monitoring tool and a surrogate marker of mucosal healing[6-8] and could then be an alternative. However, the STRIDE guidelines considered that Fcal was not a target because of insufficient evidence to recommend treatment optimization using biomarkers alone[4]. Recently, the CALM trial compared two ways of monitoring patients with inflammatory bowel disease (IBD) treated with adalimumab[9]. In the first arm (conventional care), the patients had a therapeutic intensification if the CD activity index (CDAI) did not decrease of at least 70 points. In the second group so-called "tight control group", the therapies were upgraded in cases of CDAI > 150 or C-reactive protein (CRP) > 5 mg/L or Fcal > 250 μg/g[9]. The authors reported that the group monitored using a tight control of inflammation with objective markers of disease activity and clinical symptoms to drive treatment decisions (second group), achieved better endoscopic and clinical outcomes than conventional monitoring[9]. In a post-hoc analysis of this study, the

requirements. Informed consent was obtained from each patient included in the study.

Conflict-of-interest statement: Buisson A declares lecture fees for MSD, Abbvie, Ferring, Takeda, Vifor Pharma, Hospira and consulting fees for Abbvie, Takeda and Hospira. Bouguen G received lecture fees from Abbvie, Ferring, MSD, Takeda and Pfizer and consulting fees from Takeda and Janssen. The other authors declare no conflict of interest related to this work.

Data sharing statement: The original anonymous dataset is available on request from the corresponding author at a_buisson@hotmail.fr.

STROBE statement: The manuscript was prepared according to the STROBE Checklist.

Manuscript source: Invited manuscript

Received: March 7, 2019
Peer-review started: March 7, 2019
First decision: April 11, 2019
Revised: April 16, 2019
Accepted: April 19, 2019
Article in press: April 20, 2019
Published online: May 21, 2019

P-Reviewer: Lv XP, Sachar DB, Yang MS
S-Editor: Ma RY
L-Editor: A
E-Editor: Ma YJ

authors reported that most of the therapeutic intensification were related to increased level of Fcal in the tight control group. However, even though the conclusion of this landmark trial encourages IBD physicians to use Fcal testing in daily practice, the authors did not explore specifically the value of each marker, *i.e.*, CDAI, CRP and Fcal.

In this study, we aimed to investigate the performances of CDAI, CRP and Fcal variation, alone or combined, after 12 wk of anti-tumor necrosis factor (TNF) therapy to predict corticosteroids-free remission (CFREM) at one year, in CD patients treated with anti-TNF.

MATERIALS AND METHODS

Ethical considerations

The study was performed in accordance with the Declaration of Helsinki, Good Clinical Practice and applicable regulatory requirements. The study was approved by local Ethics Committee (#2014/CE 72).

Design of the study

We conducted an observational multicenter study in three French IBD centers. All the patients with CD older than 18 years-old requiring anti-TNF therapy according to the physician's judgement with CDAI > 150, and CRP > 5 mg/L or Fcal > 250 μg/g were consecutively and prospectively enrolled. Patients who presented with usual contra-indications to anti-TNF or who received anti-TNF therapy to prevent endoscopic postoperative recurrence or to treat isolated perianal lesions were excluded. The patients were treated with infusion of infliximab (5 mg/kg at W0, W2 and W6 and then every 8 wk) or subcutaneous injection of adalimumab (160 mg at W0, 80 mg at W2 and 40 mg every other week) according to the usual guidelines. The choice of the type of anti-TNF agent and the use of concomitant immunosuppressive therapy (azathioprine from 2 to 2.5 mg/kg or methotrexate from 15 mg to 25 mg SC) were free and based on the physician's judgment. No systematic drug level monitoring was performed during the study as routinely in our centers.

Clinical parameters including the CDAI are detailed in Table 1 and were collected before starting anti-TNF therapy (W0), at W12 and W52. Blood samples were taken and used to measure high- sensitive serum CRP level by immunonephelemetric method (Vista; Siemens, Berlin, Germany) at W0, W12 and W52.

Fcal measurement

Stools samples were collected at W0, W12 and W52, in the morning to reduce intra-individual variation, and immediately stored at 4 °C. Patients were instructed to transport the stool samples in a dedicated container at 4 °C. Faecal samples were immediately transferred, upon patient arrival, to the Clermont-Ferrand hospital Biochemistry Laboratory. Stool cultures were performed on all samples to exclude gastrointestinal infection. Calprotectin was measured, as routinely performed in our IBD centre, using quantitative immunochromatographic test Quantum Blue High Range (Bühlmann Laboratories AG, Schönenbuch, Switzerland), according to the manufacturer's instructions. Laboratory personnel, who were blinded from the current clinical disease activity of the patients, performed the analyses. The lower and the upper limits of detection for calprotectin were 100 and 1800 μg/g, respectively. Consequently, all calprotectin levels < 100 and > 1800 μg/g were considered as equal to 100 and 1800 μg/g, respectively. Results were given in μg/g.

Definitions and endpoints

CFREM at W52 was defined as: CDAI < 150 and CRP < 2.9 mg/L (normal value according to the manufacturer's instruction) and faecal calprotectin < 250 μg/g, with no switch or swap of biologics and no bowel resection, and with no therapeutic intensification between W12 and W52. Therapeutic intensification was defined as an increase of anti-TNF dose or a decrease of interval between two infusions/injections or as an addition of another CD-specific medication (steroids or immunosuppressant therapy). Therapeutic intensification was based on clinical activity (CDAI > 150) and not on CRP or Fcal level.

Sample size calculation

Sample size estimation has been performed in order to assess our primary endpoint. Overall, 40 patients were necessary for a type I error at 5% and a statistical power greater than 80% to detect a true absolute difference higher than 50% to predict CFREM at week 52 using CDAI, CRP, or Fcal, alone or in combination. Consequently, we planned to include 40 patients.

Table 1 Baseline characteristics of the 40 patients with Crohn's disease included in this study

	n = 40 patients
Age at the time of inclusion, mean ± SD (yr)	34 .0 ± 13.6
Disease duration, median (IQR) (yr)	4 (0.8-11.3)
Female gender, *n* (%)	21 (52.5)
Current smokers, *n* (%)	15 (37.5)
Prior bowel resection, *n* (%)	7 (17.5)
Montreal classification	
Location	
L1, *n* (%)	18 (45.0)
L2, *n* (%)	3 (7.5)
L3, *n* (%)	19 (47.5)
Behaviour	
B1, *n* (%)	13 (32.5)
B2, *n* (%)	16 (40.0)
B3, *n* (%)	11 (27.5)
Perianal lesions, *n* (%)	7 (17.5)
Anti-TNF-naïve patients, *n* (%)	24 (60.0)
Type of anti-TNF	
Infliximab, *n* (%)	16 (40.0)
Adalimumab, *n* (%)	24 (60.0)
Concomitant medications	
Immunosuppressive therapies, *n* (%)	21 (52.5)
Steroids, *n* (%)	7 (17.5)
Faecal calprotectin level at baseline, median (IQR) (μg/g)	1010.5 (357.8-1800.0)
CRP level at baseline, median (IQR) (mg/L)	13.2 (5.2-25.9)

SD: Standard deviation; IQR: Interquartile range; TNF: Tumor necrosis factor.

Statistical analysis

Study data were collected and managed using Research Electronic Data Capture (REDCap) electronic data capture tools hosted at Clermont-Ferrand University Hospital[10]. REDCap is a secure, web-based application designed to support data capture for research studies, providing (1) an intuitive interface for validated data entry; (2) audit trails for tracking data manipulation and export procedures; (3) automated export procedures for seamless data downloads to common statistical packages; and (4) procedures for importing data from external sources.

Statistical analysis was performed using Stata software (version 13, StataCorp LP, College Station, TX, United States). The tests were two-sided, with a type I error set at $\alpha = 0.05$. Continuous data were presented as mean ± standard-deviation or median (interquartile range) according to statistical distribution (assumption of normality assessed using the Shapiro-Wilk test). Categorical parameters were presented as frequencies and associated percentages. To assess the factors associated with CFREM at W52, univariable analyses were realized using usual statistical tests: for continuous outcomes Student t-test or Mann-Whitney test when assumptions of *t*-test were not met (normality, homoscedasticity assessed by the Fisher-Snedecor test) and for categorical data chi-squared or Fisher's exact tests. Regarding Fcal, ROC curve analyses were performed to determine the best thresholds to predict CFREM. The optimal threshold was determined according to clinical relevance and usual indexes reported in medical literature (Youden, Liu and efficiency). According to univariable results, a multivariable analysis (logistic regression) was carried out considering an adjustment on relevant clinical parameters. The results were expressed as odds-ratios and 95% confidence intervals.

RESULTS

Baseline characteristics of the patients

Overall, 40 patients with CD were enrolled in this study. Their baseline characteristics

are detailed in Table 1.

Among them, 16 patients (40%) and 24 patients (60%) were treated with IFX and ADA, respectively. Twenty-one patients received concomitant thiopurines therapy (52.5%). At baseline the median CDAI was 215 (166-282) and the median levels of Fcal and CRP were 1010.5 (357.8-1800.0) μg/g and 13.2 (5.2-25.9) mg/L, respectively. Among the 40 patients treated with anti-TNF, the levels of CDAI [111 (55-198) *vs* 215 (166-282); $P < 0.0001$], CRP [3.0 (1.0-17.0) mg/L *vs* 13.2 (5.2-25.9) mg/L; p=0.011] and Fcal [374.0 (103.0-969.0) *vs* 1010.5 (357.8-1800.0) μg/g; p = 0.001] were significantly diminished after 12 wk of anti-TNF agents.

Early variation of CDAI, CRP and Fcal after anti-TNF induction therapy (W12) as predictor of CFREM at W52 in patients with CD

Overall, 13 patients (32.5%) achieved CFREM at W52. The proportion of patients achieving the different therapeutic endpoints at W12 is reported in Figure 1.

The median CDAI at W12 was significantly lower in patients presenting with CFREM at one year[46 (14-64)] compared to those who did not [165 (83-265)] ($P < 0.001$). In univariable analysis, CDAI < 150 at W12 was associated with higher likelihood of CFREM at W52 (47.9% *vs* 11.8%, $P = 0.012$). Clinical remission at W12 (CDAI < 150) predicted CFREM at W52 with the following performances: sensitivity = 84.6% (56.3-96.6), specificity = 55.6% (37.3-72.4), positive predictive value (PPV) = 47.8% (27.4-68.2), negative positive value (NPV) = 88.2% (72.9-100.0), positive likelihood ratio (LR+) = 1.904 (1.177-3.081) and negative likelihood ratio (LR-) = 0.277 (0.074-1.035) (Table 2).

The level of CRP dropped at W12 in patients with CFREM at one year [1.0 mg/L (1.0-2.9) *vs* 8.4 mg/L (2.9-29.5); $P = 0.001$]. In univariable analysis, a CRP level < 2.9 mg/L (normalized CRP) at W12 was associated with higher rate of CFREM at W52 (61.2% *vs* 4.8%, $P < 0.001$). CRP level below 2.9 mg/L at W12 predicted CFREM at W52 with the following performances: sensitivity = 92.3% (64.2-100.0), specificity = 74.1% (55.0-86.9), PPV = 63.2% (41.5-84.8), NPV = 95.2% (86.1-100.0), LR+ = 3.560 (1.846-6.865), LR- = 0.104 (0.016-0.692) (Table 2).

The combined performances of both CDAI < 150 and CRP ≤ 2.9 mg/L at W12 to predict CFREM at W52 were sensitivity = 76.9% (48.9-92.2), specificity = 85.2% (66.7-94.6), PPV = 71.4% (47.8-95.1), NPV = 88.5% (76.2-100.0), LR+ = 5.192 (2.004-13.456), LR- = 0.271 (0.099-0.740) (Table 2).

In patient with CFREM at one year, the median Fcal level at W12 was significantly lower [100.0 μg/g (100.0-193.0)] *vs* compared to those who were not [646.0 μg/g (315.0-1567.0)] ($P < 0.001$) (Figure 2).

We also observed that the relative decrease of Fcal between W0 and W12 was higher [83.3% (33.6%-83.3%) *vs* 0.0% (0.0%-33.2%), $P = 0.001$] in the patients achieving CFREM at W52 compared to the patients who failed to obtain CFREM at W52. Based on ROC curve analyses, we determined that the best threshold of Fcal after anti-TNF induction therapy (W12) to predict CFREM at one year was 300 μg/g [area under the curve (AUC) = 0.848]. The performances of this cut-off value were: sensitivity = 84.6% (56.3-96.6), specificity = 77.8% (58.8-89.6), PPV = 64.7% (42.0-87.4), NPV = 91.3% (79.8-100%), LR+ = 3.808 (1.812-8.003), LR- = 0.198 (0.054-0.719) (Table 2).

Using a ROC curve (AUC = 0.82), a decreased > 50% of Fcal was also predictive of CFREM at one year with sensitivity = 61.5% (35.4-82.2), specificity = 85.2% (66.7-94.6), PPV = 66.7% (40.0-93.3), NPV = 82.1% (68.0-96.3), LR+ = 4.154 (1.526-11.307), LR- = 0.452 (0.223-0.914).

We also studied the complementary of these two thresholds by creating a composite criterion so-called Fcal improvement [Fcal < 300 μg/g at W12; or, for patients with initial Fcal < 300 μg/g, at least 50% decrease of Fcal or normalization of Fcal (< 100 μg/g)]. Fcal improvement predicted CFREM at 1 year with the following performances: sensitivity = 76.9% (48.9-92.2), specificity = 92.6% (75.3-98.9), PPV = 83.3% (62.2-100.0), NPV = 89.3% (77.8-100.0), LR+ = 10.385 (2.648-40.721), LR- = 0.249 (0.092-0.676) (Table 2).

Concomitant CDAI < 150 and FCal improvement at W12 was predictive of CFREM at W52 with the following performances: sensitivity = 69.2% (42.0-87.4), specificity = 96.3% (79.9-100.0), PPV = 90.0% (71.4-100.0), NPV = 86.7% (74.5-98.8), LR+ = 18.692 (2.640-132.328), LR- = 0.320 (0.141-0.725) (Table 2).

Combined endpoints such as CDAI < 150 and CRP ≤ 2.9 mg/L and FCal improvement at W12 predicted CFREM at W52 with the following performances sensitivity = 69.2% (42.0-87.4), specificity = 100.0% (84.9-100.0), PPV = 100.0% (100.0-100.0), NPV = 87.1% (75.3-98.9), LR+ = not applicable, LR- = 0.308 (0.136-0.695) (Table 2).

In univariable analysis, we did not observe any additional factors associated with CFREM. In multivariable analysis including disease duration, smoking status, CDAI and CRP values, Fcal improvement at W12 was independently associated with

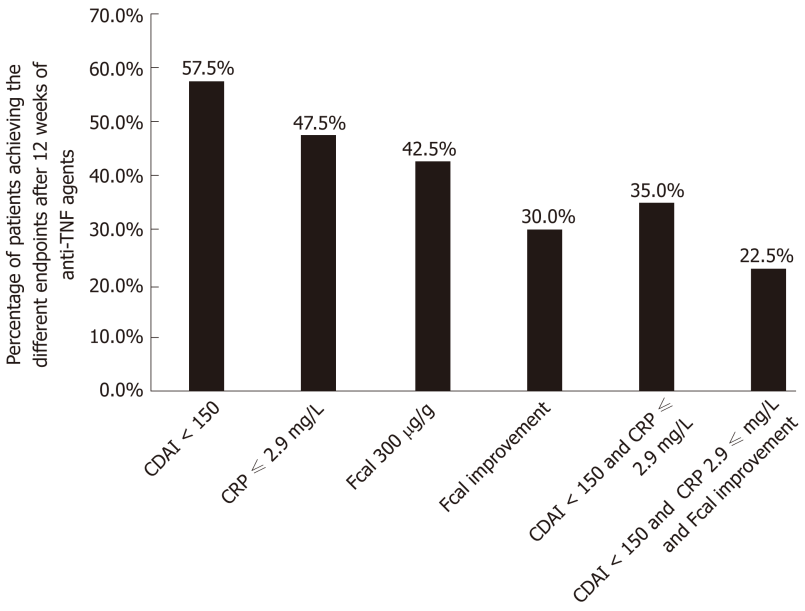

Figure 1 Rate of patients achieving the different therapeutic endpoints after 12 wk of anti-tumor necrosis factor therapy in 40 patients with Crohn's disease. CDAI: Crohn's disease activity index; CRP: C-reactive protein; Fcal: Faecal calprotectin; TNF: Tumor necrosis factor.

CFREM at W52 [odd ratio (OR) = 45.1 (2.96-687.9); P = 0.03] and was a better predictor than CDAI < 150 [9.3 (0.36-237.1); P = 0.145] and CRP < 2.9 mg/L (0.77-278.0; P = 0.073) (Figure 3).

DISCUSSION

In this prospective study, we showed the complementarity of the variation of CDAI, CRP and Fcal after anti-TNF induction therapy, to predict CFREM at one year, and confirmed that Fcal was the most effective predictor among these three markers.

According to the results of the CALM trial, we decided to use the same composite endpoint at W52 *i.e.*, CDAI < 150 and CRP normalization (< 2.9 mg/L using our assay) and Fcal < 250 μg/g, so-called CFREM, which has been shown to be associated with clinical and endoscopic remission[9]. We added the absence of therapeutic intensification including the absence of CD-related surgery to assess the impact of these biomarkers on CD outcomes and also to avoid a complete overlap between the criteria assessed at W12 and the composite primary endpoint at W52. We aimed to investigate what was the best predictor among CDAI, CRP, FCal, or combination of these biomarkers assessed at W12 to predict CFREM at W52.

In this study, we confirmed that CDAI alone is not suitable to monitor CD patients as we found a low PPV (47.3%) of clinical remission (CDAI < 150) at W12 to predict CFREM at W52. The lack of correlation between clinical symptoms and objective markers of activity is now well admitted. A *post-hoc* analysis from the SONIC trial showed that almost one half of the patients with CDAI < 150 presented with significant endoscopic lesions[11]. The STRIDE guidelines considered that resolution of symptoms alone is not a sufficient target and that objective evidence of bowel inflammation is necessary when making clinical decisions[4]. As expected, we also found that the patients, who did not achieve clinical remission (CDAI < 150) at W12, had a very high likelihood of treatment failure (with NPV of 88.2%) reminding that clinical remission is a necessary but not sufficient therapeutic goal in patients with CD.

We also investigated the measurement of CRP value at W12 in patients receiving anti-TNF agents as predictor of mid-term CFREM (W52). While CRP normalization after 12 wk demonstrated moderate performances (PPV = 63.2%) to predict CFREM at W52, the absence of CRP normalization at W12 was highly predictive of treatment failure (NPV = 95.2%). Our data seems slightly different from two studies dedicated to CRP normalization as predictor of remission. Reinisch *et al*[12] reported in a *post-hoc* analysis of the landmark ACCENT 1 trial that normalisation of CRP at week 14 led to a higher probability of maintained response or remission during one-year of infliximab maintenance therapy (P < 0.001) with PPV of 51.8% and NPV of 68.0%. Kiss

Table 2 Performances of Crohn's disease activity index, C-reactive protein, and faecal calprotectin after 12 wk of anti-tumor necrosis factor to predict steroids-free remission at week 52

Endpoints	Sensitivity	Specificity	PPV	NPV	LR+	LR-	Accuracy
CDAI < 150	84.6% (56.3-96.6)	55.6% (37.3-72.4)	47.8% (27.4-68.2)	88.2% (72.9-100.0)	1.904 (1.177-3.081)	0.277 (0.074-1.035)	60.5% (50.2-79.8)
CRP ≤ 2.9 mg/L	92.3% (64.2-100.0)	74.1% (55.0-86.9)	63.2% (41.5-84.8)	95.2% (86.1-100.0)	3.560 (1.846-6.865)	0.104 (0.016-0.692)	80.0% (67.6-92.4)
CDAI < 150 and CRP ≤ 2.9 mg/L	76.9% (48.9-92.2)	85.2% (66.7-94.6)	71.4% (47.8-95.1)	88.5% (76.2-100.0)	5.192 (2.004-13.456)	0.271 (0.099-0.740)	82.5% (70.7-94.3)
Fcal < 300 μg/g	84.6% (56.3-96.6)	77.8% (58.8-89.6)	64.7% (42.0-87.4)	91.3% (79.8-100%)	3.808 (1.812-8.003)	0.198 (0.054-0.719)	80.0% (67.6-92.4)
Fcal improvement	76.9% (48.9-92.2)	92.6% (75.3-98.9)	83.3% (62.2-100.0)	89.3% (77.8-100.0)	10.385 (2.648-40.721)	0.249 (0.092-0.676)	87.5% (77.3-97.7)
CDAI < 150 and Fcal improvement	69.2% (42.0-87.4)	96.3% (79.9-100.0)	90.0% (71.4-100.0)	86.7% (74.5-98.8)	18.692 (2.640-132.328)	0.320 (0.141-0.725)	87.5% (77.3-97.7)
CDAI < 150 and CRP ≤ 2.9 mg/L and Fcal improvement	69.2% (42.0-87.4)	100.0% (84.9-100.0)	100.0% (100.0-100.0)	87.1% (75.3-98.9)	NA	0.308 (0.136-0.695)	90.0% (80.7-99.3)

CDAI: Crohn's disease activity index; CRP: C-reactive protein; Fcal: Faecal calprotectin; PPV: Positive predictive valu; NPV: Negative positive value; LR+: Positive likelihood ratio; LR-: Negative likelihood ratio.

et al[13] showed that CD patients who had normalised CRP at week 12 were associated with clinical efficacy at 12 mo with PPV ranging from 67% to 79% and NPV from 73% to 80%. This discrepancy could be partly explained by our sample size but also by the choice of our combined endpoint, which is probably more stringent than the two former studies and could have improve the NPV.

As the capability of Fcal to change under treatment remains poorly investigated[14-16], the STRIDE guidelines did not consider Fcal as a therapeutic target[4]. Our results highlighted the performances of Fcal improvement [defined as Fcal < 300 μg/g at W12 or, for patients with baseline Fcal < 300 μg/g, at least 50% decrease or normalization of Fcal (< 100 μg/g)] to predict CFREM at 1 year: PPV = 83.3% and NPV = 89.3%. We chose to also enroll patients with moderate elevation of Fcal (100-300 μg/g) as it reflects some real-life clinical situations in daily practice. Our data are in line with the three studies available to date on this topic. In a French prospective study including 32 patients with CD receiving anti-TNF therapy, Fcal level above 82 μg/g at W14 demonstrated PPV = 85% and NPV = 87% to predict clinical remission within one year using quantitative monoclonal antibody-based enzyme-linked immunosorbent assay (Bühlmann, Schönenbuch, Switzerland). Guidi and colleagues (n = 44 patients with CD), post-induction level of Fcal ≤ 168 μg/g using enzyme-linked immunosorbent assay (ELISA, Calprest, Eurospitals.p.a., Trieste, Italy) was predictive of sustained clinical response with PPV = 81% and NPV = 77%[15]. Eventually, Molander *et al*[16] found that a post-induction level of Fcal < 139 μg/g [measured by a quantitative enzyme immunoassay (PhiCal Test, Calpro, Oslo, Norway)] predicted the risk of relapse in 34 patients with CD treated with anti-TNF agents. The heterogeneity of these thresholds is explained by the difference of assays used across the studies. IBD physicians have to be aware of these variations between the different assays to measure FCal when they make a decision based on Fcal cut-off values. We strongly encourage IBD physicians to use the same assays when assessing the variation of Fcal under treatment in a same patient. A study comparing six commercially available assays underlined that Fcal level may vary with up to 5-fold quantitative differences between assays[17].

The CALM trial was designed considering that the use of biomarkers could improve patients' outcomes without real evidence of it. Since the publication of this study, the authors insisted on the role of FCal to monitor patients with CD. However, what is the part of Fcal, CRP and CDAI remains questionable. It is why we decided to investigate the specific role and the potential complementarity of these three biomarkers. In our study, we observed that achieving CDAI < 150, CRP normalization and Fcal improvement was the best combination and led to a PPV of 100% with substantial NPV (87.1%) for the prediction of CFREM at W52. This result could mean that the surveillance scheduled every three months in the CALM trial could be slightly lightened in patients achieving this endpoint after induction therapy and extended to every 6 mo.

The main limitations of our study are the lack of endoscopic evaluation at W52 and the relative small number of patients even though our sample size calculation showed

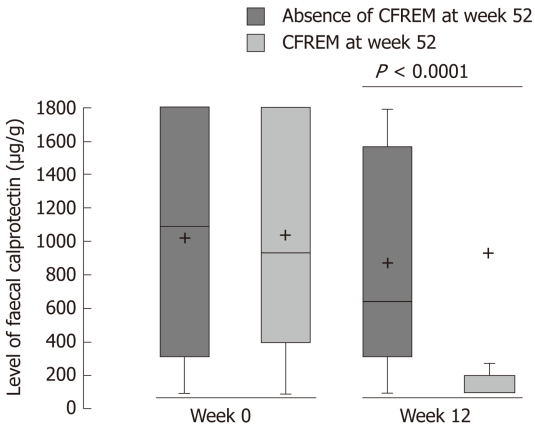

Figure 2 Level of faecal calprotectin at baseline and after 12 wk of anti-tumor necrosis factor therapy in patients with Crohn's disease achieving steroids-free remission (Crohn's disease activity index < 150 and C-reactive protein < 2.9 mg/L and faecal calprotectin < 250 µg/g with no therapeutic intensification and no surgery) or not at week 52. CFREM: Corticosteroids-free remission.

that it was appropriate. However, we investigated prospectively with a suitable power the performances of each item of the CALM criteria and their combinations to predict favorable outcomes in patients with CD.

In conclusion, the combined monitoring of CDAI, CRP and FCal after anti-TNF induction therapy is able to predict favorable outcome within one year in patients with CD. The most impactful biomarker was Fcal among these three biomarkers. Our results should lead IBD physicians to monitor patients with CD using a tight control strategy based on CDAI, CRP and Fcal in daily practice.

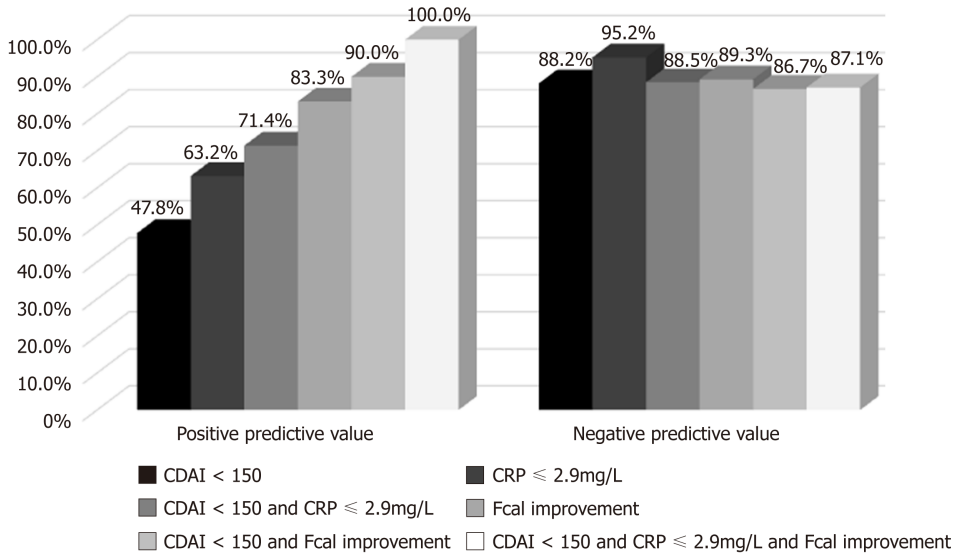

Figure 3 Positive and negative predictive values of Crohn's disease activity index, C-reactive protein and faecal calprotectin, alone or combined, after 12 wk of anti-tumor necrosis factor to predict corticosteroids-free remission at week 52. Faecal calprotectin (Fcal) improvement (Fcal < 300 μg/g at W12; or, for patients with initial Fcal < 300 μg/g, at least 50% decrease of Fcal or normalization of Fcal (< 100 μg/g). CDAI: Crohn's disease activity index; CRP: C-reactive protein; Fcal: Faecal calprotectin.

ARTICLE HIGHLIGHTS

Research background

Crohn's disease (CD) is a chronic and disabling disorder that can highly affect quality of life. Faecal calprotectin (Fcal) is a well-accepted monitoring tool and a surrogate marker of mucosal healing and could then be an alternative to endoscopy. Recently, the CALM trial compared two ways of monitoring patients with inflammatory bowel disease (IBD) treated with adalimumab. The authors reported that the group monitored using a tight control of inflammation with objective markers of disease activity and clinical symptoms to drive treatment decisions, achieved better endoscopic and clinical outcomes than conventional monitoring. In a *post-hoc* analysis of this study, the authors reported that most of the therapeutic intensification were related to increased level of Fcal in the tight control group. However, even though the conclusion of this landmark trial encourages IBD physicians to use Fcal testing in daily practice, the authors did not explore specifically the value of each marker, *i.e.*, CD activity index (CDAI), C-reactive protein (CRP) and Fcal.

Research motivation

Understanding the value of each monitoring biomarker to guide physicians to manage patients with inflammatory bowel disease is a key point.

Research objectives

In this study, we aimed to investigate the performances of CDAI, CRP and Fcal variation, alone or combined, after 12 wk of anti-tumor necrosis factor (TNF) therapy to predict corticosteroids-free remission (CFREM) at one year, in CD patients treated with anti-TNF.

Research methods

It was a multicentre prospective observational study.

Research results

Among the 40 included patients, 13 patients (32.5%) achieved CFREM at W52. In univariable analysis, CDAI < 150 at W12 (P = 0.012), CRP level < 2.9 mg/L at W12 (P = 0.001) and Fcal improvement at W12 [Fcal < 300 μg/g; or, for patients with initial Fcal < 300 μg/g, at least 50% decrease of Fcal or normalization of Fcal (<100 μg/g)] (P = 0.001) were predictive of CFREM at W52. Combined endpoint (CDAI < 150 and CRP ≤ 2.9 mg/L and FCal improvement) at W12 was the best predictor of CFREM at W52 with PPV = 100.0% (100.0-100.0) and NPV = 87.1% (75.3-98.9). In multivariable analysis, Fcal improvement at W12 [odd ratio (OR) = 45.1 (2.96-687.9); P = 0.03] was a better predictor of CFREM at W52 than CDAI < 150 [OR = 9.3 (0.36-237.1); P = 0.145] and CRP < 2.9 mg/L (0.77-278.0; P = 0.073).

Research conclusions

The combined monitoring of CDAI, CRP and FCal after anti-TNF induction therapy is able to predict favorable outcome within one year in patients with CD. The most impactful biomarker was Fcal among these three biomarkers. Our results should lead IBD physicians to monitor patients with CD using a tight control strategy based on CDAI, CRP and Fcal in daily practice.

Research perspectives

Additional studies from independent cohorts should be conducted to confirm these data.

REFERENCES

1 **Peyrin-Biroulet L**, Cieza A, Sandborn WJ, Coenen M, Chowers Y, Hibi T, Kostanjsek N, Stucki G, Colombel JF; International Programme to Develop New Indexes for Crohn's Disease (IPNIC) group. Development of the first disability index for inflammatory bowel disease based on the international classification of functioning, disability and health. *Gut* 2012; **61**: 241-247 [PMID: 21646246 DOI: 10.1136/gutjnl-2011-300049]

2 **Pariente B**, Cosnes J, Danese S, Sandborn WJ, Lewin M, Fletcher JG, Chowers Y, D'Haens G, Feagan BG, Hibi T, Hommes DW, Irvine EJ, Kamm MA, Loftus EV, Louis E, Michetti P, Munkholm P, Oresland T, Panés J, Peyrin-Biroulet L, Reinisch W, Sands BE, Schoelmerich J, Schreiber S, Tilg H, Travis S, van Assche G, Vecchi M, Mary JY, Colombel JF, Lémann M. Development of the Crohn's disease digestive damage score, the Lémann score. *Inflamm Bowel Dis* 2011; **17**: 1415-1422 [PMID: 21560202 DOI: 10.1002/ibd.21506]

3 **Pariente B**, Mary JY, Danese S, Chowers Y, De Cruz P, D'Haens G, Loftus EV, Louis E, Panés J, Schölmerich J, Schreiber S, Vecchi M, Branche J, Bruining D, Fiorino G, Herzog M, Kamm MA, Klein A, Lewin M, Meunier P, Ordas I, Strauch U, Tontini GE, Zagdanski AM, Bonifacio C, Rimola J, Nachury M, Leroy C, Sandborn W, Colombel JF, Cosnes J. Development of the Lémann index to assess digestive tract damage in patients with Crohn's disease. *Gastroenterology* 2015; **148**: 52-63.e3 [PMID: 25241327 DOI: 10.1053/j.gastro.2014.09.015]

4 **Peyrin-Biroulet L**, Sandborn W, Sands BE, Reinisch W, Bemelman W, Bryant RV, D'Haens G, Dotan I, Dubinsky M, Feagan B, Fiorino G, Gearry R, Krishnareddy S, Lakatos PL, Loftus EV, Marteau P, Munkholm P, Murdoch TB, Ordás I, Panaccione R, Riddell RH, Ruel J, Rubin DT, Samaan M, Siegel CA, Silverberg MS, Stoker J, Schreiber S, Travis S, Van Assche G, Danese S, Panes J, Bouguen G, O'Donnell S, Pariente B, Winer S, Hanauer S, Colombel JF. Selecting Therapeutic Targets in Inflammatory Bowel Disease (STRIDE): Determining Therapeutic Goals for Treat-to-Target. *Am J Gastroenterol* 2015; **110**: 1324-1338 [PMID: 26303131 DOI: 10.1038/ajg.2015.233]

5 **Buisson A**, Chevaux JB, Hudziak H, Bresler L, Bigard MA, Peyrin-Biroulet L. Colonoscopic perforations in inflammatory bowel disease: a retrospective study in a French referral centre. *Dig Liver Dis* 2013; **45**: 569-572 [PMID: 23298761 DOI: 10.1016/j.dld.2012.11.012]

6 **Buisson A**, Gonzalez F, Poullenot F, Nancey S, Sollellis E, Fumery M, Pariente B, Flamant M, Trang-Poisson C, Bonnaud G, Mathieu S, Thevenin A, Duruy M, Filippi J, L'hopital F, Luneau F, Michalet V, Genès J, Achim A, Cruzille E, Bommelaer G, Laharie D, Peyrin-Biroulet L, Pereira B, Nachury M, Bouguen G; ACCEPT study group. Comparative Acceptability and Perceived Clinical Utility of Monitoring Tools: A Nationwide Survey of Patients with Inflammatory Bowel Disease. *Inflamm Bowel Dis* 2017; **23**: 1425-1433 [PMID: 28570431 DOI: 10.1097/MIB.0000000000001140]

7 **D'Haens G**, Ferrante M, Vermeire S, Baert F, Noman M, Moortgat L, Geens P, Iwens D, Aerden I, Van Assche G, Van Olmen G, Rutgeerts P. Fecal calprotectin is a surrogate marker for endoscopic lesions in inflammatory bowel disease. *Inflamm Bowel Dis* 2012; **18**: 2218-2224 [PMID: 22344983 DOI: 10.1002/ibd.22917]

8 **Goutorbe F**, Goutte M, Minet-Quinard R, Boucher AL, Pereira B, Bommelaer G, Buisson A. Endoscopic Factors Influencing Fecal Calprotectin Value in Crohn's Disease. *J Crohns Colitis* 2015; **9**: 1113-1119 [PMID: 26351383 DOI: 10.1093/ecco-jcc/jjv150]

9 **Colombel JF**, Panaccione R, Bossuyt P, Lukas M, Baert F, Vaňásek T, Danalioglu A, Novacek G, Armuzzi A, Hébuterne X, Travis S, Danese S, Reinisch W, Sandborn WJ, Rutgeerts P, Hommes D, Schreiber S, Neimark E, Huang B, Zhou Q, Mendez P, Petersson J, Wallace K, Robinson AM, Thakkar RB, D'Haens G. Effect of tight control management on Crohn's disease (CALM): a multicentre, randomised, controlled phase 3 trial. *Lancet* 2018; **390**: 2779-2789 [PMID: 29096949 DOI: 10.1016/S0140-6736(17)32641-7]

10 **Harris PA**, Taylor R, Thielke R, Payne J, Gonzalez N, Conde JG. Research electronic data capture (REDCap)--a metadata-driven methodology and workflow process for providing translational research informatics support. *J Biomed Inform* 2009; **42**: 377-381 [PMID: 18929686 DOI: 10.1016/j.jbi.2008.08.010]

11 **Peyrin-Biroulet L**, Reinisch W, Colombel JF, Mantzaris GJ, Kornbluth A, Diamond R, Rutgeerts P, Tang LK, Cornillie FJ, Sandborn WJ. Clinical disease activity, C-reactive protein normalisation and mucosal healing in Crohn's disease in the SONIC trial. *Gut* 2014; **63**: 88-95 [PMID: 23974954 DOI: 10.1136/gutjnl-2013-304984]

12 **Reinisch W**, Wang Y, Oddens BJ, Link R. C-reactive protein, an indicator for maintained response or remission to infliximab in patients with Crohn's disease: a post-hoc analysis from ACCENT I. *Aliment Pharmacol Ther* 2012; **35**: 568-576 [PMID: 22251435 DOI: 10.1111/j.1365-2036.2011.04987.x]

13 **Kiss LS**, Szamosi T, Molnar T, Miheller P, Lakatos L, Vincze A, Palatka K, Barta Z, Gasztonyi B, Salamon A, Horvath G, Tóth GT, Farkas K, Banai J, Tulassay Z, Nagy F, Szenes M, Veres G, Lovasz BD, Vegh Z, Golovics PA, Szathmari M, Papp M, Lakatos PL; Hungarian IBD Study Group. Early clinical remission and normalisation of CRP are the strongest predictors of efficacy, mucosal healing and dose escalation during the first year of adalimumab therapy in Crohn's disease. *Aliment Pharmacol Ther* 2011; **34**: 911-922 [PMID: 21883326 DOI: 10.1111/j.1365-2036.2011.04827.x]

14 **Boschetti G**, Garnero P, Moussata D, Cuerq C, Préaudat C, Duclaux-Loras R, Mialon A, Drai J, Flourié B, Nancey S. Accuracies of serum and fecal S100 proteins (calprotectin and calgranulin C) to predict the response to TNF antagonists in patients with Crohn's disease. *Inflamm Bowel Dis* 2015; **21**: 331-336 [PMID: 25625487 DOI: 10.1097/MIB.0000000000000273]

15 **Guidi L**, Marzo M, Andrisani G, Felice C, Pugliese D, Mocci G, Nardone O, De Vitis I, Papa A, Rapaccini G, Forni F, Armuzzi A. Faecal calprotectin assay after induction with anti-Tumour Necrosis Factor α agents in inflammatory bowel disease: Prediction of clinical response and mucosal healing at one year. *Dig Liver Dis* 2014; **46**: 974-979 [PMID: 25096964 DOI: 10.1016/j.dld.2014.07.013]

16 **Molander P**, af Björkesten CG, Mustonen H, Haapamäki J, Vauhkonen M, Kolho KL, Färkkilä M, Sipponen T. Fecal calprotectin concentration predicts outcome in inflammatory bowel disease after

induction therapy with TNFα blocking agents. *Inflamm Bowel Dis* 2012; **18**: 2011-2017 [PMID: 22223566 DOI: 10.1002/ibd.22863]

17 **Labaere D**, Smismans A, Van Olmen A, Christiaens P, D'Haens G, Moons V, Cuyle PJ, Frans J, Bossuyt P. Comparison of six different calprotectin assays for the assessment of inflammatory bowel disease. *United European Gastroenterol J* 2014; **2**: 30-37 [PMID: 24918006 DOI: 10.1177/2050640613518201]

World Journal of Gastroenterology

Submit a Manuscript: https://www.f6publishing.com

World J Gastroenterol 2019 May 21; 25(19): 2365-2372

DOI: 10.3748/wjg.v25.i19.2365

ISSN 1007-9327 (print) ISSN 2219-2840 (online)

ORIGINAL ARTICLE

Prospective Study

Change in arterial tumor perfusion is an early biomarker of lenvatinib efficacy in patients with unresectable hepatocellular carcinoma

Hidekatsu Kuorda, Tamami Abe, Yudai Fujiwara, Takuya Okamoto, Miki Yonezawa, Hiroki Sato, Kei Endo, Takayoshi Oikawa, Kei Sawara, Yasuhiro Takikawa

ORCID number: Hidekatsu Kuroda (0000-0002-1471-1087); Tamami Abe (0000-0001-8314-7187); Yudai Fujiwara (0000-0002-8436-5108); Takuya Okamoto (0000-0002-8764-3951); Miki Yonezawa (0000-0002-7509-7172); Hiroki Sato (0000-0002-0258-5503); Kei Endo (0000-0003-1020-7884); Takayoshi Oikawa (0000-0002-1100-6980); Kei Sawara (0000-0003-4608-277X); Yasuhiro Takikawa (0000-0002-1729-1540).

Author contributions: Kuroda H drafted the manuscript, and assisted with data analysis; Abe T participated in design and oversight of the study, and was involved with data collection; Fujiwara Y participated in design of the study, and was involved with data collection; Okamoto T was involved with data collection, and assisted with data analysis; Yonezawa M was involved with data collection, and assisted with data analysis; Sato H was involved with data collection, and assisted with data analysis; Endo K drafted the manuscript, and assisted with data analysis; Oikawa T participated in study design and performed statistical analysis; Sawara K participated in design of the study, was involved with data collection; Takikawa Y drafted the manuscript, and assisted with data analysis; all authors read and approved the final manuscript.

Institutional review board statement: The study was

Hidekatsu Kuorda, Tamami Abe, Yudai Fujiwara, Takuya Okamoto, Miki Yonezawa, Hiroki Sato, Kei Endo, Takayoshi Oikawa, Kei Sawara, Yasuhiro Takikawa, Division of Hepatology, Department of Internal Medicine, Iwate Medical University, Morioka, Iwate 020-8505, Japan

Corresponding author: Hidekatsu Kuroda, MD, PhD, Doctor, Division of Hepatology, Department of Internal Medicine, Iwate Medical University, Uchimaru 19-1, Morioka, Iwate 020-8505, Japan. hikuro@iwate-med.ac.jp
Telephone: +81-19-6515111
Fax: +81-19-6526664

Abstract

BACKGROUND

Lenvatinib is one of the first-line tyrosine kinase inhibitors used for unresectable hepatocellular carcinoma (HCC). In the present study, we evaluated the potential of early changes in the time-intensity curve (TIC) of arterial phase on contrast-enhanced ultrasound (CEUS) as early imaging biomarkers of lenvatinib efficacy.

AIM

To evaluate the potential of the early changes in the TIC of CEUS as early imaging biomarkers of lenvatinib efficacy in patients with unresectable HCC.

METHODS

We analyzed 20 consecutive patients with unresectable HCC treated with lenvatinib from March to November 2018. Tumor response at 8 wk was assessed by computed tomography using the modified Response Evaluation Criteria in Solid Tumors (mRECIST). CEUS was performed at baseline before treatment (Day 0) and on day 7 (Day 7), and the images were analyzed in the arterial phase for 20 seconds after the contrast agent arrived at the target tumor. Three perfusion parameters were extracted from the TICs: the slope of wash-in (Slope), time to peak (TTP) intensity, and the total area under the curve (AUC) during wash-in. The rate of change in the TIC parameters between Day 0 and Day 7 was compared between treatment responders and non-responders based on mRECIST.

RESULTS

The rate of change for all TIC parameters showed significant differences between the responders (n = 9) and non-responders (n = 11) (Slope, P = 0.025; TTP, P =

reviewed and approved by the local Ethics Committee of the Iwate Medical University (MH2018-533).

Clinical trial registration statement: The clinical trial is registered at clinical hospital center Iwate medical trial registry. The registration identification number is MH2018-533.

Informed consent statement: All study participants, or their legal guardian, provided written consent prior to study enrollment.

Conflict-of-interest statement: The authors of this manuscript having no conflicts of interest to disclose.

Data sharing statement: There is no additional data available.

CONSORT 2010 statement: The manuscript was prepared according to CONSORT 2010 Checklist.

Manuscript source: Invited manuscript

Received: February 10, 2019
Peer-review started: February 12, 2019
First decision: March 20, 2019
Revised: April 12, 2019
Accepted: April 29, 2019
Article in press: April 29, 2019
Published online: May 21, 2019

P-Reviewer: Ho HK, Vradelis S, Yarmohammadi H
S-Editor: Ma RY
L-Editor: A
E-Editor: Ma YJ

0.004; and AUC, $P = 0.0003$). The area under the receiver operating curve values for slope, TTP, and AUC for the prediction of responders were 0.805, 0.869, and 0.939, respectively.

CONCLUSION
CEUS may be useful for the early prediction of tumor response to lenvatinib therapy in patients with unresectable HCC.

Key words: Hepatocellular carcinoma; Lenvatinib; Contrast-enhanced ultrasound; Time-intensity curve

Core tip: Lenvatinib is one of the first-line tyrosine kinase inhibitors used for unresectable hepatocellular carcinoma (HCC). In the present study, we evaluated the potential of early changes in the time-intensity curve (TIC) of arterial phase on contrast-enhanced ultrasound (CEUS) as early imaging biomarkers of lenvatinib efficacy. The rate of change for TIC parameters showed precisely reflect the therapeutic effects. CEUS may be useful for the early prediction of tumor response to lenvatinib therapy in patients with unresectable HCC.

Citation: Kuorda H, Abe T, Fujiwara Y, Okamoto T, Yonezawa M, Sato H, Endo K, Oikawa T, Sawara K, Takikawa Y. Change in arterial tumor perfusion is an early biomarker of lenvatinib efficacy in patients with unresectable hepatocellular carcinoma. *World J Gastroenterol* 2019; 25(19): 2365-2372
URL: https://www.wjgnet.com/1007-9327/full/v25/i19/2365.htm
DOI: https://dx.doi.org/10.3748/wjg.v25.i19.2365

INTRODUCTION

Hepatocellular carcinoma (HCC) is the most common primary malignant tumor of the liver [1]. Unfortunately, the overall prognosis for patients with HCC is poor, and more than half of the patients are diagnosed at a stage when the tumor is unresectable. The treatment options for unresectable HCC are limited, and oral administration of sorafenib, a receptor tyrosine kinase inhibitor, has been the only treatment that substantially prolongs survival[2,3]. In the SHARP study, compared to the placebo group, the sorafenib group had an improved overall survival (OS) (median OS, 7.9 mo *vs* 10.7 mo)[4]. However, the clinical benefits of sorafenib are modest, and the survival rates in patients with unresectable HCC remain low. Lenvatinib is an oral multikinase inhibitor targeting the vascular endothelial growth factor receptor (VEGFR), fibroblast growth factor receptor (FGFR), platelet-derived growth factor (PDGF) receptor α, RET, and KIT[5]. The phase III REFLECT trial including 954 patients with previously untreated unresectable HCC demonstrated that lenvatinib had a treatment effect on OS by statistical confirmation of non-inferiority when compared to sorafenib, the standard of care[6]. Furthermore, lenvatinib also demonstrated a significantly higher overall response rate (ORR) compared to sorafenib [24.1% *vs* 9.2%; odds ratio, 3.13; 95% confidence interval (CI): 2.15-4.56; $P < 0.0001$]. In recent years, lenvatinib has become available as a single agent for the first-line treatment of patients with advanced or unresectable HCC[7].

There is a critical need for effective early methods for evaluating targeted therapies to enable individualized medicine in a clinical setting. Contrast-enhanced ultrasound (CEUS) is considered to be a useful technique for evaluating microvascularization, which is essential for tumorigenesis since angiogenesis is the basis for neoplastic growth. Lassau *et al*. have reported that the time-intensity curve (TIC) parameters obtained from CEUS of tumors correlated well with prognosis[8]. Furthermore, Frampas *et al*. showed that CEUS may be a potential surrogate marker of tumor response during targeted therapy, and the area under the curve (AUC), one of the TIC parameters, was useful for assessing blood flow[9]. However, there have been no reports designed to assess the usefulness of CEUS for early prediction of the efficacy of lenvatinib therapy.

This study investigated whether early changes in the TIC parameters of CEUS are

useful indicators of the therapeutic effects of lenvatinib therapy.

MATERIALS AND METHODS

Patients

HCC was diagnosed on the basis of an increasing course of α-fetoprotein, dynamic computed tomography (CT), contrast-enhanced magnetic resonance imaging (MRI), and pathological findings. Between March and November 2018, 22 consecutive HCC patients with (1) an Eastern Cooperative Oncology Group (ECOG) performance status score of 2 or less, (2) Child-Pugh liver function class A, and (3) Barcelona Clinic Liver Cancer stage B or C were enrolled in this prospective study to assess the potential of CEUS findings as early imaging biomarkers of lenvatinib efficacy. Two patients were excluded from the analysis owing to data corruption, and so a total of 20 patients were finally included in this study. One target tumor per patient was studied. The baseline characteristics of the patients are summarized in Table 1.

The study was approved by the local Ethics Committee of the Iwate Medical University (MH2018-533). The patients provided written informed consent prior to the study, in accordance with the principles of the Declaration of Helsinki (revision of Fortaleza, 2013).

Lenvatinib treatment protocol and evaluation of therapeutic response

Lenvatinib (Eisai, Tokyo, Japan) was administered at an initial dose of 8 or 12 mg/d based on the patient's body weight. If grade 3 or 4 adverse events judged to be clinically significant were observed, either the dose was adjusted, or treatment was interrupted according to the guidelines for the administration of lenvatinib. Baseline dynamic CT or MRI was performed within a week before treatment initiation. The target tumor was evaluated using dynamic CT at 8 wk after administering lenvatinib, based on the modified Response Evaluation Criteria in Solid Tumors (mRECIST)[10]. Treatment responders were defined as patients who showed a complete response (CR) or partial response (PR). Non-responders were defined as patients who had stable disease (SD) or progressive disease (PD).

CEUS imaging

CEUS was performed at baseline before the initiation of treatment, and then on Day 7, for evaluation. We selected Day 7 for reference in previous studies on sorafenib therapy[11-15]. Ultrasonography was performed using a LOGIQ E9 XDclear 2.0 ultrasound scanner (GE Healthcare, Wauwatosa, WI, United States) and C1-6-D convex array probe (frequency, 4 MHz). Prior to CEUS, B-mode ultrasonography was performed to examine the slices of target images, and the slice with the largest diameter was selected. All ultrasound images were analyzed by one radiologist who was blinded from the treatment information. CEUS imaging was recorded for 2 min immediately after injection of a bolus (0.0075 mL/kg) of Sonazoid (Daiichi Sankyo, Tokyo, Japan) using the amplitude modulation mode. The acoustic power of the contrast harmonic sonography was set at the default setting with a mechanical index of 0.2-0.3, a rate of 17 frames per second, and a dynamic range of 66 dB. The gain, image depth and transmit focus were optimized for each patient at baseline examination, and the same settings were used at follow up. The cine sequences were saved in the DICOM file format for subsequent analyses.

TIC analysis

A specific calibration file provided by the vendor for the GE Logiq E9 was used in the analysis software to convert ultrasound images to linearized data for TIC analysis. A circular region of interest was established within the demarcated margins of the target tumor as illustrated in Figure 1, which was automatically positioned by the software to adjust for respiratory motion on the following images of the sequence. We analyzed the CEUS images in the arterial phase for 20 s after the contrast agent arrived at the target tumor. Three perfusion parameters were extracted from the TICs: the slope of wash-in (Slope), time to peak (TTP) intensity, and the total area under the TIC (AUC) during wash-in. For each parameter, the rate of change was calculated as follows: {[values after administration of lenvatinib (Day 7) minus baseline values (Day 0)]/baseline values (Day 0) × 100(%)}[16]. The resultant values were compared between the responders and non-responders based on mRECIST.

Statistical analysis

Statistical analyses were performed using the SPSS software program (version 23, IBM, Armonk, NY, United States). The values are shown as the means ± standard deviation or as the medians (range) according to the distribution of the values. The

Table 1 The baseline characteristics of patients

Variables	All (*n* = 20)
Age, yr	68.6 ± 8.4
Gender, male : female	19:1
BMI, kg/m^2	22.2 ± 4.2
ECOG PS, 0:1:	18:2
Etiology, HBV:HCV:alcohol:others	7:7:3:3
AST, IU/L	52.2 ± 38.1
ALT, IU/L	45.1 ± 26.3
T.Bil, mg/dL	0.7 ± 0.4
Alb, g/dL	3.4 ± 0.5
PT, %	82.2 ± 15.2
Plt, × 10^4/μL	19.7 ± 6.1
Child–Pugh score, 5:6 points	8:12
Median AFP, ng/mL (range)	268 (4.5-53000)
Intrahepatic tumor size, cm	6.6 ± 6.3
Number of intrahepatic tumors, single : multiple	3:17
Portal vein invasion, *n* (%)	9 (45.0)
Extrahepatic metastasis, *n* (%)	15 (75.0)
Previous treatment, *n* (%)	19 (95.0)
Initial dose of lenvatinib, 8:12 mg/d	16:4

The values represent the mean ± SD or the median (range). BMI: Body mass index; ECOG: Eastern Cooperative Oncology Group; PS: Performance Status; T.Bil: Total bilirubin; AST: Aspartate aminotransferase; ALT: Alanine aminotransferase; Alb: Albumin; PT: Prothrombin time; Plt: Platelet count; AFP: Alpha-fetoprotein.

Mann-Whitney *U* test was used to compare differences between responders and non-responders. Receiver operating characteristic (ROC) curves were constructed, and area under the ROC curve (AUROC) was calculated using the trapezoidal rule. Optimal cut-off values for prediction of responders were identified from the highest Youden index. The sensitivity, specificity, positive predictive value, and negative predictive value were calculated using cut-offs obtained from the ROC curves. *P*-values < 0.05 were considered to be statistically significant.

RESULTS

All 20 patients were evaluated based on the imaging findings obtained by enhanced CT at 8 wk after starting lenvatinib therapy. On the basis of mRECIST, 0, 9, 8, and 3 patients were found to have CR, PR, SD, and PD, respectively [ORR, 45.0%; disease control rate (DCR), 85.0%]. Thus, 9 and 11 patients were classified as responders and non-responders, respectively, after 8 wk of lenvatinib therapy. There were no statistically significant differences in the ORR and DCR from those in patients receiving the initial dose of lenvatinib.

In responders, the TIC parameters were as follows: median slope Day 0/Day 7: 1.51 dB/s/1.09 dB/s, P = 0.018; median TTP Day 0/Day 7: 10.56 s/12.43 s, P = 0.003; median AUC Day 0/Day 7: 266.51/156.44, P = 0.001. In contrast, the TIC parameters in non-responders were as follows: median slope Day 0/Day 7: 1.52 dB/s/1.33 dB/s, P = 0.511; median TTP Day 0/Day 7: 11.02 s/11.84 s, P = 0.247; median AUC Day 0/Day 7: 258.14/229.65, P = 0.322 (Table 2). There were no significant differences in any TIC parameters between patients with SD and PD.

The rate of change for all TIC parameters showed significant differences between the responders and non-responders (Slope, P = 0.022; TTP, P = 0.019; AUC, P = 0.003) (Figure 2). The AUROC values for the rate of change of slope, TTP, and AUC for prediction of responders were 0.818, 0.869, and 0.939, respectively (Table 3).

DISCUSSION

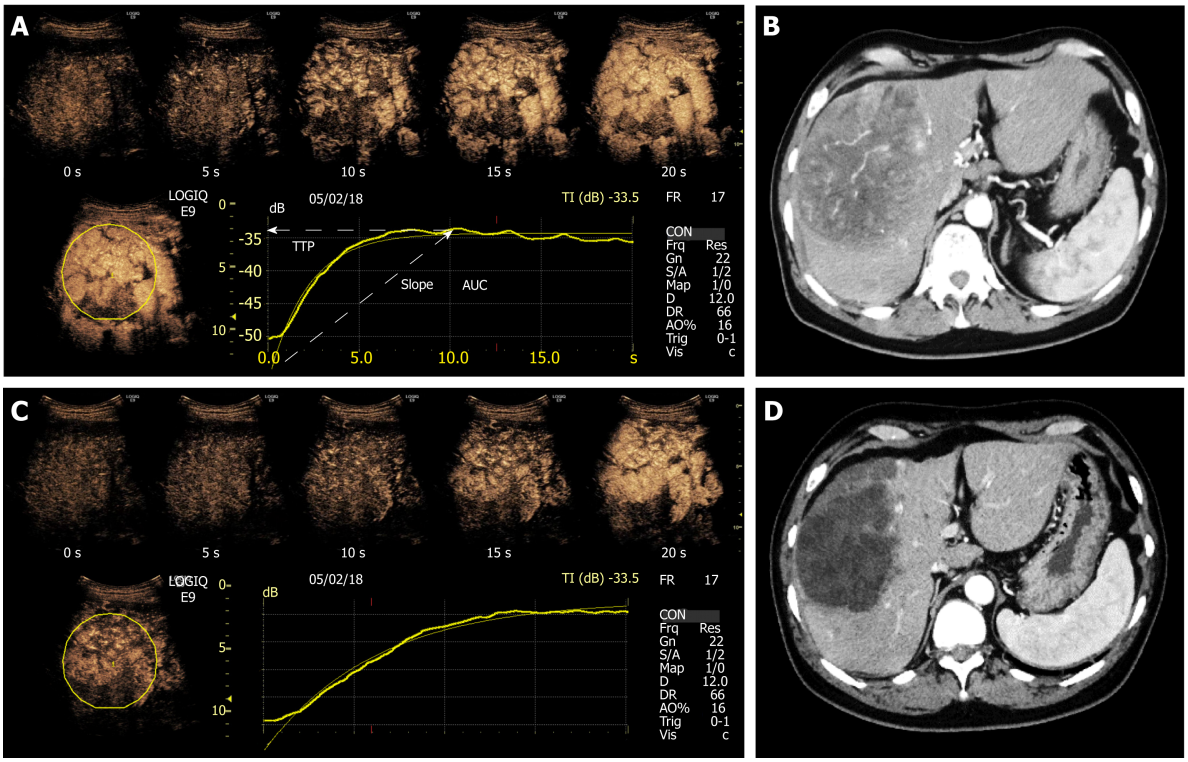

Figure 1 Representative case of a 69-year-old man with unresectable hepatocellular carcinoma treated with lenvatinib (12 mg/d). A: Contrast-enhanced ultrasound (CEUS) imaging in the arterial phase at Day 0 and time-intensity curve (TIC) analysis. The region of interest was established within the demarcation margins of the target tumor. B: CEUS imaging at Day 7 and TIC analysis. The slope became gentle, and indicated a delay in TTP and a decrease in the area under the curve. C: Computed tomography (CT) image at Day 0. D: CT image at 8 wk. Therapeutic response was evaluated as partial response using the modified Response Evaluation Criteria in Solid Tumors. TTP: Time to peak; AUC: Area under the curve.

In this study, we enrolled 20 patients with unresectable HCC and used CEUS to make an early prediction of the efficacy of lenvatinib therapy. The results of the study confirm that real-time observation of the perfusion within HCC is possible by CEUS, and responders to lenvatinib show a change in perfusion in the arterial phase on CEUS within a few days of starting the therapy. In our study, the rate of change in the slope, TTP, and AUC on Day 7 was significantly different in the responders and non-responders. The findings of CEUS performed at the earliest stage of therapy reflected the results of the CT evaluation performed 8 weeks after starting lenvatinib therapy, thereby suggesting that CEUS can predict the clinical outcomes at an early stage of therapy. To the best of our knowledge, this is the first prospective study to assess the potential of CEUS for making early predictions of clinical outcomes following lenvatinib therapy.

Besides its antitumor effects, lenvatinib is also known to be antiangiogenic based on its interaction with VEGFR2[5]. Since angiogenesis is necessary for tumor growth, the changes in tumor perfusion seem to reflect changes in tumor vitality. Therefore, CEUS is relevant as a modality for monitoring biologically essential changes in response to lenvatinib therapy. Several studies have reported that the changes in perfusion measured by CEUS may predict treatment responses in patients with HCC receiving sorafenib[11-15]. Sugimoto *et al*[14] showed that the AUC during wash-in on day 14 of sorafenib therapy was useful for the early prediction of tumor response. We observed a similar trend; the rate of change of the AUC during wash-in on day 7 of lenvatinib therapy was significantly different between the responders and non-responders. In the REFLECT trial, lenvatinib demonstrated a significantly higher ORR than sorafenib[6], which was potentially due to its stronger effect on tumor perfusion.

The evaluation of tumor perfusion by CEUS is a simple, non-invasive test that can be done in real time. Such a prediction tool is also cost-effective since it helps avoid adverse events and may enable individualized treatment for unresectable HCC in the future.

This study has some limitations. First, the sample size was small. Larger-scale prospective clinical studies will be needed to confirm these findings. Second, unlike dynamic CT and MRI, which are commonly used to assess tumor angiogenesis, CEUS is an operator-dependent examination.

In conclusion, this study demonstrates that with contrast enhancement in the

Table 2 Distribution of changes in time-intensity curve parameters in tumors from day 0 to day 7 for 20 hepatocellular carcinoma patients according to modified Response Evaluation Criteria in Solid Tumors response at 2 mo

	Responders (*n* = 9)		Non-responders (*n* = 11)	
	Day 0	Day 7	Day 0	Day 7
Slope	1.51 [1.31, 1.68]	1.09 [0.84, 1.23]	1.52 [1.22, 1.62]	1.33 [0.86, 1.71]
P value	0.018		0.511	
TTP	10.56 [9.33, 12.13]	12.43 [11.94, 13.94]	11.02 [8.53, 12.51]	11.84 [10.15, 13.82]
P value	0.003		0.247	
AUC	266.51 [225.38, 296.67]	156.44 [123.05, 178.91]	258.14 [191.61, 299.51]	229.65 [176.10, 269.50]
P value	0.001		0.322	

The values represent the median [25th-75th percentile]. HCC: Hepatocellular carcinoma; TTP: Time to peak; AUC: Area under the curve.

arterial phase, the differences in the TIC before and after lenvatinib therapy may serve as useful indicators of therapeutic outcomes for patients with unresectable HCC. In particular, the rate of change for AUC appear to precisely reflect the therapeutic effects. Therefore, TIC analysis could help in the early prediction of the clinical outcomes of lenvatinib therapy.

Table 3 The performance characteristics of the rate of change of time-intensity curve parameters for the prediction of responders

	Slope (95%CI)	TTP (95%CI)	AUC (95%CI)
AUROC	0.818 (0.602-0.944)	0.869 (0.728-0.975)	0.939 (0.812-0995)
Cut-off value (%)	-11.765	+9.495	-25.714
Sensitivity	0.889 (0.540-0.978)	0.889 (0.540-0.978)	0.896 (0.616-0.989)
Specificity	0.545 (0.304-0.786)	0.818 (0.510-0.917)	0.909 (0.648-0.995)
PPV	0.615 (0.583-0.793)	0.800 (0.611-0.907)	0.833 (0.727-0.918)
NPV	0.857 (0.731-0.922)	0.878 (0.741-0.962)	0.900 (0.747-0.992)

TIC: Time-intensity curve; CI: Confidence interval; TTP: Time to peak; AUC: Area under the curve; AUROC: Area under receiver operating curve; PPV: Positive predictive value; NPV: Negative predictive value.

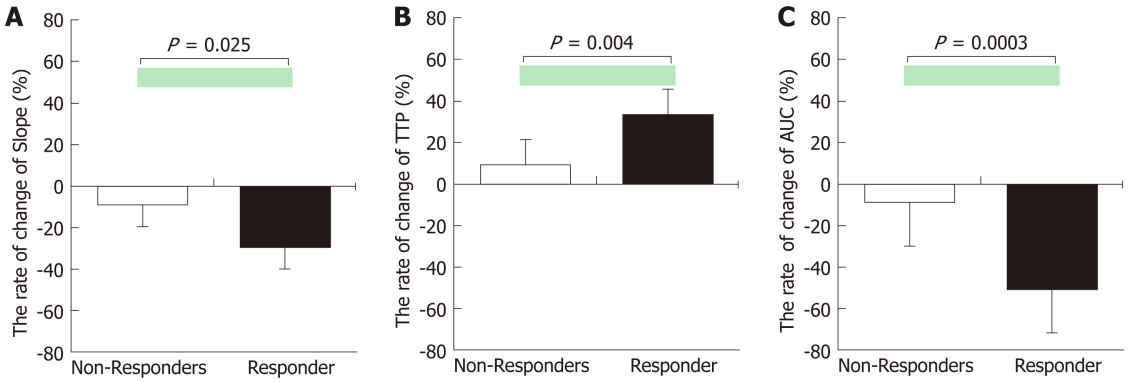

Figure 2 The rates of change of time-intensity curve parameters in responders and non-responders. A: Slope, B: time to peak, C: area under the curve. The rates of change of all time-intensity curve parameters were significantly different in responders and non-responders. TTP: Time to peak; AUC: Area under the curve.

ARTICLE HIGHLIGHTS

Research background

Lenvatinib is one of the first-line tyrosine kinase inhibitors used for unresectable hepatocellular carcinoma (HCC).

Research motivation

The overall prognosis for patients with HCC is poor, and more than half of the patients are diagnosed at a stage when the tumor is unresectable. The treatment options for unresectable HCC are limited, and oral administration of sorafenib, a receptor tyrosine kinase inhibitor, has been the only treatment that substantially prolongs survival.

Research objectives

To evaluate the potential of the early changes in the time-intensity curve (TIC) of contrast-enhanced ultrasound (CEUS) as early imaging biomarkers of lenvatinib efficacy in patients with unresectable HCC.

Research methods

We analyzed 20 consecutive patients with unresectable HCC treated with lenvatinib from March to November 2018. Tumor response at 8 wk was assessed by computed tomography using the modified Response Evaluation Criteria in Solid Tumors (mRECIST). CEUS was performed at baseline before treatment (Day 0) and on day 7 (Day 7), and the images were analyzed in the arterial phase for 20 seconds after the contrast agent arrived at the target tumor. Three perfusion parameters were extracted from the TICs: the slope of wash-in (Slope), time to peak (TTP) intensity, and the total area under the curve (AUC) during wash-in. The rate of change in the TIC parameters between Day 0 and Day 7 was compared between treatment responders and non-responders based on mRECIST.

Research results

The rate of change for all TIC parameters showed significant differences between the responders (n = 9) and non-responders (n = 11) (Slope, P = 0.025; TTP, P = 0.004; and AUC, P = 0.0003). The area under the receiver operating curve values for slope, TTP, and AUC for the prediction of responders were 0.805, 0.869, and 0.939, respectively.

Research conclusions

To the best of our knowledge, this is the first prospective study to assess the potential of CEUS for making early predictions of outcomes following lenvatinib therapy, which makes it a significant contribution to the literature.

Research perspectives

Further, we believe that this paper will be of interest to the readership especially hepatologists and oncologists because we demonstrate that CEUS may be useful for the early prediction of tumor response in patients with unresectable HCC treated with lenvatinib.

ACKNOWLEDGEMENTS

The authors thank Ms. Yuriko Mikami and Ms. Kouko Motodate for their excellent technical assistance.

REFERENCES

1 **Forner A**, Llovet JM, Bruix J. Hepatocellular carcinoma. *Lancet* 2012; **379**: 1245-1255 [PMID: 22353262 DOI: 10.1016/S0140-6736(11)61347-0]
2 **Gauthier A**, Ho M. Role of sorafenib in the treatment of advanced hepatocellular carcinoma: An update. *Hepatol Res* 2013; **43**: 147-154 [PMID: 23145926 DOI: 10.1111/j.1872-034X.2012.01113.x]
3 **Cheng AL**, Kang YK, Chen Z, Tsao CJ, Qin S, Kim JS, Luo R, Feng J, Ye S, Yang TS, Xu J, Sun Y, Liang H, Liu J, Wang J, Tak WY, Pan H, Burock K, Zou J, Voliotis D, Guan Z. Efficacy and safety of sorafenib in patients in the Asia-Pacific region with advanced hepatocellular carcinoma: a phase III randomised, double-blind, placebo-controlled trial. *Lancet Oncol* 2009; **10**: 25-34 [PMID: 19095497 DOI: 10.1016/S1470-2045(08)70285-7]
4 **Llovet JM**, Ricci S, Mazzaferro V, Hilgard P, Gane E, Blanc JF, de Oliveira AC, Santoro A, Raoul JL, Forner A, Schwartz M, Porta C, Zeuzem S, Bolondi L, Greten TF, Galle PR, Seitz JF, Borbath I, Häussinger D, Giannaris T, Shan M, Moscovici M, Voliotis D, Bruix J; SHARP Investigators Study Group. Sorafenib in advanced hepatocellular carcinoma. *N Engl J Med* 2008; **359**: 378-390 [PMID: 18650514 DOI: 10.1056/NEJMoa0708857]
5 **Tohyama O**, Matsui J, Kodama K, Hata-Sugi N, Kimura T, Okamoto K, Minoshima Y, Iwata M, Funahashi Y. Antitumor activity of lenvatinib (e7080): an angiogenesis inhibitor that targets multiple receptor tyrosine kinases in preclinical human thyroid cancer models. *J Thyroid Res* 2014; **2014**: 638747 [PMID: 25295214 DOI: 10.1155/2014/638747]
6 **Kudo M**, Finn RS, Qin S, Han KH, Ikeda K, Piscaglia F, Baron A, Park JW, Han G, Jassem J, Blanc JF, Vogel A, Komov D, Evans TRJ, Lopez C, Dutcus C, Guo M, Saito K, Kraljevic S, Tamai T, Ren M, Cheng AL. Lenvatinib versus sorafenib in first-line treatment of patients with unresectable hepatocellular carcinoma: a randomised phase 3 non-inferiority trial. *Lancet* 2018; **391**: 1163-1173 [PMID: 29433850 DOI: 10.1016/S0140-6736(18)30207-1]
7 **Kudo M**. Systemic Therapy for Hepatocellular Carcinoma: Latest Advances. *Cancers (Basel)* 2018; **10** [PMID: 30380773 DOI: 10.3390/cancers10110412]
8 **Lassau N**, Bonastre J, Kind M, Vilgrain V, Lacroix J, Cuinet M, Taieb S, Aziza R, Sarran A, Labbe-Devilliers C, Gallix B, Lucidarme O, Ptak Y, Rocher L, Caquot LM, Chagnon S, Marion D, Luciani A, Feutray S, Uzan-Augui J, Coiffier B, Benastou B, Koscielny S. Validation of dynamic contrast-enhanced ultrasound in predicting outcomes of antiangiogenic therapy for solid tumors: the French multicenter support for innovative and expensive techniques study. *Invest Radiol* 2014; **49**: 794-800 [PMID: 24991866 DOI: 10.1097/RLI.0000000000000085]
9 **Frampas E**, Lassau N, Zappa M, Vullierme MP, Koscielny S, Vilgrain V. Advanced Hepatocellular Carcinoma: early evaluation of response to targeted therapy and prognostic value of Perfusion CT and Dynamic Contrast Enhanced-Ultrasound. Preliminary results. *Eur J Radiol* 2013; **82**: e205-e211 [PMID: 23273822 DOI: 10.1016/j.ejrad.2012.12.004]
10 **Lencioni R**, Llovet JM. Modified RECIST (mRECIST) assessment for hepatocellular carcinoma. *Semin Liver Dis* 2010; **30**: 52-60 [PMID: 20175033 DOI: 10.1055/s-0030-1247132]
11 **Shiozawa K**, Watanabe M, Ikehara T, Shimizu R, Shinohara M, Igarashi Y, Sumino Y. Evaluation of sorafenib for advanced hepatocellular carcinoma with low α-fetoprotein in arrival time parametric imaging using contrast-enhanced ultrasonography. *J Med Ultrason (2001)* 2017; **44**: 101-107 [PMID: 27837395 DOI: 10.1007/s10396-016-0757-2]
12 **Knieling F**, Waldner MJ, Goertz RS, Strobel D. Quantification of dynamic contrast-enhanced ultrasound in HCC: prediction of response to a new combination therapy of sorafenib and panobinostat in advanced hepatocellular carcinoma. *BMJ Case Rep* 2012; 2012 [PMID: 23257272 DOI: 10.1136/bcr-2012-007576]
13 **Shiozawa K**, Watanabe M, Ikehara T, Kogame M, Kikuchi Y, Igarashi Y, Sumino Y. Therapeutic evaluation of sorafenib for hepatocellular carcinoma using contrast-enhanced ultrasonography: Preliminary result. *Oncol Lett* 2016; **12**: 579-584 [PMID: 27347183 DOI: 10.3892/ol.2016.4669]
14 **Sugimoto K**, Moriyasu F, Saito K, Rognin N, Kamiyama N, Furuichi Y, Imai Y. Hepatocellular carcinoma treated with sorafenib: early detection of treatment response and major adverse events by contrast-enhanced US. *Liver Int* 2013; **33**: 605-615 [PMID: 23305331 DOI: 10.1111/liv.12098]
15 **Lamuraglia M**, Escudier B, Chami L, Schwartz B, Leclère J, Roche A, Lassau N. To predict progression-free survival and overall survival in metastatic renal cancer treated with sorafenib: pilot study using dynamic contrast-enhanced Doppler ultrasound. *Eur J Cancer* 2006; **42**: 2472-2479 [PMID: 16965911 DOI: 10.1016/j.ejca.2006.04.023]
16 **Ueda N**, Nagira H, Sannomiya N, Ikunishi S, Hattori Y, Kamida A, Koyanagi Y, Shimabayashi K, Sato K, Saito H, Hirooka Y. Contrast-Enhanced Ultrasonography in Evaluation of the Therapeutic Effect of Chemotherapy for Patients with Liver Metastases. *Yonago Acta Med* 2016; **59**: 255-261 [PMID: 28070162]

World Journal of Gastroenterology

Submit a Manuscript: https://www.f6publishing.com

World J Gastroenterol 2019 May 21; 25(19): 2373-2382

DOI: 10.3748/wjg.v25.i19.2373

ISSN 1007-9327 (print) ISSN 2219-2840 (online)

ORIGINAL ARTICLE

Randomized Controlled Trial

New antireflux plastic stent for patients with distal malignant biliary obstruction

Xiang-Lei Yuan, Bin Wei, Lian-Song Ye, Chun-Cheng Wu, Qing-Hua Tan, Ming-Hong Yao, Yu-Hang Zhang, Xian-Hui Zeng, Yan Li, Yu-Yan Zhang, Bing Hu

ORCID number: Xiang-Lei Yuan (0000-0003-2281-5094); Bin Wei (0000-0003-4898-8348); Lian-Song Ye (0000-0001-5542-2508); Chun-Cheng Wu (0000-0002-8390-4202); Qing-hua Tan (0000-0001-5032-9849); Ming-Hong Yao (0000-0001-8151-6014); Yu-Hang Zhang (0000-0003-2268-6149); Xian-Hui Zeng (0000-0002-2865-7560); Yan Li (0000-0003-1731-7031); Yu-Yan Zhang (0000-0002-9094-5045); Bing Hu (0000-0002-9898-8656).

Author contributions: Hu B, Yuan XL and Ye LS designed this study; Hu B, Yuan XL, Wu CC, and Tan QH recruited the patients, performed the clinical investigations, and treated the patients; Yuan XL, Wei B, Ye LS, Zhang YH, Zeng XH, Li Y, and Zhang YY participated in trial coordination and monitoring; Yuan XL and Wu CC performed data collection and management; Yuan XL and Yao MH contributed to the statistical analyses; Hu B, Wu CC, and Tan QH analyzed and interpreted the data; Yuan XL and Wei B drafted the manuscript; Hu B, Ye LS, Tan QH, Zhang YH, Zeng XH, Li Y, and Zhang YY critically revised the manuscript; all authors approved the final version of the manuscript for publication.

Supported by the Sichuan Province Science and Technology Department, China, No. 2017SZ0009.

Institutional review board statement: The study protocol was approved by the China Ethics

Xiang-Lei Yuan, Lian-Song Ye, Chun-Cheng Wu, Qing-Hua Tan, Yu-Hang Zhang, Xian-Hui Zeng, Yan Li, Yu-Yan Zhang, Bing Hu, Department of Gastroenterology, West China Hospital, Sichuan University, Chengdu 610041, Sichuan Province, China

Bin Wei, Department of Gastroenterology, the First Hospital of Xi'an City, Xi'an 710002, Shaanxi Province, China

Ming-Hong Yao, Department of Epidemiology and Health Statistics, West China School of Public Health, Sichuan University, Chengdu 610041, Sichuan Province, China

Corresponding author: Bing Hu, MD, Professor, Department of Gastroenterology, West China Hospital, Sichuan University, No. 37, Guo Xue Xiang, Wuhou District, Chengdu 610041, Sichuan Province, China. hubingnj@163.com
Telephone: +86-18980601278

Abstract

BACKGROUND

Endoscopic biliary stenting is a well-established palliative treatment for patients with unresectable distal malignant biliary obstruction (MBO). However, the main problem with stent placement is the relatively short duration of stent patency. Although self-expanding metal stents (SEMSs) have a longer patency period than plastic stents (PSs), the higher costs limit the wide use of SEMSs. A PS with an antireflux valve is an attractive idea to prolong stent patency, but no ideal design for an antireflux PS (ARPS) has been proposed. We developed a new ARPS with a "duckbilled" valve attached to the duodenal end of the stent.

AIM

To compare the patency of ARPSs with that of traditional PSs (TPSs) in patients with unresectable distal MBO.

METHODS

We conducted a single-center, prospective, randomized, controlled, double-blind study. This study was conducted at the West China Hospital of Sichuan University. Consecutive patients with extrahepatic MBO were enrolled prospectively. Eligible patients were randomly assigned to receive either an ARPS or a TPS. Patients were followed by clinic visits or telephone interviews every 1-2 mo until stent exchange, death, or the final study follow-up in October 2018. The primary outcome was the duration of stent patency. Secondary outcomes included the rate of technical success, the rate of clinical success,

Committee of Registering Clinical Trials (Number: ChiECRCT-20150069; date of approval: December 13, 2015).

Clinical trial registration statement: The trial was registered with Chinese Clinical Trial Registry (Number: ChiCTR-IIR-16007869; date of registration: February 1, 2016).

Informed consent statement: Informed consent was obtained from all patients involved in this study.

Conflict-of-interest statement: Professor Bing Hu is one of the inventors of the antireflux plastic stent. He has worked in collaboration with Micro-Tech (Nanjing) Co. Ltd., Nanjing, China to develop the stent. No free device was offered for this study. The authors disclose no conflicts of interest.

Data sharing statement: No additional unpublished data are available.

Manuscript source: Invited manuscript

Received: March 14, 2019
Peer-review started: March 14, 2019
First decision: March 27, 2019
Revised: March 28, 2019
Accepted: April 19, 2019
Article in press: April 20, 2019
Published online: May 21, 2019

P-Reviewer: Hara K, Hillman LC
S-Editor: Yan JP
L-Editor: Wang TQ
E-Editor: Ma YJ

adverse events, and patient survival.

RESULTS

Between February 2016 and December 2017, 38 patients were randomly assigned to two groups, with 19 patients in each group, to receive ARPSs or TPSs. Stent insertion was technically successful in all patients. There were no significant differences between the two groups in the rates of clinical success or the rates of early or late adverse events (P = 0.660, 1.000, and 1.000, respectively). The median duration of stent patency in the ARPS group was 285 d [interquartile range (IQR), 170], which was significantly longer than that in the TPS group (median, 130 d; IQR, 90, P = 0.005). No significant difference in patient survival was noted between the two groups (P = 0.900).

CONCLUSION

The new ARPS is safe and effective for the palliation of unresectable distal MBO, and has a significantly longer stent patency than a TPS.

Key words: Antireflux valve; Plastic biliary stent; Distal malignant biliary obstruction; Stent patency; Endoscopic retrograde cholangiopancreatography

Core tip: There is no ideal design for an antireflux plastic stent for prolonging stent patency. In this study, a newly designed antireflux plastic stent with a "duckbilled" valve was successfully deployed in patients with unresectable distal malignant biliary obstruction. The median duration of stent patency in the antireflux plastic stent group was 285 d, which was significantly longer than that in the traditional plastic stent group (130 d).

Citation: Yuan XL, Wei B, Ye LS, Wu CC, Tan QH, Yao MH, Zhang YH, Zeng XH, Li Y, Zhang YY, Hu B. New antireflux plastic stent for patients with distal malignant biliary obstruction. *World J Gastroenterol* 2019; 25(19): 2373-2382
URL: https://www.wjgnet.com/1007-9327/full/v25/i19/2373.htm
DOI: https://dx.doi.org/10.3748/wjg.v25.i19.2373

INTRODUCTION

Distal malignant biliary obstruction (MBO) is mainly caused by cholangiocarcinoma, pancreatic cancer, and ampullary cancer. Since many of these tumors progress slowly and are usually detected at an advanced stage, curative surgical resection may not be feasible[1]. Endoscopic biliary stenting has become a well-established palliative treatment for patients with unresectable distal MBO[2,3]. However, the main problem with stent placement is the relatively short duration of stent patency[4,5]. Self-expanding metal stents (SEMSs) have longer patency periods than plastic stents (PSs). However, uncovered SEMSs are limited by their inability to be removed, and covered SEMSs are prone to migration[6-8]. Moreover, due to the problems of health insurance in China, the higher costs restrict the wide use of SEMSs[1]. PSs are still the main choice for patients in China because of their relatively low cost and easy replacement after stent dysfunction.

The actual mechanisms of PS occlusion remain largely unclear. Duodenobiliary reflux may be a major cause of stent occlusion[9,10]. In recent years, the design of PS with an antireflux valve at the duodenal end has been an attractive idea to eliminate retrograde flow from the duodenum, thereby prolonging stent patency. Some investigators have reported the effectiveness of these modified PSs[1,11,12], but no excellent results have been reported; thus, modified PSs have not been widely used in clinical practice. We developed a new antireflux PS (ARPS) with a "duckbilled" valve attached to the duodenal end of the stent (Figure 1). In this study, we aimed to compare the patency of this new ARPS with that of a traditional PS (TPS) in patients with unresectable distal MBO.

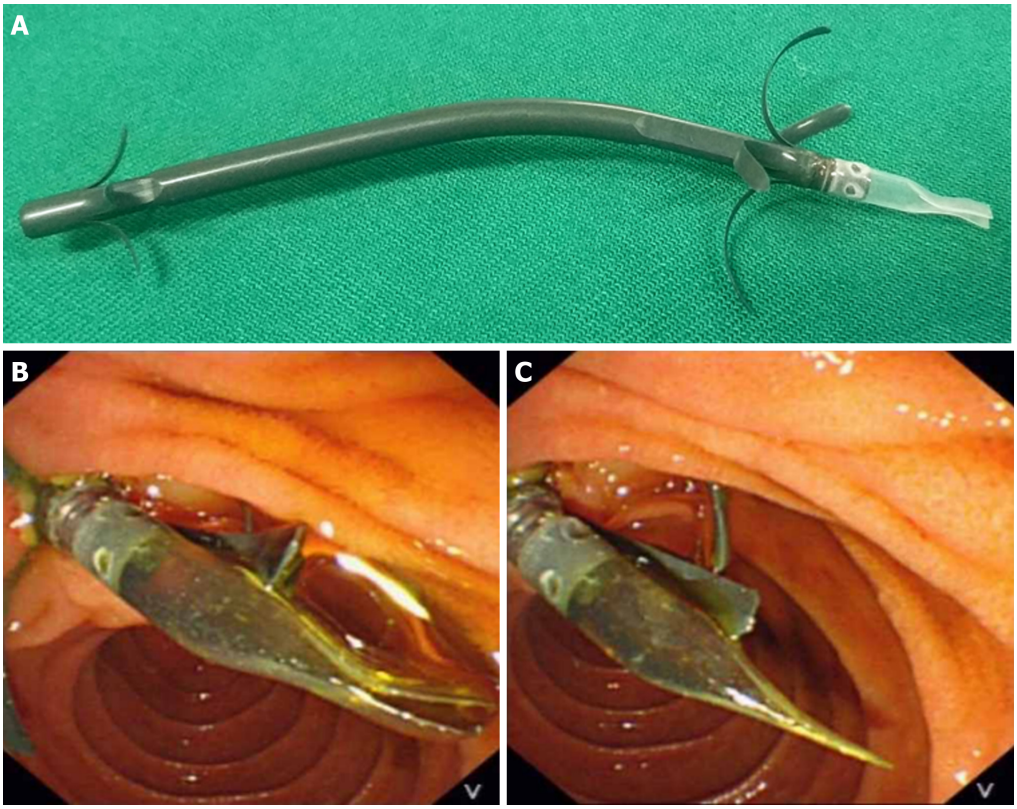

Figure 1 The new antireflux plastic biliary stent. A: The newly designed antireflux plastic stent with a "duckbilled" valve attached to the duodenal end of the stent; B: The valve remains open and allows the antegrade flow of bile; C: The valve closes as the intestinal pressure increases, preventing the reflux of the duodenal contents.

MATERIALS AND METHODS

The study was a single-center, prospective, randomized, controlled, double-blind trial. The study protocol was approved by the China Ethics Committee of Registering Clinical Trials (Number: ChiECRCT-20150069; date of approval: December 13, 2015), and registered with the Chinese Clinical Trial Registry (Number: ChiCTR-IIR-16007869; date of registration: February 1, 2016). This study was conducted at West China Hospital of Sichuan University, a tertiary hospital. Informed consent for ARPS placement and use of clinical data was obtained from all patients involved in this study.

Design of the ARPS

The ARPS (Micro-Tech (Nanjing) Co. Ltd., Nanjing, China) used in this study was made of polytetrafluoroethylene, the same material as a TPS, and had similar design (Tannenbaum design) as a TPS (Cook Ireland Ltd., Limerick, Ireland). The difference was that a 1.5 cm-long antireflux valve made of silicone rubber material was attached to the duodenal end of the ARPS. The bile flowed out when the valve was opened by increased common bile duct (CBD) pressure. Otherwise, the valve remained closed to prevent intestinal content regurgitation into the CBD when the duodenal pressure increased. The outer diameters of both types of stents were 10 Fr, and neither stent had any side holes. The length of both types of stents ranged from 5 cm to 9 cm, and the optimal length for each patient was determined by an endoscopist during the procedure.

Patients

Consecutive patients with extrahepatic MBO were prospectively enrolled. All patients were hospitalized for obstructive jaundice or elevated liver enzymes resulting from MBO. All of the patient lesions were surgically unresectable based on the stage of the tumors, the general condition of the patients, and consultations with the surgeons and anesthesiologists. Patients aged younger than 18 years old and those with a resectable tumor, hilar biliary stricture, or previous surgical drainage procedure were excluded. Patients with any contraindication to endoscopic procedures or who refused informed consent were also excluded.

Randomization and blinding

Eligible patients were randomly assigned to receive either an ARPS or a TPS during the endoscopic procedure. Group allocation schemes generated randomly by a computer program at a ratio of 1:1 were placed into serially numbered sealed envelopes. After the biliary stricture was confirmed on cholangiography, an envelope was selected in sequence to determine the group allocation.

Patients were blinded to the stent assignment until a study endpoint was reached. Although blinding of the endoscopists was not possible, the endoscopists were not involved in the assessment of outcomes. The assessments were performed by reviewing physicians blinded to the randomization process. The data manager and statistician were not blinded.

Procedures

All endoscopic retrograde cholangiopancreatography (ERCP) procedures were performed by one of four experienced endoscopists (≥300 ERCPs per year). Preoperative preparation was similar to that for general ERCPs. Prophylactic antibiotics and nonsteroidal anti-inflammatory drugs were not used before the procedure. All patients were placed in the prone position with conscious sedation, and a standard duodenoscope (TJF-260 V; Olympus Medical systems, Tokyo, Japan) was used. The endoscopist determined if sphincterotomy was necessary. Under the guidance of a guidewire (Jagwire; Boston Scientific, Natick, MA, United States), according to the group allocation, a single 10 Fr ARPS or TPS with an appropriate length was advanced into the bile duct approximately 1-2 cm above the proximal end of the stricture, leaving the distal end of the stent approximately 1 cm outside of the duodenal papilla. The flow of bile was confirmed before withdrawal of the duodenoscope (Video 1, Supplementary material).

Follow-up and outcomes

Clinical evaluation and liver function tests were performed for all patients within one month after stent insertion. Subsequently, patients were followed by clinic visits or telephone interviews every 1-2 mo until stent exchange, death, or the final study follow-up period ended in October 2018. Patients lost to follow-up were excluded from the analysis.

The primary outcome was the duration of stent patency, which was recorded in days from stent placement to stent dysfunction requiring exchange. Stent dysfunction was considered present if recurrent obstructive jaundice and/or symptoms of cholangitis were observed along with biliary dilation on imaging studies or re-ERCP findings, and these abnormalities were resolved after insertion of a new stent. Secondary outcomes included the rate of technical success, the rate of clinical success, adverse events, and patient survival. Technical success was defined as successful insertion of the stent into the bile duct above the proximal end of the stricture and in an appropriate position based on fluoroscopic confirmation. Clinical success was defined as the resolution of obstructive symptoms and normalization of serum bilirubin within one month after stent placement. Adverse events were categorized as early (within 30 d) and late (after 30 d). Patient survival was measured as the duration from stent placement to death.

Statistical analysis

The sample size calculation was based on a previous study[11]. Under the assumption of a relative difference of 40% with an assumed standard deviation (SD) of 40 d in stent patency between the ARPS and TPS groups and an attrition rate of 10% for patients lost to follow-up, a sample size of 19 patients in each group would result in a power of 80% for a targeted significance level of 5% with a two-tailed test.

Continuous variables are characterized as the mean and SD or the median and interquartile range (IQR). Categorical variables are expressed as a frequency or proportion. Student's *t*-test, Fisher's exact test, Mann-Whitney *U*-test, and log-rank test were used whenever appropriate. Stent patency and patient survival were analyzed using the Kaplan-Meier method. A P-value < 0.05 was considered to be significant. Statistical analyses were performed using SPSS Statistics v. 23.0 (IBM Corp, Armonk, NY, United States).

RESULTS

Between February 2016 and December 2017, 89 patients were screened for eligibility. Of these, 51 patients were excluded due to surgical treatment (n = 9), hilar biliary stricture (n = 13), and declined participation (n = 29). Finally, a total of 38 patients were randomized to receive an ARPS or a TPS (Figure 2). One patient in the TPS

group was lost to follow-up after discharge. Thus, clinical information was available for 19 patients [mean (SD) age, 70.3 (13.1) years; male/female, 12/7] in the ARPS group and 18 patients [mean (SD) age, 73.8 (14.6) years; male/female, 14/4] in the TPS group. Table 1 shows the baseline patient characteristics and clinical information of the patients for each group. There was no significant difference between the two groups.

Early clinical outcomes and adverse events

Stent insertion was technically successful with a single attempt in 37 patients. Clinical success was achieved in 32 patients, and no significant difference was noted between the ARPS group (n = 17) and the TPS group (n = 15) (89.5% *vs* 83.3%, P = 0.660). Early adverse events were observed in four patients, including two cases of post-ERCP cholangitis and two cases of post-ERCP mild pancreatitis. Adverse events were all successfully controlled with conservative management. One patient in the ARPS group presented a late adverse event, mild pancreatitis, on day 94; she responded well to the conservative treatment. There were no significant differences in the rates of early or late adverse events between the two groups (Table 2).

Stent patency and patient survival

During the follow-up period, stent dysfunction was noted in 12 (63.2%) patients in the ARPS group and 15 (83.3%) patients in the TPS group. All dysfunctional stents were successfully removed endoscopically using a snare or biopsy forceps, and a new TPS or SEMS was inserted. Although there was no significant difference in the duration between stent placement and the occurrence of stent dysfunction between the two groups, a trend of later occurrence of stent dysfunction was observed in the ARPS group (median, 183 *vs* 119 d, P = 0.102). In the remaining patients, stent patency was maintained until death or the final study follow-up in October 2018. The median patency period in the ARPS group was 285 d (IQR, 170), which was significantly longer than that in the TPS group (median, 130 d; IQR, 90, P = 0.005) (Table 2, Figure 3). By the time of analysis, 33 patients had died, namely, 17 in the ARPS group (89.5%) with a median (IQR) survival time of 195 d (297) and 16 in the TPS group (88.9%) with a median (IQR) survival time of 182 d (229). There was no significant difference in patient survival (P = 0.900) (Table 2, Figure 4).

DISCUSSION

Although endoscopic placement of SEMS is considered the recommended treatment for palliative drainage of unresectable distal MBO[13,14], PSs were used more frequently than SEMSs in our center. The factors for our preference for PSs in patients with unresectable distal MBO are as follows: First, tumor ingrowth via metal mesh may result in the uncovered SEMSs being embedded into the bile duct wall, making them impossible to remove even if stent dysfunction occurs[6,7]. Second, covered SEMSs are prone to migration, leading to stent dysfunction[6-8]. Third, Sawas *et al*[15] observed that the incidence of ascending cholangitis was similar between patients with distal MBO who received TPSs and SEMSs. However, SEMSs have a larger lumen than TPSs, and duodenobiliary reflux and cholangitis are more likely to occur in patients treated with SEMSs[16]. Finally, the most important point is the higher costs of SEMSs due to health insurance problems in China. Thus, many patients choose TPSs, and many endoscopists also tend to insert TPSs in such patients, especially those with a life expectancy of shorter than 6 months[1]. The major problem with TPSs is the relatively short duration of stent patency; therefore, prolonging stent patency was the focus of the current study.

The exact mechanisms of TPS occlusion remain largely unclear. Previous studies[17-19] have indicated that the initial TPS occlusion event is caused by biofilm formation by the adherence of proteins and bacteria to the inner wall of the stent. Then, β−glucuronidase and phospholipase that are secreted by bacteria act on biliary components. Bacterial products, calcium bilirubinate, and calcium fatty acid soaps precipitate, leading to biliary sludge formation and stent occlusion. Several studies[20-23] have compared PSs of different materials or special coatings that may prevent bacterial adherence and biofilm formation. However, a discrepancy in the results between the *in vitro* and clinical studies was noted[19]. Although hydrophilic-coated stents or sliver-coated stents prevented biofilm formation on the surface of the stent, this ability was not be maintained for a long time duration[20,22,23]. Therefore, there was no definite conclusion on the superiority of one material or special coating over another in terms of stent patency.

Prior studies[9,10] have also revealed that large plant fibers refluxed from the duodenum have been found in occluded TPSs. This provided further evidence that

Table 1 Baseline patient characteristics and clinical information of the antireflux plastic stent group and traditional plastic stent group

	ARPS group (*n* = 19)	TPS group (*n* = 18)	*P*-value
Age, mean (SD), years	70.3 (13.1)	73.8 (14.6)	0.452[a]
Sex, male/female, *n*	12/7	14/4	0.476[b]
Diagnosis, *n* (%)			
Pancreatic cancer	9 (47.4)	6 (33.3)	0.753[b]
Cholangiocarcinoma	7 (36.8)	9 (50)	
Ampullary cancer	3 (15.8)	3 (16.7)	
Distant metastasis, *n* (%)	9 (47.4)	7 (38.9)	0.743[b]
Comorbidity, *n* (%)[d]	12 (63.2)	14 (77.8)	0.476[b]
Adjuvant therapy, *n* (%)	6 (31.6)	7 (38.9)	
Chemotherapy	3 (50.0)	2 (28.6)	0.790[b]
Radiotherapy	1 (16.7)	3 (42.9)	
Radiochemotherapy	2 (33.3)	2 (28.6)	
Initial laboratory results			
Total bilirubin, median (IQR), μmol/L	234.6 (284.4)	206.7 (215.9)	0.761[c]
Direct bilirubin, median (IQR), μmol/L	210.2 (232.6)	191.30 (192.1)	0.671[c]
Length of stricture, median (IQR), cm	3 (2)	3 (2)	0.975[c]
Length of stent, median (IQR), cm	7 (2)	7 (3)	0.585[c]
Sphincterotomy, yes, *n* (%)	10 (52.6)	5 (27.8)	0.184[b]
Lost to follow-up, *n* (%)	0	1 (5.6)	1.000[b]

[a]Student's *t*-test;
[b]Fisher's exact test;
[c]Mann-Whitney *U*-test;
[d]Hypertension, coronary artery disease, diabetes mellitus, chronic obstructive pulmonary disease, liver cirrhosis, rheumatoid arthritis, and other neoplastic diseases. ARPS: Antireflux plastic stent; TPS: Traditional plastic stent; SD: Standard deviation; IQR: Interquartile range.

duodenobiliary reflux may play another important role in stent occlusion. To our knowledge, only three studies[1,11,12] in the published English literature have focused on changing the design of PSs to eliminate retrograde flow from the duodenum, prolonging the duration of stent patency. Dua *et al*[11] in 2007 initially reported an ARPS with a 4 cm windsock-shaped tubular valve made of expanded polytetrafluoroethylene material attached to the duodenal end. Their results showed that the median stent patency was prolonged from 101 d to 145 d when using this specialized stent. However, the clinical relevance of an increase in median stent patency of 44 d could be questioned[24]. Vihervaara *et al*[12] also conducted a clinical study using the same ARPS; however, their study was prematurely terminated owing to early stent occlusion in the ARPS group. An unplanned interim analysis was performed and showed that the median stent patency in the ARPS group was 34 d, which was significantly shorter than that in the TPS group (167 d). Thus, they suggested that this ARPS should not be used in clinical practice. In a study by Leong *et al*[1], an ARPS with a collapsible antireflux sleeve made of polytetrafluoroethylene was analyzed; however, a trend of early ARPS malfunction or failure was noted. All their ARPSs were occluded within 30 d, which may be attributed to the collapse or fold of the antireflux valve.

To date, there is no ideal design for an ARPS. In this study, we developed a new ARPS with a "duckbilled" valve. We presumed that this valve could simulate the opening and closing function of a duck's bill. When bile drainage does not impair the antegrade flow, the valve closes as the intestinal pressure increases, thereby preventing the reflux of the duodenal contents. This hypothesis was preliminarily confirmed by our study comparing stent patency between the ARPS group and the TPS group. In patients with stent dysfunction, the median stent patency in the ARPS group was 64 d longer than that in the TPS group. Although the difference was not statistically significant due to the limited sample size, the difference was impressive. In all patients enrolled in this study, the median patency of this new ARPS was 285 d, which was significantly longer than 130 d observed for the TPS. Moreover, the median patency was also better than previously reported median ARPS patency times[1,11,12]. There were no side holes in either ARPS or TPS; this avoided the

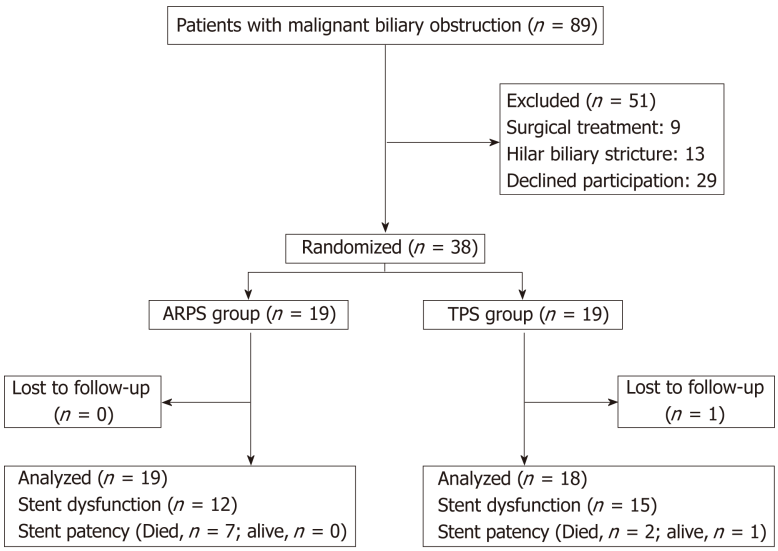

Figure 2 Flowchart of patients involved in the trial. ARPS: Antireflux plastic stent; TPS: Traditional plastic stent.

possibility of duodenal contents entering the bile duct to bypass the valve. Malignant ingrowth rarely played a role in PS occlusion[10] and sludge was noted in occluded ARPSs; thus, in this study, ARPS dysfunction may have been due to sludge occlusion, but the exact causes were not clear. Further studies are needed to address the mechanisms of occlusion.

In the present study, a similar delivery system was used to deploy ARPSs or TPSs. Although ARPSs had a valve, there was no additional difficulty in placing such a stent. All patients presented technical success with a single placement attempt. After ARPS placement, bile flowed easily through the valve. No significant difference was noted in clinical success between the two groups, suggesting that the ARPS had good efficacy for palliation of jaundice caused by extrahepatic MBO. Some studies[11,16] have reported that duodenal contents may enter the bile duct from the side of the stent in patients with sphincterotomy; thus, no routine sphincterotomy was performed in these studies. In our experience, the placement of a 10 Fr stent in some patients without sphincterotomy is technically challenging; therefore, in this study, the endoscopist determined if sphincterotomy was necessary. No significant difference was noted between the two groups.

There were several limitations to our study. The main limitation was the small sample size. The calculation of sample size was based on a previous study. Although the sample size was small, the patency of ARPS was significantly longer than that of TPS. Another limitation was that microscopic examination of dysfunctional stents was not performed, and the exact causes of ARPS dysfunction were unclear. In addition, many cases were censored due to patient death without stent dysfunction, or patient survival with stent patency until the day of last follow-up. The accurate duration of stent patency might be underestimated. Although this new stent showed good and promising results in this study, further studies with larger samples are required to evaluate its safety and efficacy.

In conclusion, this new ARPS is safe and effective for the palliation of unresectable distal MBO, and has the potential advantage of prolonging stent patency markedly. Additional multicenter studies involving larger samples are needed to confirm and strengthen our results.

Table 2 Outcomes of the antireflux plastic stent group and the traditional plastic stent group

	ARPS group(*n* = 19)	TPS group(*n* = 18)	*P*-value
Technical success, *n* (%)	19 (100)	18 (100)	-
Clinical success, *n* (%)	17 (89.5)	15 (83.3)	0.660[a]
Early adverse events, *n* (%)	2 (10.5)	2 (11.1)	
Cholangitis	1	1	1.000[a]
Mild pancreatitis	1	1	
Late adverse event, *n* (%)			
Mild pancreatitis	1 (5.3)	0	1.000[a]
Stent dysfunction, *n* (%)	12 (63.2)	15 (83.3)	0.269[a]
Stent patency, median (IQR), d	285 (170)	130 (90)	0.005[b]
Mortality, *n* (%)	17 (89.5)	16 (88.9)	0.677[a]
Patient survival, median (IQR), d	195 (297)	182 (229)	0.900[b]

[a]Fisher exact test;
[b]Log-rank test. ARPS: Antireflux plastic stent; TPS: Traditional plastic stent; IQR: Interquartile range.

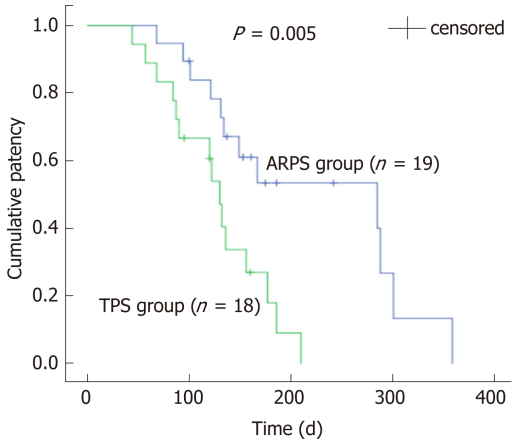

Figure 3 Kaplan-Meier curve comparing the cumulative patency of stent between the antireflux plastic stent group and the traditional plastic stent group (*P* = 0.005, log-rank test). ARPS: Antireflux plastic stent; TPS: Traditional plastic stent.

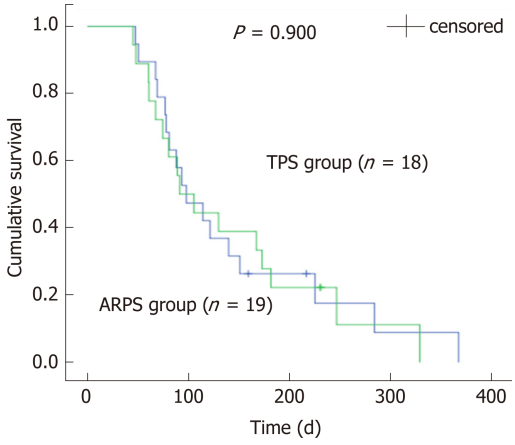

Figure 4 Kaplan-Meier curve comparing the cumulative survival of patients between the antireflux plastic stent group and the traditional plastic stent group (*P* = 0.900, log-rank test). ARPS: Antireflux plastic stent; TPS: Traditional plastic stent.

ARTICLE HIGHLIGHTS

Research background

Endoscopic biliary stenting has become an established palliative treatment for patients with unresectable malignant biliary obstruction (MBO). However, stent occlusion is considered to be the most frequent delayed adverse event of stent placement. Since duodenobiliary reflux is discussed to be a major risk factor of stent occlusion, in recent years, the design of plastic stents with an anti-reflux valve has been an attractive idea for prolonging stent patency, unfortunately without convincing results and therefore limiting their use in clinical practice.

Research motivation

To reduce duodenobiliary reflux and thereby prolonging stent patency, we developed a new antireflux plastic stent (ARPS) with a "duckbilled" valve attached to the duodenal end of the stent. We presumed that this valve could simulate the opening and closing function of the duck's bill. This geometry allows unimpaired antegrade bile flow into the duodenum, while it closes instantly when the intestinal pressure increases, thereby preventing the reflux of duodenal contents.

Research objectives

In this study, we compared the patency of ARPSs with that of traditional plastic stents (TPSs) in patients with unresectable distal MBO. The results of the study will guide the treatment of unresectable distal MBO in the future.

Research methods

From February 2016 to December 2017, consecutive patients with extrahepatic MBO were recruited in our randomized clinical trial. Eligible patients were assigned to receive either an ARPS or a TPS in a randomized manner. Patients were followed by clinic visits or telephone interviews every 1-2 mo until stent exchange, death, or the final study follow-up in October 2018. The duration of stent patency, the rates of technical and clinical success, adverse events, and patient survival were documented. All data were analyzed statistically to evaluate the efficacy and safety of this new ARPS.

Research results

During the study period, 89 patients were screened for eligibility. Of these, 51 patients were excluded; thus, 38 patients were randomized to receive ARPSs or TPSs (19 per group). Stent insertion was technically successful in all patients. No significant differences were noted in the rates of clinical success, the rates of early or late adverse events, or patient survival. There was a significant difference when comparing the duration of stent patency, which was significantly longer in the ARPS group than in the TPS group.

Research conclusions

This new ARPS is safe and effective for the palliation of unresectable distal MBO, and has a significantly longer stent patency compared with TPS. This ARPS may be an alternative option for the treatment of unresectable distal MBO.

Research perspectives

Multiple center studies with larger samples are expected in the future to confirm and strengthen our results.

ACKNOWLEDGEMENTS

The abstract of this article has been accepted for a lecture presentation at Digestive Disease Week®, held in San Diego, California, USA, May 18-21, 2019.

REFERENCES

1 **Leong QW**, Shen ML, Au KW, Luo D, Lau JY, Wu JC, Chan FK, Sung JJ. A prospective, randomized study of the patency period of the plastic antireflux biliary stent: An interim analysis. *Gastrointest Endosc* 2016; **83**: 387-393 [PMID: 26024583 DOI: 10.1016/j.gie.2015.04.027]

2 **Andersen JR**, Sørensen SM, Kruse A, Rokkjaer M, Matzen P. Randomised trial of endoscopic endoprosthesis versus operative bypass in malignant obstructive jaundice. *Gut* 1989; **30**: 1132-1135 [PMID: 2475392 DOI: 10.1136/gut.30.8.1132]

3 **Smith AC**, Dowsett JF, Russell RC, Hatfield AR, Cotton PB. Randomised trial of endoscopic stenting versus surgical bypass in malignant low bileduct obstruction. *Lancet* 1994; **344**: 1655-1660 [PMID: 7996958 DOI: 10.1016/S0140-6736(94)90455-3]

4 **Tringali A**, Mutignani M, Perri V, Zuccalà G, Cipolletta L, Bianco MA, Rotondano G, Philipper M, Schumacher B, Neuhaus H, Schmit A, Devière J, Costamagna G. A prospective, randomized multicenter trial comparing DoubleLayer and polyethylene stents for malignant distal common bile duct strictures. *Endoscopy* 2003; **35**: 992-997 [PMID: 14648409 DOI: 10.1055/s-2003-44601]

5 **Kaassis M**, Boyer J, Dumas R, Ponchon T, Coumaros D, Delcenserie R, Canard JM, Fritsch J, Rey JF, Burtin P. Plastic or metal stents for malignant stricture of the common bile duct? Results of a randomized prospective study. *Gastrointest Endosc* 2003; **57**: 178-182 [PMID: 12556780 DOI: 10.1067/mge.2003.66]

6 **Saleem A**, Leggett CL, Murad MH, Baron TH. Meta-analysis of randomized trials comparing the patency of covered and uncovered self-expandable metal stents for palliation of distal malignant bile duct obstruction. *Gastrointest Endosc* 2011; **74**: 321-327.e1-3 [PMID: 21683354 DOI:

10.1016/j.gie.2011.03.1249]
7 **Chen MY**, Lin JW, Zhu HP, Zhang B, Jiang GY, Yan PJ, Cai XJ. Covered Stents versus Uncovered Stents for Unresectable Malignant Biliary Strictures: A Meta-Analysis. *Biomed Res Int* 2016; **2016**: 6408067 [PMID: 27051667 DOI: 10.1155/2016/6408067]
8 **Jang S**, Stevens T, Parsi M, Lopez R, Zuccaro G, Dumot J, Vargo JJ. Association of covered metallic stents with cholecystitis and stent migration in malignant biliary stricture. *Gastrointest Endosc* 2018; **87**: 1061-1070 [PMID: 28867074 DOI: 10.1016/j.gie.2017.08.024]
9 **van Berkel AM**, van Marle J, Groen AK, Bruno MJ. Mechanisms of biliary stent clogging: Confocal laser scanning and scanning electron microscopy. *Endoscopy* 2005; **37**: 729-734 [PMID: 16032491 DOI: 10.1055/s-2005-870131]
10 **Weickert U**, Venzke T, König J, Janssen J, Remberger K, Greiner L. Why do bilioduodenal plastic stents become occluded? A clinical and pathological investigation on 100 consecutive patients. *Endoscopy* 2001; **33**: 786-790 [PMID: 11558033 DOI: 10.1055/s-2001-16519]
11 **Dua KS**, Reddy ND, Rao VG, Banerjee R, Medda B, Lang I. Impact of reducing duodenobiliary reflux on biliary stent patency: An in vitro evaluation and a prospective randomized clinical trial that used a biliary stent with an antireflux valve. *Gastrointest Endosc* 2007; **65**: 819-828 [PMID: 17383650 DOI: 10.1016/j.gie.2006.09.011]
12 **Vihervaara H**, Grönroos JM, Hurme S, Gullichsen R, Salminen P. Antireflux Versus Conventional Plastic Stent in Malignant Biliary Obstruction: A Prospective Randomized Study. *J Laparoendosc Adv Surg Tech A* 2017; **27**: 53-57 [PMID: 27754790 DOI: 10.1089/lap.2016.0178]
13 **Dumonceau JM**, Tringali A, Blero D, Devière J, Laugiers R, Heresbach D, Costamagna G; European Society of Gastrointestinal Endoscopy. Biliary stenting: Indications, choice of stents and results: European Society of Gastrointestinal Endoscopy (ESGE) clinical guideline. *Endoscopy* 2012; **44**: 277-298 [PMID: 22297801 DOI: 10.1055/s-0031-1291633]
14 **Dumonceau JM**, Tringali A, Papanikolaou IS, Blero D, Mangiavillano B, Schmidt A, Vanbiervliet G, Costamagna G, Devière J, García-Cano J, Gyökeres T, Hassan C, Prat F, Siersema PD, van Hooft JE. Endoscopic biliary stenting: Indications, choice of stents, and results: European Society of Gastrointestinal Endoscopy (ESGE) Clinical Guideline - Updated October 2017. *Endoscopy* 2018; **50**: 910-930 [PMID: 30086596 DOI: 10.1055/a-0659-9864]
15 **Sawas T**, Al Halabi S, Parsi MA, Vargo JJ. Self-expandable metal stents versus plastic stents for malignant biliary obstruction: A meta-analysis. *Gastrointest Endosc* 2015; **82**: 256-267.e7 [PMID: 25982849 DOI: 10.1016/j.gie.2015.03.1980]
16 **Hu B**, Wang TT, Wu J, Shi ZM, Gao DJ, Pan YM. Antireflux stents to reduce the risk of cholangitis in patients with malignant biliary strictures: A randomized trial. *Endoscopy* 2014; **46**: 120-126 [PMID: 24477367 DOI: 10.1055/s-0034-1364872]
17 **Leung JW**, Ling TK, Kung JL, Vallance-Owen J. The role of bacteria in the blockage of biliary stents. *Gastrointest Endosc* 1988; **34**: 19-22 [PMID: 3280393 DOI: 10.1016/S0016-5107(88)71223-7]
18 **Coene PP**, Groen AK, Cheng J, Out MM, Tytgat GN, Huibregtse K. Clogging of biliary endoprostheses: A new perspective. *Gut* 1990; **31**: 913-917 [PMID: 2387517 DOI: 10.1136/gut.31.8.913]
19 **Kwon CI**, Gromski MA, Sherman S, Easler JJ, El Hajj II, Watkins J, Fogel EL, McHenry L, Lehman GA. Time Sequence Evaluation of Biliary Stent Occlusion by Dissection Analysis of Retrieved Stents. *Dig Dis Sci* 2016; **61**: 2426-2435 [PMID: 27154511 DOI: 10.1007/s10620-016-4135-0]
20 **van Berkel AM**, Bruno MJ, Bergman JJ, van Deventer SJ, Tytgat GN, Huibregtse K. A prospective randomized study of hydrophilic polymer-coated polyurethane versus polyethylene stents in distal malignant biliary obstruction. *Endoscopy* 2003; **35**: 478-482 [PMID: 12783344 DOI: 10.1055/s-2003-39666]
21 **Costamagna G**, Mutignani M, Rotondano G, Cipolletta L, Ghezzo L, Foco A, Zambelli A. Hydrophilic hydromer-coated polyurethane stents versus uncoated stents in malignant biliary obstruction: A randomized trial. *Gastrointest Endosc* 2000; **51**: 8-11 [PMID: 10625787 DOI: 10.1016/S0016-5107(00)70378-6]
22 **Yamabe A**, Irisawa A, Wada I, Shibukawa G, Fujisawa M, Sato A, Igarashi R, Maki T, Hoshi K. Application of a silver coating on plastic biliary stents to prevent biofilm formation: An experimental study using electron microscopy. *Endosc Int Open* 2016; **4**: E1090-E1095 [PMID: 27747284 DOI: 10.1055/s-0042-115173]
23 **Jansen B**, Goodman LP, Ruiten D. Bacterial adherence to hydrophilic polymer-coated polyurethane stents. *Gastrointest Endosc* 1993; **39**: 670-673 [PMID: 8224690 DOI: 10.1016/S0016-5107(93)70220-5]
24 **Kahaleh M**. Antireflux biliary stents: Is it time to go with the flow? *Gastrointest Endosc* 2007; **65**: 829-831 [PMID: 17466201 DOI: 10.1016/j.gie.2006.10.025]

World Journal of Gastroenterology

Submit a Manuscript: https://www.f6publishing.com

World J Gastroenterol 2019 May 21; 25(19): 2383-2401

DOI: 10.3748/wjg.v25.i19.2383

ISSN 1007-9327 (print) ISSN 2219-2840 (online)

META-ANALYSIS

High-risk symptoms and quantitative faecal immunochemical test accuracy: Systematic review and meta-analysis

Noel Pin Vieito, Sara Zarraquiños, Joaquín Cubiella

ORCID number: Noel Pin Vieito (0000-0003-0526-4104); Sara Zarraquiños (0000-0002-8222-618X); J. Cubiella (0000-0002-9994-4831).

Author contributions: Pin Vieito N and Cubiella J conception and design of the study; Pin Vieito N, Zarraquiños S, and Cubiella J acquisition of data, analysis and interpretation of data, and final approval; Pin Vieito N and Cubiella J drafted the article; Cubiella J contributed to critical revision.

Conflict-of-interest statement: Dr. Pin reports non-financial support from ABBVIE, non-financial support from GILEAD SCIENCES, outside the submitted work; Dr. Zarraquiños reports non-financial support from CASEN RECORDATI, non-financial support from MYLAN, non-financial support from ALLERGAN, non-financial support from OLYMPUS, non-financial support from ABBVIE, outside the submitted work; Dr. Cubiella reports grants from Instituto de Investigación Sanitaria Galicia Sur, grants from Fondo de Investigaciones Sanitarias (FIS), during the conduct of the study; personal fees from NORGINE, personal fees from IMC, outside the submitted work;

PRISMA 2009 Checklist statement: The authors have read the PRISMA 2009 Checklist, and the manuscript was prepared and revised according to the PRISMA 2009 Checklist.

Noel Pin Vieito, Sara Zarraquiños, Joaquín Cubiella, Department of Gastroenterology, Complexo Hospitalario Universitario de Ourense, Ourense 32005, Spain

Noel Pin Vieito, Sara Zarraquiños, Joaquín Cubiella, Instituto de Investigación Sanitaria Galicia Sur, Ourense 32005, Spain

Noel Pin Vieito, Department of Biochemistry, Genetics and Immunology, Faculty of Biology University of Vigo, Vigo 36310, Pontevedra, Spain

Corresponding author: Noel Pin Vieito, MD, Staff Physician, Statistician, Department of Gastroenterology, Complexo Hospitalario Universitario de Ourense, C/ Ramón Puga 52-54, Ourense 32005, Spain. noel.pin.vieito@sergas.es
Telephone: +34-988385399
Fax: +34-988385399

Abstract

BACKGROUND

The quantitative faecal immunochemical test for haemoglobin (FIT) has been revealed to be highly accurate for colorectal cancer (CRC) detection not only in a screening setting, but also in the assessment of patients presenting lower bowel symptoms. Therefore, the National Institute for Health and Care Excellence has recommended the adoption of FIT in primary care to guide referral for suspected CRC in low-risk symptomatic patients using a 10 μg Hb/g faeces threshold. Nevertheless, it is unknown whether FIT´s accuracy remains stable throughout the broad spectrum of possible symptoms.

AIM

To perform a systematic review and meta-analysis to assess FIT accuracy for CRC detection in different clinical settings.

METHODS

A systematic literature search was performed using MEDLINE and EMBASE databases from inception to May 2018 to conduct a meta-analysis of prospective studies including symptomatic patients that evaluated the diagnostic accuracy of quantitative FIT for CRC detection. Studies were classified on the basis of brand, threshold of faecal haemoglobin concentration for a positive test result, percentage of reported symptoms (solely symptomatic, mixed cohorts) and CRC prevalence (< 2.5%, ≥ 2.5%) to limit heterogeneity and perform subgroup analysis to assess the influence of clinical spectrum on FIT´s accuracy to detect CRC.

RESULTS

Manuscript source: Invited manuscript

Received: February 3, 2019
Peer-review started: February 6, 2019
First decision: March 5, 2019
Revised: March 20, 2019
Accepted: March 29, 2019
Article in press: March 30, 2019
Published online: May 21, 2019

P-Reviewer: Biondi A, Lieto E P
S-Editor: Yan JP
L-Editor: A
E-Editor: Ma YJ

Fifteen cohorts including 13073 patients (CRC prevalence 0.4% to 16.8%) were identified. Pooled estimates of sensitivity for studies using OC-Sensor at 10 μg Hb/g faeces threshold (n = 10400) was 89.6% [95% confidence interval (CI): 82.7% to 94.0%). However, pooled estimates of sensitivity for studies formed solely by symptomatic patients (n = 4035) and mixed cohorts (n = 6365) were 94.1% (95%CI: 90.0% to 96.6%) and 85.5% (95%CI: 76.5% to 91.4%) respectively (P < 0.01), while there were no statistically significant differences between pooled sensitivity of studies with CRC prevalence < 2.5% (84.9%, 95%CI: 73.4% to 92.0%) and ≥ 2.5% (91.7%, 95%CI: 83.3% to 96.1%) (P = 0.25). At the same threshold, OC-Sensor® sensitivity to rule out any significant colonic lesion was 78.6% (95%CI: 75.6% to 81.4%). We found substantial heterogeneity especially when assessing specificity.

CONCLUSION
The results of this meta-analysis confirm that, regardless of CRC prevalence, quantitative FIT is highly sensitive for CRC detection. However, FIT ability to rule out CRC is higher in studies solely including symptomatic patients.

Key words: Bowel disease; Colorectal cancer; Diagnostic accuracy; Faecal haemoglobin; Faecal immunochemical test; Faecal occult blood test; Inflammatory bowel disease; Significant colonic lesion

Core tip: The quantitative faecal immunochemical test for haemoglobin (FIT) has been recommended to guide referral for suspected colorectal cancer (CRC) in people with unexplained symptoms without rectal bleeding. However, the information regarding its accuracy in different settings is scarce. Our meta-analysis reveals that sensitivity for CRC may change across populations with differences in clinical symptoms, irrespective of CRC prevalence. On the other hand, we should not use this to rule out CRC if its prevalence is high. In addition, FIT is not sensitive enough to exclude other significant colonic diseases.

Citation: Pin Vieito N, Zarraquiños S, Cubiella J. High-risk symptoms and quantitative faecal immunochemical test accuracy: Systematic review and meta-analysis. *World J Gastroenterol* 2019; 25(19): 2383-2401
URL: https://www.wjgnet.com/1007-9327/full/v25/i19/2383.htm
DOI: https://dx.doi.org/10.3748/wjg.v25.i19.2383

INTRODUCTION

The quantitative faecal immunochemical test for haemoglobin (hereinafter referred to as 'FIT') has been revealed to be highly accurate for colorectal cancer (CRC) detection not only in a screening setting, but also in the assessment of patients presenting lower bowel symptoms[1,2]. Therefore, the National Institute for Health and Care Excellence (NICE) has recently recommended adoption of FIT in primary care to guide referral for suspected CRC in people without rectal bleeding who have unexplained symptoms but do not meet the criteria for a suspected cancer pathway referral. Results should be reported using a threshold of 10 micrograms of haemoglobin per gram of faeces (μg Hb/g faeces)[3,4].

However, a clinical concern has been highlighted on transference of research results to clinical practice[5]. The NICE recommendation applies only to patients who present low-risk symptoms. In contrast, most available studies include patients who had symptoms (*e.g.*, rectal bleeding) associated with higher probability of CRC and most were performed in a secondary care setting. Although other population variables could be involved, this difference in the clinical spectrum could account for the high CRC prevalence shown in the meta-analysis used to support this recommendation (range 2.15% to 5.4%), compared to the estimated 1.5% for the relevant symptomatic group used in NICE guidance 'NG12'[3].

Thus, since the prevalence of the target condition may affect estimates of test performance by means of mechanisms other than patient spectrum[6], there is

insufficient information to elucidate whether the presence of high-risk symptoms or another clinical difference involving a higher CRC prevalence in the studies that fitted this meta-analysis inclusion criteria, will affect the expected performance of FIT in primary care. With the aim of assessing the stability of FIT´s accuracy across the broad spectrum of situations we could face outside a screening setting, we decided to perform an additional systematic review expanding upon previous inclusion criteria.

MATERIALS AND METHODS

We designed a systematic review and meta-analysis following the Preferred Reporting Items for Systematic Reviews and Meta-Analyses (PRISMA) statement to conduct and report our systematic review[7].

Data sources and searches

We included all studies identified by a sensitive search of "FIT for CRC" in MEDLINE (*via* PubMed) and EMBASE (*via* Ovid) databases from inception to 21 May 2018. Data sources were also extended to the reference lists of all articles extracted from the search strategy detailed in Appendix 1.

Study selection

Two authors (NP and SZ) independently reviewed and screened titles and abstracts of articles retrieved and determined final eligibility by means of examination of full texts. Any disagreement was resolved through discussion or by consulting a third author (JC). We regarded studies as suitable for our review if they m*et al*l the following inclusion criteria:

Population, setting and study design

We included all prospective cohort studies performed on adult patients out of CRC screening programme setting either including patients: (1) Consulting with a physician for non-acute lower abdominal symptoms; or (2) consecutively scheduled for elective colonoscopy, when at least a fraction of symptomatic patients was included. No language restriction was applied.

Index test

Studies that evaluated the diagnostic accuracy of the quantitative FIT for CRC detection either reporting absolute numbers of true-positive, false-negative, true-negative, and false-positive observations, or data from which sensitivity and specificity could be extrapolated. In the case of studies reporting more than one FIT specimen, we only included the results of the first determination.

Reference test

We included studies that reported an appropriate reference standard (colonoscopy or ≥ 2-year longitudinal follow-up of the controls).

Endpoints

Our main objective was to estimate the diagnostic accuracy of FIT for CRC detection. Secondary goals included assessing the usefulness of FIT to detect advanced neoplasia (AN) and significant colonic lesions (SCLs) in symptomatic patients. The definitions of AN and SCL differ from country to country, which should be considered when interpreting data. This issue will be subsequently outlined in detail for each study.

Data extraction and risk of bias

One reviewer (NP) extracted data and extractions were checked by a second reviewer (JC); any disagreements were resolved by means of discussion and consensus. In each study, potential risks of bias were calculated using the Quality Assessment of Diagnostic Accuracy Studies 2 tool (QUADAS-2)[8]. An inverted funnel or "Christmas tree" scatterplot was used to detect publication bias.

Data synthesis and statistical analysis

We classified studies on the basis of brand and threshold of faecal haemoglobin (f-Hb) concentration for a positive test result to limit heterogeneity. When four or more studies on a specific subgroup were available, bivariate analyses were applied to calculate pooled estimates of sensitivity, specificity and likelihood ratios using the statistical software package STATA (v14)[9,10]. A hierarchical summary receiver operating characteristic (HSROC) curve was generated to present the summary estimates of sensitivities and specificities along with their corresponding 95% confidence interval (CI) and prediction region. An area under the HSROC curve

(AUC) between 0.9 and 1.0 indicated that diagnostic accuracy was good[11].

When a bivariate random-effects approach was not possible due to limited number of studies, we applied a random effects model following DerSimonian's method using MetaDisc software[12]. In that case a summary receiver operating characteristics (sROC) curve was plotted using DerSimonian and Lair's model to present summary sensitivity and specificity estimates through the AUC or Q* index[13-15].

Subgroup analysis

To determine whether FIT´s accuracy to detect CRC out of screening setting was influenced by high-risk symptoms, studies were classified by percentage of reported symptoms and CRC prevalence. Cohorts formed solely by patients who consult for abdominal symptoms represent a population with a better chance of high-risk symptoms of CRC (*e.g.*, rectal bleeding). Prespecified CRC prevalence values (< 2.5% and ≥ 2.5%) were used to ensure an adequate number of data sets for each analysis. A bivariate model was fitted for each subgroup; direct comparison between them was performed using STATA (xtmelogit command)[16].

Threshold effect and other sources of heterogeneity

Threshold effect was examined by calculating Spearman's rank correlation ($P < 0.1$ was considered to be statistically significant), and ROC space plots were used to represent the sensitivity against 1-specificity of each study. In addition to the visual inspection of the forest plots of accuracy estimates, statistical tests, including Chi-square and Cochran's *Q* tests, were used to ascertain whether inter-study differences were greater than expected based on chance alone ($P < 0.1$ suggested heterogeneity); the inconsistency index (*I2*) was used as a measure to quantify the degree of heterogeneity. The statistical methods of this study were reviewed by Noel Pin Vieito from Complexo Hospitalario Universitario de Ourense.

RESULTS

Literature search and study characteristics

Our initial literature search yielded a total of 12657 references. After abstract review, we identified 342 complete papers retrieved for manual searching, yielding 5919 additional potential sources of information; of these, 81 articles were selected for full-text review and 14 studies were ultimately considered relevant for our purpose (Figure 1)[17-30]. Inter-rater reliability was moderate (kappa 0.58). Individual unpublished data from derivation[29] and validation[31] cohorts included in the COLONPREDICT study were also used as these patients fitted the inclusion criteria. In total, 15 cohorts (13073 patients) were selected for qualitative synthesis. Full details of these studies are shown in Tables 1 and 2, and Appendix 2.

Quality assessment

The QUADAS-2 instrument highlighted an important risk of bias in the patient selection domain (Figure 2). Some patients could have been enrolled in a non-consecutive manner[17], and another five studies also evaluated diseases or situations that could compete with CRC as a cause of a positive FIT as exclusion criteria[18,21,22,24,25]. The greatest applicability concern arose from the patient selection category, as none of the samples analysed was fully representative of patients with low risk gastrointestinal symptoms reported in NG12[3].

Diagnostic performance for colorectal cancer

Table 3 and Figure 3 present summary sensitivity and specificity estimates calculated with a random effects model following the approach of DerSimonian's method for each screening modality using OC-Sensor®. Figure 4 shows the sROC curves at different thresholds. The highest AUC was obtained at a 20 μg Hb/g faeces threshold (AUC = 0.93, 95%CI 0.90-0.96). Furthermore, studies using OC-Sensor® with various thresholds higher than 20 μg Hb/g faeces[17,18,23], and also studies using HM-JACK®[19,24], HM-JACKarc®[28] and FOB Gold®[30] have been published but their data could not be pooled due to the scarce number of studies in those thresholds. Individual data are shown in Table 4.

Heterogeneity assessment

We found substantial heterogeneity between studies when calculating the pooled sensitivity for almost every threshold analysed in the studies evaluating OC-Sensor® (Table 3). Spearman's rank correlation coefficient was higher than 0.1, suggesting an absence of threshold effect in all cases. The scarce number of studies limited our intent to determine the existence of publication bias using funnel plots. However, when

Table 1 Characteristics of the studies included in the meta-analysis

Test	Study, Year	Demographic characteristics				CRC	AN	SC-L	Exclusion criteria			Symptoms, %							
		N	Age (m/-md)	Sex (W%)	Area	%	%	%	IBD	OB	AD	AnS	WeL	AbPa	Hem	ChBo	Co	Di	An
Mixed cohorts																			
OC-S	Rozen, 2010[17]	1682	63.7	49.6	IL	1.2	8.9	0	yes	yes	yes	23	NA	NA	0	NA	NA	NA	NA
OC-S	Mc Donald, 2012[20]	280	63[1]	59.6	UK (S)	2.1	NA	21.4	NA	no	no	NA	NA	NA	NA	NA	NA	NA	NA
OC-S	Ou, 2013[21]	694	59.5[1]	55.9	CN	0.4	6.1	NA	yes	yes	no	NA	NA	NA	NA	NA	NA	NA	NA
OC-S	van Turenhout, 2014[18]	3022	59.7	55.0	NL	2.3	12.3	NA	yes	yes	no	44	2.9	11.7	0	18.1	3	4.2	0
OC-S	Symonds, 2016[23]	1381	64.1[1]	50.6	AU	4.8	17.2	NA	no	no	no	34.8	NA	NA	NA	NA	NA	NA	NA
HM-J	Woo, 2005[19]	85	56[1]	52.9	KR	7.1	NA	NA	NA	no	no	49.4	0	15.3	4.7	1.2	0	17.6	4.7
HM-Ja	Auge, 2016[22]	208	63[1]	55.8	ES	1.0	14.0	NA	yes	yes	yes	NA	NA	NA	0	NA	NA	NA	NA
FOB Gold®	Auge, 2018[30]	487	62	51.2	ES	2.5	14.6	NA	no	no	yes	54.2	NA	NA	NA	NA	NA	NA	NA
100% Symptomatic cohorts																			
OC-S	Mowat, 2016[26]	750	64[1]	54.7	UK (S)	3.7	NA	13.6	no	no	no	100	0.9	11	34.2	42.8	NA	16.8	8.9
OC-S	Rodriguez-Alonso, 2015[25]	1003	NA	46.8	ES	3.0	13.3	23.4	yes	no	no	100	19	36.4	34.2	NA	12.1	23.5	8.8
OC-S	Cubiella, 2014 (DC)[29]	1567	66.9	48.6	ES	13.7	26.7	29.5	no	no	no	100	24.5	43.8	59.9	57.2	14.5	22.2	34.8
OC-S	Cubiella, 2017 (VC)[31]	715	64.4	53.3	ES	9.4	21.1	25.3	no	no	no	100	NA	NA	54	47.9	NA	NA	NA
HM-J	Parente, 2012[24]	280	67	43.9	IT	16.8	47.2	0	yes	no	no	100	11.1	17.9	26.1	23.9	NA	NA	15
HM-Ja	Godber, 2016[27]	484	59[1]	60.1	UK (S)	2.3	NA	9.3	no	no	no	100	1.7	18.8	15.9	39.7	NA	NA	4.8
HM-Ja	Widlack, 2017[28]	430	67[1]	51.0	UK (E)	5.6	NA	NA	no	no	no	100	15.8	30	43	64.2	NA	NA	17.2

[1]Age is expressed as median; AbPa: Abdominal pain; AD: Antithrombotic discontinuity; An: Anaemia; AN: advanced neoplasia; AnS: Any symptom; AU: Australia; CN: China; Co: Constipation; CRC: Colorectal cancer; ChBo: Change in bowel habit; DC: Derivation cohort; Di: Diarrhoea; ES: Spain; HM-J: HM-JACK®; HM-Ja: HM-JACKarc®; Hem: Haematochezia; IBD: Inflammatory bowel disease; IL: Israel; IT: Italy; KR: South Korea; m: mean; md: median; NA: Non-available; NL: Netherlands; OC-S: OC-Sensor®; OB: Overt bleeding; SCL: Significant colonic lesion; UK (E): United Kingdom (England); UK (S): United Kingdom (Scotland); VC: Validation cohort; W%: Women%; WeL: Weight loss.

plotting each study's diagnostic odds ratio (dOR) in a logarithmic scale against its sample size, we did not identify any trends towards asymmetry around the axis traced by the pooled dOR value for any analysed threshold, which suggests the absence of this possibility (Figure 5).

Subgroup and bivariate analysis

Although the number of studies limited our ability to use bivariate and HSROC models for most subgroups, the number of available studies performed with the OC-Sensor® enabled us to perform a subgroup analysis based on CRC prevalence and percentage of symptoms at the 10 μg Hb/g faeces threshold (10400 patients). Pooled estimates of sensitivity for studies comprised solely by symptomatic patients (n = 4035) and mixed cohorts (n = 6365) were 94.1% (95%CI: 90.0% to 96.6%) and 85.5% (95%CI: 76.5% to 91.4%) respectively (P < 0.01), while there were no statistically significant differences between pooled sensitivity of studies with CRC prevalence < 2.5% (84.9%, 95%CI: 73.4% to 92.0%) and ≥ 2.5% (91.7%, 95%CI: 83.3% to 96.1%) (P = 0.25). FIT sensitivity was equal or higher than 90% for almost every situation analysed (Table 3 and Figure 6).

Conversely, pooled specificities were significantly different when comparing studies both by percentage of symptoms (solely symptomatic = 66.0%; 95%CI: 47.1% to 80.9% *vs* lesser percentage of reported symptoms = 89.3%; 95%CI: 84.1% to 93.0%, P = 0.01) as by CRC prevalence (CRC prevalence < 2.5% = 90.5%; 95%CI: 89.0% to 91.9% *vs* CRC prevalence ≥ 2.5% = 69.3%; 95%CI: 53.5% to 81.6%, P < 0.01).

A comparison between summary sensitivity and specificity estimates calculated with both methods is shown in Table 5 and generated HSROC curves in Figure 7. OC-Sensor® accuracy parameters (threshold 10 μgHb/g faeces) estimated by bivariate model from both '100% symptomatic' and ´mixed cohort´ subgroups, were used to calculate different post-test probabilities through Fagan nomograms on the basis of various CRC prevalence (Figures 8 and 9).

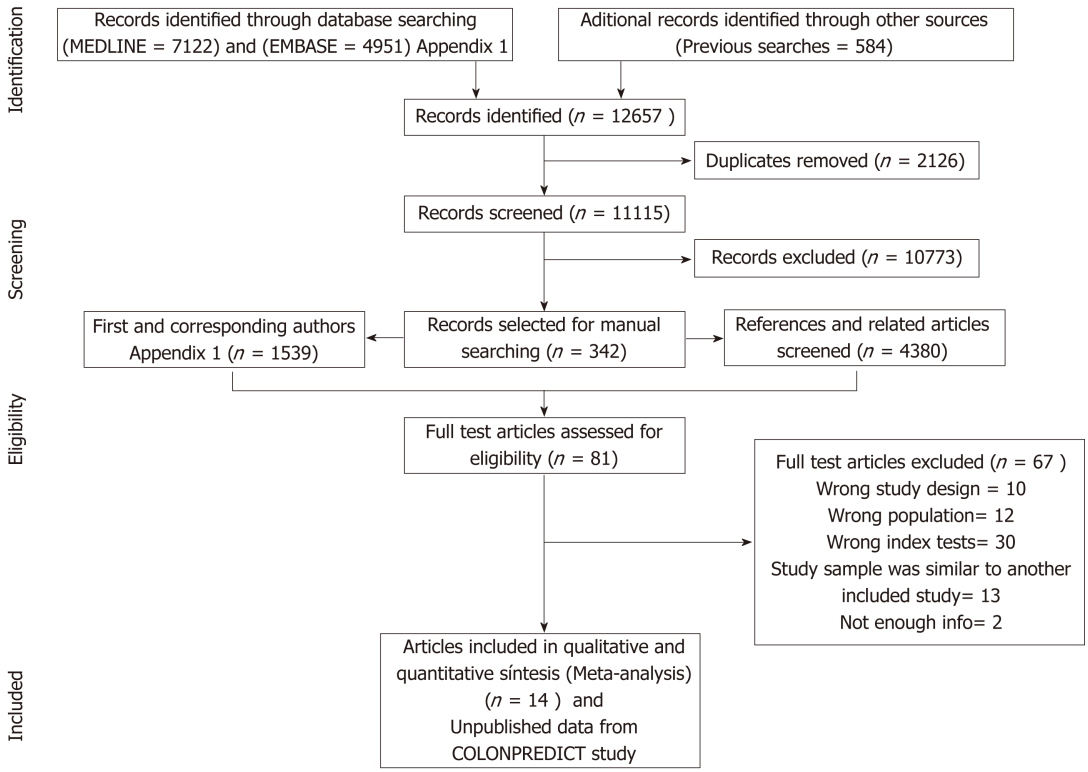

Figure 1 Summary of evidence search and selection.

Secondary endpoints: diagnostic performance for AN and SCL

Besides the COLONPREDICT study cohorts[29,31], nine[17,19-22,24-26,30] and four[20,26-28] studies provided information on the FIT's accuracy for AN and SCL detection, respectively, with heterogeneous definitions. Furthermore, Terhaar sive Droste *et al*[32] published data on FIT´s accuracy for AN detection in 2145 patients included in van Turenhout´s study[18]. AN was defined as CRC plus high-risk[19-21,26]*vs* advanced[17,22,24,25,30-32] adenoma. This variability was greater for the definition of SCL. Some studies defined SCL as cancer plus high-risk adenoma plus inflammatory bowel disease[20,26], whereas Godber *et al*[27] expanded that definition to include other types of colitis. A broader definition was used by Cubiella *et al*[29,31] including CRC, advanced adenoma, polyposis, colitis, polyps ≥ 10 mm, complicated diverticular disease, colonic ulcer and bleeding angiodysplasia. Auge *et al*[30] provided data about FOB Gold® accuracy for colonic lesion detection regardless of its importance. Finally, as long as Widlack *et al*[28] added a single case of high-grade dysplasia to 24 cases of CRC, we decided to include their study within the CRC group.

Summary sensitivity and specificity estimates for AN and SCL detection are shown in Table 6. Once again, studies evaluating OC-Sensor® with different thresholds[17,21,29,31,32], HM-JACK®[24], HM-JACKarc®[22,27] or FOB Gold®[30] have been published but their number was insufficient to enable pooling of data in homogeneous groups. Individual data are shown in Tables 7 and 8.

DISCUSSION

Statement of principal findings

This meta-analysis confirms that FIT is useful for triaging referrals in people with lower abdominal symptoms. Most studies have been performed using OC-Sensor® assay; using this brand, the high pooled estimates of sensitivity for CRC shown at f-Hb thresholds from limit of detection (LoD) to 20 μg Hb/g faeces, demonstrates this brand's ability to stratify which symptomatic patients are more likely to have CRC.

Furthermore, the optimal OC-Sensor® performance (maximising both sensitivity and specificity) appeared to occur with f-Hb thresholds between 10 and 20 μg Hb/g faeces as FIT specificity is too low at a LoD f-Hb threshold. Since fewer cases of CRC will be missed with the former, 10 μg Hb/g faeces may be the most suitable threshold for CRC assessment of patients with symptoms (sROC AUC 0.92). In fact, subgroup analysis at this threshold demonstrates that regardless of CRC prevalence, summary

Table 2 Possibility of data extraction on the accuracy of quantitative faecal immunochemical test for haemoglobin for detecting colorectal cancer, advanced neoplasia and significant colonic lesion

Study	CRC							AN						SCL						
	Threshold (U)					SxD	SD	Threshold (U)					SxD	Threshold (U)					SxD
	0	10	15	20	Other			0	10	15	20	Other		0	10	15	20	Other	
Rozen, 2010[17]		x	x	x	25; 30; 40				x	x	x	25; 30; 40							
Van Turenhout, 2014[18]		x	x	x	40	x													
Mc Donald, 2012[20]		x							HRA						x				
Ou, 2013[21]					5							5; HRA							
Symonds, 2016[23]		x			60; 80		x												
Auge, 2016[22]								x	x		x	30; 40	x						
Woo, 2005[19]					33							3; HRA							
Auge, 2018[30]		x		x	30; 40; 50; 60		x		x		x	30; 40; 50; 60			x		x	30; 40; 50; 60	
Cubiella, 2014 (DC)[29]	x	x	x	x		x		x	x	x	x		x	x	x	x	x		x
Cubiella, 2016 (VC)[31]	x	x	x	x		x		x	x	x	x		x	x	x	x	x		x
Rodríguez-Alonso 2015[25]	x	x	x	x				x	x	x	x								
Mowat, 2016[26]	x	x						HRA	HRA					x	x				
Parente, 2012[24]				x							x								
Godber, 2016[27]															x	x	x	25; 30; 35; 40	
Widlack, 2017[28]																		7; HGD	

AN: Advanced neoplasia; CRC: Colorectal cancer; DC: Derivation cohort; HDG: High-grade dysplasia; HRA: High risk adenoma; SCL: Significant colonic lesion; SxD and SD: Differences between sex and stage respectively can be calculated VC: Validation cohort; (U): Threshold units: µgrams of haemoglobin per gram of faeces.

estimates of sensitivity are higher when calculated from studies where all patients are overtly symptomatic than from mixed cohorts. Moreover, if we aim to rule out not only CRC but also other SCL using the same threshold, OC-Sensor® accuracy decreases showing lower sensitivities without improving specificity.

Finally, although information related to FIT accuracy to detect different targets have been reported using other brands and thresholds (HM-JACK, HM-JACKarc and FOB Gold), we could not pool their data due to the scarce number of homogeneous studies. Consequently, we could not assume the same degree of evidence for them.

Strengths and weaknesses

The limited number of studies did not enable us to tackle the high expected heterogeneity for all the different thresholds and assays available. Several factors could account for the heterogeneity detected: CRC prevalence[33], demographic characteristics[34], tumour location and stage[35], sample contamination (*e.g.*, haemorrhoids)[36], or FITs[37]. As reported in Table 1, there were many inter-study differences, but the low number of studies included in our review did not enable us to perform a subgroup analysis for most of them. This also limited our ability to conduct statistical pooling using bivariate and HSROC models, which offer the strongest conclusions regarding diagnostic performance. In contrast, random effects methods incorporate a slight degree of heterogeneity among study results[38]. Where possible, we applied both models to calculate pooled estimates of accuracy showing very similar results. Despite this, the strategy to include both studies performed on different percentages of symptomatic patients and the individual data of the COLONPREDICT study[31], enabled us to determine the diagnostic accuracy of the FIT at different thresholds and check the test's diagnostic accuracy at different patient spectra with a different percentage of symptomatic patients and CRC prevalence.

An additional focal point of our review was to ascertain whether all FIT brands shared similar accuracy values. Only four studies with varying thresholds and settings reported the accuracy parameters of the HM-JACK®[19,24] HM-JACKarc®[28] and FOB Gold®[30] systems to detect CRC and no study to date has directly compared the

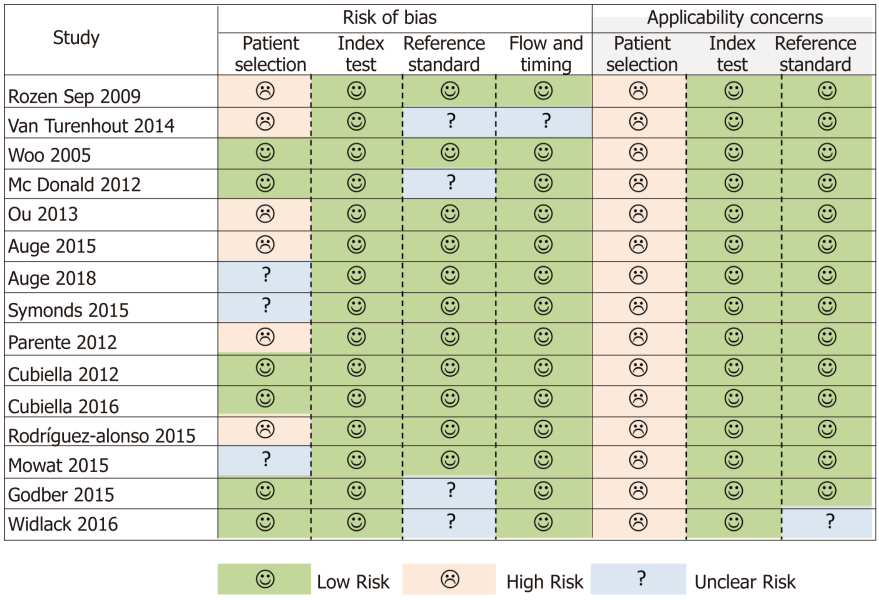

Figure 2 Quality Assessment of Diagnostic Accuracy Studies.

performance of different FITs. Finally, we evaluated the diagnostic performance of the FIT in detecting SCLs. However, we must highlight that the main limitations of our analysis were the varying definitions and diagnostic criteria for both advanced (or high-risk) adenoma and SCL among the studies.

Strengths and weaknesses in relation to other studies

A prior systematic review assessed the value of symptoms and additional diagnostic tests for CRC assessing, including FIT, in symptomatic primary care patients[39]. This review was completed in 2008 and included only three studies involving quantitative FITs. Another systematic review[2] was recently performed to provide information on the new NICE DG30 diagnostic guidelines[4]. We expanded previous inclusion criteria to assess the performance of FIT on samples with different percentage of symptoms and CRC prevalence, since the population included in that meta-analysis was not representative of the criteria reported in NG12[3]. In fact, the studies included had major variability in terms of CRC prevalence[6].

Moreover, to ascertain whether FIT´s accuracy to detect CRC changes in symptomatic patients may be challenging. There are few studies on heterogeneous populations outside a screening setting and categorising those studies according to the presence and type of symptoms is difficult due to unspecific abdominal symptoms commonly associated with bowel cancer (such as abdominal pain or changing bowel habit) are common and sometimes unreported among apparently healthy people[40]. This not only diminishes the value of symptoms as a diagnostic tool as previously reported[39,41,42], but means that even a significant proportion of individuals taking part in CRC screening programmes could suffer from unreported lower gastrointestinal symptoms. This could also explain why in some studies SCL prevalence has been revealed to be similar between patients suffering from nonspecific abdominal symptoms and supposedly 'asymptomatic' symptoms, unlike what is expected[43,44].

Our results suggest that although FIT may play a key role in the evaluation of symptomatic patients, it should not be used alone to rule out CRC. In fact, FIT should be interpreted considering the whole clinical spectrum including variables such as sex and age[34]. Moreover, high-risk symptoms like rectal bleeding or diarrhoea may affect the amount of f-Hb detected. FIT accuracy could be higher in this setting than in unspecific low-risk symptoms which are also more in line with the NG12 scenario reported[3].

This clinical concern may affect the expected number of missed CRC as previously discussed elsewhere[5]. Therefore, we checked the performance of FIT in different theoretical situations defined in Figure 8 by means of what we try to represent as the sources of uncertainty of actual decision-making. For example, if we 'erroneously' assumed that FIT sensitivity to rule out CRC is 94.1% for any symptomatic patient after being estimated by pooling '100% symptomatic' studies which have higher percentages of high-risk symptoms such as rectal bleeding, but the 'true value' were 85.5% (estimated by 'mixed cohorts') we would miss 1, 2 and 10 unexpected additional CRCs in populations with a CRC prevalence of 1%, 3% and 13%,

Table 3 Colorectal cancer detection: Diagnostic accuracy parameters based on quantitative faecal immunochemical test for haemoglobin threshold concentration and brand (DerSimonian´s method)"

Variable	Studies (*n*)	Sensitivity[1]	*I2*[2]	Specificity[1]	*I2*[2]	Positive LR[3]	*I2*[2]	Negative LR[3]	*I2*[2]	Diagnostic OR[3]	*I2*[2]	*P*[a]
OC-Sensor, > LoD μg Hb/g faeces												
All studies	4	98.2 (96.2-99.3)	0.0	35.8 (34.2-37.3)	96.1	1.55 (1.37-1.75)	94.2	0.07 (0.03-0.14)	0.0	21.41 (10.07-45.5)	0.0	0.6
OC-Sensor, ≥ 10 μg Hb/g faeces												
All studies	8	90.8 (87.9-93.2)	69.7	79.9 (79.1-80.7)	99.4	4.79 (2.96-7.76)	99.1	0.15 (0.09-0.23)	52.7	31.44 (19.50-50.68)	44.7	0.09
100% Symptomatic	4	94.4 (91.4-96.6)	0.0	65.9 (64.4-67.4)	99.3	2.97 (1.78-4.95)	99.0	0.10 (0.06-0.15)	0.0	28.49 (17.77-45.67)	0.0	0.6
Mixed patients	4	83.2 (76.5-88.6)	44.5	88.2 (87.4-89.0)	96.7	7.78 (4.72-12.82)	95.1	0.21 (0.13-0.33)	30.7	35.36 (14.19-88.10)	71.0	0.6
CRC prevalence ≥ 2.5%	5	91.9 (88.7-94.3)	76.0	69.7 (68.5-71.0)	99.2	3.16 (1.99-5.0)	98.8	0.13 (0.07-0.25)	66.5	23.20 (14.76-36.47)	20.0	0.2
CRC prevalence < 2.5%	3	86.3 (77.7-92.5)	48.0	90.2 (89.4-91.1)	72.6	9.21 (7.23-11.74)	55.1	0.17 (0.09-0.33)	26.4	52.33 (27.23-100.58)	10.0	0.7
OC-Sensor, ≥ 15 μg Hb/g faeces												
All studies	5	91.0 (87.8-93.6)	73.3	81.8 (80.9-82.7)	99.7	4.77 (2.34-9.71)	99.4	0.15 (0.09-0.25)	57.3	36.64 (20.43-65.71)	49.7	0.04
100% Symptomatic[4]	3	93.6 (90.2-96.0)	32.6	65.8 (64.1-67.5)	99.5	2.91 (1.46-5.78)	99.3	0.11 (0.07-0.16)	0.0	29.10 (12.74-66.46)	35.5	0.67
OC-Sensor, ≥ 20 μg Hb/g faeces												
All studies	5	90.3 (86.9-93.0)	75.6(86.9-93.0)	83.4 (82.5-84.2)	99.7	5.30 (2.47-11.34)	99.4	0.15 (0.09-0.27)	67.2	39.02 (21.48-70.88)	56.1	0.04
100% Symptomatic[4]	3	92.9 (89.5-95.5)	26.1	68.0 (66.3-69.7)	99.5	3.14 (1.52-6.50)	99.3	0.11 (0.07-0.17)	0.0	29.81 (15.05-59.04)	29.2	0.67

[1]Values are expressed as percentages and its 95% confidence interval;
[2]Values are expressed as percentages;
[3]Values are expressed as absolute numbers and its 95% confidence interval;
[4]The studies that comprise the 100% symptomatic subgroup also have colorectal cancer prevalence ≥ 2.5%; *P*[a]: Significance of the threshold effect using the Spearman rank correlation ($P < 0.01$ is considered statistically significant). *I2*: Inconsistency index; LoD: Limit of detection; LR: Likelihood ratio; OR: Odds ratio; CRC: Colorectal cancer.

respectively, for each 1000 symptomatic patients with CRC assessed.

Nevertheless, it is important to note that the aim of performing a FIT in a symptomatic patient is not only to rule out CRC as long as other conditions, such as IBD, may also present the same symptoms. Unfortunately, we could only estimate the pooled accuracy parameters of three studies performed with the OC-Sensor® at LoD and 10 μg Hb/g faeces thresholds respectively, with sensitivity estimates ranging from 91.7% to 80.4%. Despite the weakness previously discussed, these results are consistent with the results of Hogberg *et al*'s study[45], which demonstrated that a qualitative FIT with a LoD f-Hb threshold could identify 87.5% and 90% of cases of CRC and IBD in unselected primary care patients, respectively.

Unanswered questions and future research

Although our results support the use of FIT in optimising the number of urgent referrals and helping to define a patient cohort with a negligible risk of CRC that would not require any referral, caution is recommended when using it outside the screening setting for symptomatic patients. FIT´s accuracy for detecting SCL appears to be not equally reliable in every patient subgroup. Finally, whether to exclude the use of further diagnostic tests in symptomatic patients with high CRC prevalence is doubtful, especially if symptoms persist. Thus, existing FIT-based prediction models[25,31,46] and recently published results[47,48] should also be validated directly, comparing different FIT brands and stratifying by clinical spectrum, while future biomarkers[49,50] should also be evaluated and compared with the FIT to incorporate objective criteria that can safely rule out CRC diagnosis.

In conclusion, our meta-analysis reveals that sensitivity for CRC may change across populations with differences in clinical symptoms, irrespective of CRC prevalence. In addition, FIT is not sensitive enough to exclude other significant colonic diseases. Future studies solely concerned with patients consulting for low risk symptoms are needed to better assess the role of FIT in ruling out CRC in this subgroup. Meanwhile,

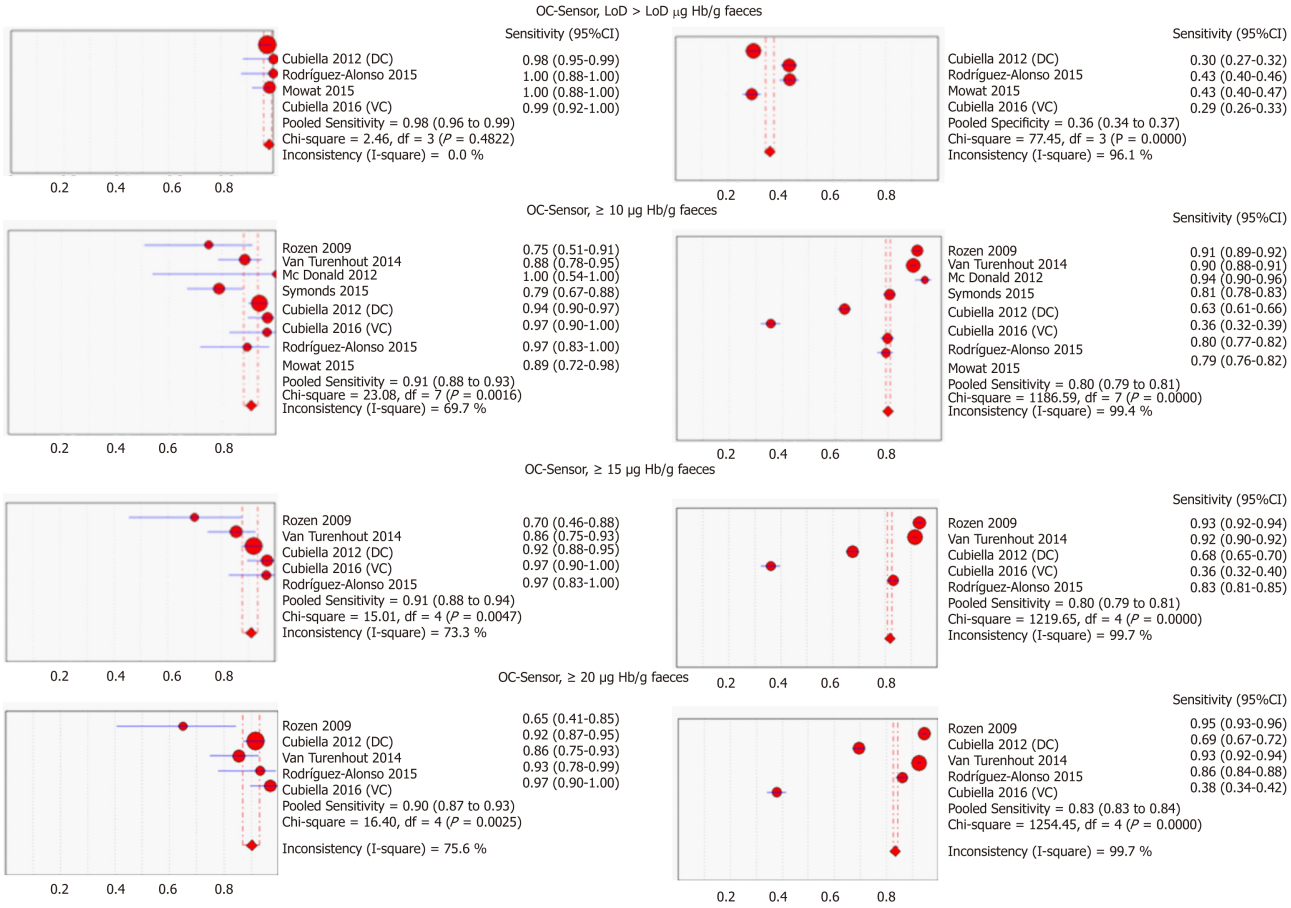

Figure 3 Pooled sensitivity and specificity of faecal immunochemical tests for colorectal cancer detection based on threshold and branch (DerSimonian´s method). CI: Confidence interval; DC: Derivation cohort; VC: Validation cohort.

a single f-Hb cut-off of 10 mg Hb/g faeces could be used in this population to identify which patients may benefit from a "watching and waiting" strategy without this involving to avoid further workup, irrespective of FIT result, if there is no response to treatment.

Table 4 Diagnostic accuracy parameters for colorectal cancer detection based on quantitative faecal immunochemical test for haemoglobin threshold concentration and brand

Brand	Threshold(μg/g faeces)	Author, year	Sensitivity[1]	Specificity[1]
Mixed cohorts				
OC-Sensor®	25	Rozen, 2010[17]	60.0 (36.1-80.9)	95.2 (94.0-96.2)
OC-Sensor®	30	Rozen, 2010[17]	55.0 (31.5-76.9)	95.8 (94.7-96.7)
OC-Sensor®	40	Rozen, 2010[17]	55.0 (31.5-76.9)	96.3 (95.3-97.2)
OC-Sensor®	40	van Turenhout, 2014[18]	75.4 (63.5-84.9)	94.8 (93.9-95.6)
OC-Sensor®	60	Symonds 2016[23]	63.6 (50.9-75.1)	91.9 (90.3-93.3)
OC-Sensor®	80	Symonds 2016[23]	59.1 (46.3-71.0)	93.4 (91.9-94.7)
HM-JACK®	33	Woo, 2005[19]	50.0 (11.8-88.2)	83.5 (73.5-90.9)
FOB Gold®	10	Auge, 2018[30]	91.7 (71.5-98.5)	82.2 (79.6-84.5)
FOB Gold®	20	Auge, 2018[30]	87.5 (66.5-96.7)	86.0 (83.6-88.1)
FOB Gold®	30	Auge, 2018[30]	83.3 (61.8-94.5)	89.2 (87.0-91.1)
FOB Gold®	40	Auge, 2018[30]	83.3 (61.8-94.5)	90.3 (88.2-92.1)
FOB Gold®	50	Auge, 2018[30]	83.3 (61.8-94.5)	91.4 (89.4-93.1)
FOB Gold®	60	Auge, 2018[30]	83.3 (61.8-94.5)	91.8 (89.9-93.5)
100% Symptomatic				
HM-JACK®	20	Parente, 2012[24]	61.7 (46.4-75.5)	88.8 (84.1-92.6)
HM-JACKarc®	7	Widlak, 2017[28]	84.0 (63.9-95.5)	93.1 (90.2-95.4)

[1]Values are expressed as percentages and its 95% confidence interval.

Table 5 OC-Sensor® diagnostic accuracy parameters for colorectal cancer detection (Threshold 10 μg Hb/g faeces) estimated with DerSimonian *vs* Bivariate methods

Variable	Studies (*n*)	Sensitivity[1]	Specificity[1]	Positive LR[2]	Negative LR[2]	Diagnostic OR[2]
All studies (DS)	8	90.8 (87.9-93.2)	79.9 (79.1-80.7)	4.79 (2.96-7.76)	0.15 (0.09-0.23)	31.44 (19.50-50.68)
All studies (Bv)	8	89.6 (82.7-94.0)	80.2 (67.2-88.9)	4.52 (2.73-7.50)	0.13 (0.08-0.20)	34.85 (20.74-58.57)
100% Symptomatic (DS)	4	94.4 (91.4-96.6)	65.9 (64.4-67.4)	2.97 (1.78-4.95)	0.10 (0.06-0.15)	28.49 (17.77-45.67)
100% Symptomatic (Bv)	4	94.1 (90.0-96.6)	66.0 (47.1-80.9)	2.77 (1.69-4.55)	0.09 (0.06-0.14)	30.93 (16.09-59.45)
Mixed patients (DS)	4	83.2 (76.5-88.6)	88.2 (87.4-89.0)	7.78 (4.72-12.82)	0.21 (0.13-0.33)	35.36 (14.19-88.10)
Mixed patients (Bv)	4	85.5 (76.5-91.4)	89.3 (84.1-93.0)	8.01 (5.07-12.65)	0.16 (0.10-0.28)	49.35 (19.88-122.5)
CRC prevalence ≥ 2.5% (DS)	5	91.9 (88.7-94.3)	69.7 (68.5-71.0)	3.16 (1.99-5.0)	0.13 (0.07-0.25)	23.20 (14.76-36.47)
CRC prevalence ≥ 2.5% (Bv)	5	91.7 (83.3-96.1)	69.3 (53.5-81.6)	2.99 (1.97-4.53)	0.12 (0.07-0.21)	24.95 (16.02-38.86)
CRC prevalence < 2.5% (DS)	3	86.3 (77.7-92.5)	90.2 (89.4-91.1)	9.21 (7.23-11.74)	0.17 (0.09-0.33)	52.33 (27.23-100.58)
CRC prevalence < 2.5% (Bv)	3	84.9 (73.4-92.0)	90.5 (89.0-91.9)	8.96 (7.63-10.53)	0.17 (0.09-0.30)	53.77 (26.99-107.11)

[1]Values are expressed as percentages and its 95% confidence interval;
[2]Values are expressed as absolute numbers and its 95% confidence interval. Bv: Bivariate; CRC: Colorectal cancer; D: DerSimonian; LR: Likelihood ratio; OR: Odds ratio.

Table 6 Advanced neoplasia and significant colonic lesion detection: Diagnostic accuracy parameters based on quantitative faecal immunochemical test threshold concentration and brand (DerSimonian´s method)

Variable	Studies(*n*)	Sensitivity[1]	I^2[2]	Specificity[1]	I^2[2]	Positive LR[3]	I^2[2]	Negative LR[3]	I^2[2]	Diagnostic OR[3]	I^2[2]	*P*[a]
Advanced neoplasia												
OC-Sensor, > LoD μg Hb/g faeces												
All studies	3	91.0 (88.7-93.0)	87.9	36.9 (35.0-38.8)	95.2	1.40 (1.35-1.45)	0.0	0.26 (0.16-0.44)	76.6	5.44 (3.48-8.48)	58	< 0.001
OC-Sensor, ≥ 10 μg Hb/g faeces												
All studies	5	67.9 (65.1-70.5)	97.4	81.0 (80.0-82.0)	99.5	3.42 (1.97-5.94)	98.8	0.41 (0.30-0.57)	93.4	9.43 (8.10-10.98)	0.0	< 0.001

100% Symptomatic	3	79.7 (76.5-82.6)	94.6	67.3 (65.5-69.1)	99.4	2.43 (1.41-4.17)	98.5	0.32 (0.21-0.49)	86.5	8.67 (6.96-10.80)	5.8	< 0.001
Prevalence CRC ≥ 2.5%	4	71.7 (68.8-74.5)	97.1	76.7 (75.4-77.9)	99.5	2.96 (1.65-5.30)	98.9	0.36 (0.25-0.53)	91.8	9.29 (7.79-11.09)	9.3	< 0.001
OC-Sensor, ≥ 15 μg Hb/g faeces												
All studies	5	65.0 (62.2-67.8)	97.6	83.5 (82.5-84.4)	99.6	3.90 (2.04-7.47)	99.0	0.43 (0.31-0.60)	94.2	10.06 (8.14-12.44)	42.4	< 0.001
100% Symptomatic	3	76.8 (73.5-79.9)	95.6	70.3 (68.5-72.1)	99.4	2.63 (1.39-4.97)	98.8	0.34 (0.22-0.52)	88.4	8.88 (7.23-10.91)	0.0	< 0.001
Prevalence CRC ≥ 2.5%	4	69.3 (66.3-72.1)	97.1	79.4 (78.2-80.6)	99.6	3.33 (1.67-6.66)	99.1	0.38 (0.27-0.54)	91.1	9.72 (7.46-12.66)	55.4	< 0.001
OC-Sensor, ≥ 20 μg Hb/g faeces												
All studies	5	62.9 (60.1-65.7)	97.8	85.1 (84.2-86.0)	99.6	4.34 (2.16-8.73)	99.0	0.45 (0.32-0.62)	95.3	10.62 (8.24-13.67)	57.4	< 0.001
100% Symptomatic	3	75.1 (71.7-78.3)	96.1	72.4 (70.7-74.1)	99.5	2.85 (1.43-5.65)	98.8	0.35 (0.23-0.55)	90.4	9.19 (7.47-11.32)	1.8	< 0.001
Prevalence CRC ≥ 2.5%	4	67.5 (64.5-70.4)	97.3	81.2 (80.0-82.3)	99.6	3.66 (1.74-7.71)	99.1	0.40 (0.29-0.55)	91.7	10.19 (7.49-13.86)	66.5	< 0.001
Significant colonic lesion												
OC-Sensor, LoD μg Hb/g faeces												
All studies	3	91.7 (89.5-93.6)	0.0	36.9 (35.0-39.0)	94.2	1.45 (1.32-1.59)	80.4	0.24 (0.19-0.30)	0.0	6.01 (4.57-7.92)	0.0	< 0.001
OC-Sensor, ≥ 10 μg Hb/g faeces												
All studies	4	78.6 (75.6-81.4)	91.5	69.8 (67.9-71.6)	99.2	3.75 (2.08-6.76)	98.3	0.34 (0.27-0.42)	59.6	11.72 (6.41-21.45)	82.8	< 0.001
100% Symptomatic[4]	3	80.4 (77.4-83.2)	89.6	67.0 (65.0-68.9)	99.2	2.54 (1.45-4.46)	98.5	0.31 (0.26-0.37)	23.7	8.56 (6.18-11.86)	49.8	< 0.001

[1]Values are expressed as percentages and its 95% confidence interval;
[2]Values are expressed as percentages;
[3]Values are expressed as absolute numbers and its 95% confidence interval;
[4]The studies that comprise the 100% symptomatic subgroup also have CRC prevalence ≥ 2.5%; P^a: Significance of the threshold effect using the Spearman rank correlation ($P < 0.01$ is considered statistically significant). *I2*: Inconsistency index; LoD: Limit of detection; LR: Likelihood ratio; OR: Odds ratio; CRC: Colorectal cancer.

Table 7 Diagnostic accuracy parameters for advanced neoplasia detection based on quantitative faecal immunochemical test for haemoglobin threshold concentration and brand

Brand	Threshold(μg/g faeces)	Author, year	Sensitivity[1]	Specificity[1]
		Mixed cohorts		
OC-Sensor®	5	Ou, 2013[21]	56.8 (39.5-72.9)	88.7 (85.7-91.2)
OC-Sensor®	25	Rozen, 2010[17]	27.5 (20.3-34.7)	96.7 (95.8-97.6)
OC-Sensor®	25	Terhaar sive Droste, 2010[32]	48.3 (42.6-53.9)	94.3 (93.2-95.3)
OC-Sensor®	30	Rozen, 2010[17]	26.8 (19.9-34.7)	97.3 (96.5-98.1)
OC-Sensor®	30	Terhaar sive Droste, 2010[32]	46.0 (40.4-51.7)	95.1 (94.1-96.1)
OC-Sensor®	40	Rozen, 2010[17]	26.2 (19.1-33.2)	97.8 (97.0-98.5)
OC-Sensor®	40	Terhaar sive Droste, 2010[32]	43.2 (37.6-48.9)	95.8 (94.8-96.7)
HM-JACKarc®	LoD	Auge, 2016[22]	96.6 (82.8-93.4)	10.6 (6.9-15.9)
HM-JACKarc®	10	Auge, 2016[22]	34.5 (19.9-52.7)	87.2 (81.6-91.3)
HM-JACKarc®	20	Auge, 2016[22]	31.0 (17.3-49.2)	92.8 (88.0-95.7)
HM-JACKarc®	30	Auge, 2016[22]	31.0 (17.3-49.2)	93.3 (88.7-96.1)
HM-JACKarc®	40	Auge, 2016[22]	27.6 (14.7-45.7)	93.9 (89.4-96.6)
FOB Gold®	10	Auge, 2018[30]	45.7 (33.7-58.1)	84.7 (80.8-88.0)
FOB Gold®	20	Auge, 2018[30]	37.1 (26.1-49.6)	87.9 (84.2-90.8)
FOB Gold®	30	Auge, 2018[30]	35.7 (24.6-48.1)	90.3 (87.0-93.1)
FOB Gold®	40	Auge, 2018[30]	32.9 (22.4-45.2)	91.1 (87.8-93.6)
FOB Gold®	50	Auge, 2018[30]	31.4 (20.9-43.6)	92.3 (89.3-94.7)
FOB Gold®	60	Auge, 2018[30]	30.0 (19.9-42.3)	92.3 (89.2-94.6)
		100% symptomatic		

HM-JACK®	20	Parente, 2012[24]	35.6 (27.9-44.1)	94.5 (89.7-97.2)

[1]Values are expressed as percentages and its 95% confidence interval.

Table 8 Diagnostic accuracy parameters for significant colonic lesion detection based on quantitative faecal immunochemical test for haemoglobin threshold concentration and brand

Brand	Threshold(μg/g faeces)	Author, year	Sensitivity[1]	Specificity[1]
Significant colonic lesion (100% symptomatic)				
OC-Sensor®	15	Cubiella (DC), 2014[29]	76.2 (72.0-80.0)	74.4 (71.7-76.9)
OC-Sensor®	15	Cubiella (VC), 2017[31]	89.5 (84.1-93.6)	40.6 (36.4-44.9)
OC-Sensor®	20	Cubiella (DC), 2014[29]	74.7 (70.5-78.6)	76.1 (73.5-78.6)
OC-Sensor®	20	Cubiella (VC), 2017[31]	87.8 (82.2-92.2)	42.1 (37.9-46.5)
HM-JACKarc®	10	Godber, 2016[27]	68.9 (53.2-81.4)	80.2 (76.1-83.7)
HM-JACKarc®	15	Godber, 2016[27]	66.7 (50.9-79.6)	83.1 (79.2-86.5)
HM-JACKarc®	20	Godber, 2016[27]	64.4 (48.7-77.7)	85.7 (81.9-88.7)
HM-JACKarc®	25	Godber, 2016[27]	64.4 (48.7-77.7)	87.5 (83.9-90.3)
HM-JACKarc®	30	Godber, 2016[27]	64.4 (48.7-77.7)	88.6 (85.2-91.4)
HM-JACKarc®	35	Godber, 2016[27]	64.4 (48.7-77.7)	89.2 (85.9-92.0)
HM-JACKarc®	40	Godber, 2016[27]	64.4 (48.7-77.7)	90.0 (86.7-92.5)

[1]Values are expressed as percentages and their 95% confidence interval. DC: Derivation cohort; VC: Validation cohort.

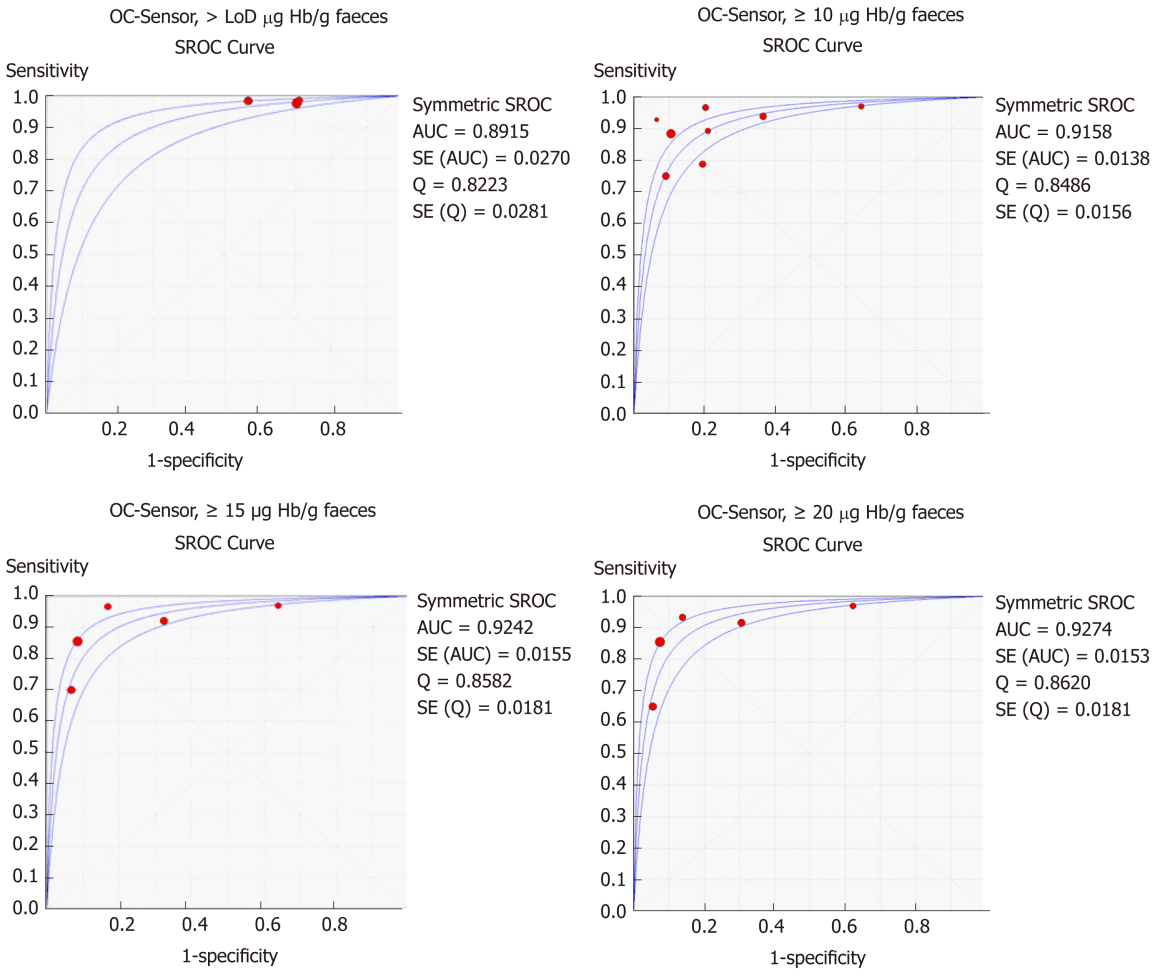

Figure 4 Summary receiver operating characteristic curve for colorectal cancer detection at different thresholds and branches (DerSimmonian and Lair´s model). LoD: Limit of detection; AUC: Area under the curve; SROC: Summary receiver operating characteristic.

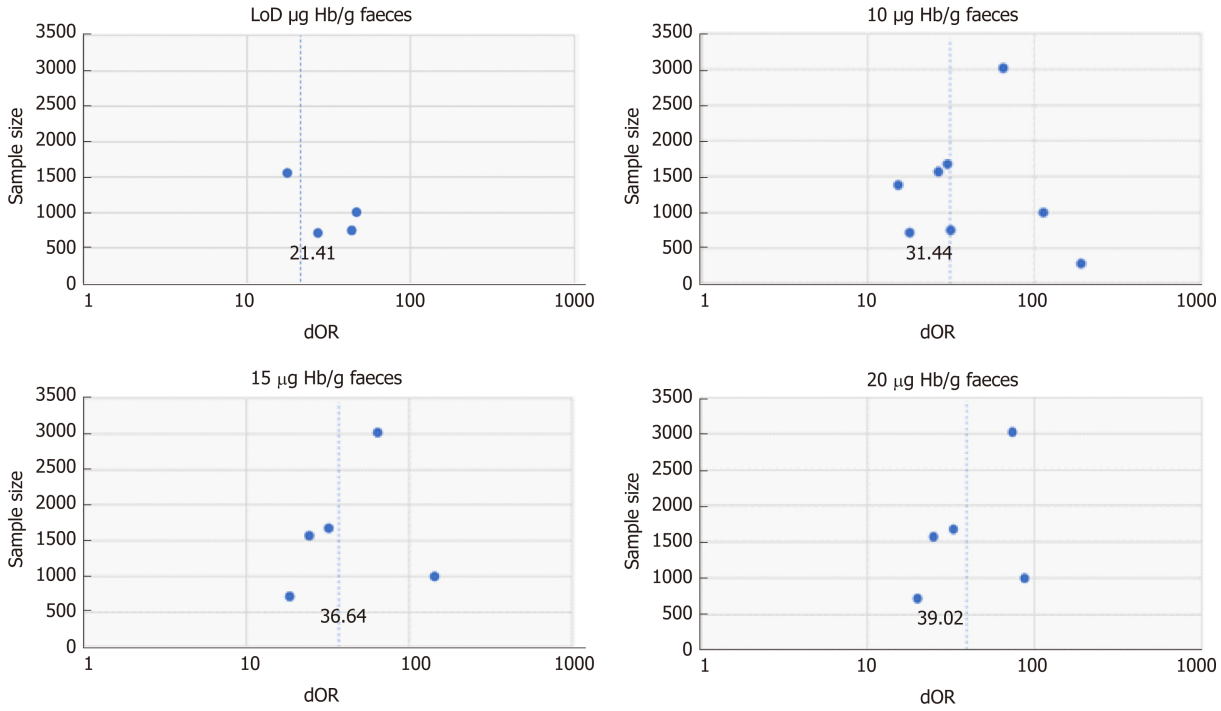

Figure 5 Funnel scatterplot to evaluate publication bias for studies using OC-Sensor® with different thresholds to detect colorectal cancer. Each point in the plot represents a study with its diagnostic odds ratio (dOR) and sample size. A symmetric image around an axis traced by the pooled dOR value suggests absence of publication bias. Asymmetry with study concentration on the right side (the side with higher diagnostic odds ratio values) suggests publication bias with less negative studies published. dOR: Diagnostic odds ratio.

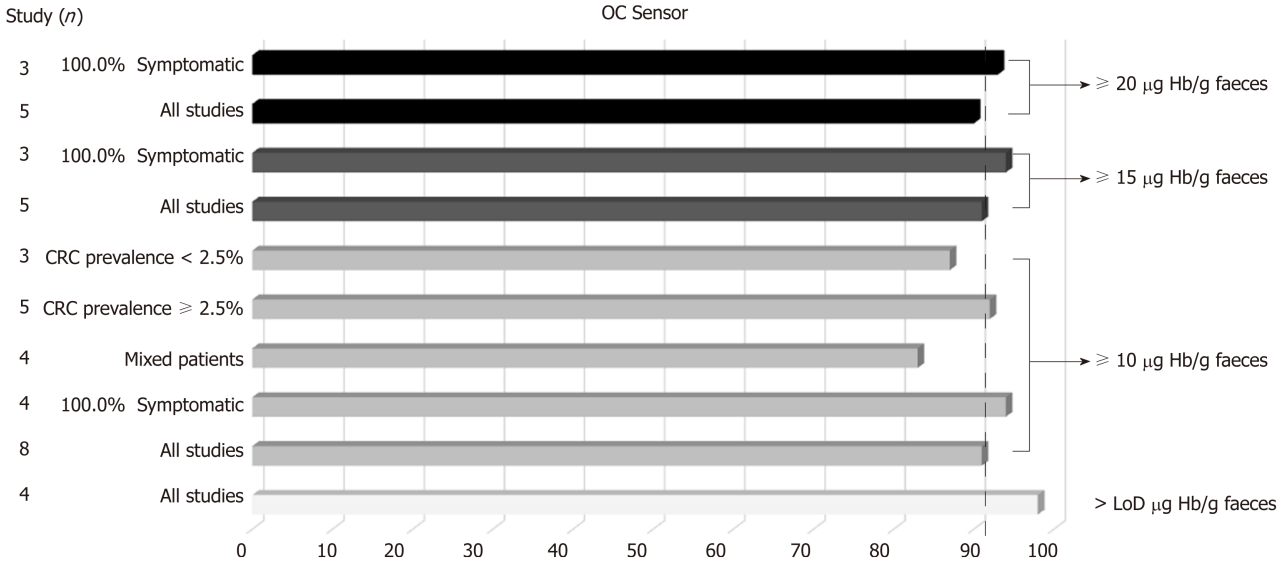

Figure 6 OC-Sensor® pooled sensitivity estimates for colorectal cancer detection (subgroup analysis using DerSimonian´s method). CRC: Colorectal cancer.

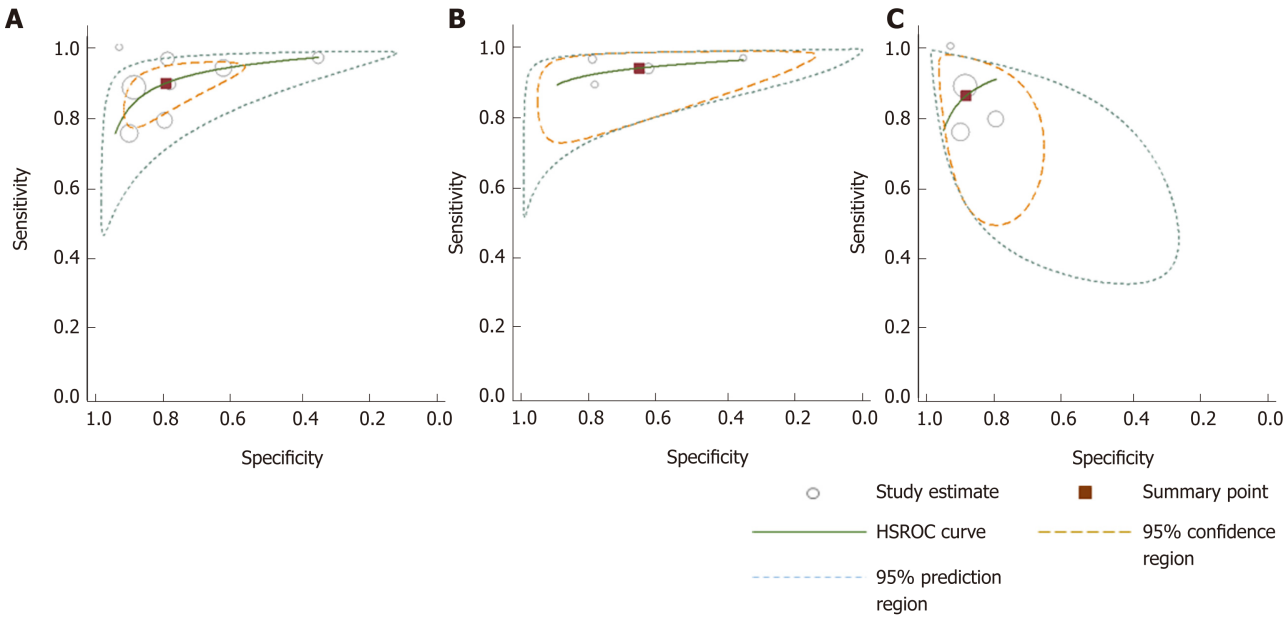

Figure 7 Hierarchical summary receiver-operating characteristic curves for colorectal cancer detection generated using different subgroups of studies. A: All studies; B: 100% symptomatic; C: Mixed cohorts. HSROC: Hierarchical summary receiver operating characteristic.

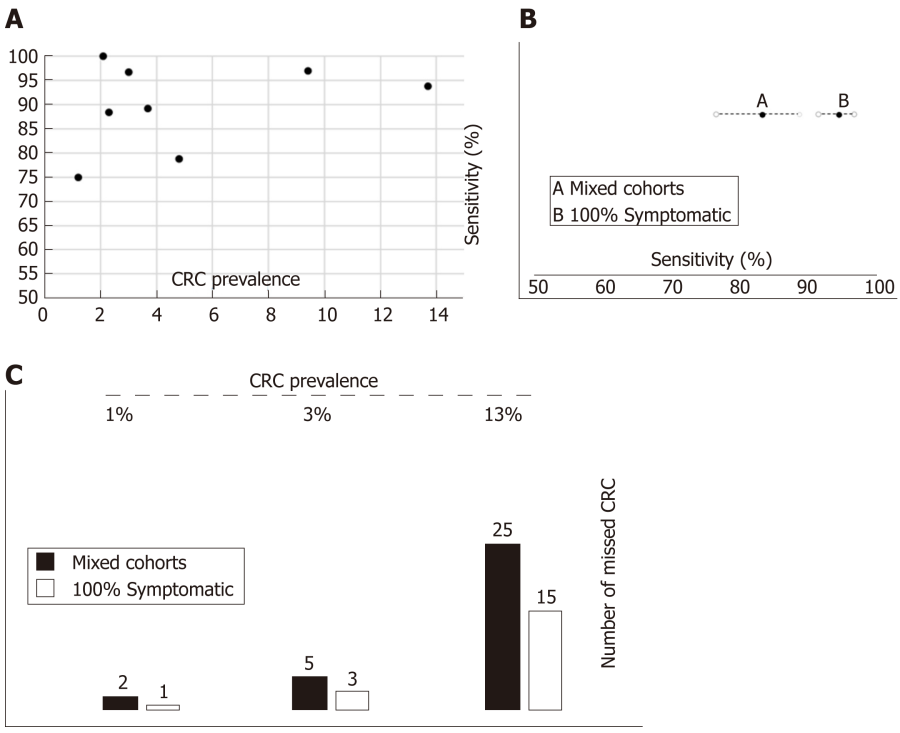

Figure 8 Relationship between colorectal cancer prevalence, clinical spectrum and accuracy of faecal immunochemical test for haemoglobin to rule out colorectal cancer. A: There is no correlation between colorectal cancer (CRC) prevalence and faecal immunochemical test for haemoglobin (FIT) sensitivity; B: Pooled FIT sensitivity to detect CRC cancer estimated from studies with 'Mixed cohorts' is significantly lower than estimated with '100% symptomatic' cohorts; C: Number of missed CRC per 1000 assessed symptomatic patients with colorectal cancer calculated through Fagan nomograms under various assumptions (FIT accuracy parameters estimated with mixed cohorts or 100% symptomatic cohorts) and CRC prevalence. CRC: Colorectal cancer; FIT: Faecal immunochemical test for haemoglobin.

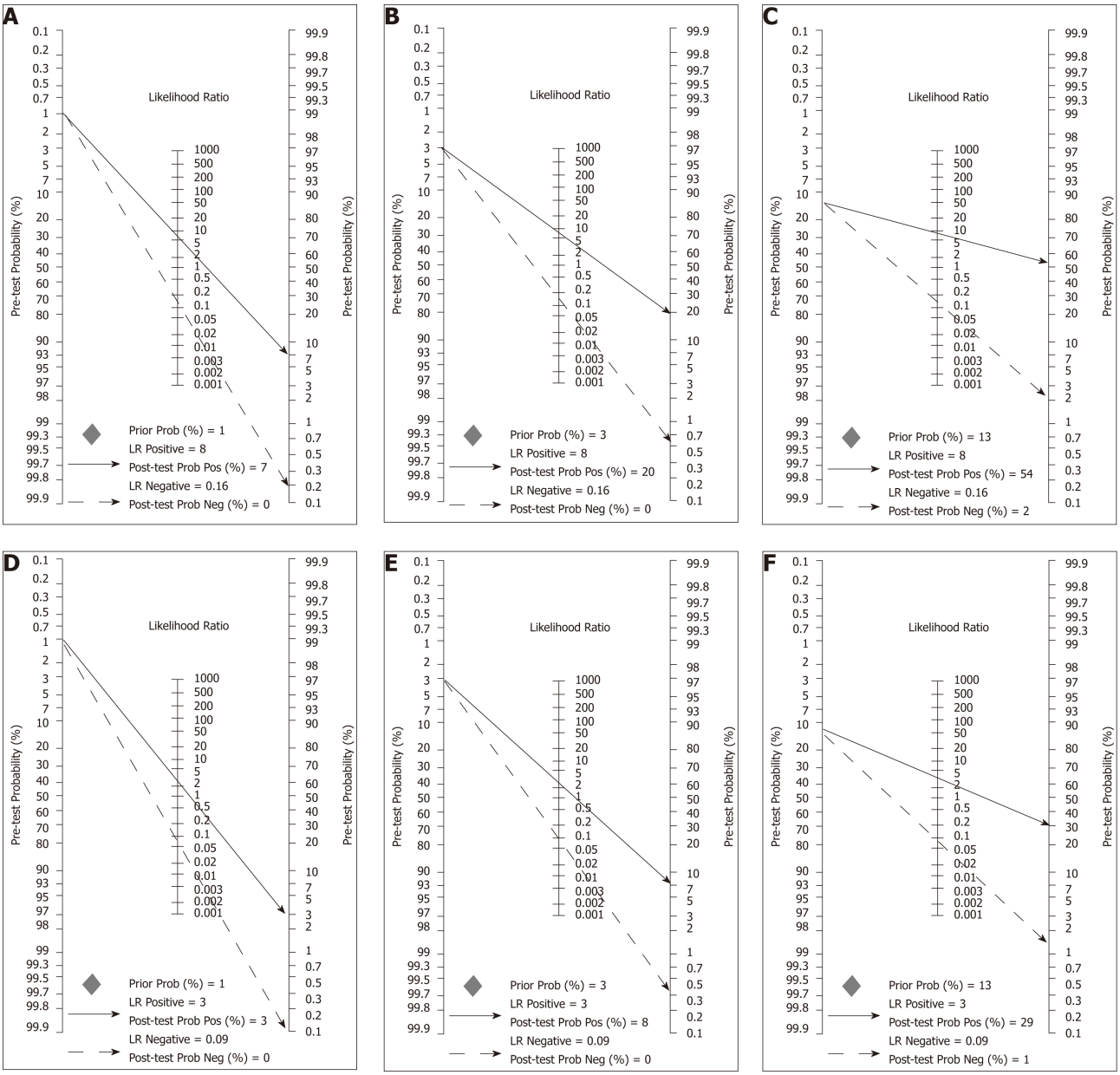

Figure 9 Fagan nomograms used to calculate post-test probabilities based on different scenarios defined by colorectal cancer prevalence and supposed accuracy of OC-Sensor (Threshold 10 μg Hb/g faeces). A-C; These scenarios are defined by colorectal cancer (CRC) prevalence of 1%, 3% and 13% respectively and faecal immunochemical test for haemoglobin (FIT) accuracy parameters used were the pooled estimates calculated with 'mixed cohorts' studies; D-F; These scenarios are defined by CRC prevalence of 1%, 3% and 13% respectively and FIT accuracy parameters used were the pooled estimates calculated with '100% symptomatic' studies. CRC: Colorectal cancer; FIT: Faecal immunochemical test for haemoglobin.

ARTICLE HIGHLIGHTS

Research background

Colorectal cancer (CRC) is the third most common cancer worldwide and the fourth leading cause of cancer-related death. The majority of cancers are still diagnosed after symptomatic presentation, and the quantitative faecal immunochemical test for haemoglobin (FIT) has been revealed to be more accurate for the detection of CRC than multiple clinical referral criteria in symptomatic patients referred for colonoscopy. Hence, The National Institute for Health and Care Excellence (NICE) has recently issued referral guidance for suspected CCR in which FIT is recommended for certain low risk symptomatic patients using a 10 μg Hb/g faeces threshold.

Research motivation

Although NICE recommendation applies only to patients with low risk symptoms in primary care, the studies done to date were mainly concerned with patients who had already been referred to secondary care and were not only concerned with patients with low risk symptoms. Thus, further work is required to find out if FIT´s ability to rule out CRC may change through the broad spectrum of symptomatic patients.

Research objectives
We aimed to systematically review the literature for published studies out of CRC screening programme setting, to compare FIT accuracy for CRC detection in different clinical spectrum through a meta-analysis. Secondary goal included assessing the usefulness of FIT to detect significant colonic lesions (SCLs) in symptomatic patients.

Research methods
We performed an electronic search in MEDLINE and EMBASE databases (from database inception to May 2018) using a sensitive search of "FIT for CRC" narrowing our search to prospective cohort studies performed on adult patients when at least a fraction of symptomatic patients was included. To identify further relevant studies, we checked the reference lists of all articles extracted. We classified studies on the basis of brand and threshold of faecal haemoglobin (f-Hb) concentration for a positive test result to limit heterogeneity. Finally, a bivariate model was fitted for subgroups defined by CRC prevalence and percentage of symptoms, for direct comparison between them.

Research results
We identified fourteen studies that matched the search criteria, and individual unpublished data from cohorts included in the COLONPREDICT study were also used enrolling 10400 patients using OC-Sensor® at the f-Hb cut-off of 10 mg Hb/g faeces. Pooled estimates of sensitivity for studies formed solely by symptomatic patients (94.1%) were significantly higher than for mixed cohorts (85.5%), while there were no statistically significant differences between pooled sensitivity of studies with different CRC prevalence (< 2.5% and ≥ 2.5%). At the same threshold, OC-Sensor® sensitivity to rule out any SCL was 78.6%.

Research conclusions
This meta-analysis suggests that FIT sensitivity to detect CRC is higher in studies solely including symptomatic patients irrespective of CRC prevalence, but may not be sensitive enough to rule out all SCLs. We hypothesize that differences between both groups could be justified due to cohorts solely including symptomatic patients could present a higher percentage of symptoms related to higher amounts of f-Hb as rectal bleeding or diarrhoea, but the study design is not suitable to prove this hypothesis.

Research perspectives
More data are warranted in order to compare FIT accuracy for CRC detection in patients with different clinical spectrum, to identify a subgroup of symptomatic patients where FIT can safely rule out CRC. Future prospective cohort studies solely concerned with patients consulting for low risk symptoms and stratifying by sex and age could help to get this aim.

REFERENCES

1 **Lee JK**, Liles EG, Bent S, Levin TR, Corley DA. Accuracy of fecal immunochemical tests for colorectal cancer: Systematic review and meta-analysis. *Ann Intern Med* 2014; **160**: 171 [PMID: 24658694 DOI: 10.7326/M13-1484]

2 **Westwood M**, Lang S, Armstrong N, van Turenhout S, Cubiella J, Stirk L, Ramos IC, Luyendijk M, Zaim R, Kleijnen J, Fraser CG. Faecal immunochemical tests (FIT) can help to rule out colorectal cancer in patients presenting in primary care with lower abdominal symptoms: A systematic review conducted to inform new NICE DG30 diagnostic guidance. *BMC Med* 2017; **15**: 189 [PMID: 29061126 DOI: 10.1186/s12916-017-0944-z]

3 National Institute for Health and Care Excellence NICE Guideline 12. Suspected cancer: Recognition and referral 2015; Available from: https://www.nice.org.uk/guidance/ng12

4 NICE Diagnostics guidance DG30. Quantitative faecal immunochemical tests to guide referral for colorectal cancer in primary care. 2017; Available from: https://www.nice.org.uk/guidance/dg30

5 **Fraser CG**. Faecal immunochemical tests (FIT) in the assessment of patients presenting with lower bowel symptoms: Concepts and challenges. *Surgeon* 2018; **16**: 302-308 [PMID: 29548552 DOI: 10.1016/j.surge.2018.01.004]

6 **Leeflang MM**, Rutjes AW, Reitsma JB, Hooft L, Bossuyt PM. Variation of a test's sensitivity and specificity with disease prevalence. *CMAJ* 2013; **185**: E537-E544 [PMID: 23798453 DOI: 10.1503/cmaj.121286]

7 **Moher D**, Liberati A, Tetzlaff J, Altman DG; PRISMA Group. Preferred reporting items for systematic reviews and meta-analyses: The PRISMA statement. *PLoS Med* 2009; **6**: e1000097 [PMID: 19621072 DOI: 10.1371/journal.pmed.1000097]

8 **Whiting PF**, Rutjes AW, Westwood ME, Mallett S, Deeks JJ, Reitsma JB, Leeflang MM, Sterne JA, Bossuyt PM; QUADAS-2 Group. QUADAS-2: A revised tool for the quality assessment of diagnostic accuracy studies. *Ann Intern Med* 2011; **155**: 529-536 [PMID: 22007046 DOI: 10.7326/0003-4819-155-8-201110180-00009]

9 StataCorp 2015. Stata Statistical Software: Release 14. College Station, TX: StataCorp LP

10 **Reitsma JB**, Glas AS, Rutjes AW, Scholten RJ, Bossuyt PM, Zwinderman AH. Bivariate analysis of sensitivity and specificity produces informative summary measures in diagnostic reviews. *J Clin Epidemiol* 2005; **58**: 982-990 [PMID: 16168343 DOI: 10.1016/j.jclinepi.2005.02.022]

11 **Rutter CM**, Gatsonis CA. A hierarchical regression approach to meta-analysis of diagnostic test accuracy evaluations. *Stat Med* 2001; **20**: 2865-2884 [PMID: 11568945 DOI: 10.1002/sim.942]

12 **Zamora J**, Abraira V, Muriel A, Khan K, Coomarasamy A. Meta-DiSc: A software for meta-analysis of test accuracy data. *BMC Med Res Methodol* 2006; **6**: 31 [PMID: 16836745 DOI: 10.1186/1471-2288-6-31]

13 **Walter SD**. Properties of the summary receiver operating characteristic (SROC) curve for diagnostic test

data. *Stat Med* 2002; **21**: 1237-1256 [PMID: 12111876 DOI: 10.1002/sim.1099]
14 **DerSimonian R**, Laird N. Meta-analysis in clinical trials. *Control Clin Trials* 1986; **7**: 177-188 [PMID: 3802833 DOI: 10.1016/0197-2456(86)90046-2]
15 **Swets JA**. Measuring the accuracy of diagnostic systems. *Science* 1988; **240**: 1285-1293 [PMID: 3287615 DOI: 10.1126/science.3287615]
16 **Takwoingi Y**. Meta-analysis of test accuracy studies in Stata: a bivariate model approach. Version 1.1. April 2016.. Available from: http://methods.cochrane.org/sdt/
17 **Rozen P**, Comaneshter D, Levi Z, Hazazi R, Vilkin A, Maoz E, Birkenfeld S, Niv Y. Cumulative evaluation of a quantitative immunochemical fecal occult blood test to determine its optimal clinical use. *Cancer* 2010; **116**: 2115-2125 [PMID: 20186820 DOI: 10.1002/cncr.25012]
18 **van Turenhout ST**, Oort FA, van der Hulst RW, Visscher AP, Terhaar sive Droste JS, Scholten P, Bouman AA, Meijer GA, Mulder CJ, van Rossum LG, Coupé VM. Prospective cross-sectional study on faecal immunochemical tests: Sex specific cut-off values to obtain equal sensitivity for colorectal cancer? *BMC Gastroenterol* 2014; **14**: 217 [PMID: 25528043 DOI: 10.1186/s12876-014-0217-7]
19 **Woo HY**, Mok RS, Park YN, Park DI, Sung IK, Sohn CI, Park H. A prospective study of a new immunochemical fecal occult blood test in Korean patients referred for colonoscopy. *Clin Biochem* 2005; **38**: 395-399 [PMID: 15766742 DOI: 10.1016/j.clinbiochem.2005.01.003]
20 **McDonald PJ**, Digby J, Innes C, Strachan JA, Carey FA, Steele RJ, Fraser CG. Low faecal haemoglobin concentration potentially rules out significant colorectal disease. *Colorectal Dis* 2013; **15**: e151-e159 [PMID: 23199241 DOI: 10.1111/codi.12087]
21 **Ou CH**, Kuo FC, Hsu WH, Lu CY, Yu FJ, Kuo CH, Wang JY, Wu MT, Shiea J, Wu DC, Hu HM. Comparison of the performance of guaiac-based and two immunochemical fecal occult blood tests for identifying advanced colorectal neoplasia in Taiwan. *J Dig Dis* 2013; **14**: 474-483 [PMID: 23701988 DOI: 10.1111/1751-2980.12077]
22 **Auge JM**, Fraser CG, Rodriguez C, Roset A, Lopez-Ceron M, Grau J, Castells A, Jimenez W. Clinical utility of one versus two faecal immunochemical test samples in the detection of advanced colorectal neoplasia in symptomatic patients. *Clin Chem Lab Med* 2016; **54**: 125-132 [PMID: 26124057 DOI: 10.1515/cclm-2015-0388]
23 **Symonds EL**, Pedersen SK, Baker RT, Murray DH, Gaur S, Cole SR, Gopalsamy G, Mangira D, LaPointe LC, Young GP. A Blood Test for Methylated BCAT1 and IKZF1 vs. a Fecal Immunochemical Test for Detection of Colorectal Neoplasia. *Clin Transl Gastroenterol* 2016; **7**: e137 [PMID: 26765125 DOI: 10.1038/ctg.2015.67]
24 **Parente F**, Marino B, Ilardo A, Fracasso P, Zullo A, Hassan C, Moretti R, Cremaschini M, Ardizzoia A, Saracino I, Perna F, Vaira D. A combination of faecal tests for the detection of colon cancer: A new strategy for an appropriate selection of referrals to colonoscopy? A prospective multicentre Italian study. *Eur J Gastroenterol Hepatol* 2012; **24**: 1145-1152 [PMID: 22735608 DOI: 10.1097/MEG.0b013e328355cc79]
25 **Rodríguez-Alonso L**, Rodríguez-Moranta F, Ruiz-Cerulla A, Lobatón T, Arajol C, Binefa G, Moreno V, Guardiola J. An urgent referral strategy for symptomatic patients with suspected colorectal cancer based on a quantitative immunochemical faecal occult blood test. *Dig Liver Dis* 2015; **47**: 797-804 [PMID: 26055489 DOI: 10.1016/j.dld.2015.05.004]
26 **Mowat C**, Digby J, Strachan JA, Wilson R, Carey FA, Fraser CG, Steele RJ. Faecal haemoglobin and faecal calprotectin as indicators of bowel disease in patients presenting to primary care with bowel symptoms. *Gut* 2016; **65**: 1463-1469 [PMID: 26294695 DOI: 10.1136/gutjnl-2015-309579]
27 **Godber IM**, Todd LM, Fraser CG, MacDonald LR, Younes HB. Use of a faecal immunochemical test for haemoglobin can aid in the investigation of patients with lower abdominal symptoms. *Clin Chem Lab Med* 2016; **54**: 595-602 [PMID: 26457785 DOI: 10.1515/cclm-2015-0617]
28 **Widlak MM**, Thomas CL, Thomas MG, Tomkins C, Smith S, O'Connell N, Wurie S, Burns L, Harmston C, Evans C, Nwokolo CU, Singh B, Arasaradnam RP. Diagnostic accuracy of faecal biomarkers in detecting colorectal cancer and adenoma in symptomatic patients. *Aliment Pharmacol Ther* 2017; **45**: 354-363 [PMID: 27910113 DOI: 10.1111/apt.13865]
29 **Cubiella J**, Salve M, Díaz-Ondina M, Vega P, Alves MT, Iglesias F, Sánchez E, Macía P, Blanco I, Bujanda L, Fernández-Seara J. Diagnostic accuracy of the faecal immunochemical test for colorectal cancer in symptomatic patients: comparison with NICE and SIGN referral criteria. *Colorectal Dis* 2014; **16**: O273-O282 [PMID: 24456168 DOI: 10.1111/codi.12569]
30 **Auge JM**, Rodriguez C, Espanyol O, Rivero L, Sandalinas S, Grau J, Jimenez W, Castells A. An evaluation of the SENTiFIT 270 analyser for quantitation of faecal haemoglobin in the investigation of patients with suspected colorectal cancer. *Clin Chem Lab Med* 2018; **56**: 625-633 [PMID: 29150989 DOI: 10.1515/cclm-2017-0605]
31 **Cubiella J**, Digby J, Rodríguez-Alonso L, Vega P, Salve M, Díaz-Ondina M, Strachan JA, Mowat C, McDonald PJ, Carey FA, Godber IM, Younes HB, Rodriguez-Moranta F, Quintero E, Álvarez-Sánchez V, Fernández-Bañares F, Boadas J, Campo R, Bujanda L, Garayoa A, Ferrandez Á, Piñol V, Rodríguez-Alcalde D, Guardiola J, Steele RJ, Fraser CG. COLONPREDICT study investigators. The fecal hemoglobin concentration, age and sex test score: Development and external validation of a simple prediction tool for colorectal cancer detection in symptomatic patients. *Int J Cancer* 2017; **140**: 2201-2211 [PMID: 28187494 DOI: 10.1002/ijc.30639]
32 **Terhaar sive Droste JS**, Oort FA, van der Hulst RW, van Heukelem HA, Loffeld RJ, van Turenhout ST, Ben Larbi I, Kanis SL, Neerincx M, Räkers M, Coupé VM, Bouman AA, Meijer GA, Mulder CJ. Higher fecal immunochemical test cutoff levels: Lower positivity rates but still acceptable detection rates for early-stage colorectal cancers. *Cancer Epidemiol Biomarkers Prev* 2011; **20**: 272-280 [PMID: 21135261 DOI: 10.1158/1055-9965.EPI-10-0848]
33 **Brenner H**, Gefeller O. Variation of sensitivity, specificity, likelihood ratios and predictive values with disease prevalence. *Stat Med* 1997; **16**: 981-991 [PMID: 9160493 DOI: 10.1002/(SICI)1097-0258(19970515)16:9<981::AID-SIM510>3.0.CO;2-N]
34 **McDonald PJ**, Strachan JA, Digby J, Steele RJ, Fraser CG. Faecal haemoglobin concentrations by gender and age: Implications for population-based screening for colorectal cancer. *Clin Chem Lab Med* 2011; **50**: 935-940 [PMID: 22149740 DOI: 10.1515/CCLM.2011.815]
35 **Digby J**, Fraser CG, Carey FA, McDonald PJ, Strachan JA, Diament RH, Balsitis M, Steele RJ. Faecal haemoglobin concentration is related to severity of colorectal neoplasia. *J Clin Pathol* 2013; **66**: 415-419 [PMID: 23418340 DOI: 10.1136/jclinpath-2013-201445]
36 **Kim NH**, Park JH, Park DI, Sohn CI, Choi K, Jung YS. Are Hemorrhoids Associated with False-Positive

Fecal Immunochemical Test Results? *Yonsei Med J* 2017; **58**: 150-157 [PMID: 27873508 DOI: 10.3349/ymj.2017.58.1.150]

37 **Chiang TH**, Chuang SL, Chen SL, Chiu HM, Yen AM, Chiu SY, Fann JC, Chou CK, Lee YC, Wu MS, Chen HH. Difference in performance of fecal immunochemical tests with the same hemoglobin cutoff concentration in a nationwide colorectal cancer screening program. *Gastroenterology* 2014; **147**: 1317-1326 [PMID: 25200099 DOI: 10.1053/j.gastro.2014.08.043]

38 **Moayyedi P**. Meta-analysis: Can we mix apples and oranges? *Am J Gastroenterol* 2004; **99**: 2297-2301 [PMID: 15571572 DOI: 10.1111/j.1572-0241.2004.40948.x]

39 **Jellema P**, van der Windt DA, Bruinvels DJ, Mallen CD, van Weyenberg SJ, Mulder CJ, de Vet HC. Value of symptoms and additional diagnostic tests for colorectal cancer in primary care: Systematic review and meta-analysis. *BMJ* 2010; **340**: c1269 [PMID: 20360221 DOI: 10.1136/bmj.c1269]

40 **Dent OF**, Goulston KJ, Zubrzycki J, Chapuis PH. Bowel symptoms in an apparently well population. *Dis Colon Rectum* 1986; **29**: 243-247 [PMID: 3485035 DOI: 10.1007/BF02553027]

41 **Ford AC**, Veldhuyzen van Zanten SJ, Rodgers CC, Talley NJ, Vakil NB, Moayyedi P. Diagnostic utility of alarm features for colorectal cancer: Systematic review and meta-analysis. *Gut* 2008; **57**: 1545-1553 [PMID: 18676420 DOI: 10.1136/gut.2008.159723]

42 **Astin M**, Griffin T, Neal RD, Rose P, Hamilton W. The diagnostic value of symptoms for colorectal cancer in primary care: A systematic review. *Br J Gen Pract* 2011; **61**: e231-e243 [PMID: 21619747 DOI: 10.3399/bjgp11X572427]

43 **Rajasekhar PT**, Ritchie M, Rutter MD, Clifford G, Waddup G, Dempsey N, Rubin GP, Rees CJ. Lower gastrointestinal symptoms are prevalent among individuals colonoscoped within the Bowel Cancer Screening Programme. *Colorectal Dis* 2012; **14**: e603-e607 [PMID: 22554066 DOI: 10.1111/j.1463-1318.2012.03066.x]

44 **Lieberman DA**, de Garmo PL, Fleischer DE, Eisen GM, Chan BK, Helfand M. Colonic neoplasia in patients with nonspecific GI symptoms. *Gastrointest Endosc* 2000; **51**: 647-651 [PMID: 10840294 DOI: 10.1067/mge.2000.105082]

45 **Högberg C**, Karling P, Rutegård J, Lilja M. Diagnosing colorectal cancer and inflammatory bowel disease in primary care: The usefulness of tests for faecal haemoglobin, faecal calprotectin, anaemia and iron deficiency. A prospective study. *Scand J Gastroenterol* 2017; **52**: 69-75 [PMID: 27623716 DOI: 10.1080/00365521.2016.1228120]

46 **Williams TG**, Cubiella J, Griffin SJ, Walter FM, Usher-Smith JA. Risk prediction models for colorectal cancer in people with symptoms: A systematic review. *BMC Gastroenterol* 2016; **16**: 63 [PMID: 27296358 DOI: 10.1186/s12876-016-0475-7]

47 **Herrero JM**, Vega P, Salve M, Bujanda L, Cubiella J. Symptom or faecal immunochemical test based referral criteria for colorectal cancer detection in symptomatic patients: A diagnostic tests study. *BMC Gastroenterol* 2018; **18**: 155 [PMID: 30359225 DOI: 10.1186/s12876-018-0887-7]

48 **Quyn AJ**, Steele RJ, Digby J, Strachan JA, Mowat C, McDonald PJ, Carey FA, Godber IM, Younes HB, Fraser CG. Application of NICE guideline NG12 to the initial assessment of patients with lower gastrointestinal symptoms: Not FIT for purpose? *Ann Clin Biochem* 2018; **55**: 69-76 [PMID: 28661203 DOI: 10.1177/0004563217707981]

49 **Vacante M**, Borzì AM, Basile F, Biondi A. Biomarkers in colorectal cancer: Current clinical utility and future perspectives. *World J Clin Cases* 2018; **6**: 869-881 [PMID: 30568941 DOI: 10.12998/wjcc.v6.i15.869]

50 **Godos J**, Biondi A, Galvano F, Basile F, Sciacca S, Giovannucci EL, Grosso G. Markers of systemic inflammation and colorectal adenoma risk: Meta-analysis of observational studies. *World J Gastroenterol* 2017; **23**: 1909-1919 [PMID: 28348498 DOI: 10.3748/wjg.v23.i10.1909]

Published By Baishideng Publishing Group Inc
7041 Koll Center Parkway, Suite 160, Pleasanton, CA 94566, USA
Telephone: +1-925-2238242
Fax: +1-925-2238243
E-mail: bpgoffice@wjgnet.com
Help Desk:http://www.f6publishing.com/helpdesk
http://www.wjgnet.com